Universidade do Minho
Escola de Engenharia

Simone dos Santos Silva

Processing and surface modification of novel natural-origin architectures aimed for biomedical applications

Junho de 2008

Processing and surface modification of novel natural-origin architectures aimed for biomedical applications
Simone dos Santos Silva
UMinho|2008

Universidade do Minho
Escola de Engenharia

Simone dos Santos Silva

Processing and surface modification of novel natural-origin architectures aimed for biomedical aplications

Tese de Doutoramento em Ciências e Tecnologia de Materiais
Área de conhecimento em Biomateriais

Trabalho efectuado sob a orientação de
Professor Doutor Rui Luís Gonçalves dos Reis
Professor Doutor João Filipe Colardelle da Luz Mano

Junho de 2008

To my parents

“ A ciência tem as raízes amargas mas os frutos são muito doces” – Aristóteles

ACKNOWLEDGEMENTS

I would like to acknowledge my supervisor, Prof. Rui Reis for the confidence, and for accepting me as part of the 3B´s family. I am also very grateful for giving me the freedom to explore my ideas not only within the group but also abroad at the University of Aveiro and at the University of Trento (Italy). I was fortunate to have you as my supervisor, whose expertise, leadership and patience contributed positively to the construction of my professional profile.

A special thanks to my co-supervisor, Prof. João F. Mano, who greatly enriched my knowledge with his insightful conversations into engineering. I would like acknowledge your attention, guidance and helpful comments on the present thesis.

Thank you to Prof. Claudio Migliaresi and Prof. Antonella Motta for the attention and guidance throughout the work period at the University of Trento.

My acknowledgements to Prof. João Rocha and Prof. Luis Carlos for the help and guidance throughout of the work at the University of Aveiro.

I hereby express my deepest gratitude to the '*Fundação para a Ciência e Tecnologia*', for the financial support through a PhD grant.

To my colleagues from the 3B's group, all of you were equally important throughout this work. I appreciate all the help, encouragement and friendship! I specially thank Manuela who received me in my first day in the lab, showing me with a big smile "how the things work"!
I also thank the Management Team, Ariana, Tânia, Berta, Virginia, Liliana for the help with the bureaucratic matters. To Elsa, thanks for the patience and help in the analysis of the samples.

A particular thanks to some people, namely Belinha, João Oliveira, Ana Pinheiro, Tó, Rui Amandi, Vitor, Elizabeth, Emanuel, Ana Rita, Xana, Bruno, Gabriela, Ana Leite, Luciano, Paulo Bessa, Ana Martins, Patrícia, Esther, Ricardo and Sofia for all the friendship and collaboration.

A special thank to Márcia, Iva, Marina, Gabriela, Marta, Johan and Sandra Luna. You were "important pieces" in the development of this work.

To Miguel and Jessica, a special hug by the constant friendship and affection during this long course. Thank you!!!!

To my colleagues namely Eva, Devid, Eleonora, Michelle and Matteo for the attention and help during my work abroad in Italy.

I would like to acknowledge my friend and teacher, Prof. Rosangela Balaban for the constant attention and friendship.

To my dear Carlos, for encouraging me especially throughout the late nights. Thank you for your patience, dedication, sense of humour and love all over those months!

To my parents, for encouraging my dreams and supporting my decisions and, especially 'keeping the rope always stretched, even at a distance'. I would be lost without your advices, support, friendship and love.

ABSTRACT

In the last decades, tissue engineering has emerged as a potential therapeutical tool aimed at developing substitutes that are able to restore proper function of the damaged organs/tissues. Nature-inspired routes involving natural origin polymer-based systems represent an attractive alternative to produce novel materials by mimicking the tissue environment required for tissue regeneration. Moreover, further modifications of these systems allow the adjustment of their properties in accordance with the requirements for successful biomedical applications.

The main goal of the present thesis is to develop and modify natural origin polymer-based systems using simple methodologies such as sol-gel, surface modification by means of plasma treatment and blending of chitosan with proteins (soy protein isolate and silk fibroin).

A sol-gel method was used to improve the bulk properties of chitosan by the incorporation of an inorganic component at the sub-nanometric level. Chitosan/siloxane hybrid materials were synthesised, where essentially urea bridges covalently bond the chitosan to the polysiloxane network. These bifunctional materials exhibit interesting photoluminescence features and a bioactive behaviour.

In most situations in the biomedical field, the surface of a biomaterial is in direct contact with living tissues. Therefore, the surface characteristics play a fundamental role on the implant biocompatibility. In this thesis, nitrogen and argon plasma treatment was applied on chitosan membranes in order to improve their surface properties. The applied modifications promoted differences on surface chemistry, wettability and roughness, which reflected in a significant improvement of fibroblast adhesion and proliferation onto chitosan membranes. Besides the surface modification, blending of chitosan with proteins such as soy protein isolate and silk fibroin was also used to modify the bulk properties of chitosan. *In situ* cross-linking with glutaraldehyde solutions was used to enhance the interaction between the components of the blend. Hence, membranes with different morphologies, water absorption and degradability were obtained. The biological assays suggested that the cross-linking with lower glutaraldehyde concentration promotes better cell adhesion on the membranes. The morphological characterization showed that both surface roughness surface and surface energy were dependent on soy protein content. Structural investigations by FTIR and NMR indicated that the blends are not completely miscible due to a weak polysaccharide-protein interaction. In another related work, novel hydrogels were produced combining *Bombyx mori* silk fibroin and chitosan. In this case, these systems were cross-linked with genipin. These hydrogels were freeze-

dried to obtain cross-linked chitosan/silk sponges. Rheological and mechanical properties, structural aspects and morphological features of the porous structures were evaluated. The results revealed stable and ordered structures, similar porosities, and swelling capability that depended on the pH. The cytotoxicity assay indicated that cellular viability was about 100% in all sponges and for all time points studied (1, 3, 7 and 14 days), demonstrating the extremely low cytotoxicity levels of the materials. Cell studies using chondrocytes-like cells seeded onto sponges, including cell viability (MTS assay), proliferation (DNA test), morphology (SEM analysis) and matrix production (GAGs quantification), showed a significant high adhesion, proliferation and matrix production with the time of culture. The findings in this work suggested that the properties of the sponges can be manipulated by either change chitosan/silk fibroin ratio or through genipin cross-linking. Parallel to this study, the possibility of obtaining modified silk nanometric nets using electrospinning processing from regenerated silk fibroin/formic acid with addition of genipin was explored. Modified silk nanofibers with diameters ranging from 140 nm to 590 nm were developed. The changes on the secondary structure of nanofibers, induced by the reaction of silk fibroin with genipin, promoted a higher integrity of these modified nanofibers in water.

In summary, the findings from these works demonstrated the potential and versatility of the proposed strategies in obtaining different structures (*e.g.* membranes, hydrogels) using mixtures of chitosan with proteins or with inorganic agents for improving the performance of natural origin polymer-based materials to be used in biomedical applications.

RESUMO

Nas últimas décadas, a engenharia de tecidos emergiu como uma solução terapêutica alternativa dentro das estratégias possíveis relacionadas com a reparação e regeneração de órgãos/tecidos danificados, no sentido de restabelecer a sua capacidade funcional. As estratégias envolvendo sistemas à base de biopolímeros representam uma alternativa promissora para a produção de novos materiais para a regeneração de tecidos. Materiais de origem natural e, consequentemente, de fontes renováveis, surgem como uma escolha interessante para recriar o ambiente envolvente do tecido afectado. No entanto, modificações químicas nos biomateriais poderão ser necessárias para melhorar as suas propriedades, ajustando-as a determinadas aplicações biomédicas.

O principal objectivo da presente tese consistiu no desenvolvimento e modificação de sistemas à base de polímeros de origem natural usando metodologias como o "sol-gel", a modificação superficial através do tratamento por plasma e combinações de quitosano com proteínas da soja e da fibroína da seda.

De modo a modificar as propriedades internas do quitosano, uma parte inorgânica foi incorporada ao sistema macromolecular através do método "sol-gel". Como resultado, materiais híbridos de quitosano/siloxano foram sintetizados, onde se estabeleceram ligações covalentes entre o quitosano e a rede inorgânica. Estes materiais bifuncionais demonstraram características interessantes de fotoluminescência e um comportamento bioactivo.

É frequente a superfície de um biomaterial estar em contacto directo com os tecidos vivos. Assim sendo, as características da sua superfície têm um papel fundamental na biocompatibilidade do implante. Com o objectivo de melhorar as propriedades de superfície de membranas de quitosano, estas foram tratadas por plasma utilizando azoto e árgon, resultando em diferenças na química de superfície, molhabilidade e na rugosidade das membranas. Estas modificações estimularam a adesão e proliferação celulares de fibroblastos quando cultivados nas membranas de quitosano. Além das modificações de superfície, as propriedades internas do quitosano foram modificadas através da adição da proteína da soja e da fibroína da seda. Foram usadas reacções de reticulação *in situ*, com soluções de glutaraldeído em sistemas à base de quitosano com soja, de modo a aumentar a interacção entre os componentes do sistema. As membranas reticuladas apresentaram morfologias, absorção de água e degradabilidade diferentes. As membranas reticuladas com uma baixa concentração de glutaraldeído apresentaram melhor adesão celular quando comparadas às restantes membranas. Através da caracterização morfológica demonstrou-se que

tanto a rugosidade de superfície como a energia de superfície estava directamente relacionada com o conteúdo da proteína de soja usada no sistema. Estudos estruturais utilizando as técnicas de FTIR e RMN indicaram que as misturas não são completamente miscíveis devido às fracas interacções entre polímero e proteína. Novos hidrogéis foram também produzidos combinando a fibroina da seda e o quitosano reticulados com "genipin". Em seguida, os hidrogéis foram liofilizados para obter esponjas de quitosano/seda. Os resultados relativos às propriedades reológicas e mecânicas assim como os aspectos estruturais e as características morfológicas, revelaram estruturas estáveis e ordenadas, porosidades similares e capacidade de inchamento dependentes do pH. A análise de citoxicidade indicou uma viabilidade celular de aproximadamente 100% em todas as esponjas produzidas e em todos os tempos de cultura estudados (1, 3, 7 e 14 dias), evidenciando os níveis extremamente baixos de citoxicidade dos materiais. Estudos de cultura celular utilizando uma linha celular de condrócitos cultivados nas esponjas, nomeadamente viabilidade (teste MTS), proliferação (teste do ADN) e morfologia (análise do SEM) celulares bem como a produção de matriz extracelular (quantificação dos GAGs), mostrou melhoramento a todos os níveis ao longo dos tempos de cultura. Os resultados deste trabalho sugeriram que as propriedades das esponjas podem ser controladas, quer pela composição de quitosano e de fibroina da seda, quer pela reticulação com o "genipin". Paralelamente a este estudo, foi explorada a possibilidade de se obterem fibras nanométricas de proteína de seda modificadas usando o processo de "electrospinning" a partir de soluções de fibroina da seda regenerada dissolvida em ácido fórmico com adição de genipin como agente de reticulação. Deste modo, nanofibras de seda modificadas foram desenvolvidas com diâmetro entre 140 nm e 590 nm. As mudanças na estrutura secundária das nanofibras, induzidas pela reacção de fibroina da seda com "genipin", promoveram uma maior integridade das nanofibras em água.

Os resultados obtidos a partir destes trabalhos experimentais demonstraram o potencial e versatilidade das estratégias e materiais propostos para a obtenção de diferentes estruturas (por exemplo, membranas, hidrogéis) utilizando soluções à base de quitosano, e suas combinações com proteínas ou mesmo com agentes inorgânicos para melhorar o desempenho de materiais à base de polímeros naturais em aplicações biomédicas.

TABLE OF CONTENTS

Chapter VII

Novel Genipin Cross-linked Chitosan/Silk fibroin Sponges for Cartilage Tissue Engineering Strategies

LIST OF ABBREVIATIONS AND NOMENCLATURES

A

AA- acetic acid

ACL- human anterior cruciate ligament

AgSD- silver sulfadiazine

AFM- Atomic force microscopy

APTES- 3- aminopropyltriethyoxysilane

Ar – argon

ARES- Advanced Rheometric Expansion System

B

bFGF - basic fibroblast growth factor

C

CAE- constant analyser energy

$CaCl_2$ - chloride calcium

Cht – Chitosan

CMC – carboxymethylchitosan

CNS- central nervous system

CS- Chitosan/soy protein blended membranes

CS- collagen/chitosan

CSG – cross-linked chitosan/silk fibroin sponges

CP- cross polarization

^{13}C CP/MAS NMR- solid state carbon nuclear magnetic resonance

D

DAH - 1,6-diaminohexane

D_2O- deuterated water

DCl – deuterium chloride

DD- degree of deacetylation

DHT- dehydrothermal treatment

DMA- Dynamic mechanical analysis

DMEM- Dulbecco's Modified Eagle's Medium

DMF – dimethylformamide

DNA - Desoxyribonucleic Acid

DSC- Differential Scanning Calorimetry

E

E´- storage modulus

E´´´- loss modulus

ECM- extracellular matrix

ECACC- European collection of cell cultures

EDC- 1-Ethyl-3-[3-dimethylaminopropyl]carbodiimide

EDS- energy dispersive spectrometer

EGF- epidermal growth factor

ELE – electrospinning

ESE- endothelialized skin equivalent

ESEM- Environmental scanning electronic microscopy

Et – ethanol

F

FDA- US Food and Drug Administration

FGF- fibroblast growth factor

FTIR- Fourier Transform Infrared Spectroscopy

FTIR-ATR- Fourier Transform Infrared with Attenuated Total Reflection (FTIR-ATR)

FWHM –full-width-at-half-maximum

G

G, GE – genipin

G´- elastic modulus

G´´ - viscous modulus

GA- glutaraldehyde

GAGs - glycosaminoglycans

GC – galactosylated chitosan

GHC6S – gelatin/hyaluronic acid/chondroitin-6-sulphate

GPTMS – 3-glycidyloxypropyl-trimethyoxysilane

H

HA - hyaluronic acid, hyaluronan

Hep-2 - human larynx carcinoma cells

HMDIC- Hexamethylenediisocyanate

HPLC- High Performance Liquid Chromatography

HT- hydrothermal treatment.

HUVEC- human umbilical vein endothelial cells

I

ICPTES - isocyanatopropyltriethoxysilane

IGF-1- insulin-like growth factor

ISO- International Standard Operations

IUPAC - International Union of Pure and Applied Chemistry

K

KBr- potassium bromide

KGF - keratinocyte growth factor

KOH - potassium hydroxyde

L

LM – low molecular weight

LiBr- lithium bromide

M

micro-CT- Micro-Computed Tomography

MC – microbial cellulose

MSCs- mesenchymal stem cells

ml – milliliters

MM – medium molecular weight

MMPs – matrix mettalloproteases

MTS - (3-(4,5-dimethylthiazol-2-yl)-5-(3-carboxymethoxyphenyl)-2-(4-sulfophenyl)-2H-tetrazolium) assay

Mv – molecular viscosimetry weight

N

η´- dynamic viscosity

N_2 – nitrogen

NaCl – sodium chloride

NaOH – sodium hydroxide

NHS – N-hydroxyusuccinimide

NMR - Solid State Nuclear Magnetic Resonance

O

ORC- oxidised regenerated cellulose

O/W emulsion: Oil/water emulsion

OD – optical density

P

PA - Proanthocyanidins

PBS – phosphate buffer solution

PDFG- platelet-derived growth factor

PEC- polyelectrolyte complex

PEG – poly(ethylene glycol)

PEO- polyethylene oxide

PIC – polyionic complex

PLA – poly(lactic acid)

PL- emission photoluminescence

PLE – excitation photoluminescence

PLGA - poly-(lactic-co-glycolic acid)

PMN – polymorphonuclear neutrohils

PNS - peripheral nervous system

POP – poly(oxypropylene)

PSM- Plasma surface modification

R

ROS – reactive oxygen species

RT- room temperature

S

SAXS- Small Angle X-Ray Scattering

SBF- simulated body fluid

SDS-PAGE - Sodium dodecyl sulfate-polyacrylamide gel electrophoresis

SEM- scanning electronic microscopy

SF – Silk fibroin

SFF- solid free-form fabrication method

T

$T_{1\beta}$ (^{1}H) - proton spin –lattice relaxation time in the rotating frame

TCPS -Tissue Culture Polystyrene

TE- Tissue Engineering

TEOS – tetraethylorthosilicate

Tg - glass transition temperature

TGF-β1- Transforming growth factor

TMS- tetramethylsilane

TPP- tripolyphosphate

U

UV – ultra-violet

V

VEGF- Vascular endothelial growth factor

W

W/O- Water-in- oil emulsion

Wt – weight

X

XPS- X- ray photoelectron spectroscopy

XRD- Powder X-ray Diffraction

LIST OF FIGURES

CHAPTER I

CHAPTER II

CHAPTER III

Functional Nanostructured Chitosan/Siloxane Hybrids

CHAPTER IV

Plasma Surface Modification of Chitosan Membranes: Characterization and preliminary cell response studies

CHAPTER V

Physical Properties and Biocompatibility of Chitosan/Soy Blended Membranes

CHAPTER VII

Novel Genipin Cross-linked Chitosan/Silk Fibroin-based Sponges for Cartilage Tissue Engineering Strategies

CHAPTER VIII

Genipin Modified Silk Fibroin Nanometric-Nets

LIST OF TABLES

CHAPTER I

CHAPTER III

Functional Nanostructured Chitosan-Siloxane Hybrids

CHAPTER IV

Plasma Surface Modification on Chitosan Membranes: Characterization and preliminary cell response studies

CHAPTER VI

Miscibility and Morphology of Chitosan/Soy protein Blended Membranes

CHAPTER VII

Novel Genipin Cross-linked Chitosan/Silk fibroin Sponges for Cartilage Tissue Engineering Strategies

CHAPTER VIII

Genipin Modified Silk Fibroin Nanometric Nets

LIST OF PUBLICATIONS

This thesis is based on the following publications:

International Journals with referee

S. S. Silva, R. A. S. Ferreira, L. Fu, L. D. Carlos, J. F. Mano, R. L. Reis, J. Rocha. "Functional nanostructured chitosan/siloxane hybrids". *Journal of Materials Chemistry*, 15, 3952-3961, 2005.

S. S. Silva, M. I. Santos, O. P. Coutinho, J. F. Mano, R. L. Reis, " Physical properties and biocompatibility of chitosan/soy blended membranes", *Journal of Materials Science: Materials in Medicine* 16, 575-579, 2005.

S. S. Silva, J. Benesch, J. F. Mano, B. Goodfellow, R. L. Reis, "Miscibility and morphology of chitosan/soy protein blended membranes", *Carbohydrate Polymers* 70, 25-31, 2007.

S. S. Silva, S. M. Luna, M. E. Gomes, J. Benesch, J. F. Mano, R. L. Mano, " Plasma surface modification on chitosan membranes: characterization and preliminary cell response studies", *Macromolecular Bioscience* 2008, 8(6):568-576.

S. S. Silva, D. Maniglio, A. Motta, J. F. Mano, R. L. Reis, C. Migliaresi, "Genipin modified silk fibroin nanometric nets", *Macromolecular Bioscience* 2008, DOI:10.1002/mabi.200700300.

S. S. Silva, M. Rodrigues, A. Motta, A. Pinheiro, M. E. Gomes, J. F. Mano, R. L. Reis, C. Migliaresi, "Novel Genipin Cross-linked Chitosan-Silk Fibroin Sponges for Cartilage Tissue Engineering Strategies", *Biomacromolecules*, *Submitted* 2008.

S. S. Silva, J. F. Mano, R. L. Reis, "Potential Applications of Natural Origin Polymer-based Systems in Soft Tissue Regeneration", Biotechnology Advances, *Submitted* 2008.

Participations in international conferences:

S. S. Silva, M. T. Rodrigues, A. Motta, M. E. Gomes, J. F. Mano, C. Migliaresi, R. L. Reis, "pH-sensitive cross-linked chitosan-silk based sponges for cartilage tissue engineering strategies: An *in vitro* approach", 8th World Biomaterials Congress, Amsterdam, 2008.

S. S. Silva, M. T. Rodrigues, A. Motta, M. E. Gomes, João F. Mano, C. Migliaresi, R. L. Reis, " Novel genipin cross-linked chitosan-silk based sponges for the regeneration and repair of cartilage using a tissue engineering approach", TERMIS 2008, Porto, Portugal,2008.

S. S. Silva, S. M. Luna, M. E. Gomes, J. Benesch, J. F. Mano, R. L. Reis, " Plasma surface modification of chitosan membranes and its effect on cell adhesion and proliferation", Society for Biomaterials 2006 Annual Meeting, Pittsburg, Pennsylvania, USA, 2006.

S. S. Silva, J. M. Oliveira, S. M. Luna, M. E. Gomes, J. F. Mano, R. L. Reis, " Biocompatibility assessment of novel chitosan hybrid bioactive membranes prepared by means of an in situ cross-linking process, 6th International Symposium on Frontiers in Biomedical Polymers, Granada, Span, 2005.

S. S. Silva, J. M. Oliveira, S. M. Luna, M. E. Gomes, J. F. Mano, R. L. Reis, " Development of chitosan hybrid bioactive membranes prepared through an in situ cross-linking process", 19th European Conference on Biomaterials, Sorrento, Italy, 2005.

S. S. Silva, J. M. Oliveira, J. F. Mano, R. L. Reis, " Preparation and characterization of novel chitosan/soy protein porous hybrids for tissue engineering applications", XII Portuguese Materials Society Meeting, Aveiro, Portugal, 2005.

S. S. Silva, J. M. Oliveira, J. F. Mano, R. L. Reis, " Preparation of novel chitosan/soy protein porous structures for tissue engineering applications", Biomaterials in Regenerative Medicine: The Advent of Combination Products, Philadelphia, USA, 2004.

S. S. Silva, M. I. Santos, O. P. Coutinho, B. J. Goodfellow, J. Rocha, J. F. Mano, R. L. Reis, " Nano-scale interactions, miscibility and physical properties of novel biomedical membranes composed by chitosan/soy protein blends, 7th World Biomaterials Congress, Sydney, Australia, 2004.

S. S. Silva, L. D. Carlos, J. Rocha, J. F. Mano, R. L. Reis, " Evaluation of the properties of novel chitosan/sílica hybrids", 12th Annual Polychar World Forum on Advanced Materials, Guimarães, Portugal, 2004.

S. S. Silva, L. D. Carlos, J. Rocha, J. F. Mano, R. L. Reis, " Evaluation of the biomineralization ability of novel chitosan/sílica hybrids", NATO-ASI Course – Learning From Nature How to Design New Implantable Biomaterials: From Biomineralization Fundamentals to Biomimetic Materials and Processing Routes; Alvor, Portugal, 2003.

S. S. Silva, J. F. Mano, R. L. Reis," Properties of soy protein/chitosan membranes in simulated physiological conditions", 18th European Conference on Biomaterials, Stuttgart, Germany, 2003.

CHAPTER I

CHAPTER I

Potential Applications of Natural Origin Polymer-based Systems in Soft Tissue Regeneration

Abstract

Despite many advances in tissue engineering approaches, scientists still face significant challenges in trying to repair and replace soft tissues. Nature-inspired routes involving the creation of natural origin polymer-based systems constitute an interesting alternative route to produce novel materials. Composition in multi-component systems can be manipulated allowing to mimic the tissue environment required for cellular regeneration of soft tissues. Factors such as design, choice and compatibility of the polymers are key factors for successful strategies in soft tissue regeneration. The present manuscript overviews the potential applications of natural origin polymer-based systems, especially those investigated from polysaccharide-protein systems, and proposed for the treatment of soft tissues, in articles published in the last 10 years. Emphasis will be made on properties and compatibility of the resulting materials as well as matrices commercially available or currently under investigation.

This chapter is based on the following publication:

S. S. Silva, J. F. Mano, R. L. Reis, "Potential Applications of Natural Origin Polymer-based Systems in Soft Tissue Regeneration, Biotechnology Advances, 2008, *submitted*.

1. **Introduction**

Despite many advances in tissue engineering (TE) approaches, scientists still face significant challenges in repairing or replacing soft tissues such as tendons, ligaments, skin, liver, nerve and cartilage to improve the quality of people life. Conventional therapeutic treatments targeted to reconstruct the injured tissues or organs have some limitations such as donor limitations and graft rejections. Based on the principles of TE[1,2], alternative therapeutic strategies have been developed to current treatments involving biodegradable constructs containing specific populations of living cells and growth factors. For example, the skin can be regenerated using epidermal sheets, dermal replacements and complex skin substitutes[3-5], while cartilage defects can be treated with cells seeded on three-dimensional (3D) matrices[6-8]. To meet all the necessary requirements for the success of these approaches, the choice of polymer, design of the matrices and knowledge of the factors affecting cell/tissue-material interactions should be investigated. Nature-inspired routes involving the creation of natural origin polymer-based systems constitute an interesting alternative to produce novel materials. The properties of these systems will depend on the intrinsic characteristics (*e.g.* molecular weight, charge) of each component, their degree of interaction, and their miscibility[9,10]. Both polysaccharides and proteins exhibit relevant characteristics such as availability in the nature, chemical diversity, biodegradability and may be modified in relatively easy ways[11-14]. These features when combined have proven to be a useful route to obtain bioengineered biomatrices with better mechanical and biological properties compared to individual components[14,15]. In this review, the attention was focused in natural origin polymer-based systems composed mainly by chitin/chitosan, glycosaminoglycans, alginate and cellulose combined with different proteins, recently proposed for applications in soft tissue repair and regeneration.

2. **Natural origin polymers and their combinations**

Most of the current researchers have headed toward to study the use of natural biodegradable polymers such as collagen[13,16,17], chitosan [13,18-21], hyaluronic acid [13,22-24], cellulose [13,25], starch[13,26-30], soy protein[13,31,32], gelatin[13,33], silk fibroin[13,34-37], and alginate[13,38] separately, or combined themselves for TE applications[13,14,39-45]. The creation of new materials from natural origin polymer based-systems offer new opportunities for mimicking the tissue microenvironment and stimulate appropriate physiological responses required for cellular regeneration. It seems that these features associated to a controlled biodegradation rate and biocompatibility of these natural based-systems is advantageous when compared to synthetic polymers. The resulting materials can be conjugated as membranes, hydrogels, scaffolds and microspheres to be used in specific biomedical applications. Figure 1 shows some devices organized according to its geometrical dimension. The polymeric matrices can be produced using several techniques. For example, membranes can be obtained by solvent casting of polymeric solutions, while hydrogels can be processed by traditional synthesis, including cross-linking reactions and copolymerization reactions[46,47]. However, some methods are limited in the control of their resulting structure due to side reactions, unreacted pendant groups and entanglements. Scaffolds are usually prepared by freeze-drying technique, emulsion freeze-drying method, salt leaching method, rapid prototyping, fibre bonding, melt based methodologies, among many others [14,15,48-50]. Among them, the freeze-drying technique is the most used widely method [21,49] to produce scaffolds with different shapes, porosities and pore size distributions by varying some parameters such as polymer concentration, type of solvent, freezing temperature and type of moulds. Therefore, the selection of design and method of fabrication of a scaffold could influence its final characteristics in terms of porosity, mechanical properties, degradation behavior and surface properties[15]. Ideally, scaffolds, in forms of hydrogels, sponges and fibrous meshes proposed for TE

applications should posses a structure with an adequate pore size and morphology, controlled degradation rate, suitable mechanical and surface properties[2]. However, these requirements depend on the tissue to be regenerated. For example, successful nerve regeneration to require tissue-engineered scaffolds that provide not only mechanical support for growing neuritis, but also biological signals to direct axonal growth cone to the distal stump[51,52]. Particularly for osteochondral defects, the use of single scaffolds to regenerated cartilage may not be effective, and the employ of bilayered constructs has been purposed as alternative solutions[53-56]. These approaches consists on developing a 3D porous structure that combine a mechanical support resembling the subchondral bone, while also providing a chondrogenic support for the repairing of cartilage.

Tables 1 to 4 summarizes of natural origin polymer-based systems composed by chitin/chitosan, glycosaminoglycans, alginate and cellulose with different proteins. These tables also include the methods for production of these systems, the matrix shape, the aimed TE application, the biologically active biomolecule to be delivered, the source of cell used to *in vitro* tests. When applicable the used animal model is also refereed. More details about characteristics of the natural origin polymers described in the scope of this review can be found elsewhere[13,14,18,24,31,34,39,57,58].

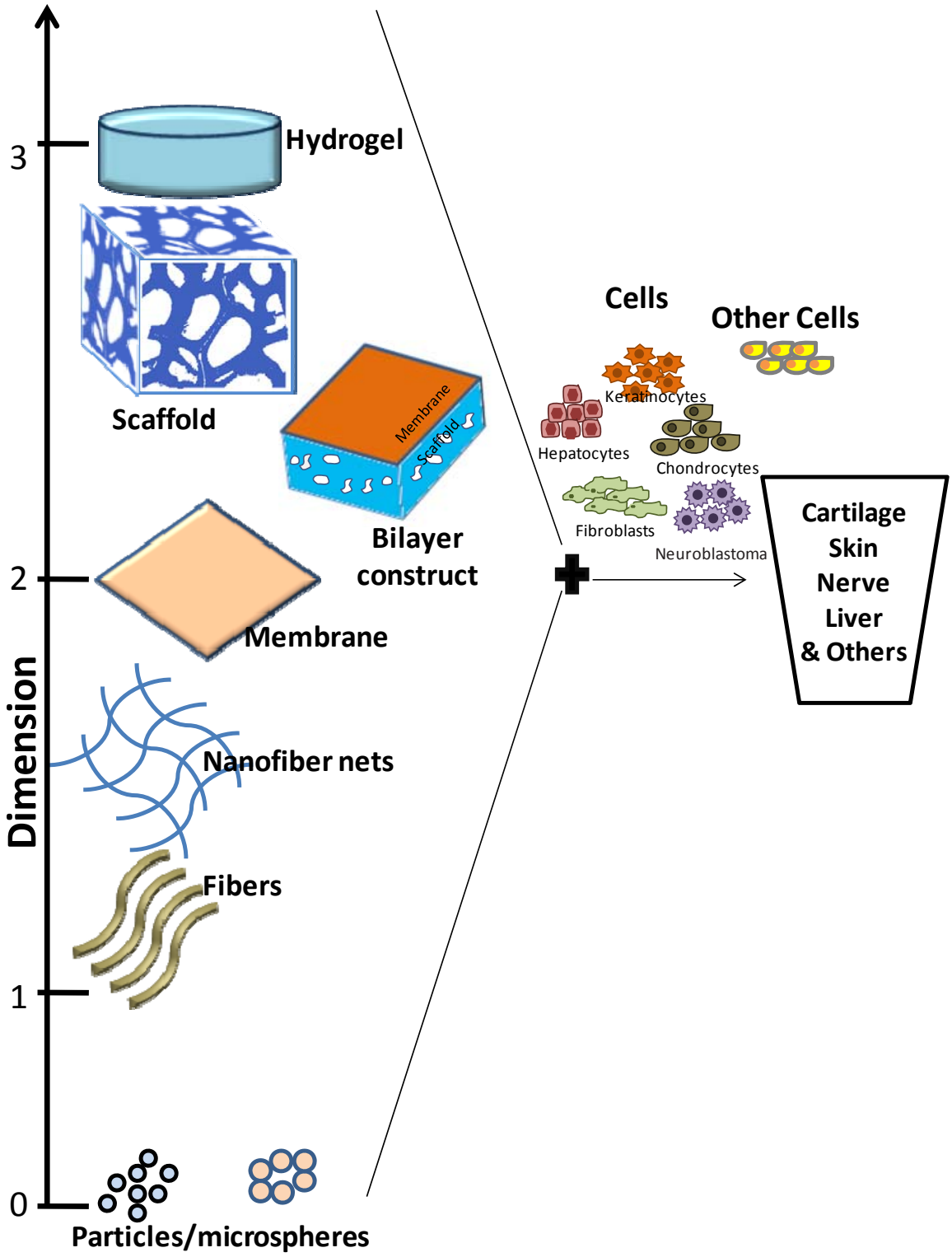

Figure 1. Scheme of different polymeric architectures proposed for soft tissue repair.

2.1. *Chitin/chitosan*

Chitin is the second most abundant natural polymer in the nature, found in the shell of crustacean, cuticles of insects, and cell walls of fungi[18,58,59]. Chitin has bacteriostatic and fungiostatic activities, which are favorable for promoting rapid dermal regeneration and accelerating wound healing[18]. However, applications of chitin have been limited due to its insolubility in water and in most common organic solvents[18]. Nevertheless, chitin is soluble in hexafluoroisopropanol, hexafluoroacetone and dimethylacetamide containing 5% lithium chloride[18]. Some types of chitin-based materials (filaments, granules, sponges) were adapted for uses in wound dressing applications[60,61]. Also, the potential application of flexible chitin films has been proposed as occlusive, semi-permeable film wound dressing[62,63]. Additionally, chitin derivatives (*e.g.* carboxymethyl chitin, water-soluble chitin, dibutyl chitin) with better solubility have been found to be particularly effective as wound healing accelerator and as wound dressings[64-66]. Lee *et al* [67]designed a chitin/collagen hybrid scaffold prepared by coating the collagen solution into the macropores of the chitin scaffold to improve the attachment of the fibroblast on the scaffold. Hirano *et al* [68] developed a biodegradable dressing material made of wet spun chitin-glycosaminoglycans fibers. Softness and easy handling of these fibers could be useful to heal epidermal tissue injuries.

Chitosan is a polysaccharide obtained by alkaline deacetylation of chitin[18,58]. This polymer has interesting properties including biodegradability, bioadhesiveness, bacteriostatic, fungistatic and haemostatic activities[18]. Besides, its chemical structure allow introducing desired properties into chitosan by its chemical modification or its conjugation with other polymers[19,58,69]. Particularly, chitosan-based matrices have been extensively investigated in wound healing since chitosan promote rapid dermal regeneration and accelerated wound healing[19,70]. A wide range of research works[71-82] are based on the aspects associated to preparation, properties and characterization of films[70-78] and bilayer membranes[79-82] as wound dressings. Some bilayer chitosan wound dressings[80,81] are composed of a dense

top-layer that protects the wound and serves as an artificial epidermis, and an underlying porous sponge-like layer for the drainage of wound exudates (see Figure 2).

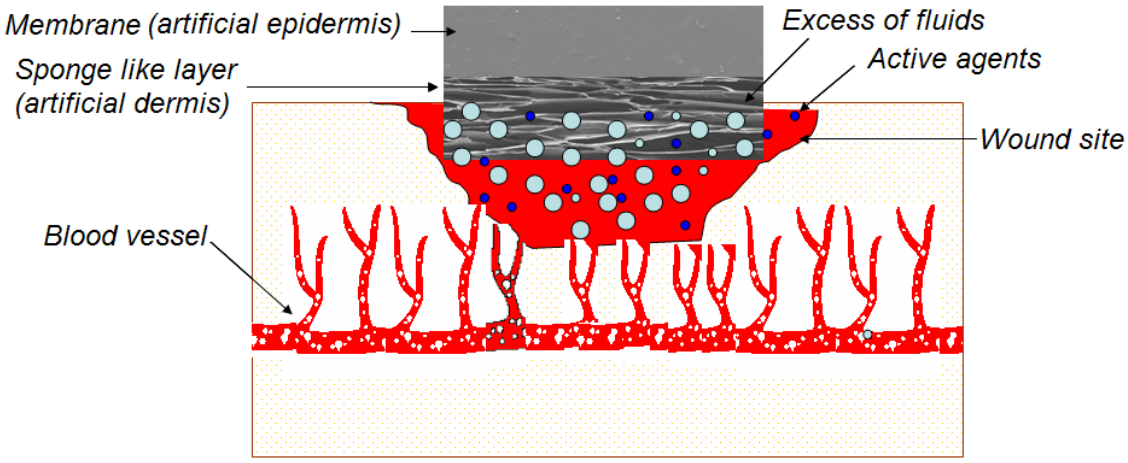

Figure 2. Example of a bilayer wound dressing. Adapted from[80,81].

On the other hand, systems based on the association of the cationic character of chitosan in acidic conditions with negatively charged molecules (*e.g.* proteins, anionic polysaccharides and nucleic acids) are proposed to develop dermal substitutes. Table 1 summarizes natural origin polymers that are currently conjugated to chitosan and their proposed applications for soft tissue repair.

Many studies[83-85] investigated different aspects of the interactions between chitosan and collagen. They have shown that chitosan can modify the properties of collagen when biological or mechanical properties are considered. Interesting strategies suggested the use of collagen/chitosan matrices in the form of scaffolds[45] or bilayers[86] (scaffold/membrane) as dermal equivalent. The bilayer dermal equivalent has the ability to regenerate a damaged dermis and to support the angiogenesis of the regenerated dermis[86]. Ma and co-workers[45] produced collagen/chitosan (CS) scaffolds by cross-linking with glutaraldehyde and freeze-drying to improve the biostability of CS scaffold. Amino groups of chitosan acted as binding sites to increase the glutaraldehyde cross-linking efficiency whereas

collagen should facilitate the attachment and proliferation of skin fibroblasts. In other strategy[87], an endothelialized skin equivalent (ESE) was designed with chitosan/collagen/glycosaminoglycans scaffolds. These scaffolds were seeded with co-cultures of human umbilical vein endothelial cells (HUVECs), fibroblasts and keratinocytes. This ESE promoted spontaneous formation of capillary-like structures in a highly differentiated extracellular matrix.

Polyelectrolyte complexes (PEC) can be formed by chitosan and gelatin in different gel states depending on their concentrations, ionic strength and the pH of the solution[88,89]. This PEC formation involves the formation of hydrogen bonding between amino groups in chitosan with carboxyl groups in gelatin[89,90]. Promising features of this PEC is its excellent ability to be processed into sponges[91] and both monolayer and bilayer scaffolds for use in human skin fibroblast and keratinocyte transplantation and skin regeneration[88,92]. The chitosan-gelatin sponge wound dressing was shown to be reliable, have good antibacterial property and a healing effect superior to vaseline sterile gauze[91]. In a different approach[93], chitosan-gelatin microspheres loaded with basic fibroblast growth factor (bFGF) were incorporated into chitosan-gelatin scaffolds, where the sustained release of bFGF increased the production of laminin by human fibroblasts, which may be helpful to angiogenesis in skin regeneration. Further studies[92,94] included hyaluronic acid (HA) into chitosan/gelatin PEC system to enhance its water uptake ability, flexibility and biocompatibility. Chitosan-gelatin-hyaluronic acid scaffolds showed higher stability in terms of shape and volume during cell culture with co-cultures of fibroblasts and keratinocytes[94]. In addition, it was observed that only the concentrations of HA ranging between 0.01- 0.1% could promote the cell adhesion, migration and proliferation[95]. Other polyelectrolyte complex (PEC) systems are formed with the addition of sodium alginate[96] or heparin[97,98] to chitosan solutions. Macroporous chitosan-alginate PEC membranes were used for sustained release of silver sulfadiazine in a controlled way[99], while *in vivo* studies in a rat model suggested that chitosan-alginate PEC membranes has a accelerated healing of incisional wounds[96]. Additionally, ease of handling, cost effectiveness, biodegradability,

stability upon storage and high batch-to-batch reproducibility are advantages of these PECs as wound dressings. Some researchers[97,98,100] suggested that heparin-chitosan complex stimulates re-epithelialization of full-thickness wound in human skin, in a heparin dose dependent effect[97]. Moreover, the mixture of heparin and chitosan inhibited the inflammatory reaction on early extension of deep partial thickness burns[100]. Recent investigations have focused on the interactions between chitosan and silk fibroin[101], soy protein[102-104], keratin[105] and their resulting properties for skin applications. Variations of chitosan content in the chitosan/silk fibroin blended films influenced the structure, morphology and properties of the films, whereas 40-50% chitosan content showed very high oxygen permeability[101]. In our group, Silva and co-workers[102,103] explored the blending of chitosan with soy protein isolate, the major component of the soybean[31], in the development of a series of blended membranes. These membranes have higher surface roughness and surface energy when compared to their individual components. Nevertheless, chitosan/soy protein (CS) blended systems are not completely miscible and *in situ* chemical cross-linking with glutaraldehyde solutions was used to enhance the interaction degree between chitosan and soy protein and, thus overcome the immiscibility drawback. The addition of soy protein associated to the cross-linking have a positive effect on enhancing fibroblast-like cell attachment on cross-liked CS membranes in comparison with chitosan membranes (see Figure 3). Later on, CS membranes in direct contact with human polymorphonuclear neutrophils (PMNs*)* were not able to stimulat*e* PMN*s in vitro* neither for the release of lysozyme or for the production of reactive oxygen species (ROS) found in the "respiratory burst"[106]. Recently, *in vivo* studies[104] demonstrated that the CS membranes accelerated skin wound healing in rats after two weeks of dressing. All these findings supporting the suitability of the CS membranes as wound dressing materials.

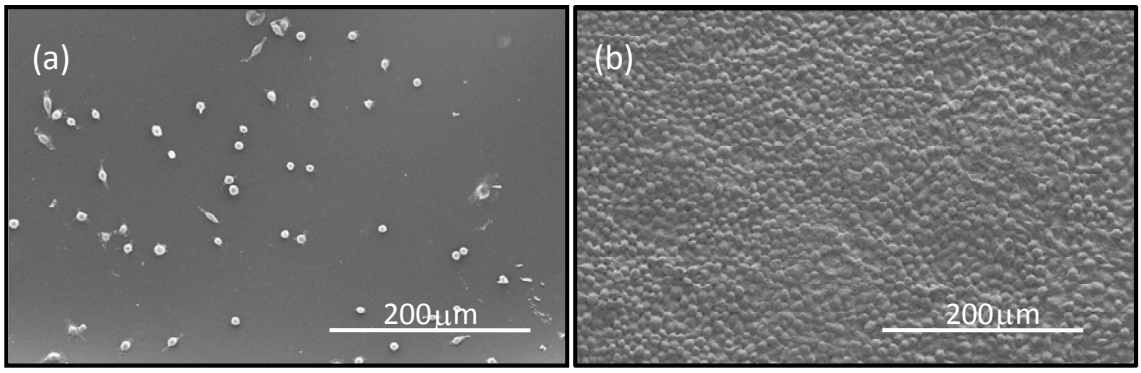

Figure 3. SEM micrographs of L929 cells cultured on chitosan membrane (a) and chitosan/soy protein blended membrane cross-linked with 0.1 M Ga (b). Culture time: 3 days. [Unpublished results].

Particularly for cartilage tissue engineering applications, chitosan seems to be a good candidate given that its structure and characteristics resemble those of glycosaminoglycan (GAGs), which are well known constituents of cartilage extracellular matrix, and it has also a critical role in supporting chondrogenesis both *in vitro* and *in vivo*[21]*.* Chitosan scaffolds with various geometries can be produced by freezing and lyophilising chitosan solutions in appropriate moulds[20,21,55,107] aimed at tissue regeneration. Silva *et al* [107] proposed to prepare cross-linked chitosan/soy protein scaffolds by means of combining a sol-gel process with the freeze-drying for cartilage TE applications. In another approach, Correlo *et al* [108-110] developed scaffolds made from blends of chitosan and biodegradable synthetic aliphatic polyesters using melt-based processing methodologies combined with salt leaching. These scaffolds have been reported to exhibit a wide range of porosities, pore morphologies and adequate mechanical properties for bone and cartilage applications. Other studies[111] demonstrated that through blending of silk fibroin and chitosan, followed by genipin cross-linking, chondrocytes-like cell adhesion, viability, proliferation and matrix production could be improved as compared with chitosan sponges. Medrado *et al* [112] suggested that the association of chitosan-gelatin matrix and chondrogenic media supplemented with dexamethasone may stimulate the proliferation of mesenchymal stem cells. To achieve cartilage tissue regeneration, some researchers developed multi-component scaffolds, whose

composition to mimic the natural cartilage matrix. Collagen-chitosan-chondroitin sulphate scaffolds were used to culture rabbit articular chondrocytes, where the findings evidenced that these scaffolds have good cell growth and proliferation, and facilitated the formation of articular cartilaginous tissue formation *in vitro* and *in vivo*[113]. Hsu *et al*[114] indicated the potential of chitosan-alginate-hyaluronan scaffolds modified RGD peptides for cartilage regeneration. Chondrocytes seeded scaffolds implanted into rabbit knee defects, promoted the partial repair after 1 month. In another approach[115], porous collagen/chitosan/GAG loaded with transforming growth factor-β1 (TGF-β1) acted as controlled released systems. These scaffolds provided the controlled release of TGF-β1 and promoted cartilage regeneration.

Apart the promising results of chitosan-based matrices in skin and cartilage regeneration, researchers suggested that collagen/chitosan (CS) matrices[116] can create an appropriate environment for the regeneration of liver cells. However, the low mechanical strength and poor blood compatibility of these natural polymers have limited their further use in liver TE. Further studies[117] included an ammonia treatment on chitosan/collagen systems to create interpenetrating networks, which showed a high porosity, high mechanical strength and good hepatocytes adhesion and growth. Additionally, the collagen/chitosan/heparin matrix showed superior blood compatibility[118]. On the other hand, porous sponges composed by association of galactosylated chitosan (GC) with alginate had a viability, spheroid formation and functions of hepatocytes higher than those obtained with alginate alone[119,120]. Another approach in liver TE focuses on design of the complex 3D architectures with predefined internal vascular channels to favour angiogenesis[121,122]. Recently[121], a novel 3D chitosan/gelatin scaffold with predefined multilevel internal morphologies (see Figure 4) and porosities between 90.6 % and 98.1%, were fabricated combining solid freeform fabrication (SFF), microreplication and lyophilization techniques.

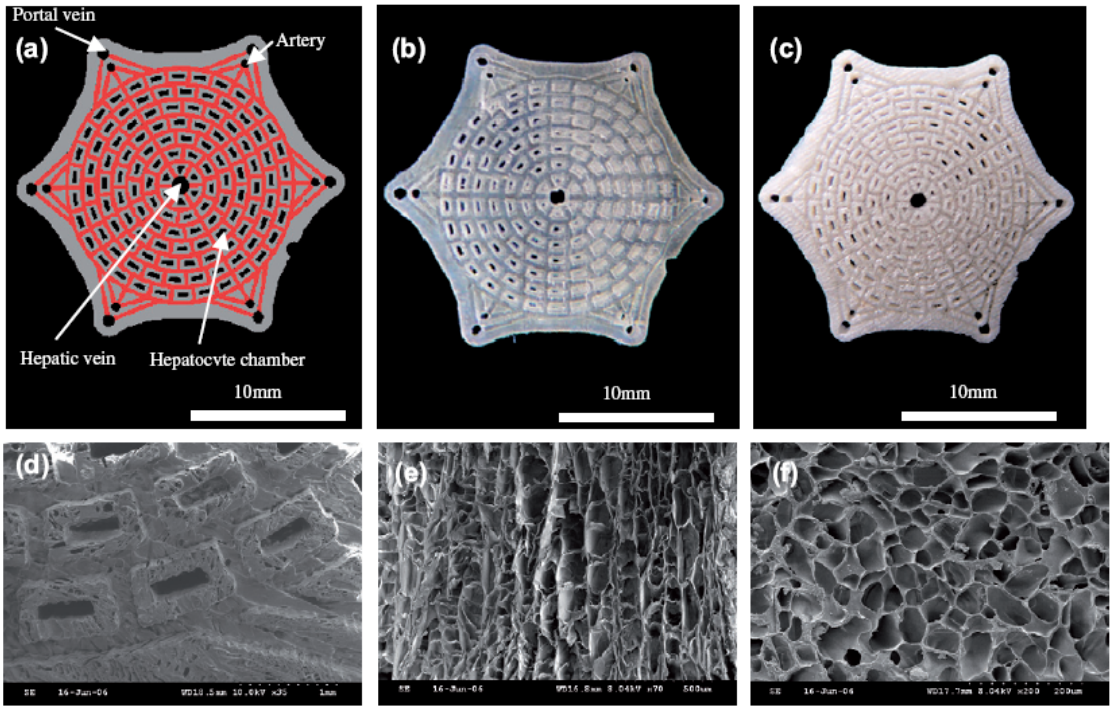

Figure 4. Chitosan/gelatin scaffold with specific external shape and predefined internal morphology: (a) CAD model, (b) resin mould fabricated using SL technique, (c) chitosan/gelatin scaffold, (d) SEM of the predefined internal morphology, (e) microstructures segmented longitudinally, and (f) microstructures segmented transversely [121].

With respect to nerve regeneration, studies have focused on nerve guidance conduits made from chitosan and their combinations with proteins. Chitosan modified by blending with proteins (collagen, albumin and gelatin) or poly-L-lysine [123,124] had significantly improvement of the nerve cell affinity when compared to chitosan, as indicated by increased attachment, differentiation, and growth of nerve cells. Besides, rat PC12 cells cultured on the chitosan/gelatin films with 60wt% gelatin differentiated more rapidly and extended longer neuritis than on chitosan film[124]. Regarding chitosan applications to tendons and ligaments TE, fiber-based scaffolds were developed through combination of chitosan with alginate[125] and hyaluronan[42,126]. Funakoski *et al*[42] revealed that hyaluronan hybridization with chitosan fibers enhanced fiber mechanical properties and *in vitro* biological effects on the cultured fibroblasts.

Table 1. Chitosan-based matrices proposed for applications in soft tissue repair. Targeted tissues and organs include cartilage, skin, liver, nerve, tendons and ligaments. Compiled from references [42,43,86-88,92,94,96,97-102,104,105,107,111,113-122,124-151].

Composition	Processing Methodology	Matrix Type	Active Substance	Potential TE application	Cell type (source)/line	Animal model	Ref.
Chitosan-alginate	Solvent casting	Membranes	_	Wound dressing	Fibroblasts like cells	Sprague Dawley rats	96
	Interpolyelectrolyte complex method	Macroporous Membranes	AgSD	Wound dressing	_	_	99
	Freeze-drying	Scaffolds	_	Cartilage	Chondrocyte-like cells	_	127
	Coagulation bath Spinning	Fibers	_	Cartilage	Chondrocytes (rabbit)	_	139
	Wet spinning	Fibers	_	Tendons and ligaments	Fibroblast (rabbit)	_	125
	Spinning mandrel technology	Hydrogels	_	Nerve conduit	_	_	128
Galactosylated chitosan -alginate	Freeze-drying Cross-linking ($CaCl_2$)	Sponges	_	Liver	Hepatocytes (mouse)	_	119,120
	Freeze-drying Cross-linking ($CaCl_2$)	Scaffolds	_	Bioartificial liver	Co-culture of Hepatocytes (mice), NIH 3T3 Fibroblasts	_	129
Galactosylated chitosan –alginate-heparin	Freeze-drying Cross-linking ($CaCl_2$)	Scaffolds	_	Bioartificial liver	Hepatocytes (mice) NIH 3T3 Fibroblasts	_	130

Composition	Processing Methodology	Matrix Type	Active Substance	Potential TE application	Cell type (source) line	Animal model	Ref.
Chitosan-alginate-hyaluronan	Solvent casting Freeze-drying	Membranes and scaffolds	_	Cartilage	Chondrocytes	_	[114]
Chitosan-bacterial cellulose	Biosynthesis	Hydrogels	_	Wound dressing	_	_	[131]
Chitosan-chondroitin-6-sulphate-dermatan	Freeze-drying cross linking	Scaffolds	_	Cartilage	Chondrocytes (Winstar rats)	_	[132]
Chitosan-collagen	Freeze-gelation method Cross-linking (EDC)	Scaffolds	_	Skin	Embryonic fibroblasts (human)	_	[133]
	Quenching ethanol extraction	Porous membranes	_	Dermal regeneration template	_	_	[134]
	Freeze-drying DHT Cross-linking (GA)	Scaffolds	_	Dermal equivalent	Human fibroblast	Rabbit ear	[135]
	Solvent casting	Films	HN-300	Antimicrobial wound dressing	Fibroblasts-like cells (mouse)	_	[136]
	Solvent casting Cross-linking (EDC)	Films	_	Artificial livers	Hepatocytes (rats)	_	[116]
	Freeze-drying Ammonia treatment	Scaffolds	_	Liver	Hepatocytes (rats)	_	[117]
Carboxymethylchitosan-collagen	Freeze-drying Cross-linking (EDC)	Porous matrices	_	Wound dressing	Fibroblasts (human)	Wistar rats	[137]

Composition	Processing Methodoloy	Matrix Type	Active substance	Potential TE application	Cell type (source) line	Animal model	Ref.
Chitosan-collagen-chondroitin sulphate	Emulsion Freeze-drying Cross-linking (EDC)	Microspheres encapsulated in scaffolds	TGF-β1	Cartilage	Chondrocytes (rabbits)	_	115
	Freeze-drying Cross linking (EDC)	Scaffolds	-	Cartilage	Chondrocytes (rabbits)	_	43
	Freeze-drying Cross-linking (EDC)	Scaffolds	_	Cartilage	Chondrocytes (rabbits)	Athymic male mice	113
	Freeze-drying	Sponges	-	Skin equivalent	Co-cultures of keratinocytes, fibroblasts, and HUVEC (human) foreskin and adult dermal fibroblast	_	87
	Freeze-drying	Scaffolds	-	Dermal substitute		Rats	138
Chitosan-collagen-heparin	Freeze-drying Solvent casting Ammonia treatment	Scaffolds Membranes	_	Liver	Hepatocytes (rats)	_	118
	Freeze-drying Cross-linking (EDC)	Scaffolds	_	Liver	Hepatocytes (rats)	_	140
Chitosan-collagen-hyaluronan	Freeze-drying Cross-linking (EDC)	Scaffolds	_	Cartilage	Chondrocytes (rabbits)	_	141
Chitosan-collagen-PEO	Electrospinning Cross-linking (GA vapour)	Nanofibres membranes	_	Wound dressing	Fibroblasts-like cells	SD rats	142

Composition	Processing methodology	Matrix Type	Active substance	Potential TE application	Cell type (source) line	Animal model	Ref.
Chitosan-collagen-silicone	Freeze drying cross-linking (GA)	Bilayers (scaffold/ membrane)	_	Dermal equivalent	Fibroblasts (human)	_	[143]
	Freeze-drying Cross-linking (GA)	Bilayers (scaffold/ membrane)	_	Dermal equivalent	Fibroblasts (human)	Pigs	[86]
Chitosan-gelatin	Freeze-drying Cross-linking (GA)	Scaffolds	_	Artificial bilayer skin *in vitro*	Co-cultures of keratinocytes and fibroblasts	_	[88]
	Freeze-drying	Scaffolds	plasmid DNA	Cartilage	Chondrocytes (rabbit)	_	[144]
	Solvent casting Cross-linking (EDC)	Films	Dexamethasone	Cartilage	Mesenchymal stem (bone marrow of rabbits)	_	[145]
	Freeze-drying	Scaffolds	_	Cartilage	Autologous chondrocytes (pigs)	Pigs	[146]
	Solvent casting	Films	_	Nerve regeneration	Rat PC12 cells	_	[124]
	_	Gels	_	Liver	_	Rats	[147]
	Freeze-drying, SFF Microreplication Cross-linking (GA)	Scaffolds	_	Liver	Hepatocytes (rats)	_	[121]

Composition	Processing methodology	Matrix Type	Active substance	Potential TE application	Cell type (source) line	Animal model	Ref.
Chitosan-gelatin	3D cell assembly technique Gelation Cross-linking (TPP and GA)	3D structures	_	Bioartificial liver	Hepatocytes (rats)	_	122
	Solvent casting Cross-linking (G)	Membranes	_	Nerve repair	Fibroblasts-like cells Neuroblastoma-like cells	_	148
Chitosan-gelatin-hyaluronan	Freeze-drying Cross-linking (EDC)	Scaffolds	_	Artificial skin	Co-cultures of keratinocytes and fibroblasts	_	92,94
	Freeze-drying Cross-linking (EDC)	Scaffolds	bFGF	Cartilage	Chondrocytes (rabbits)	_	149
Chitosan-heparin	Solvent casting	Membranes	_	Wound healing	*In vitro* model	-	97
	-	Powder	_	Wound healing	-	Wistar rats	100
	-	Powder ointment	_	Wound healing	_	Rats	98
Chitosan-hyaluronan	Solvent casting	Films	_	Wound dressing	Fibroblasts (human)	SD mice	150
	Wet spinning	Fibres	_	Cartilage	Chondrocytes (rabbits)	_	151
	Wet spinning	Fiber scaffolds	_	Ligament	Fibroblasts (rabbits)	_	42

Composition	Processing methodology	Matrix Type	Active substance	Potential TE application	Cell type (source) line	Animal model	Ref.
Chitosan-hyaluronan	Wet spinning	Fiber scaffolds	_	Ligament and tendons	Fibroblasts (rabbits)	Wistar-King rats	126
Chitosan-keratin	Solvent casting	Films	_	Wound dressing	Fibroblasts- like cells	_	105
Chitosan-silk fibroin	Solvent casting	Membranes	_	Wound dressing	_	_	101
	Cross-linking (G) Freeze-drying	Sponges	_	Cartilage	Chondrocytes-like cells	_	111
Chitosan-soy protein	Solvent casting Cross-linking (GA)	Membranes	_	Wound dressing	Fibroblasts-like cells	_	102
	Solvent casting	Membranes	_	Wound dressing	_	Sprague Dawley rats	104
	Sol-gel process Freeze-drying	Scaffolds	_	Cartilage	_	-	107

Abbreviatures. AgSD: silver sulfadiazine; bFGF: basic fibroblast growth factor ; $CaCl_2$: calcium chloride; EDC: (*N*-(3-dimethylaminopropyl)-*N*ethylcarbodiimide; DHT: dehydrothermal treatment; GA: glutaraldehyde ; PEO: polyethylene oxide ; TPP: tripolyphosphate; 3D structures: three dimensional structures; TE: Tissue Engineering; SFF : solid free form : W/O: Water-in- oil emulsion; O/W emulsion: Oil/water emulsion; G- genipin.

2.2. ***Glycosaminoglycans (hyaluronic acid and chondroitin-sulphate)***

Glycosaminoglycans (GAGs), including hyaluronan (HA) and chondroitin sulphate (CS), are amino sugar containing polysaccharides present in the extracellular matrix (ECM) of all vertebrates[152]. Hyaluronic acid or hyaluronan (HA), is a water-soluble polysaccharide that is widely distributed throughout the ECM of all connective tissues in human and other animals[24]. HA has a high capacity for water sorption and retention, and influences several cellular functions such as adhesion, migration and proliferation[24]. Based on its positive biological effects on cell behaviour *in vitro*, HA have participated in many polymeric systems for different TE applications. Examples are summarized in Table 2. In skin application, HA has been mixed mainly with collagen and gelatin (see examples in Table 2). Collagen/HA based systems has a tendency to form polyionic complexes (PICs), in aqueous solution due to their electrostatic charges. These PICs are dense precipitates that can interfere with the process of forming sponge-like scaffolds[153,154]. However, the presence of 0.4M NaCl in the preparation of these scaffolds could suppress the PIC formation due to screening effect of sodium and chloride ions[154]. Matrices formed by collagen and HA have shown good biological response in tissue environment, low local irritability and ingrowth of autologous tissue[155,156]. In most studies[153-159], the collagen/HA mixtures were cross-linked to stabilize the structure of the materials. Park *et al* [159]showed that the dermis treated with EDC–cross linked-collagen-HA matrix was thicker than the control (porous polyurethane matrix), and epithelial regeneration was accelerated *in vivo*. Besides, the presence of growth factors into collagen-hyaluronan matrices significantly enhanced the wound healing[160]. Kubo and Kuroyanagi *et al* [158,161,162] developed a series of studies on hyluronic acid/collagen bilayer sponges to be used as dermal substitute. The collagen layer was essential for attachment and proliferation of fibroblasts on the bilayer sponge while hyaluronan layer, facilitating early formation of granulation tissue in rats and maintained the moisture environment on the wound surface. Another related works[163,164] chondroitin sulphate and collagen were used to produce a more

porous structure in the bilayer artificial skin invented by Burke and Yannas, actually called Integra® (Integra Life Sciences Holding Corporation, New Jersey, USA). Integra® is widely used for coverage of excised burn wounds. The collagen-chondroitin sulphate dermal layer served as biodegradable template that induces organized regeneration of dermal tissue by the body and the infiltration by fibroblasts and other cells from the wound bed. Similarly, bi-layered gelatin-chondroitin sulphate-HA constructs with different pore sizes on either side were prepared to mimic skin composition and to create an appropriate microenvironment for cell growth, differentiation and migration[165]. On the other hand, studies indicated that the combination of chondroitin sulphate with collagen in the form of scaffolds had a positive effect on chondrocytes phenotype[166] and supported chondrogenic differentiation of adult rat stem cells[167]. Novel strategies to mimic the natural cartilage matrix are also based on the development of multi-component scaffolds[41,168,169]. For instance, chondrocytes seeded on gelatin/chondroitin sulphate/hyaluronan scaffolds were evenly distributed in matrices, secreted new ECM, retained their phenotype, and secreted type II collagen[41]. Moreover, TGF-β1 was immobilized onto the surface of gelatin/hyaluronic acid/chondroitin-6-sulphate (GHC6S) to suppress the undesired differentiation during the cartilage growth *in vitro*[170]. However, the authors described also that these matrices presented problems on cell seeding and cell distribution [171]. To provide better mechanical strength, cell distribution and seeding, the GHC6S sponges were transformed in small particles and added to fibrin glue[171]. In other approach[172], the addition of selected growth factors to medium for an implantable collagen-glycosaminoglycan (CG) scaffold may enhance ligament cell behaviour within CG scaffold. The findings suggested that this approach may facilitate the ligament healing in the gap between the ruptured ends of the human anterior cruciate ligament (ACL).

Regarding to nerve regeneration, a collagen-glycosaminoglycans matrix[173] was synthesized with an average pore diameter (35 mm) and orientation of pore channel axes. Nerves regenerated through tubes fabricated from large-pore

collagen and filled with the CG matrix had higher number of axons per nerve. The presence of CG matrix in the tubes provided a specific surface for the attachment and migration of cells.

Table 2. Glycosaminoglycans-based matrices proposed for applications in soft tissue repair. Targeted tissues and organs include cartilage, skin, liver, nerve, and ligaments. Compiled from references [41, 44,152-156,158-162,165,167-170,172-190].

Composition	Processing Methodology	Matrix Type	Active Substance	Potential TE Application	Cell type (source)/line	Animal model	Ref.
Chondroitin-sulphate-collagen	Freeze-drying Cross-linking (EDC)	Scaffolds	_	Skin substitute	Co-cultures of keratinocytes and fibroblasts (human)	_	174
	Freeze-drying Cross-linking (HT)	Scaffolds	TGF-01, PDGF-AB, EGF, or FGF-2*	Ligaments	Explants (human ACL)	_	172
	Freeze-drying Cross-linking (UV)	Scaffolds	_	Cartilage	Chondrocytes (dogs)	_	175
	Freeze-drying Cross-linking (HT)	Scaffolds	_	Cartilage	_	Dogs	176
	Freeze-drying Cross-linking (EDC, NHS)	Scaffolds	FGF-2, IGF-1	Cartilage	Chondrocytes (dogs)	_	177
	Freeze-drying Cross-linking (EDC, HT,GA, UV)	Scaffolds	_	Cartilage	Chondrocytes (dogs)	_	178
	Freeze-drying	Scaffolds	_	Cartilage/bone	MSCs	_	167
	Freeze-drying	Porous matrices	_	Nerve regeneration	_	Rats	173,179

Composition	Processing Methodology	Matrix Type	Active substance	Potential TE Application	Cell type (source)/line	Animal model	Ref.
Chondroitin-sulphate-collagen-chitosan	Freeze-drying	Scaffolds	_	Skin equivalent model	Keratinocytes Fibroblasts HUVEC	_	[180]
Chondroitin-sulphate-collagen-heparin	Solvent casting Cross-linking (DAH)	Films	_	Liver	Hepatocytes (rats)	_	[181]
Chondroitin sulphate -gelatin-hyaluronan	Emulsion Freeze-drying Cross-linking (EDC)	Scaffolds containing microspheres	TGF-β1	Cartilage	Mesenchymal stem cells (rabbits)	Rabbits	[169]
	Freeze-drying Cross-linking (EDC)	Scaffolds	_	Cartilage	Chondrocytes (porcine knee joints)	Pigs	[41,168]
	Solvent casting Freeze drying cross-linking (EDC)	Porous-bilayered membrane	_	Skin	Keratinocytes Fibroblasts (human)	_	[182,183]
	Freeze drying cross-linking (EDC)	Bilayer scaffolds	_	Skin	Keratinocytes Fibroblasts (human)	Rats	[165]
Chondroitin-hyaluronan-gelatin-PLGA	Low temperature-deposition Cross-linking (EDC) Freeze-drying	Scaffolds	_	Cartilage	Mesenchymal stem cells	Rabbits	[184]
Hyaluronan-chitosan	Freeze-drying	Sponges	AgSD	Wound dressing	_	Wistar rats	[185]

Composition	Processing Methodology	Matrix Type	Active substance	Potential TE Application	Cell type (source)/line	Animal model	Ref.
Hyluronan-chondroitin sulphate	Solvent casting Cross-linking (PEG, propiondialdehyde)	Films	_	Bio-interactive dressing	_	Mouse	[152]
Hyaluronan-collagen	Freeze-drying cross-linking (EDC)	Porous matrices	_	Dermal tissue regeneration	Fibroblasts (human)	Guinea pig	[159]
	Freeze drying cross-linking (EDC)	Porous matrices	bFGF, PDGF-BB, tobramycin, ciprofloxacin	Skin substitute	Fibroblasts (human)	Male Dunking-Hartley guinea pigs	[160]
	Freeze-drying Cross-linking (EDC)	Scaffolds	_	Cartilage	Chondrocytes (dogs)	_	[153]
	Cross-linking (EDC)	Composite matrices	_	Cartilage	_	_	[154]
	Solvent casting Cross-linking (HMDIC)	Membranes	_	Dermal substitutes	_	Wistar rats and IPR mice	[155,156]
	Freeze-drying Cross-linking (Ethylene glycol**)	Sponges	VEGF Fibronectin	Dermal substitutes	Fibroblasts	Sprague-Dawley rats	[158,161,162]
	Image-based design and SFF method	Hydrogels	_	Cartilage	Chondrocytes (pigs)	Mice	[44]

Composition	Processing Methodology	Matrix Type	Active substance	Potential TE Application	Cell line (source)/line	Animal model	Ref.
Hyaluronan-gelatin	Freeze-drying Cross-linking (EDC)	Sponges	AgSD	Wound dressing	_	Wistar rats	186
	Freeze drying Cross-linking (EDC)	Sponges	EGF AgSD	Wound dressing	_	Wistar rats	187
	Salt leaching	Sponges	TGF-β1	Cartilage/bone	Bone marrow (rabbit)	_	188
Hyaluronan-gelatin-beta glucan	Freeze-drying Cross-linking (EDC)	Scaffolds	_	Artificial dermis	_	_	189
Hyaluronan-gelatin-chondroitin-6-sulphate	Freeze-drying cross-linking (EDC)	Scaffolds	TGF-β1	Cartilage	Chondrocytes (porcine knee joints)	_	170
Oxidized chondroitin sulphate-gelatin	Periodate oxidation	Hydrogels	_	Wound dressings	Fibroblasts- like cells	_	190

Abbreviatures: AgSD: silver sulfadiazine; HUVEC: human umbilical vein endothelial cells; Hep-2: human larynx carcinoma cells; PLGA: poly-(lactic-co-glycolic acid); TGF-β1: transforming growth factor- β1; VEGF: vascular endothelial growth factor; HMDIC:hexamethylenediisocyanate; EDC: 1-Ethyl-3-[3-dimethylaminopropyl]carbodiimide; SFF: solid free-form fabrication method; HT: hydrothermal treatment. TGF-01, PDGF-AB, EGF, or FGF-2*: The culture medium was supplemented with these growth factors; human ACL- human anterior cruciate ligament; MSCs: mesenchymal stem cells; DAH: 1,6-diaminohexane; Ethylene glycol*: Ethylene glycol diglycidylether.; NHS: *N*-hydroxysuccinimide.; UV – ultraviolet.; FGF-2: fibroblast growth factor; IGF-1: insulin-like growth factor; PEG : poly(ethylene glycol).

2.3. ***Alginate***

Alginate is a water-soluble at room temperature and in the presence of certain divalent cations, such as calcium, barium, and strontium, it forms stable hydrogels[13,38]. Although alginate is considered a non- or slowly-biodegradable polymer (there are no known enzymes in the human body for alginate), its high water solubility enables efficient removal (especially when molecular weight is less than 50 kDa) once the hydrogel is dissolved. The ease and mild conditions of dissolving alginate hydrogels enable its use in 3-D cell cultivation *in vitro.* Alginate has been widely used[191-193] in the wound management industry for the production of absorbent products such as gels, foams and fibrous dressings that are used to cover wounds. The shape that the alginate dressings will retain is dependent on the relative amount of each unit (mannuronic acid and guloronic acid) in polymer. Those rich in mannuronic acid can be washed off the wound easily with saline, but those high in guluronic acid tend to retain their basic structure, and should be remove from the wound bed in one piece[191,194]. Examples of alginate-based matrices are shown in Table 3. For instance, silk fibroin/alginate sponges significantly increased the size of re-epithelialization via rapid proliferation of epithelial cells when compared to gauze dressings[195]. Clinical studies[196] indicated the efficacy and safety of a collagen-alginate topical wound dressing (FIBRACOL PLUS Dressing, Johnson & Johnson Gateway®) in the treatment of diabetic foot ulcers. In this commercial dressing, the combination of collagen (90%) and alginate (10%) provides the versatility needs for a variety of wound types. It maintains a moist wound environment, which is conducive to granulation tissue formation and epithelialization that enables healing to proceed optimally. In cartilage studies[197], alginate-hyaluronan mixtures were prepared in form of beads in order to combine the alginate gel forming ability with the biological and rheological properties of hyaluronan. Moreover, encapsulated articular chondrocytes within alginate beads containing fibrin showed good cellular growth and remained stable for over 60 days[198]. It was also observed that the hydrophilic nature of alginate scaffold enable

the efficient seeding of hepatocytes into the scaffolds, but this matrix was incapable of hepatocyte anchorage[199]. To circumvent these limitations, alginate scaffolds were conjugated with galactosylated chitosan[129] and, also with heparin[130] for enhance liver-specific functions in the design of bioartificial liver devices. Recently[200], a 3D structure composed of a calcium gelatin/alginate hydrogel was produced using cell controlled assemblying technology. The gelatin/alginate hydrogel act as an extracellular matrix (ECM) able to maintain the functions of the implanted cells, and plays an important role in supporting the whole structure.

Table 3. Alginate-based matrices proposed for applications in soft tissue repair. Targeted tissues and organs include cartilage, skin and liver.

Compiled from references [195,198,200-207].

Composition	Processing Methodology	Matrix Type	Active Substance	Potential TE Application	Cell type (source)/line	Animal model	Ref.
Alginate-laminin derived peptide Alginate- elastin derived peptide	Peptide synthesis Cross-linking (EDC)	Gels	_	Wound dressing	Fibroblasts (human)	Rabbit ear skin	201
Alginate-gelatin	Freeze-drying Cross-linking (EDC)	Sponges	AgSD Gentamicin sulphate	Wound dressing	_	Wistar rats	202,203
	Spinning Coagulation	Fibers	_	Wound dressing	_	_	204
	Cell assembly Cross-linking ($CaCl_2$; GA)	Gels /3D structure	_	Liver	Hepatocytes (rats)	_	200
Alginate-hyaluronan	-	Beads	-	Cartilage	Chondrocytes(pigs)	-	198
	Freeze-drying	Sponges	-	Cartilage	Chondrocytes (Winstar rats)	-	205
Alginate-silk fibroin	Freeze-drying	Sponges	_	Wound dressing	_	_	206
	Freeze-drying	Sponges	_	Wound dressing	_	Male Sprague Dawley rats	195
Oxidized alginate-gelatin	Periodate oxidation	Hydrogels	_	Wound dressing	_	Rat model	207

Abbreviatures: AgSD: silver sulfadiazine. EDC: 1-Ethyl-3-[3-dimethylaminopropyl]carbodiimide;$CaCl_2$:calcium chloride; GA: glutaraldehyde;

2.4. ***Cellulose***

Cellulose is the most abundant organic polymer in the world. It is insoluble in most solvent due to strong intra-or intermolecular hydrogen bonding[208]. Even so, it is used in the mass production of conventional dressing materials[194], as sponge for cartilage tissue engineering[25] and scaffolds for clinical settings in wound repair[209-211]. Some researchers[209,211] studied the oxidized regenerated cellulose/collagen in terms of its ability to promote fibroblast migration and proliferation *in vitro*, and the role of this system as modifier of the chronic wound environment. Commercially, a spongy matrix containing oxidized regenerated cellulose (45%, ORC) and collagen (55%) named Promogran® manufactured by Johnson & Johnson Medical had been introduced to both USA and EU market. In the presence of chronic wound exudates, ORC/collagen forms a soft, conformable and biodegradable gel that physically binds and inactivates matrix mettalloproteases (MMPs), stabilizing its level and contributing to a positive effect on wound healing process, since a high level of MMPs in chronic wounds may lead to degradation of important proteins and inactivate growth factors[211]. Cellulose can also be produced by *Gluconacetobacter xylinus (=Acetobacter xylinum*) [208,212,213]. Although identical to cellulose of plant origin in terms of molecular formula, bacterial cellulose is characterized by a crystalline nano- and microfibril structure that determines its extraordinary physical and mechanical properties [208,213]. Bacterial cellulose or microbial cellulose has unique properties, including high purity, high crystallinity, moldability *in situ*, biocompatibility and high water-holding ability. In addition to its cost-efficient production, it has high mechanical strength in the wet state[212,213]. Due to its versatility, bacterial cellulose has been studied as wound dressings, tubular implants and scaffolds for cartilage repair, among other applications[208,212,213]. *In vivo* tests on animal models showed that microbial cellulose membranes protected burn wounds from excessive external fluid loss, and thus accelerating the entire process of healing[214]. Bacterial cellulose/chitosan wound dressings have good antibacterial and barrier properties as well as mechanical

properties in wet state and optimal moisture conditions for rapid wound healing without irritation[131]. In cartilage studies[212], bacterial cellulose can be a potential scaffold for cartilage TE since that chondrocytes maintained their differentiated form and that the scaffold support cell ingrowth.

Table 4. Cellulose-based matrices proposed for applications in soft tissue repair. Compiled from references [209-211,215].

Composition	Processing Methodology	Matrix Type	Active Substance	Potential TE Application	Cell type (source)/line	Animal model	Ref.
Cellulose-silk fibroin	Wet spinning	Fibers	_	Wound dressing	_	_	[215]
ORC-collagen	Freeze-drying cross-linking (dehydrothermal)	Scaffolds	_	Clinical settings in wound repair	Fibroblasts (human)	Diabetic mouse	[209]
	Freeze-drying cross-linking (dehydrothermal)	Scaffolds	PDGF	Clinical setting in acute wounds	_	Sprague-Dawley rats	[210]
	Freeze-drying cross-linking (dehydrothermal)	Scaffolds	PDGF	Chronic wounds	_	_	[211]

Abbreviatures. ORC: oxidised regenerated cellulose; GA: glutaraldehyde; PDGF: platelet-derived growth factor.

3. **Considerations of polysaccharide and proteins interactions**

In biological systems, proteins and polysaccharides have an important role in the organization of the living cells, and the interactions between these natural origin polymers leads to the formation of macromolecular structures through association. Basic information related to the phase behaviour and interactions between polysaccharides and proteins has been obtained during the last three decades, mainly in the field of food science[9,10,216-219]. Mixed systems of globular proteins and polysaccharides have been widely used to control the structure, texture and stability of food products[220,221], whereas natural origin polymer-based systems can also be used towards biomedical applications. Different examples of biomedical applications of these systems are shown in Tables 1 to 4. Besides the low cost and versatility of this strategy, proteins into matrix materials may improve its cell behaviour because they are able to interact favourably with cells through specific recognition domains present in their structure. Also, the interaction between natural polymers of different chemical structure through hydrogen bonding or electrostatic in nature may reinforce the mechanical properties of the materials obtained from such mixtures. Nevertheless, most polymer blends are immiscible or only partially miscible. Even so many combinations have good mechanical, thermal and biological properties. Depending on the polymers characteristics (molecular weight, polysaccharide/protein ratio, conformation, and charge density), and on the solution conditions (pH, ionic strength, total concentration, solvent quality, etc.), the association of biomacromolecules may result in the formation of a complex or a phase separation[10]. When polysaccharides and proteins attract each other through electrostatic interactions, the polymers associate excluding the solvent from their vicinity (complex coacervation), allowing the formation of soluble complexes or an aggregative phase separation (precipitate)[218,222]. Sometimes the complex coacervates are highly unstable, and a structural stabilization by chemical agents becomes necessary[223]. The formation of complexes and coacervates induced by electrostatic interactions is a fundamental physico-

chemical phenomenon, which is relevant to a number of known biological processes such as protein transcription and antigen-antibody reactions[224]. Additionally, protein-polysaccharide complexes are also important in the design of multi-layers structures[225], encapsulation processes[226] and formation and stabilization of food emulsions[227]. On the other hand, the phase separation can occur due to a strong repulsion between the polymers caused by similar electrical charges or then because one or both polymers are uncharged[9,218]. At low concentrations, the polymers can be intimately mixed and form a one-phase solution. But, when the total concentration of system increases, exceeding a certain critical value (about 4% for globular proteins and polysaccharides mixture[220]), the phase separation occurs. As a result, the system exhibits one phase rich in protein and the other rich in polysaccharide[9,218]. Miscibility in a polymer blend is associated to specific interactions between polymeric components. The major forces responsible for polymer interactions are electrostatic in nature but other common interactions such as hydrogen bonding or hydrophobic interactions may be significant in the stabilization of the interactions[9,228]. Several authors[84,89,90,103,221,229-232] have studied the interactions between natural origin-polymers regarding to its promising applications in food formulation and biotechnological and biomedical areas. For example, studies performed by Taravel and Domard[83,84] and Sionskowsha *et al* [232] suggested that chitosan/collagen blends are miscible and that the interactions between them are polyelectrolytic, *i.e.* allows the formation of complexes. These matrices have been proposed as films for dermal regeneration template[134], as wound dressings[136] and scaffolds for liver TE[116]. Malay *et al* [229] investigated the formation of pH-induced complexation of silk fibroin and hyaluronic acid, while Naidu *et al* [231] evaluated the compatibility of sodium alginate/hydroxyethylcellulose blends in solution and as solid films. Certain studies[233] indicated that the compatibility between polymers in solution would remain even when the solvent is absent ("memory effect"). Besides, the miscibility and the nature and strength of interactions involved between natural origin polymers-based systems can be studied using a wide variety of analytical

techniques. For example, in polymer blend solutions, the existence of thermodynamic interaction (attraction or repulsion) between polymers will induce a non-ideal mixing, resulting in changes of viscosity. Therefore, viscosimetry is an effective, quick and inexpensive method to determine the miscibility of polymers[231]. Also, the compatibility of a blend system can be studied by its glass transition temperature (T_g), usually determined by Differential Scanning Calorimetry (DSC). An immiscible blend usually exhibits the T_{gs} of the components, while miscible polymers involve thermodynamic solubility and should have one phase and only a single T_g . On the other hand, the type of morphology in a blend system is dependent on the nature and amount of the polymers in the mixture, viscosity, and also on their miscibility[229,234]. Heterogeneous blends can appear as a dispersion of one polymer in the matrix of the other polymer, and formation of co-continuous morphology.

4. **Strategies for compatibilization and surface modification on polymeric blends**

Compatibilizers and chemical cross-linking treatments

As most polymeric blends are immiscible, compatibilization could be required. The compatibilization of polymer blends can be possible adding to the system non- or reactive compatibilizers [228,234]. Reactive compatibilizers chemically react with blend components, while non- compatibilizers are block and graft copolymers having chain segments identical or similar to the components to be mixed[228,234]. Graft copolymers works as emulsifiers reducing the interfacial tension of blends. This lead to a phase size small enough for that the material to be considered as macroscopically homogeneous, and consequently improving the mechanical properties of the system[228]. Besides usual compatibilizers, cross-linking methods has been used to improve structural stability and mechanical properties of binary systems. A particular cross-linker should be chosen based on its chemical reactivity, solubility, spacer length and compatibility of the reaction with the application.

Glutaraldehyde (GA), formaldehyde, 1-ethyl-3-(3-dimethylaminopropyl)-carbodiimide (EDC), polyepoxide, and polyglycidyl ether are commonly used as cross-linking agents[47,102,159,235-238]. Among them, glutaraldehyde and EDC are the most widely used for polymeric systems due to its high cross-linking efficiency. However, depending of the concentration used, extracts from the cross-linked materials can be released into the tissue, resulting in cytotoxicity and inflammation. In contrast to glutaraldehyde, water-soluble carbodiimide (EDC) does not remain as a part of linkage but simply change to water-soluble urea derivatives that have low cytotoxicty. Park *et al* [235] reported that collagen/HA matrix cross-linked with EDC had good resistance to enzymatic degradation and acceptable toxicity. Actually, genipin have been considered a natural cross-linking agent with lower cytotoxicity when compared to alternative cross-linkers like glutaraldehyde[239]. It is obtained from its parent compound geniposide, which it extracted from fruits of *Gardenia jasminoides Ellis*[240]. Genipin has been used to cross-linking gelatin[241,242], collagen[243], kappa-carrageenan[244], chitosan[245-247], alginate/chitosan[248], chitosan/gelatin blends[148] and chitosan/silk fibroin system[111]. One interesting characteristic of the reaction of genipin with amino acids consists in the formation of dark blue pigments, which are result of oxygen radical induced polymerization of genipin[239]. These blue pigments are used as a natural colorant in the food[249], and can also aid to follow the evolution of the genipin cross-linking reactions[247]. Typically, matrices cross-linked with genipin presented good mechanical properties, reduced swelling extent, slower degradation rate and good biocompatibility[241].[245] Proanthocyanidins (PAs) have also been indicated as nontoxic cross-linker[250]. PAs are widespread in fruits and vegetables and belong to the category known as condensed tannins, which consist of highly hydroxylated structures capable of forming insoluble complexes with carbohydrates and proteins[250]. Studies indicated that PAs are less cytotoxic than glutaraldehyde, and it could efficiently cross-link collagen matrices[250] and chitosan/gelatin membranes[251]. Kim *et al* [251] reported that proanthocyanidins cross-linked chitosan/gelatin membranes have good mechanical and thermal properties and slower degradation

rate *in vivo* and no inflammatory reaction in all implants tested when compared to uncross-linked gelatin films and chitosan/gelatin membranes.

Surface modification

A biomaterial with good bulk properties does not necessarily possess the surface characteristics suitable for a given biomedical application. Therefore, the modification of the biomaterial surface is often needed[252,253]. Various methods are employed for modifying polymer surfaces including chemical modification[254,255], ultra-violet (UV)[256-258], gamma irradiation[259,260] and plasma surface modification[252,254,261-266]. These modifications will determine for instance the possible interactions of polymers with bioactive agents, namely drugs, growth factors as well as the possibility of allowing for clinical use on the regeneration of hard/soft tissues[263,266,267]. Depending of the chosen method and used conditions, a surface can be modified to become hydrophilic or hydrophopic, be functionalized or only be activated to further reactions[263,267]. Chemical etching with potassium permanganate-nitric acid system has been shown to enhance surface energy and wettabiliy of starch based blends[254]. UV irradiation has been used to create patterned polystyrene substrates for tissue engineering applications, especially in neuroscience[257]. Plasma surface modification is a method widely used to tailor surface functionality using different atmospheres[253,263]. Usually, plasma treatment only affects the outermost layers (2.5-10 nm) of material surface, while the bulk properties of the polymer remain intact[252]. When a material is exposed to a partially ionized gas, its surface is bombarded with ions, electrons and radicals from the plasma. This process results in radicals formation on the polymer surface. So-formed highly reactive species combine with the radicals from the working gas to modify the surface[253]. Depending on the interaction between the plasma and polymer, and on the operating conditions (gas, power, and exposure time), reactions of modification and degradation can occur[252,253,268]. When degradation is prominent, etching will take place on the polymer surface. An etching reaction

occurs when polymers are exposed to plasma for a long period, and the exposed layers of the polymers are etched off[253]. As a result, etching produces nanoroughness on the polymer surface, which can create the desirable features on biomaterials to meet the requirements of biocompatibility *in vivo*[253]. In Figure 5, for instance, we can see that the prolonged exposure time on chitosan/soy protein membranes to argon plasma (Fig. 5b and 5c) promoted an increase of surface roughness when compared to initial surface membrane (Fig. 5a). On the other hand, plasma can also be used to create a functionalized surfaces using attachment of new chemical groups or their inclusion after surface activation by plasma treatment[253,265]. For example, oxygen (-OH, -C=O, -COOH groups) or nitrogen ($-NO_2$, $-NH_2$, $-CONH_2$ groups) plasma have been used to increase the material hidrophilicity[269]. As a result, improved adhesion strength, biocompatibility, and other relevant properties were observed[253,269]. Similar results were obtained in our group by Silva *et al* [261] who have investigated the surface modification of chitosan membranes using nitrogen and argon plasma to improve its fibroblast cell adhesion *in vitro.* The proposed modifications would facilitate the use of chitosan-based materials as wound dressings. In addition, plasma grafting polymerization can be used to modify inert surfaces. This includes activation of the surface by plasma followed by polymerization reactions, resulting from the contact between the activated surface with monomers in the liquid or gas phase[253,263,265,270]. Therefore, grafted copolymers are formed on the surface. Using such procedures, smart surfaces may be produced, where the wettability can be responsive to the change of external variables, being useful for some biomedical applications[271,272]. Recently, Huang *et al* [264] suggested that oxygen plasma is a better method to incorporate laminin onto the surface of chitosan membrane, resulting in a significant increase of Schwann cells attachment and affinity for directing peripheral nerve regeneration.

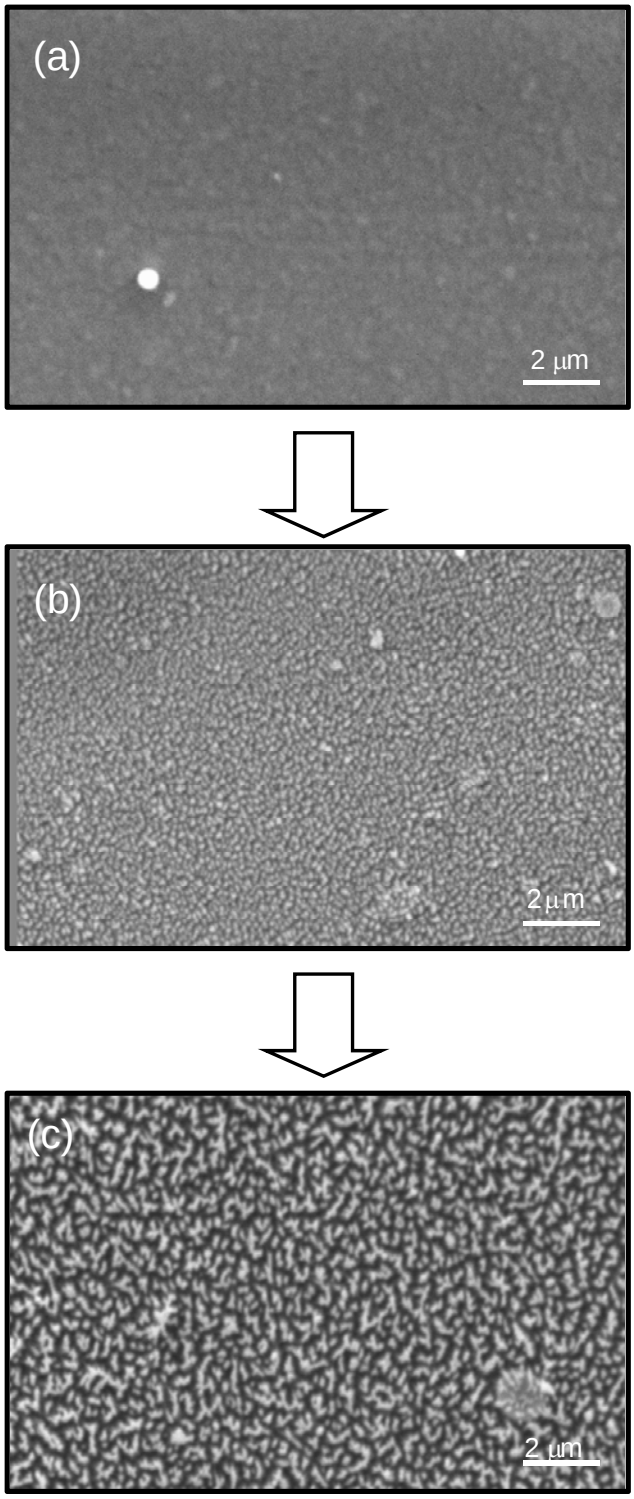

Figure 5. SEM micrographs showing the effect of the prolonged time exposure to argon plasma on surface of chitosan-soy protein (CS) based membranes; (a) CS membrane without treatment, (b) CS after argon plasma (40 watts, 5 minutes) and (c) CS after argon plasma (40 watts, 20 minutes). [Unpublished results]

5. **Final remarks**

Several natural origin polymer-based systems are proposed to be used in soft tissue repair. In general, the features of a particular blended system must be modulated and designed in an appropriate form for a determined application. Improvements of the properties of binary systems can be made through cross-linking reactions in order to enhance the structural stability and mechanical properties of the resulting materials. In addition, surface modification on a matrix might be necessary to improve their surface properties, and further its tissue/cell interface. On what concerns to the target tissue, interesting strategies such as co-cultures of keratinocytes and fibroblasts on bilayer constructs (scaffold/membrane) as dermal equivalent and development of multi-component scaffolds with living cells for cartilage repair shown promising results. In some cases, a sustained release of a bioactive substance (drugs or growth factors) incorporated into biomatrices enhance the cell response, and thus the tissue regeneration. Moreover, advanced processing techniques like solid-free form have been proposed to produce porous matrices with complex geometric shapes and suitable porosities tailored to tissue target, for example in the design of bioartificial livers. Although the approaches described have demonstrated promising results both *in vitro* and some cases *in vivo*, there are still many challenges to obtain clinically successful materials as well as to create novel therapeutic approaches, possibly with a more extensive and optimized use of stem cells and genetic engineering.

6. **Acknowledgements**

The authors to thank J. Benesch, I. Paskuleva, J. Grech and M. Oliveira for useful discussions. S. S. Silva would like to acknowledged to the Portuguese Foundation for Science and Technology (FCT) for providing her with a PhD scholarship (SFRH/BD/8658/2002). This work was partially supported by the European Union funded STREP Project HIPPOCRATES and was carried out under the scope of the European NoE EXPERTISSUES.

7. **References**

1. Langer, R. and Vacanti, J., Tissue engineering, *Science* 260, 920-926, 1993.
2. Lanza, R., Langer, R., and Vacanti, J. P., *Principles of Tissue Engineering* Academic Press, New York, 2000.
3. Metcalfe, A. D. and Ferguson, M. W., Tissue engineering of replacement skin: the crossroads of biomaterials, wound healing, embryonic development, stem cells and regeneration, *Journal of Royal Society Interface* 4, 413-437, 2007.
4. Macneil, S., Progress and opportunities for tissue -engineered skin, *Nature* 445, 874-880, 2007.
5. Barbul, A., Wound healing: Physiology and possible role of skin substitutes, in *Cultured human keratinocytes and tissue engineered skin substitutes*, Horch, R. E., Munster, A. M., andAchauer, B. M. Georg Thieme Verlag, New York, 2001, pp. 23-36.
6. Chung, C. and Burdick, J. A., Engineering cartilage tissue, *Advanced Drug Delivery Reviews* 60, 243-262, 2008.
7. Temenoff, J. S. and Mikos, A. G., Review: tissue engineering for regeneration of articular cartilage, *Biomaterials* 21, 431-440, 2000.
8. Hutmacher, D. W., Scaffolds in tissue engineering bone and cartilage, *Biomaterials* 21, 2529-2543, 2000.
9. McClements, D. J., Non-covalent interactions between proteins and polysaccharides, *Biotechnology Advances* 24, 621-625, 2006.
10. Turgeon, S. L., Beaulieu, M., Schmitt, C., and Sanchez, C., Protein-polysaccaride interactions: phase-ordering kinetics, thermodynamic and structural aspects, *Current Opinion in Colloid and Interface Science* 8, 401-414, 2003.
11. Damodaran, S., *Food Proteins and Their Applications*, 1 edition ed. Marcel Dekker Inc., New York, 1997.
12. Lloyd, L. L., Kennedy, J. F., Methacanon, P., Paterson, M., and Knill, C. J., Carbohydrate polymers as wound management aids, *Carbohydrate Polymers* 37, 315-322, 1998.
13. Gomes, M. E., Azevedo, H. S., Malafaya, P. B., Silva, S. S., Oliveira, J. M., Sousa, R. A., Mano, J. F., and Reis, R. L., Natural polymers in tissue engineering applications, in *Tissue engineering*, Blitterswijk, C., Lindahl, A., Thomsen, P., Williams, D., Hubbell, J., andCancedda, R. Elsevier, Amsterdam, 2008, pp. 145-192.
14. Mano, J. F., Silva, G. A., Azevedo, H. S., Malafaya, P. B., Sousa, R. A., Silva, S. S., Boesel, L. F., Oliveira, J. M., Santos, T. C., Marques, A. P., Neves, N. M., and Reis, R. L., Natural origin

biodegradable systems in tissue engineering and regenerative medicine: present status and some moving trends, *Journal of The Royal Society Interface* 4, 999-1030, 2007.
15. Gomes, M. E. and Reis, R. L., Biodegradable polymers and composites in biomedical applications: from catgut to tissue engineering. Part 2 Systems for temporary replacement and advanced tissue regeneration, *International Materials Reviews* 49, 274-285, 2004.
16. Stark, Y., Suck, K., Kasper, C., Wieland, M., van Griensven, M., and Scheper, T., Application of collagen matrices for cartilage tissue engineering, *Experimental and Toxicologic Pathology* 57, 305-311, 2006.
17. Pieper, J. S., van der Kraan, P. M., Hafmans, T., Kamp, J., Buma, P., van Susante, J. L. C., van den Berg, W. B., Veerkamp, J. H., and van Kuppevelt, T. H., Crosslinked type II collagen matrices: preparation, characterization, and potential for cartilage engineering, *Biomaterials* 23, 3183-3192, 2002.
18. Kumar, M. N. V. R., A review of chitin and chitosan applications, *Reactive & Functional Polymers* 46, 1-27, 2000.
19. Kim, I.-Y., Seo, S.-J., Moon, H.-S., Yoo, M.-K., Park, I.-Y., Kim, B.-C., and Cho, C.-S., Chitosan and its derivatives for tissue engineering applications, *Biotechnology Advances* 26, 1-21, 2008.
20. Madihally, S. V. and Matthew, H. W. T., Porous chitosan scaffolds for tissue engineering, *Biomaterials* 20, 1133-1142, 1999.
21. Suh, J. K. F. and Matthew, H. W. T., Application of chitosan-based polysaccharide biomaterials in cartilage tissue engineering: a review, *Biomaterials* 21, 2589-2598, 2000.
22. Yoo, H. S., Lee, E. A., Yoon, J. J., and Park, T. G., Hyaluronic acid modified biodegradable scaffolds for cartilage tissue engineering, *Biomaterials* 26, 1925-33, 2005.
23. Aigner, J., Tegeler, J., Hutzler, P., Campoccia, D., Paveio, A., Hammer, C., Kastenbauer, E., and Naumann, A., Cartilage tissue engineering with novel nonwoven structured biomaterial based on hyaluronic acid benzyl ester, *Journal of Biomedical Materials Research* 42, 172-181, 1998.
24. Kogan, G., Soltes, L., Stern, T., and Gemeiner, P., Hyaluronic acid: a natural biopolymer with a broad range of biomedical and industrial applications, *Biotechnology Letters* 29, 17-25, 2007.
25. Pulkkinen, H., Virpi Tiitu, V., Lammentaust, E., Hämäläinen, E. R., Kiviranta, I., and Lammi, M. J., Cellulose sponge as a scaffold for cartilage tissue engineering, *Bio-Medical Materials and Engineering* 16, S29-S35, 2006.
26. Malafaya, P. B., Stappers, F., and Reis, R. L., Starch-based microspheres produced by emulsion crosslinking with a potential media dependent responsive behavior to be used as drug delivery carriers, *Journal of Materials Science- Materials in Medicine* 17, 371-377, 2006.
27. Gomes, M. E., Holtorf, H. L., Reis, R. L., and Mikos, A. G., Influence of the porosity of starch-based fiber mesh scaffolds on the proliferation and osteogenic differentiation of bone marrow stromal cells cultured in a flow perfusion bioreactor, *Tissue Engineering* 12, 801-809, 2006.
28. Oliveira, J. T., Crawford, A., Mundy, J. M., Moreira, A. R., Gomes, M. E., Hatton, P. V., and Reis, R. L., A cartilage tissue engineering approach combining starch-polycaprolactone fibre mesh scaffolds with bovine articular chondrocytes, *Journal of Materials Science- Materials in Medicine* 18, 295-302, 2007.
29. Santos, M. I., Fuchs, S., Gomes, M. E., Unger, R. E., Reis, R. L., and Kirkpatrick, J., Response of micro- and macrovascular endothelial cells to starch-based fiber meshes for bone tissue engineering, *Biomaterials* 28, 240-248, 2007.
30. Silva, G. A., Coutinho, O. P., Ducheyne, P., Shapiro, I. M., and Reis, R. L., Starch-based microparticles as vehicles for the delivery of active platelet-derived growth factor, *Tissue Engenering* 13, 1259-1268, 2007.
31. Vaz, C. M., Graaf, L. A., Reis, R. L., and Cunha, A. M., Soy protein-based systems for different tissue regeneration applications, in *Polymer Based Systems on Tissue Engineering, Replacement and Regeneration*, Reis, R. L. and Cohn, D. Kluwer Academic Publishers, 2002, pp. 93-110.

32. Vaz, C. M., de Graaf, L. A., Reis, R. L., and Cunha, A. M., In vitro degradation behaviour of biodegradable soy plastics: effects of crosslinking with glyoxal and thermal treatment, *Polymer Degradation and Stability* 81, 65-74, 2003.
33. Kang, H.-W., Tabata, Y., and Ikada, Y., Fabrication of porous gelatin scaffolds for tissue engineering, *Biomaterials* 20, 1339-1344, 1999.
34. Vepari, C. and Kaplan, D. L., Silk as a biomaterial, *Progress in Polymer Science* 32, 991-1007, 2007.
35. Altman, G. H., Diaz, F., Jakuba, C., Calabro, T., Horan, R. L., Chen, J. S., Lu, H., Richmond, J., and Kaplan, D. L., Silk-based biomaterials, *Biomaterials* 24, 401-416, 2003.
36. MacIntosh, A. C., Kearns, V. R., Crawford, A., and Hatton, P. V., Skeletal tissue engineering using silk biomaterials, *Journal of Tissue Engineering and Regenerative Medicine* 2, 71-80, 2008.
37. Unger, R. E., Peters, K., Wolf, M., Motta, A., Migliaresi, C., and Kirkpatrick, C. J., Endotheliazation of a non-woven silk fibroin net for use in tissue engineering: growth and gene regulation of human endothelial cells, *Biomaterials* 25, 5137-5146, 2004.
38. Eiselt, P., Julia Yeh, J., Latvala, R. K., Shea, L. D., and Mooney, D. J., Porous carriers for biomedical applications based on alginate hydrogels, *Biomaterials* 21, 1921-1927, 2000.
39. Malafaya, P. B., Silva, G. A., and Reis, R. L., Natural-origin polymers as carriers and scaffolds for biomolecules and cell delivery in tissue engineering applications, *Advanced Drug Reviews* 59, 207-233, 2007.
40. Seal, B. L., Otero, T. C., and Panitch, A., Polymeric biomaterials for tissue and organ regeneration, *Materials Science and Engineering Reviews* 34, 147-230, 2001.
41. Chang, C. H., Liu, H. C., Lin, C. C., Chou, C. H., and Lin, F. H., Gelatin-chondroitin-hyaluronan tri-copolymer scaffold for cartilage tissue engineering, *Biomaterials* 24, 4853-4858, 2003.
42. Funakoshi, T., Majima, T., Iwasaki, N., Yamane, S., Masuko, T., Minami, A., Harada, K., Tamura, H., Tokura, S., and Nishimura, S.-I., Novel chitosan-based hyaluronan hybrid polymer fibers as a scaffold in ligament tissue engineering, *Journal of Biomedical Materials Research-Part A* 74A, 338-346, 2005.
43. Lee, J. E., Jeong, M. H., Ahn, H. J., Kim, J. K., Choi, K., Chang, C. B., Kim, H. J., Seong, S. C., and Lee, M. C., Evaluation of chondrogenesis in collagen/chitosan/glycosaminoglycan scaffolds for cartilage tissue engineering, *Tissue Engineering and Regenerative Medicine* 2, 41-49, 2005.
44. Liao, E., Yaszemski, M., Krebsbach, P., and Hollister, S., Tissue-engineered cartilage constructs using composite hyaluronic acid/collagen I hydrogels and designed poly(propylene fumarate) scaffolds, *Tissue Engineering* 13, 537-550, 2007.
45. Ma, L., Gao, C., Mao, Z., Zhou, J., Shen, J., Hu, X., and Han, C., Collagen/chitosan porous scaffolds with improved biostability for skin tissue engineering, *Biomaterials* 24, 4833-41, 2003.
46. Kopecek, J. and Yang, J., Review- Hydrogels as smart biomaterials, *Polymer International* 56, 1078-1098, 2007.
47. Hennink, W. E. and van Nostrum, C. F., Novel crosslinking methods to design hydrogels, *Advanced Drug Reviews* 54, 13-36, 2002.
48. Mikos, A. G. and Temenoff, J. S., Formation of highly porous biodegradable scaffolds for tissue engineering, *Electronic Journal of Biotechnology* 3, 1-6, 2000.
49. Correlo, V. M., Gomes, M. E., Tuzlakoglu, K., Oliveira, J. M., Malafaya, P. B., Mano, J. F., Neves, N. M., and Reis, R. L., Tissue engineering using natural polymers, in *Biomedical polymers*, Jenkins, M. Woodhead publishing and Maney Publishing, 2007, pp. 197-217.
50. Chen, G., Ushida, T., and Tateishi, T., Scaffold design for tissue engineering, *Macromolecular Bioscience* 2, 67-77, 2002.
51. Schmidt, C. and Leach, J. B., Neural tissue engineering: strategies for repair and regeneration, *Annual Review Biomedical Engineering* 5, 293-347, 2003.
52. Huang, Y.-C. and Huang, Y.-Y., Biomaterials and strategies for nerve regeneration, *Artificial Organs* 30, 514-522, 2006.

53. Mano, J. F. and Reis, R. L., Osteochondral defects: present situation and tissue engineering approaches, *Journal of Tissue Engineering and Regenerative Medicine* 1, 261-273, 2007.
54. Malafaya, P. B., Pedro, A. J., Peterbauer, A., Gabriel, C., Redl, H., and Reis, R. L., Chitosan particles agglomerated scaffolds for cartilage and osteochondral tissue engineering approaches with adipose tissue derived stem cells, *Journal of Materials Science: Materials in Medicine* 16, 1077-1085, 2005.
55. Oliveira, J. M., Rodrigues, M. T., Silva, S. S., Malafaya, P. B., Gomes, M. E., Viegas, C. A., Dias, I. R., Azevedo, J. T., Mano, J. F., and Reis, R. L., Novel hydroxyapatite/chitosan bilayered scaffold for osteochondral tissue-engineering applications: Scaffold design and its performance when seeded with goat bone marrow stromal cells, *Biomaterials* 27, 6123-6137, 2006.
56. Gao, J., Dennis, J. E., Solchage, L. A., Golberg, V. M., and Caplan, A. L., Repair of osteochondral defect with tissue-engineered two-phase composite material of injectable calcium phosphate and hyaluronan sponge, *Tissue Engineering* 8, 827-837, 2002.
57. Gelse, K., Poschl, E., and Aigner, T., Collagens—structure, function, and biosynthesis, *Advanced Drug Reviews* 55, 1531-1546, 2003.
58. Kumar, M. N. V. R., Muzzarelli, R. A. A., Muzzarelli, C., Sashiwa, H., and Domb, A. J., Chitosan chemistry and pharmaceutical perspectives, *Chemical Reviews* 104, 6017-6084, 2004.
59. Kurita, K., Controlled functionalization of the polysaccharide chitin, *Progress in polymer science* 26, 1921-1971, 2001.
60. Koji, K., Yasuhiko, Y., and Hiroyuki, T., US Patent No. 4651725, 1987, Wound dressing.
61. Fox, A. S. and Allen, A. E., US Patent No. 5578661, 1996, Gel forming system for use as wound dressing.
62. Yusof, N. L. B. M., Wee, A., Lim, L. Y., and Khor, E., Flexible chitin films as potential wound-dressing materials: wound model studies, *Journal of Biomedical Materials Research Part A* 66A, 224-232, 2003.
63. Yusof, N. L. B. M., Lee, L. Y., and Khor, E., Flexible chitin films: structural studies, *Carbohydrate Research* 339, 2701-2711, 2004.
64. Pielka, S., Paluch, D., Kus, J. S., Zywicka, B., Solski, L., Szosland, L., and Zaczynska, E., Wound healing acceleration by a textile dressing containing dibutyrylchitin and chitin, *Fibres & Textiles in Eastern Europe* 11, 79-84, 2003.
65. Muzzarelli, R. A. A., Guerrieri, M., Goteri, G., Muzzarelli, C., Armeni, T., Ghiselli, R., and Cornelissen, M., The biocompatibility of dibutyryl chitin in the context of wound dressings, *Biomaterials* 26, 5844-5854, 2005.
66. Cho, Y.-W., Cho, Y.-N., Chung, S.-H., Yoo, G., and Ko, S.-W., Water-soluble chitin as a wound healing accelerator, *Biomaterials* 20, 2139-2145, 1999.
67. Lee, S. B., Kim, Y. H., Chong, M. S., and Lee, Y. M., Preparation and characteristics of hybrid scaffolds composed of beta-chitin and collagen, *Biomaterials* 25, 2309-2317, 2004.
68. Hirano, S., Zhang, M., and Nakagawa, M., Release of glycosaminoglycans in physiological saline and water by wet-spun chitin-acid glycosaminoglycan fibers, *Journal of Biomedical Materials Research* 56, 556-561, 2001.
69. Jayakumar, R., Prabaharan, M., Reis, R. L., and Mano, J. F., Graft copolymerized chitosan-present status and applications, *Carbohydrate Polymers* 62, 142-158, 2005.
70. Khor, E. and Lim, L. Y., Implantable applications of chitin and chitosan, *Biomaterials* 24, 2339-2349, 2003.
71. Aoyagi, S., Onishi, H., and Machida, Y., Novel chitosan wound dressing loaded with minocycline for the treatment of severe burn wounds, *International Journal of Pharmaceutics* 330, 138-145, 2007.
72. Khan, T. A., Peh, K. K., and Ch'ng, H. S., Mechanical, bioadhesive strength and biological evaluations of chitosan films for wound dressing, *Journal of Pharmacy and Pharmaceutical Sciences* 3, 303-311, 2000.
73. Khan, T. A. and Peh, K. K., A preliminary investigation of chitosan film as dressing for punch biopsy wounds in rats, *Journal of Pharmacy and Pharmaceutical Science* 6, 20-26, 2003.

74. Azad, A. K., Sermsintham, N., Chandrkrachang, S., and Stevens, W. F., Chitosan membrane as a wound-healing dressing: Characterization and clinical application, *Journal of Biomedical Materials Research Part B-Applied Biomaterials* 69B, 216-222, 2004.
75. Marreco, P. R., da Luz Moreira, P., Genari, S. C., and Moraes, A. M., Effects of different sterilization methods on the morphology, mechanical properties, and cytotoxicity of chitosan membranes used as wound dressings, *Journal of Biomedical Materials Research Part B-Applied Biomaterials* 71B, 268-277, 2004.
76. Azevedo, E. P., Saldanha, T. D. P., Navarro, M. V. M., Medeiros, A. C., Ginani, M. F., and Raffin, F. N., Mechanical properties and release studies of chitosan films impregnated with silver sulfadiazine, *Journal of Applied Polymer Science* 102, 3462-3470, 2006.
77. Mizuno, K., Yamamura, K., Yano, K., Osada, T., Saeki, S., Takimoto, N., Sakura, T., and Nimura, Y., Effect of chitosan film containing basic fibroblast growth factor on wound healing in genetically diabetic mice, *Journal of Biomedical Materials Research* 64, 177-181, 2003.
78. Queiroz, A. A. A., Ferraz, H. G., Abraham, G. A., Fernandez, M., Bravo, A. L., and Roman, J. S., Development of new hydroactive dressings based on chitosan membranes: characterization and in vivo behavior, *Journal of Biomedical Materials Research- Part A* 64A, 147-154, 2003.
79. Mi, F.-L., Shyu, S.-S., Wu, Y.-B., Lee, S.-T., Shyong, J.-Y., and Huang, R.-N., Fabrication and characterization of a sponge-like asymmetric chitosan membrane as a wound dressing, *Biomaterials* 22, 165-173, 2001.
80. Mi, F. L., Wu, Y. B., Shyu, S. S., Schoung, J. Y., Huang, Y. B., Tsai, Y. H., and Hao, J. Y., Control of wound infections using a bilayer chitosan wound dressing with sustainable antibiotic delivery, *Journal of Biomedical Materials Research* 59, 438-449, 2002.
81. Mi, F. L., Wu, Y. B., Shyu, S. S., Chao, A. C., Lai, J. Y., and Su, C. C., Asymmetric chitosan membranes prepared by dry/wet phase separation: a new type of wound dressing for controlled antibacterial release, *Journal of Membrane Science* 212, 237-254, 2003.
82. Ma, J., Wang, H., He, B., and Chen, J., A preliminary in vitro study on the fabrication and tissue engineering applications of a novel chitosan bilayer material as a scaffold of human neofetal dermal fibroblasts, *Biomaterials* 22, 331-336, 2001.
83. Taravel, M. N. and Domard, A., Relation between the physicochemical characteristics of collagen and its interactions with chitosan, *Biomaterials* 14, 930-938, 1993.
84. Taravel, M. N. and Domard, A., Collagen and its interaction with chitosan II. Influence of the physicochemical characteristics of collagen, *Biomaterials* 16, 665-671, 1995.
85. Taravel, M. N. and Domard, A., Collagen and its interactions with chitosan. III. Some biological and mechanical properties, *Biomaterials* 17, 451-455, 1996.
86. Ma, L., Shi, Y., Chen, Y., Zhao, H., Gao, C., and Han, C., In vitro and in vivo biological performance of collagen-chitosan/silicone membrane bilayer dermal equivalent, *Journal of Materials Science - Materials in Medicine* 18, 2185-2191, 2007.
87. Black, A. F., Berthod, F., L'Heureux, N., Germain, L., and Auger, F. A., In vitro reconstruction of a human capillary-like network in a tissue-engineered skin equivalent, *FASEB Journal* 12, 1331-1340, 1998.
88. Mao, J., Zhao, L., De Yao, K., Shang, Q., Yang, G., and Cao, Y., Study of novel chitosan-gelatin artificial skin in vitro, *Journal of Biomedical Materials Research - Part A* 64, 301-308, 2003.
89. Yin, Y., Li, Z., Sun, Y., and Yao, K., A preliminary study on chitosan/gelatin polyelectrolyte complex formation, *Journal of Materials Science* 40, 4649-4652, 2005.
90. Yin, Y. J., Yao, K. D., Cheng, G. X., and Ma, J. B., Properties of polyelectrolyte complex films of chitosan and gelatin, *Polymer International* 48, 420-432, 1999.
91. Deng, C. M., He, L. Z., Zhao, M., Yang, D., and Liu, Y., Biological properties of the chitosan-gelatin sponge wound dressing, *Carbohydrate Polymers* 69, 583-589, 2007.
92. Liu, H. F., Yin, Y. J., and Yao, K. D., Construction of chitosan-gelatin-hyaluronic acid artificial skin in vitro, *Journal of Biomaterials Applications* 21, 413-430, 2007.

93. Liu, H. F., Fan, H. B., Cui, Y. L., Chen, Y. P., Yao, K. D., and Goh, J. C. H., Effects of the controlled-released basic fibroblast growth factor from chitosan-gelatin microspheres on human fibroblasts cultured on a chitosan-gelatin scaffold, *Biomacromolecules* 8, 1446-1455, 2007.
94. Liu, H., Mao, J., Yao, K., Yang, G., Cui, L., and Cao, Y., A study on a chitosan-gelatin-hyaluronic acid scaffold as artificial skin in vitro and its tissue engineering applications, *Journal of Biomaterials Science Polymer Edition* 15, 25-40, 2004.
95. Liu, H., Yin, Y., Yao, K., Ma, D., Cui, L., and Cao, Y., Influence of the concentrations of hyaluronic acid on the properties and biocompatibility of Cs–Gel–HA membranes, *Biomaterials* 25, 3523-3530, 2004.
96. Wang, L. H., Khor, E., Wee, A., and Lim, L. Y., Chitosan-alginate PEC membrane as a wound dressing: Assessment of incisional wound healing, *Journal of Biomedical Materials Research* 63, 610-618, 2002.
97. Kratz, G., Amander, C., Swedenborg, J., Back, M., Falk, C., Gouda, I., and Larm, O., Heparin-chitosan complexes stimulate wound healing human skin, *Scandinavian Journal Plastic Reconstruction Hand Surgery* 31, 119-123, 1997.
98. Kweon, D.-K., Song, S.-B., and Park, Y.-Y., Preparation of water-soluble chitosan/heparin complex and its application as wound healing accelerator, *Biomaterials* 24, 1595-1601, 2003.
99. Yu, S.-H., Mi, F.-L., Wu, Y.-B., Peng, C.-K., Shyu, S. S., and Huang, R. N., Antibacterial activity of chitosan-alginate sponges incorporating silver sulfadiazine: effect of ladder-loop transition of interpolyelectrolyte complex and ionic crosslinking on the antibiotic release, *Journal of Applied Polymer Science* 98, 538-549, 2005.
100. Jin, Y., Ling, P. X., He, Y. L., and Zhang, T. M., Effects of chitosan and heparin on early extension of burns, *Burns* 33, 1027-1031, 2007.
101. Kweon, H., Ha, H. C., Um, I. C., and Park, Y. H., Physical properties of silk fibroin/chitosan blend films, *Journal of Applied Polymer Science* 80, 928-934, 2001.
102. Silva, S. S., Santos, M. I., Coutinho, O. P., Mano, J. F., and Reis, R. L., Physical properties and biocompatibility of chitosan/soy blended membranes, *Journal of Materials Science-Materials in Medicine* 16, 575-579, 2005.
103. Silva, S. S., Goodfellow, B. J., Benesch, J., Rocha, J., Mano, J. F., and Reis, R. L., Morphology and miscibility of chitosan/soy protein blended membranes, *Carbohydrate Polymers* 70, 25-31, 2007.
104. Santos, T. C., Marques, A. P., Silva, S. S., Oliveira, J. M., Mano, J. F., and Reis, R. L., In vivo performance of chitosan/soy-based membranes for skin wound dressing, *Submitted*, 2008.
105. Tanabe, T., Okitsu, N., Tachibana, A., and Yamauchi, K., Preparation and characterization of keratin-chitosan composite film, *Biomaterials* 23, 817-825, 2002.
106. Santos, T. C., Marques, A. P., Silva, S. S., Oliveira, J. M., Mano, J. F., Castro, A. G., and Reis, R. L., In vitro evaluation of the behaviour of human polymorphonuclear neutrophils in direct contact with chitosan-based membranes, *Journal of Biotechnology* 132, 218-226, 2007.
107. Silva, S. S., Oliveira, J. M., Mano, J. F., and Reis, R. L., Physicochemical characterization of novel chitosan-soy protein/TEOS porous hybrids for tissue engineering applications, *Advanced Materials Forum* 514-516, 1000-1004, 2006.
108. Correlo, V. M., Boesel, L. F., Bhattacharya, M., Mano, J. F., Neves, N. M., and Reis, R. L., Hydroxyapatite reinforced chitosan and polyester blends for biomedical applications, *Macromolecular Materials and Engineering* 290, 1157-1165, 2005.
109. Correlo, V. M., Pinho, E. D., Pashkuleva, I., Bhattacharya, M., Neves, N. M., and Reis, R. L., Water absorption and degradation characteristics of chitosan-based polyesters and hydroxyapatite composites, *Macromolecular Bioscience* 7, 354-363, 2007.
110. Correlo, V. M., Boesel, L. F., Pinho, E. D., Costa-Pinto, A. R., Alves da Silva, M. L., Bhattacharya, M., Mano, J. F., Neves, N. M., and Reis, R. L., Melt-based compression moulded scaffolds from chitosan-polyester blends and composites: morphology and mechanical properties, *Journal of Biomedical Materials Research: Part A* accepted, 2008.

111. Silva, S. S., Rodrigues, M. T., Motta,A, Pinheiro,A.F.M., Gomes, M. E., Mano, J. F., Reis, R. L.,and Migliaresi, C., Novel genipin cross-linked chitosan-silk sponges for cartilage tissue engineering strategies, Biomacromolecules, *submitted*, 2008.
112. Medrado, G. C. B., Machado, C. B., Valerio, P., Sanches, M. D., and Goes, A. M., The effect of a chitosan-gelatin matrix and dexamethasone on the behavior of rabbit mesenchymal stem cells, *Biomedical Materials* 1, 155-161, 2006.
113. Yan, J. H., Qi, N. M., and Zhang, Q. Q., Rabbit articular chondrocytes seeded on collagen-chitosan-GAG scaffold for cartilage tissue engineering in vivo, *Artificial Cells Blood Substitutes and Biotechnology* 35, 333-344, 2007.
114. Hsu, S. H., Whu, S. W., Hsieh, S. C., Tsai, C. L., Chen, D. C., and Tan, H. S., Evaluation of chitosan-alginate-hyaluronate complexes modified by an RGD-containing protein as tissue-engineering scaffolds for cartilage regeneration, *Artificial Organs* 28, 693-703, 2004.
115. Lee, J. E., Kim, K. E., Kwon, I. C., Ahn, H. J., Lee, S.-H., Cho, H., Kim, H. J., Seong, S. C., and Lee, M. C., Effects of the controlled-released TGF-b1 from chitosan microspheres on chondrocytes cultured in a collagen/chitosan/glycosaminoglycan scaffold, *Biomaterials* 25, 4163-4173, 2004.
116. Wang, X. H., Li, D. P., Wang, W. J., Feng, Q. L., Cui, F. Z., Xu, Y. X., Song, X. H., and Werf, M., Crosslinked collagen/chitosan matrix for artificial livers, *Biomaterials* 24, 3213-3220, 2003.
117. Wang, X., Yan, Y., Xiong, Z., Lin, F., Wu, R., Zhang, R., and Lu, Q., Preparation and evaluation of ammonia-treated collagen/chitosan matrices for liver tissue engineering, *Journal of Biomedical Materials Research Part B: Applied Biomaterials* 75B, 91-98, 2005.
118. Wang, X., Yan, Y., Lin, F., Xiong, Z., Wu, R., Zhang, R., and Lu, Q., Preparation and characterization of a collagen/chitosan/heparin matrix for an implantable bioartificial liver, *Journal Biomaterials Science- Polymer Edition* 16, 1063-1080, 2005.
119. Yang, J., Chung, T. W., Nagaoka, M., Goto, M., Cho, C.-S., and Akaike, T., Hepatocyte-specific porous polymer-scaffolds of alginate/galactosylated chitosan sponge for liver-tissue engineering, *Biotechnology Letters* 23, 1385-1389, 2001.
120. Chung, T. W., Yang, J., Akaike, T., Cho, K. Y., Nah, J. W., Kim, S., and Cho, C. S., Preparation of alginate/galactosylated chitosan scaffold for hepatocyte attachment, *Biomaterials* 23, 2827-2834, 2002.
121. Jiankang, H., Dichen, L., Yaxiong, L., Bo, Y., Bingheng, L., and Qin, L., Fabrication and characterization of chitosan/gelatin porous scaffolds with predefined internal microstructures, *Polymer* 48, 4578-4588, 2007.
122. Yan, Y., Wang, X., Pan, Y., Liu, H., Cheng, J., Xiong, Z., Lin, F., Wu, R., Zhang, R., and Lu, Q., Fabrication of viable tissue-engineered constructs with 3D cell-assembly technique, *Biomaterials* 26, 5864-5871, 2005.
123. Cheng, M., cao, W., Gao, Y., Gong, Y., Zhao, N., and Zhang, X., Studies on nerve cell affinity of biodegradable modified chitosan films, *Journal Biomaterials Science- Polymer Edition* 14, 1155-1167, 2003.
124. Cheng, M., Deng, J., Yang, F., Gong, Y., Zhao, N., and Zhang, X., Study on physical properties and nerve cell affinity of composite films from chitosan and gelatin solutions, *Biomaterials* 24, 2871-2880, 2003.
125. Majima, T., Funakosi, T., Iwasaki, N., Yamane, S.-T., Harada, K., Nonaka, S., Minami, A., and Nishimura, S.-H., Alginate and chitosan polyion complex hybrid fibers for scaffolds in ligament and tendon tissue engineering, *Journal of Orthopaedic Science* 10, 302-307, 2005.
126. Majima, T., Irie, T., Sawaguchi, N., Funakoshi, T., Iwasaki, N., Harada, K., Minami, A., and Nishimura, S. I., Chitosan-based hyaluronan hybrid polymer fibre scaffold for ligament and tendon tissue engineering, *Proceedings of the Institution of Mechanical Engineers, Part H: Journal of Engineering in Medicine* 221, 537-46, 2007.
127. Li, Z. and Zhang, M., Chitosan-alginate as scaffolding material for cartilage tissue engineering, *Journal of Biomedical Materials Research Part A* 75, 485-493, 2005.

128. Pfister, L. A., Papaloızos, M. I., Merkle, H. P., and Gander, B., Hydrogel nerve conduits produced from alginate/chitosan complexes, *Journal of Biomedical Materials Research* 80A, 932-937, 2007.
129. Seo, S. J., Kim, I. Y., Choi, Y. J., Akaike, T., and Cho, C. S., Enhanced liver functions of hepatocytes cocultured with NIH 3T3 in the alginate/galactosylated chitosan scaffold, *Biomaterials* 27, 1487-95, 2006.
130. Seo, S. J., Choi, Y. J., Akaike, T., Higuchi, A., and Cho, C. S., Alginate/galactosylated chitosan/heparin scaffold as a new synthetic extracellular matrix for hepatocytes, *Tissue Engineering* 12, 33-44, 2006.
131. Ciechanska, D., Multifunctional bacterial cellulose/chitosan composite materials for medical applications, *Fibres & Textiles in Eastern Europe* 12, 69-72, 2004.
132. Chen, Y. L., Lee, H. P., Chan, H.-Y., Sung, L.-Y., Chen, H.-C., and Hu, Y.-C., Composite chondroitin-6-sulfate/dermatan sulfate/chitosan scaffolds for cartilage tissue engineering, *Biomaterials* 28, 2294-2305, 2007.
133. Tsai, S. P., Hsieh, C. Y., Hsieh, C. Y., Wang, D. M., Huang, L. L. H., Lai, J. Y., and Hsieh, H. J., Preparation and cell compatibility evaluation of chitosan/collagen composite scaffolds using amino acids as crosslinking bridges, *Journal of Applied Polymer Science* 105, 1774-1785, 2007.
134. Gao, C. Y., Wang, D. Y., and Shen, J. C., Fabrication of porous collagen/chitosan scaffolds with controlling microstructure for dermal equivalent, *Polymers for Advanced Technologies* 14, 373-379, 2003.
135. Ma, L., Gao, C., Mao, Z., Shen, J., Hu, X., and Han, C., Thermal dehydration treatment and glutaraldehyde cross-linking to increase the biostability of collagen-chitosan porous scaffolds used as dermal equivalent, *Journal Biomaterials Science- Polymer Edition* 14, 861-874, 2003.
136. Guan, M., Ren, L., Wu, T., Sun, L. P., Li, L. R., and Zhang, Q. Q., Potential wound dressing with improved antimicrobial property, *Journal of Applied Polymer Science* 105, 1679-1686, 2007.
137. Chen, R. N., Wang, G. M., Chen, C. H., Ho, H. O., and Sheu, M. T., Development of N,O-(carboxymethyl)chitosan/collagen matrixes as a wound dressing, *Biomacromolecules* 7, 1058-1064, 2006.
138. Kellouche, S., Martin, C., Korb, G., Rezzonico, R., Bouard, D., Benbunan, M., Dubertret, L., Soler, C., Legrand, C., and Dosquet, C., Tissue engineering for full-thickness burns: A dermal substitute from bench to bedside, *Biochemical and Biophysical Research Communications* 363, 472-478, 2007.
139. Iwasaki, N., Yamane, S. T., Majima, T., Kasahara, Y., Minami, A., Harada, K., Nonaka, S., Maekawa, N., Tamura, H., Tokura, S., Shiono, M., Monde, K., and Nishimura, S., Feasibility of polysaccharide hybrid materials for scaffolds in cartilage tissue engineering: evaluation of chondrocyte adhesion to polyion complex fibers prepared from alginate and chitosan, *Biomacromolecules* 5, 828-33, 2004.
140. Yu, X., Bichtelen, A., Wang, X., Yan, Y., Lin, F., Xiong, Z., Wu, R., Zhang, R., and Lu, Q., Collagen/chitosan/heparin complex with improved biocompatibility for hepatic tissue engineering, *Journal of Bioactive and Compatible Polymers* 20, 15-28, 2005.
141. Yan, J. H., Li, X. M., Liu, L. R., Wang, F. J., Zhu, T. W., and Zhang, Q. Q., Potential use of collagen-chitosan-hyaluronan tri-copolymer scaffold for cartilage tissue engineering, *Artificial Cells Blood Substitutes and Biotechnology* 34, 27-39, 2006.
142. Chen, J.-P., Chang, G.-Y., and Chen, J.-K., Electrospun collagen/chitosan nanofibrous membrane as wound dressing, *Colloids and Surfaces A: Physicochemical and Engineering Aspects* 313-314, 183-188, 2007.
143. Shi, H., Ma, L., Zhou, J., Mao, Z., and Gao, C., Collagen/chitosan-silicone membrane bilayer scaffold as a dermal equivalent, *Polymers for Advanced Technologies* 16, 789-794, 2005.
144. Guo, T., Zhao, J. N., Chang, J. B., Ding, Z., Hong, H., Chen, J. N., and Zhang, J. F., Porous chitosan-gelatin scaffold containing plasmid DNA encoding transforming growth factor-beta 1 for chondrocytes proliferation, *Biomaterials* 27, 1095-1103, 2006.

145. Medrado, G. C. B., Machado, C. B., Valerio, P., Sanches, M. D., and Goes, A. M., The effect of a chitosan-gelatin matrix and dexamethasone on the behavior of rabbit mesenchymal stem cells, *Biomedical Materials* 1, 155-161, 2006.
146. Xia, W. Y., Liu, W., Cui, L., Liu, Y. C., Zhong, W., Liu, D. L., Wu, J. J., Chua, K. H., and Cao, Y. L., Tissue engineering of cartilage with the use of chitosan-gelatin complex scaffolds, *Journal of Biomedical Materials Research Part B-Applied Biomaterials* 71B, 373-380, 2004.
147. Wang, X., Yu, X., Yan, Y., and Zhang, R., Liver tissue responses to gelatin and gelatin/chitosan gels, *Journal of Biomedical Materials Research Part A* DOI: 10.1002/jbm.a.31712, 2007.
148. Chiono, V., Pulieri, E., Vozzi, G., Ciardelli, G., Ahluwalia, A., and Giusti, P., Genipin-crosslinked chitosan/gelatin blends for biomedical applications, *Journal of Materials Science - Materials in Medicine* 19, 889-898, 2008.
149. Tan, H. P., Gong, Y. H., Lao, L. H., Mao, Z. W., and Gao, C. Y., Gelatin/chitosan/hyaluronan ternary complex scaffold containing basic fibroblast growth factor for cartilage tissue engineering, *Journal of Materials Science-Materials in Medicine* 18, 1961-1968, 2007.
150. Xu, H., Ma, L., Shi, H., Gao, C., and Han, C., Chitosan–hyaluronic acid hybrid film as a novel wound dressing: in vitro and in vivo studies, *Polymers for advanced technologies* 18, 869-875, 2007.
151. Yamane, S., Iwasaki, N., Majima, T., Funakoshi, T., Masuko, T., Harada, K., Minami, A., Monde, K., and Nishimura, S., Feasibility of chitosan-based hyaluronic acid hybrid biomaterial for a novel scaffold in cartilage tissue engineering, *Biomaterials* 26, 611-619, 2005.
152. Kirker, K. R., Luo, Y., Nielson, J., Shelby, J., and Prestwic, G. D., Glycosaminoglycan hydrogel films as bio-interactive dressings for wound healing, *Biomaterials* 23, 3661-3671, 2002.
153. Tang, S. Q., Vickers, S. M., Hsu, H. P., and Spector, M., Fabrication and characterization of porous hyaluronic acid-collagen composite scaffolds, *Journal of Biomedical Materials Research Part A* 82A, 323-335, 2007.
154. Taguchi, T., Ikoma, T., and Tanaka, J., An improved method to prepare hyaluronic acid and type II collagen composite matrices, *Journal of Biomedical Materials Research* 61, 330-336, 2002.
155. Koller, J., Bakos, D., and Sadlonova, I., Biocompatibility studies of a new biosynthetic dermal substitute based on collagen/hyaluronan conjugate, *Cell and Tissue Banking* 1, 75-80, 2000.
156. Koller, J., Bakos, D., and Sadlonova, I., Biocompatibility studies of modified collagen /hyaluronan membranes after implantation, *Cell and Tissue Banking* 2, 135-142, 2001.
157. Bakos, D. and Koniarova, D., Collagen and collagen/hyaluronan complex modifications, *Chemical Papers* 53, 431-435, 1999.
158. Kubo, K. and Kuroyanagi, Y., Spongy matrix of hyaluronic acid and collagen as a cultured dermal substitute: evaluation in an animal test, *Journal of Artificial Organs* 6, 64-70, 2003.
159. Park, S. N., Lee, H. J., Lee, K. H., and Suh, H., Biological characterization of EDC-crosslinked collagen-hyaluronic acid matrix in dermal tissue restoration, *Biomaterials* 24, 1631-1641, 2003.
160. Park, S. N., Kim, J. K., and Suh, H., Evaluation of antibiotic-loaded collagen-hyaluronic acid matrix as a skin substitute, *Biomaterials* 25, 3689-3698, 2004.
161. Kubo, K. and Kuroyanagi, Y., Development of a cultured dermal substitute composed of a spongy matrix of hyaluronic acid and atelo-collagen combined with fibroblasts: fundamental evaluation, *Journal of Biomaterials Science Polymer Edition* 14, 625-641, 2003.
162. Kubo, K. and Kuroyanagi, Y., Development of a cultured dermal substitute composed of a spongy matrix of hyaluronic acid and atelo-collagen combined with fibroblasts: cryopreservation, *Artificial Organs* 28, 182-188, 2004.
163. Yannas, I. V. and Burke, J. F., Design of an artificial skin. I. Basic design principles, *Journal of Biomedical Materials Research* 14, 65-81, 1980.

164. Burke, J. F., Yannas, I. V., Quinby, W. C., Bondoc, C. C., and Jung, W. K., Successful use of a physiologically acceptable artificial skin in the treatment of extensive burn injury., *Annals of Surgery* 194, 413-428, 1981.
165. Wang, T. W., Wu, H. C., Huang, Y. C., Sun, J. S., and Lin, F. H., Biomimetic bilayered gelatin-chondroitin-6-sulfate-hyaluronic acid biopolymer as a scaffold for skin equivalent tissue engineering, *Artificial Organs* 30, 141-149, 2006.
166. van Susante, J. L. C., Pieper, J., Buma, P., van Kuppevelt, T. H., van Beuningen, H., van der Kraan, P. M., Veerkamp, J. H., van den Berg, W. B., and Veth, R. H. P. H., Linkage of chondroitin-sulfate to type I collagen scaffolds stimulates the bioactivity of seeded chondrocytes in vitro, *Biomaterials* 22, 2359-2369, 2001.
167. Farrell, E., O'Brien, F. J., Doyle, P., Fischer, J., Yannas, I., Harley, B. A., O´Connell, B., Prendergast, P. J., and Campbell, V. A., A collagen-glycosaminoglycan scaffold supports sdult rat mesenchymal stem cell differentiation along osteogenic and chondrogenic routes, *Tissue Engineering* 12, 459-469, 2006.
168. Chang, C. H., Kuo, T. F., Lin, C. C., Chou, C. H., Chen, K. H., Lin, F. H., and Liu, H. C., Tissue engineering-based cartilage repair with allogenous chondrocytes and gelatin-chondroitin-hyaluronan tri-copolymer scaffold: A porcine model assessed at 18, 24, and 36 weeks, *Biomaterials* 27, 1876-1888, 2006.
169. Fan, H., Hu, Y., Qin, L., Li, X., Wu, H., and Lv, R., Porous gelatin-chondroitin-hyaluronate tri-copolymer scaffold containing microspheres loaded with TGF-beta1 induces differentiation of mesenchymal stem cells in vivo for enhancing cartilage repair, *Journal of Biomedical Materials Research - Part A* 77, 785-794, 2006.
170. Chou, C. H., Cheng, W. T., Lin, C. C., Chang, C. H., Tsai, C. C., and Lin, F. H., TGF-beta1 immobilized tri-co-polymer for articular cartilage tissue engineering, *Journal of Biomedical Materials Research Part B - Applied Biomaterials* 77, 338-348, 2006.
171. Chou, C. H., Cheng, W. T. K., Kuo, T. F., Sun, J. S., Lin, F. H., and Tsai, J. C., Fibrin glue mixed with gelatin/hyaluronic acid/chondroitin-6-sulfate tri-copolymer for articular cartilage tissue engineering: The results of real-time polymerase chain reaction, *Journal of Biomedical Materials Research Part A* 82A, 757-767, 2007.
172. Murray, M. M., Rice, K., Wright, R. J., and Spector, M., The effect of selected growth factors on human anterior cruciate ligament cell interactions with a three-dimensional collagen-GAG scaffold, *Journal of Orthopaedic Research* 21, 238-244, 2003.
173. Chamberlain, L. J., Yannas, I. V., Hsu, H.-P., Strichartz, G., and Spector, M., Collagen-GAG substrate enhances the quality of nerve regeneration through collagen tubes up to level of autograft, *Experimental Neurology* 154, 315-329, 1998.
174. Powell, H. M. and Boyce, S. T., EDC cross-linking improves skin substitute strength and stability, *Biomaterials* 27, 5821-5827, 2006.
175. Nehrer, S., Breinan, H. A., Ramappa, A., Young, G., S., S., Louie, L. K., Sledge, C. B., Yannas, I. V., and Spector, M., Matrix collagen type and pore size influence behaviour of seeded canine chondrocytes, *Biomaterials* 16, 769-776, 1997.
176. Nehrer, S., Breinan, H. A., Ramappa, A., Hsu, H.-P., Minas, T., Shortkro, S., Sledge, C. B., Yannas, I. V., and Spector, M., Chondrocyte-seeded collagen matrices implanted in a chondral defect in a canine model, *Biomaterials* 19, 2313-2328, 1998.
177. Veilleux, M. S. and M. Spector, M., Effects of FGF-2 and IGF-1 on adult canine articular chondrocytes in type II collagen-glycosaminoglycan scaffolds in vitro, *OsteoArthritis and Cartilage* 13, 278-286, 2005.
178. Lee, C. R., Grodzinsky, A. J., and Spector, M., The effects of cross-linking of collagen-glycosaminoglycan scaffolds on compressive stiffness, chondrocyte-mediated contraction, proliferation and biosynthesis, *Biomaterials* 22, 3145-3154, 2001.
179. Chamberlain, L. J., Yannas, I. V., Hsu, H. P., Strichartz, G. R., and Spector, M., Near-terminus axonal structure and function following rat sciatic nerve regeneration through a

collagen-GAG matrix in a ten-millimeter gap, *Journal of Neuroscience Research* 60, 666-677, 2000.
180. Dambuyant, C. D., Black, A., Bechetoille, N., Bouez, C., Maréchal, S., Auxenfans, C., Cenizo, V., Pascal, P., Perrier, E., and Damour, O., Evolutive skin reconstructions: From the dermal collagen–glycosaminoglycan–chitosane substrate to an immunocompetent reconstructed skin, *Biomedical Materials and Engineering* 16, S85-S94, 2006.
181. Kataropoulou, M., Henderson, C., and Grant, H., Metabolic studies of hepatocytes cultured on collagen substrata modified to contain glycosaminoglycans, *Tissue Engineering* 11, 1263-1273, 2005.
182. Wang, T. W., Sun, J. S., Wu, H. C., Tsuang, Y. H., Wang, W. H., and Lin, F. H., The effect of gelatin-chondroitin sulfate-hyaluronic acid skin substitute on wound healing in SCID mice, *Biomaterials* 27, 5689-5697, 2006.
183. Wang, -. T.-W., Sun, J.-S., Wu, H.-C., Huang, Y.-C., and Lin, F.-H., Evaluation and biological characterization of bilayer gelatin/chondroitin-6-sulphate/hyaluronic acid membrane, *Journal of Biomedical Materials Research - Part B: Applied Biomaterials* 82B, 390-399, 2007.
184. Fan, H., Hu, Y., Zhang, C., Li, X., Lv, R., Qin, L., and Zhu, R., Cartilage regeneration using mesenchymal stem cells and a PLGA-gelatin/chondroitin/hyaluronate hybrid scaffold, *Biomaterials* 27, 4573-4580, 2006.
185. Lee, S. B., Lee, Y. M., Song, K. W., and Park, M. H., Preparation and properties of polyelectrolyte complex sponges composed of hyaluronic acid and chitosan and their biological behaviors, *Journal of Applied Polymer Science* 90, 925-932, 2003.
186. Choi, Y. S., Hong, S. R., Lee, Y. M., Song, K. W., Park, M. H., and Nam, Y. S., Studies on gelatin-containing artificial skin: II. Preparation and characterization of cross-linked gelatin-hyaluronate sponge, *Journal of Biomedical Materials Research - Applied Biomaterials* 48, 631-639, 1999.
187. Hong, S. R., Lee, S. J., Shim, J. W., Choi, Y. S., Lee, Y. M., Song, K. W., Park, M. H., Nam, Y. S., and Lee, S. I., Study on gelatin-containing artificial skin IV: a comparative study on the effect of antibiotic and EGF on cell proliferation during epidermal healing, *Biomaterials* 22, 2777-2783, 2001.
188. Angele, P., Kujat, R., nerlich, M., Yoo, J., Goldberg, V., and Johnstone, B., Engineering of osteochondral tissue with bone marrow mesenchymal progenitor cells in a derivatized hyaluronan-gelatin composite sponge, *Tissue Engineering* 5, 545-553, 1999.
189. Lee, S. B., Jeon, H. W., Lee, Y. W., Lee, Y. M., Song, K. W., Park, M. H., Nam, Y. S., and Ahn, H. C., Bio-artificial skin composed of gelatin and (1 -> 3), (1 -> 6)-beta-glucan, *Biomaterials* 24, 2503-2511, 2003.
190. Dawlee, S., Sugandhi, A., Balakrishnan, B., Labarre, D., and Jayakrishnan, A., Oxidized chondroitin sulfate-cross-linked gelatin matrixes: A new class of hydrogels, *Biomacromolecules* 6, 2040-2048, 2005.
191. Qin, Y., Alginate fibres: an overview of the production processes and applications in wound management, *Polymer International* 57, 171-180, 2008.
192. Suzuki, Y. N., Y., Tanihara, M. S., K., Kitahara, A. K. Y., Y., Nakamura, T. S., Y., and Kakimaru, Y., Development of alginate gel dressing, *Journal of Artificial Organs* 1, 28-32, 1998.
193. Chiu, C.-T., Lee, J.-S., Chu, C.-S., Chang, Y.-P., and Wang, Y.-J., Development of two alginate-based wound dressings, *Journal of Materials Science: Materials in Medicine* 19, 2503-2513, 2008.
194. Boateng, J. S., Matthews, K. H., Stevens, H. N., and Eccleston, G. M., Wound healing dressings and drug delivery systems: A review, *Journal of Pharmaceutical Sciences* 97,2892–2923, 2008.
195. Roh, D. H., Kang, S. Y., Kim, J. Y., Kwon, Y. B., Kweon, H. Y., Lee, K. G., Park, Y. H., Baek, R. M., Heo, C. Y., Choe, J., and Lee, J. H., Wound healing effect of silk fibroin/alginate-blended sponge in full thickness skin defect of rat, *Journal of Materials Science-Materials in Medicine* 17, 547-552, 2006.

196. Donaghue, V. M., Chrzan, J. S., Rosenblum, B. I., Giurini, J. M., Habershaw, G. M., and Veves, A., Evaluation of a collagen-alginate wound dressing in the management of diabetic foot ulcers, *Advances in Wound Care: The Journal for Prevention and Healing* 11, 114-119, 1998.
197. Gerard, C., Catuogno, C., Amargier-Huin, C., Grossin, L., Hubert, P., P., G., Netter, P., Dellacherie, E., and Payan, E., The effect of alginate, hyaluronate and hyaluronate derivatives biomaterials on synthesis of non-articular chondrocyte extracellular matrix, *Journal of Materials Science - Materials in Medicine* 16, 541-551, 2005.
198. Lindenhayn, K., Perka, C., Spitzer, R. S., Heilmann, H. H., Pommerening, K., Mennicke, J., and Sittinger, M., Retention of hyaluronic acid in alginate beads: Aspects for in vitro cartilage engineering, *Journal of Biomedical Materials Research* 44, 149-155, 1999.
199. Smetana, K., Cell biology of hydrogels, *Biomaterials* 14, 1046-1050, 1993.
200. Yan, Y., Wang, X., Xiong, Z., Liu, H., Liu, F., Wu, R., Zhang, R., and Lu, Q., Direct construction of a three dimensional structure with cells and hydrogel, *Journal of Bioactive and Compatible Polymers* 20, 259-269, 2005.
201. Hashimoto, T., Suzuki, Y., Tanihara, M., Kakimaru, Y., and Suzuki, K., Development of alginate wound dressings linked with hybrid peptides derived from laminin and elastin, *Biomaterials* 25, 1407-1414, 2004.
202. Choi, Y. S., Hong, S. R., Lee, Y. M., Song, K. W., Park, M. H., and Nam, Y. S., Study on gelatin-containing artificial skin: I. Preparation and characteristics of novel gelatin-alginate sponge, *Biomaterials* 20, 409-417, 1999.
203. Choi, Y. S., Lee, S. B., Hong, S. R., Lee, Y. M., Song, K. W., and Park, M. H., Studies on gelatin-based sponges. Part III: a comparative study of cross-linked gelatin/alginate, gelatin/hyaluronate and chitosan/hyaluronate sponges and their application as a wound dressing in full-thickness skin defect of rat, *Journal of Materials Science: Materials in Medicine* 12, 67-73, 2001.
204. Fan, L., Du, Y., Huang, R., Wang, Q., Wang, X., and Zhang, L., Preparation and characterization of alginate/gelatin blend fibers, *Journal of Applied Polymer Science* 96, 1625-1629, 2005.
205. Miralles, G., Baudoin, R., Dumas, D., Baptiste, D., Hubert, P., Stoltz, J. F., Dellacherie, E., Mainard, D., Netter, P., and E. Payan, E., Sodium alginate sponges with or without sodium hyaluronate: In vitro engineering of cartilage, *Journal Biomedical Materials Research* 57, 268-278, 2001.
206. Lee, K. G., Kweon, H. Y., Yeo, J. H., Woo, S. O., Lee, J. H., and Park, Y. H., Structural and physical properties of silk fibroin/alginate blend sponges, *Journal of Applied Polymer Science* 93, 2174-2179, 2004.
207. Balakrishnan, B., Mohanty, M., Umashankar, P. R., and Jayakrishnan, A., Evaluation of an in situ forming hydrogel wound dressing based on oxidized alginate and gelatin, *Biomaterials* 26, 6335-6342, 2005.
208. Klemm, D., Heublein, B., Fink, H. P., and Bohn, A., Cellulose: fascinating biopolymer and sustainable raw material, *Angewandte Chemie International Edition* 44, 3358-3393, 2005.
209. Hart, J., Silcock, D., Gunnigle, S., Cullen, B., D., L. N., and Watt, P. W., The role of oxidised regenerated cellulose/collagen in wound repair: effect in vitro on fibroblast biology and in vivo in a model of compromised healing, *The International Journal of Biochemistry& Cell Biology* 34, 1557-1570, 2002.
210. Jeschke, M. G., Sandmann, G., Schubert, T., and Klein, D., Effect of oxidized regenerated cellulose/collagen matrix on dermal and epidermal healing and growth factors in an acute wound, *Wound Repair and Regulation* 13, 324-331, 2005.
211. Cullen, B., Watt, P. W., Lundqvist, C., Silcock, D., Schmidt, R. J., Bogan, D., and Light, N. D., The role of oxidised regenerated cellulose/collagen in chronic wound repair and its potential mechanism of action, *The International Journal of Biochemistry& Cell Biology* 34, 1544-1556, 2002.

212. Svensson, A., Nicklasson, E., Harrah, T., Panlaitis, B., Kaplan, D. L., Brittberg, M., and Gatenholm, P., Bacterial cellulose as a potential scaffold for tissue engineering of cartilage, *Biomaterials* 26, 419-431, 2005.
213. Czaja, W. K., Young, D. J., Kawecki, M., and Brown, R. M., The future prospects of microbial cellulose in biomedical applications, *Biomacromolecules* 8, 1-12, 2007.
214. Helenius, G., Backdahl, H., Bodin, A., Nannmark, U., Gatenholm, P., and Risberg, B., In vivo biocompatibility of bacterial cellulose, *Journal of Biomedical Materials Research* 76A, 431-438, 2006.
215. Strobin, G., Wawro, D., Stęplewski, W., Ciechanska, D., Jóźwicka, J., Sobczak, S., and Haga, A., Formation of cellulose/silk-fibroin blended fibres, *Fibres & Textiles* 14, 32-35, 2006.
216. Ya, G. V. and Tolstoguzov, V. B., Thermodynamic incompatibility of proteins and polysaccharides in solutions, *Food Hydrocolloids* 11, 145-158, 1997.
217. Tolstoguzov, V. B., Phase behaviour of macromolecular components in biological and food systems, *Nahrung/Food* 44, 299-308, 2000.
218. Doublier, J. L., Garnier, C., Renard, D., and Sanchez, C., Protein-polysacharide interactions, *Current Opinion in Colloid and Interface Science* 5, 202-214, 2000.
219. Kruif, C. G. and Tuinier, R., Polysaccharide protein interactions, *Food Hydrocolloids* 15, 555-563, 2001.
220. Musampa, R. M., Alves, M. M., and Maia, J. M., Phase separation, rheology and microstructure of pea protein–kappa-carrageenan mixtures, *Food Hydrocolloids* 21, 92-99, 2007.
221. Berthand, M. E. and Turgeon, S. L., Improved gelling properties of whey protein isolate by addition of xantham gum, *Food Hydrocolloids* 21, 159-166, 2007.
222. de Kruif, C. G., Weinbreck, F., and de Vries, R., Complex coacervation of proteins and anionic polysaccharides, *Current Opinion in Colloid and Interface Science* 9, 340-349, 2004.
223. Sanchez, C. and Renard, D., Stability and structure of protein–polysaccharide coacervates in the presence of protein aggregates, *International Journal of Pharmaceutics* 242, 319-324, 2002.
224. Turgeon, S. L., Schmitt, C., and Sanchez, C., Protein–polysaccharide complexes and coacervates, *Current Opinion in Colloid and Interface Science* 12, 166-178, 2007.
225. Noel, T. R., Krzeminski, A., Moffat, J., Parker, R., Wellner, N., and Ring, S. G., The deposition and stability of pectin/protein and pectin/poly-L-lysine/protein multilayers, *Carbohydrate Polymers* 70, 393-405, 2007.
226. Xing, F., Cheng, G. X., Yang, B., and Ma, L., Nanoencapsulation of capsaicin by complex coacervation of gelatin, acacia, and tannins, *Journal of Applied Polymer Science* 96, 2225-2229, 2005.
227. Dickinson, E., Colloid science of mixed ingredients, *Soft Matter* 2, 642-652, 2006.
228. Feldman, D., Polyblend compatibilization, *Journal of Macromolecular Science - Part A: Pure and Applied Chemistry* 42, 587-605, 2005.
229. Malay, O., Bayraktar, O., and Batigun, A., Complex coacervation of silk fibroin and hyaluronic acid, *International Journal of Biological Macromolecules* 40, 387-93, 2007.
230. Palmiere, G. P., Lauri, D., Martelli, S., and Wehrle, P., Methoxybutropate microencapsulation by gelatin-acacia complex coacervation, *Drug Development and Industrial Pharmacy* 25, 399-407, 1999.
231. Naidu, B. V. K., Sairam, M., Raju, K. V. S. N., and Aminabhavi, T. M., Thermal, viscoelastic, solution and membrane properties of sodium alginate/hydroxyethylcellulose blends, *Carbohydrate Polymers* 61, 52-60, 2005.
232. Sionkowska, A., Wisniewski, M., Skopinska, J., Kennedy, C. J., and Wess, T. J., Molecular interactions in collagen and chitosan blends, *Biomaterials* 25, 795-801, 2004.
233. Christopoulou, V., Papanagopoulos, D., and Dondos, A., Relation between the repulsion of incompatible and compatible polymers in solution and their degree of mixing in the solid state: the memory effect, *Polymer International* 49, 1365-1370, 2000.

234. Koning, C., van Duin, M., Pagnoulle, C., and Jerome, R., Strategies for compatibilization of polymer blends, *Progress in Polymer Science* 23, 707-757, 1998.
235. Park, S. N., Park, J. C., Kim, H. O., Song, M. J., and Suh, H., Characterization of porous collagen/hyaluronic acid scaffold modified by 1-ethyl-3-(3-dimetylaminopropyl)carbodiimide cross-linking, *Biomaterials* 23, 1205-1212, 2002.
236. Harriger, M. D., Supp, A. P., Warden, G. D., and Boyce, S. T., Glutaraldehyde crosslinking of collagen substrates inhibits degradation in skin substitutes grafted to athymic mice, *Journal of Biomedical Materials Research* 35, 137-145, 1997.
237. Silva, R. M., Mano, J. F., and Reis, R. L., Preparation and characterization in simulated body conditions of glutaraldehyde crosslinked chitosan membranes, *Journal of Materials Science-Materials in Medicine* 15, 1105-112, 2004.
238. Sung, H. W., Hsu, C. S., Lee, Y. S., and Lin, D. S., Crosslinking characteristics of an epoxy-fixed porcine tendon: effects of pH, temperature and fixative concentration, *Journal of Biomedical Materials Research* 31, 511-518, 1996.
239. Sung, H. W., Huang, R. N., Huang, L. L. H., Tsai, C. C., and Chiu, C. T., Feasibility study of a natural crosslinking reagent for biological tissue fixation, *Journal of Biomedical Materials Research* 42, 560-567, 1998.
240. Koo, H. J., Song, Y. S., Kim, H. J., Lee, Y. H., Hong, S. M., Kim, S. J., Kim, B. C., Jin, C., Lim, C. J., and Park, E. H., Antiinflammatory effects of genipin, an active principle of gardenia, *European Journal of Pharmacology* 495, 201-208, 2004.
241. Chang, W. H., Chang, Y., Lai, P. H., and Sug, H. W., A genipin-crosslinked gelatin membrane as wound-dressing material: in vitro and in vivo studies, *Journal of Biomaterials Science-Polymer Edition* 14, 481-495, 2003.
242. Liu, B. S., Yao, C. H., Hsu, S. H., Yeh, T. S., Chen, Y. S., and Kao, S. T., A novel use of genipin-fixed gelatin as extracellular matrix for peripheral nerve regeneration, *Journal of Biomaterials Applications* 19, 21-34, 2004.
243. Sundararaghavan, H. G., Monteiro, G. A., Lapin, N. A., Chabal, Y. J., Miksan, J. R., and Shreiber, D. I., Genipin-induced changes in collagen gels: Correlation of mechanical properties to fluorescence, *Journal of Biomedical Materials Research Part A* DOI:10.1002/jbm.a.31715, 2008.
244. Meena, R., Prasad, K., and Siddhanta, A. K., Effect of genipin, a naturally occurring crosslinker on the properties of kappa-carrageenan, *Int J Biol Macromol* 41 (1), 94-101, 2007.
245. Mi, F. L., Tan, Y. C., Liang, H. F., and Sung, H. W., In vivo biocompatibility and degradability of a novel injectable-chitosan-based implant, *Biomaterials* 23, 181-191, 2002.
246. Kuo, Y. C. and Lin, C. Y., Effect of genipin-crosslinked chitin-chitosan scaffolds with hydroxyapatite modifications on the cultivation of bovine knee chondrocytes, *Biotechnology and Bioengineering* 95, 132-144, 2006.
247. Chen, H., Ouyang, W., Lawuyi, B., Martoni, C., and Prakash, S., Reaction of chitosan with genipin and its fluorogenic attributes for potential microcapsule membrane characterization, *Journal of Biomedical Materials Research Part A* 75, 917-927, 2005.
248. Chen, H., Ouyang, W., Lawuyi, B., and Prakash, S., Genipin cross-linked alginate-chitosan microcapsules: membrane characterization and optimization of cross-linking reaction, *Biomacromolecules* 7, 2091-8, 2006.
249. Park, J. E., Isolation and characterizaton of water-soluble intermediates of blue pigments transformed from geniposide of gardenia jasminoides, *Journal of Agriculture and Food Chemistry* 50, 6511-6514, 2002.
250. Han, B., Jaurequi, J., Tang, B. W., and Nimni, M. E., Proanthocyanidin: A natural crosslinking reagent for stabilizing collagen matrices, *Journal of Biomedical Materials Research Part A* 65, 118-124, 2003.
251. Kim, S., Nimni, M. E., Yang, Z., and Han, B., Chitosan-gelatin–based films crosslinked by proanthocyanidin, *Journal of Biomedical Materials Research Part B: Applied Biomaterials* 75B, 442-450, 2005.

252. Oehr, Plasma surface modification of polymers for biomedical use, *Nuclear Instruments and Methods in Physics Research B* 208, 40-47, 2003.
253. Chu, P. K., Chen, J. Y., Wang, L. P., and Huang, N., Plasma surface modification of biomaterials, *Materials Science and Engineering Reviews* 36, 143-206, 2002.
254. Pashkuleva, I., Marques, A. P., Vaz, F., and Reis, R. L., Surface modification of starch based blends using potassium permanganate-nitric acid system and its effect on the adhesion and proliferation of osteoblast-like cells, *Journal of Materials Science - Materials in Medicine* 16, 81-92, 2005.
255. Tangpasuthadol, V., Pongchaisirikul, N., and Hoven, V. P., Surface modification of chitosan films. Effects of hydrophobicity on protein adsorption, *Carbohydrate Research* 338, 937-942, 2003.
256. Olbrich, M., Punshon, G., Frischauf, I., Salacinski, H., Rebollar, E., Romanin, C., Seifalian, A. M., and Heitz, J., UV surface modification of a new nanocomposite polymer to improve cytocompatibility, *Journal Biomaterials Science- Polymer Edition* 18, 453-468, 2007.
257. Welle, A., Horn, S., Schimmelpfeng, J., and Kalka, D., Photo-chemically patterned polymer surfaces for controlled PC-12 adhesion and neurite guidance, *Journal of Neuroscience Methods* 142, 243-250, 2005.
258. Gumpenberger, T., Heitz, J., Bäuerle, D., Kahr, H., Graz, I., Romanin, C., Svorcik, V., and Leisch, F., Adhesion and proliferation of human endothelial cells on photochemically modified polytetrafluoroethylene, *Biomaterials* 24, 5139-5144, 2003.
259. Yang, F., Li, X., Cheng, M., Gong, Y., Zhao, N., and Zhang, X., Performance modification of chitosan membranes induced by gamma irradiation, *Journal of Biomaterials Applications* 16, 215-226, 2002.
260. Mao, C., Qiu, Y., Sang, H., Mei, H., Zhu, A., Shen, J., and Lin, S., Various approaches to modify biomaterial surfaces for improving hemocompatibility, *Advances in Colloid and Interface Science* 110, 5-17, 2004.
261. Silva, S. S., Luna, S. M., Gomes, M. E., Benesch, J., Paskuleva, I., Mano, J. F., and Reis, R. L., Plasma surface modification of chitosan membranes: characterization and preliminary cell response studies, *Macromolecular Bioscience* 8,568-576, 2008.
262. Zhu, X., Chian, K. S., Chan-Park, M. B. E., and Lee, S. T., Effect of argon-plasma treatment on proliferation of human-skin-derived fibroblast on chitosan membrane in vitro, *Journal of Biomedical Materials Research Part A* 73A, 264-274, 2005.
263. Pashkuleva, I. and Reis, R. L., Surface activation and modification - a way for improving the biocompatibility of degradable biomaterials, in *Biodegradable systems in tissue engineering and regenerative medicine*, Reis, R. L. and Román, J. S. CRC Press, 2005, pp. 430.
264. Huang, Y.-C., Huang, C.-C., Huang, Y.-Y., and Chen, K.-S., Surface modification and characterization of chitosan or PLGA membrane with laminin by chemical and oxygen plasma treatment for neural regeneration, *Journal of Biomedical Materials Research - Part A* 82A, 842-851, 2007.
265. Pérez, P. M. L., Marques, A. P., Silva, R. M. P., Pashkuleva, I., and Reis, R. L., Effect of chitosan´surface modification via plasma induced polymerization on the adhesion of osteoblast-like cells, *Journal of Materials Chemistry* 17, 4064-4071, 2007.
266. Ratner, B. D., Surface modification of polymers: chemical, biological and surface analytical challenges, *Biosensors & Bioelectronics* 10, 797-804, 1995.
267. Goddard, J. M. and Hotchkiss, J. H., Polymer surface modification for the attachment of bioactive compounds, *Progress in Polymer Science* 32, 698-725, 2007.
268. Khonsari, F. A., Tatoulian, M., Shahidzadeh, N., and Amouroux, J., Study of the plasma treated polymers and the stability of the surface properties, in *Plasma processing of polymers*, Agostino, R., Favia, P., and Fracassi, F.2003, pp. 165-193.
269. Inagaki, N., Plasma modification by implantation, in *Plasma Surface Modification and Plasma Treatment* Technomic Publishing Company, Inc., Basel, 1996, pp. 63.

270. Forch, R., Zhang, Z., and Knoll, W., Soft plasma treated surfaces: tailoring of structure and properties for biomaterial applications, *Plasma Processes and Polymers* 2, 351-372, 2005.
271. Shi, J., Alves, N. M., and Mano, J. F., Thermally responsive biomineralization on biodegradable substrates, *Advanced Functional Materials* 17, 3312-3318, 2007.
272. RMP, d. S., Mano, J. F., and Reis, R. L., Smart thermo-responsive coatings and surfaces for tissue engineering:switching cell-material boudaries, *Trends in Biotechnology* 25, 577-583, 2007.

CHAPTER II

CHAPTER II

Materials and Methods

The main of this chapter is to describe in more detail the experimental work that was employed throughout the thesis. Each of the following six chapters has a section on "Materials and Methods", but due to constraints of article length it is not possible to show all the details necessary for the correct understanding of the experiments performed.

1. Materials

Many materials with different properties and shapes (membranes, hydrogels, sponges, nanofibers) were produced from chitosan, soy protein isolate and silk fibroin or by conjugated them. The methodologies used to obtain and modify the materials were based on sol-gel process, solvent casting, plasma surface modification, chemical cross-linking and electrospining processing.

- *Chitosan*

Chitosan (Cht) is the N-deacetylated derivative chitin, a natural polysaccharide polymer [1,2]. Important parameters of this polysaccharide are its molecular weight and the degree of deacetylation[3] that means the number percentage of glucosamine in the chitosan structure (see structure in Chapter III)[2]. In general, these parameters will determine the physico-chemical and biological properties of the polymer [2]. Chitosan used in the studies was purchased from Sigma Aldrich with low (LM) and medium molecular weight (MM). As the chitosan used is a commercial product, impurities can be present in the material resulting of the obtaining process. To remove these impurities, Cht was purified by a re-precipitation method[4]. For this process, Cht powder was dissolved at a concentration of 1% (w/v) in 2% (v/v) aqueous acetic acid. The system was

maintained under stirring overnight at room temperature (RT). After that, the solution was filtered twice to remove the insoluble material. From the clear solution, Cht was precipitated using 1M aqueous sodium hydroxide (NaOH), while stirring. Finally, the precipitate was separated by filtration from liquid, and the Cht powder was repeatedly washed with distilled water until neutrality (pH ≈7). White flakes of Cht were obtained after lyophilization for 4 days. After purification, the degree of N-deacetylation [3] of polymer was determined using ^{1}H Liquid state nuclear magnetic resonance (^{1}H NMR) [5]. For this analysis, Cht (10 mg) was dissolved in deuterium chloride (DCl) in D_2O at room temperature. The DD value was found to be 81.2% (LM) and 83.8 % (MM). Also, the molecular viscosimetric weight (Mv) was determined by viscosimetry in 0.1M acetic acid/0.2 M sodium acetate as described previously [6]. The Mv values were 591 kDa (LM) and 662 kDA (MM).

Regarding to solubility, chitosan is soluble in acid conditions but insoluble in neutral or basic pH conditions, while soluble in acid pH, the amino units ($-NH_2$) of the structure become protonated to form cationic amine units ($-NH_3^+$) [7]. This cationic character associated to availability of its functional groups (amino and hydroxyl) allows to modify its structure, and also conjugate it with other biopolymers and bioactive agents [1].

- *Soy protein isolate*

Soybeans are processed into three kinds of protein-rich products: soy flour, soy concentrate, and soy isolate [8]. Soy protein, the major component of the soybean (30-45%) is readily available from renewable resources, economically competitive and present good water resistance as well as storage stability[9]. Soy protein isolate used in this thesis was provided by Loders Crocklaan (The Netherlands). Structurally soy protein is formed by two subunits, namely 35% conglycinin (7S) and 52% glycinin (11S) [10]. The determination of molecular weight of these soy components was performed using sodium dodecyl sulfate-polyacrylamide gel electrophoresis (SDS-PAGE). For that, soy protein was dispersed in solvent buffer systems namely, 182mM $NaHCO_3$ and 31.8 mM Na_2CO_3 (pH 10.6) and 8M urea plus

0.1 M beta-mercaptoethanol (pH 10.6), conform described previously [11]. The molecular weight values found were 18kDa for conglycinin and 38kDa for glycinin. On the other hand, soy protein has many reactive groups, such as $–NH_2$, -OH and –SH, which are susceptible to chemical modifications [12] and, also allow its combination with others biopolymers [13]. In this context, a series of blended membranes composed by chitosan and soy protein dispersion was prepared by solvent casting in order to join their intrinsic properties in a unique material.

- *Silk fibroin*

Silk fibroin (SF) is a highly insoluble fibrous protein produced by domestic silk worms *(Bombyx mori)* containing up to 90% of the amino acids glycine, alanine, and serine leading to antiparallel β-pleated sheet formation in the fibers [14]. Fibroin is a structural protein of silk fibers and sericins are the water-soluble glue-like proteins that bind the fibroin fibers together [15]. Traditionally, silk fibroin has been used for decades as suture material [15]. Nowadays, several studies demonstrated the utility of silk matrices for biomaterials in skin, cartilage and bone applications [15,16]. Silk from cocoons of *Bombyx mori* used in the studies was kindly provided from Cooperativa Socio Lario, Como, Italy. Silk was first degummed to remove the sericins (Figure 1). Degumming was achieved by boiling the silk filaments for 1hour in water containing 1.1 g/L of Na_2CO_3 and, then for 30 min in water with 0.4g/L of Na_2CO_3. The resulting fibroin filaments were extensively rinsed in hot distilled water and dried in the air at room temperature. Removal of the sericin coating before use removes the thrombogenic and inflammatory response of silk fibroin [3]. To prepare solutions to be used in the production of materials, fibroin was dissolved in 9.3 M lithium bromide (LiBr) overnight at 65°C. The solutions were dialyzed to get pure fibroin solutions, which were added to chitosan solution for preparation of hydrogels. Alternatively, the silk fibroin water solution was frozen in liquid nitrogen and lyophilized to obtain pure fibroin powder to preparation of nanofibers. The amino acid composition of silk fibroin was assessed by High

Performance Liquid Chromatography (HPLC) reverse phases (RP-HPLC) on a AccQ•Tag column (3.9 x150mm, Waters Corporation) with a gradient of Waters AccQ.Tag Eluent A, Milli-Q water and Acetonitrile (HPLC grade) at a flow rate of 1ml/min. The amino acids were detected with UV detector (JascoUV1570) at 254 nm. Silk fibroin molecule was formed mainly of glycine (46.7%), alanine (31.4%), and serine (8.5%).

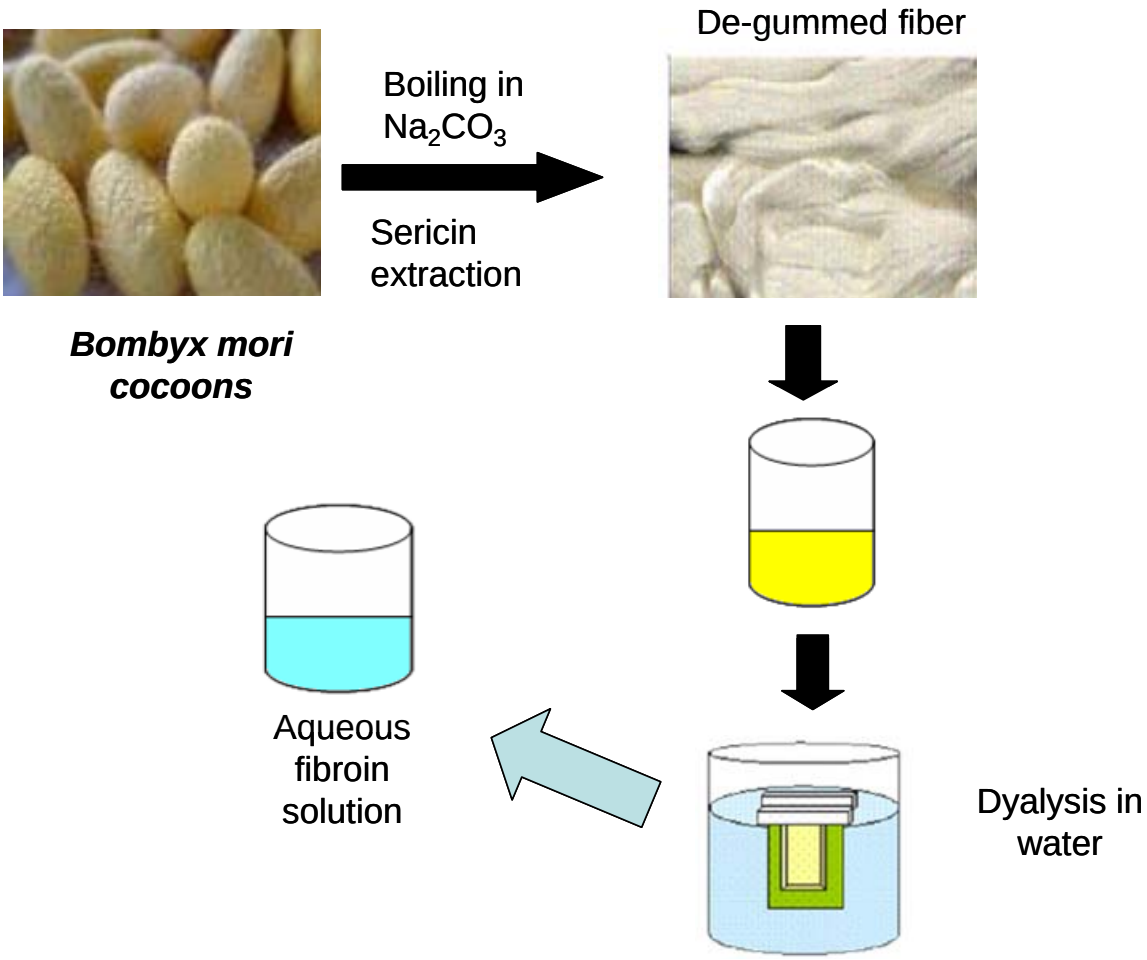

Figure 1. Schematic diagram for purification of silk fibroin.

2. **Methods and production of the materials**

2.1. *Sol gel process*

Sol-gel chemistry constitutes a versatile method that allows not only manufacturing inorganic glasses, but also to combine organic and inorganic or even bioactive components in a single hybrid material [17]. Usually, an appropriate choice of the organic (*i.e.* synthetic or natural, chemical functionalities, wettability, etc) and inorganic components (chemical nature, structure and the size) as well as reaction parameters (solvent, catalyst, concentration of the reactants) allow to tailor hybrids in various shapes that may be both biodegradable and bioactive and therefore can construct matrices appropriate for soft and or hard tissue replacement [18]. In conventional sol-gel pathways inorganic networks are obtained through hydrolysis and further condensation reactions of functionalized silane-coupling agents to form a colloidal suspension of siloxane polymers (sol) and gelation of the sol to create a network in a continuous liquid phase (gel) [17]. Moreover, the characteristics and properties of a particular sol-gel inorganic network are related to a number of factors that affect the rate of hydrolysis and condensation, such as temperature, pH, reaction time, solvent, concentration and nature of the reactants and catalyst. For example, the presence of an organic component could influence the reaction kinetics, morphology, and the mechanical and thermal properties of the resultant hybrid materials [18]. In this way, a sol-gel method was used in the production of chitosan/siloxane hybrids (Chapter III). With this purpose, chitosan was previously dispersed in dimethylformamide (DMF) and reacted with a silane coupling agent, 3-isocyanatopropyltriethoxysilane (ICPTES), for 48 hours at 105 °C under N_2 atmosphere. As ICPTES is an isocyanate that reacted rapidly in the presence of water, DMF was used instead acetic acid solution for dispersion of the polymer, and also to enhance the efficiency of the reaction. As a second step, an acetic/ethanol mixture in the ratio molar ICPTES: acetic acid: ethanol of 1:3:6 and 1:6:6 was added to dispersion prepared in step 1 to promote the hydrolysis and condensations reactions. The mixture was stirred in a sealed

flask for 24 h at room temperature in inert atmosphere. The materials were obtained as fine powders (see Figure 2). Subsequently, the DMF was separated from the product by centrifugation and washed several times with methanol, after which this solvent was evaporated and the solid allowed to dry overnight in an oven at 60°C.

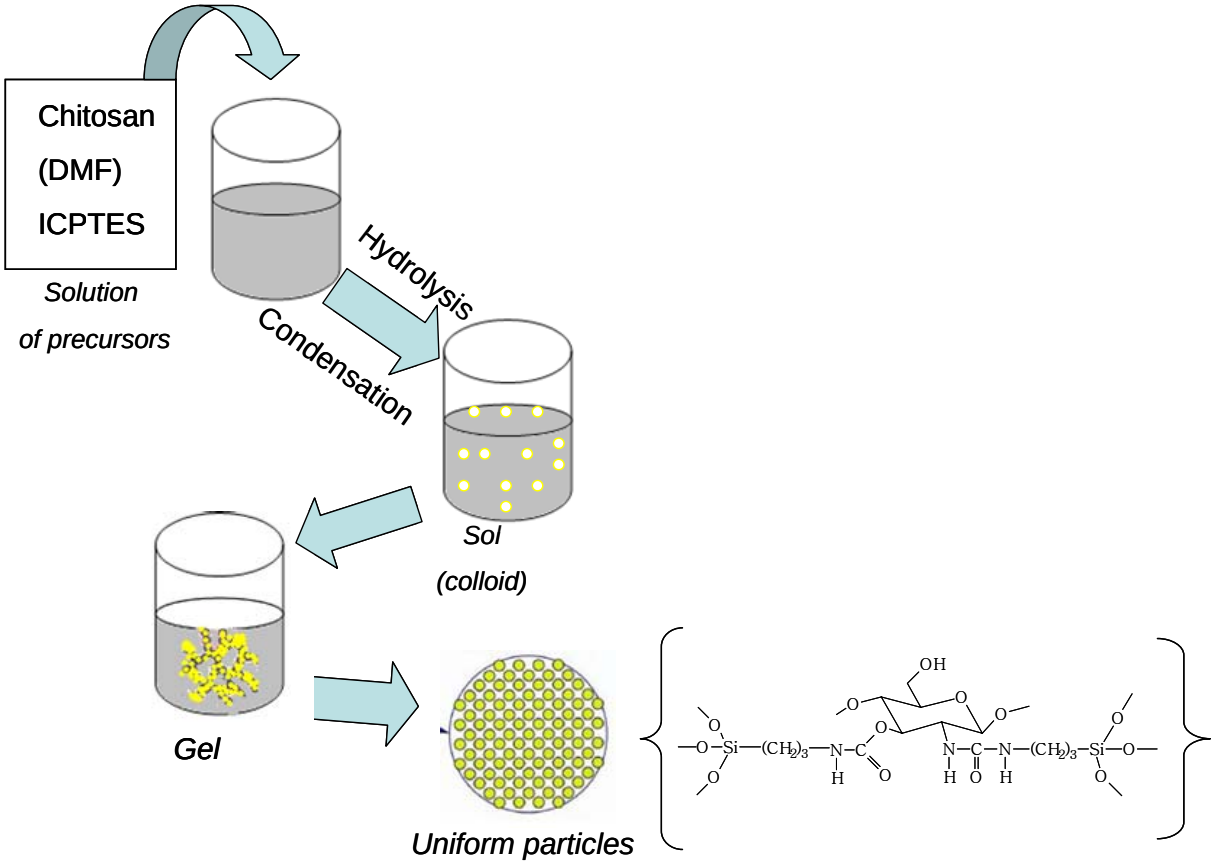

Figure 2. Schematic representation for preparation of the chitosan/siloxane hybrids by a sol-gel method.

2.2. *Plasma surface modification (PSM)*

PSM is a method widely used to modify material surface keeping its bulk properties [19]. When the plasma contacts with the surface of polymers within the reactor, the activated species initiate chemical and physical reactions, which depending on operating conditions (gas, power, and exposure time), will modify the material surface properties *e.g.* wettability, surface chemistry and roughness [19,20]. These surface changes can provide the appropriate answer in biological environments. Based on this principle, chitosan membranes (average thickness of 47μm) were prepared by solvent casting technique and submitted to plasma treatment. In preliminary studies, oxygen, nitrogen and argon were tested. However, the oxygen treated membranes were fragile and highly hydrophilic while membranes treated with argon and nitrogen showed good handling with good wettability. Besides, a study of variation of power (20, 40 and 60 watts) showed that a power higher than 20 watts produced fragile membranes. The plasma treatment was carried out in a radio frequency plasma reactor (PlasmaPrep5, Germany). The plasma chamber was thoroughly purged with a continuous flow of the gas used during the treatment to reduce trace amounts of air and moisture. During the treatment the gas flow was adjusted in order to keep a constant pressure of 0.2 mbar insight the chamber. A power of 20W was applied. The duration of the treatment was varied from 10 min to 40 min. Two different working gases, namely nitrogen (N_2) and argon (Ar) were used in order to evaluate the effect of the working gas on the induced changes in the surface functionalities and, subsequently how they will affect the cell responses of biomaterial.

2.3. *Chemical cross-linking*

Usually, crosslinking agents are used for covalently linking distinct chemical functional groups present in a determined biopolymer [21] in order to improve its stiffness, to reduce its hydrophilicity, to control the degradation rate or even to

increase the interaction between components in a binary system. The preparation of cross-linked chitosan-based materials focused on the use of glutaraldehyde (GA) and genipin (G) as cross-linking reagents (Figure 3). Glutaraldehyde is one of the chemical reagents frequently used to covalently cross-link chitosan [22]. The reaction between glutaraldehyde with the primary amine groups forms a Schiff base reaction, which can occur by three different ways as explained by different authors [22,23]. In Chapter V, chitosan/soy protein (CS) blended systems were prepared by different compositions the ratios, namely CS75, CS50 and CS25, corresponding to 75/25, 50/50, 25/75 wt% chitosan/soy. Cross-linking on these blended systems was performed *in situ* with GA solutions (5. 10^{-3} M – 0.1M) to enhance the interaction between the blended components and thus, to obtain different morphologies and a wide range of characteristics. Additionally, the influence of chemical cross-linking with GA on CS blended system was evaluated by water uptake, degradation rate and cell adhesion on CS membranes.

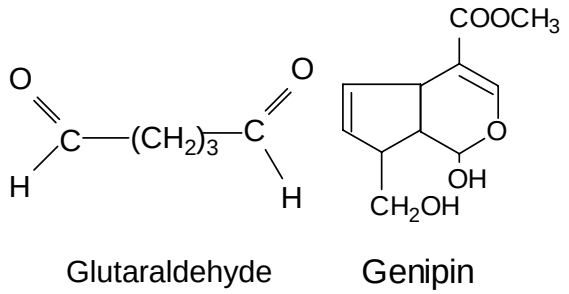

Figure 3. Chemical structures of the selected cross-linking reagents.

Also, genipin have also been proposed to cross-link chitosan and certain proteins [24]. In the reaction mechanism, the ester groups of genipin interact with the amino groups of chitosan and/or proteins leading to the formation of secondary amide linkages. Additionally, the amino groups initiate a nucleophilic attacks to genipin, resulting in the opening of the dihydropyran ring followed by a number of reaction steps [25]. Genipin powder (12% related to total weight of fibroin in solution) was used in the preparation of chitosan/silk fibroin (CS) based sponges. For that, Cht

and SF solutions prepared in aqueous acetic acid and water, respectively, were mixed in different ratios corresponding to 20/80 (CS80), 50/50 (CS50) and 80/20 (CS20) wt% CS. After homogenization, genipin powder was added to the CS systems, which were maintained under stirring for 24 hours at 37°C. The resulting hydrogels were freeze-dried to obtain cross-linked chitosan/silk fibroin (CSG) sponges. An evaluation of the structural changes, morphological and mechanical properties of the CSG sponges was performed. Additionally, the degree of cross-linking of the CSG sponges was determined by the ninhydrin assay [24]. Briefly, a lyophilized sample (3mg) was heated with a ninhydrin solution (2wt%, w/v), and the optical absorbance was measured. The number of free amine groups in the sample before and after cross-linking, after heating with ninhydrin, was considered be proportional to the optical absorbance of the solution [24], making possible to determine the cross-linking degree of the samples.

2.4. *Electrospinning (ELE)*

Electrospinning is a method used to produce nano-scale polymer fibers from natural and synthetic polymers [26,27]. The resulting nanofibers have useful properties such as high surface area and high porosity. In ELE process, fibers are formed as the surface charge of the polymer droplet overcomes its surface tension in an applied field, causing an instability that creates jets of polymer that are collected as solvent evaporates [27]. In general, the fiber diameter depends on the electrospinning parameters (*e.g*. voltage, flow rate, distance needle tip-target) and the polymer characteristics (concentration, viscosity, conductivity) [27]. ELE was used for the development of modified silk nanofiber nets as described in Chapter VIII. Briefly, the polymeric solution with a concentration of 12% was prepared by dissolving regenerated silk fibroin in neat formic acid with the addition of genipin. Formic acid was used to enhance the conductivity of the polymer solution for this process. The systems were maintained under stirring for pre-determined time (2, 15 and 24 hours) at 37°C. After that, the SF solutions were processed using ELE process,

which is presented schematically in Figure 4. A syringe with the SF solution was placed on an automatic syringe pump to maintain a constant volume flow rate. The operating parameters selected for producing the nanofibers were the following: voltage 21kV, flow rate 0.005 ml/min, distance between the needle tip and the target (aluminium foil set at ground voltage) was set to 10 cm and room temperature. Nitrogen gas was injected continuously in the system during the electrospinning process to control the humidity, which was regulated to a range of 20-30%. The resulting nanofibers were dried in vacuum for 1 week prior the analysis.

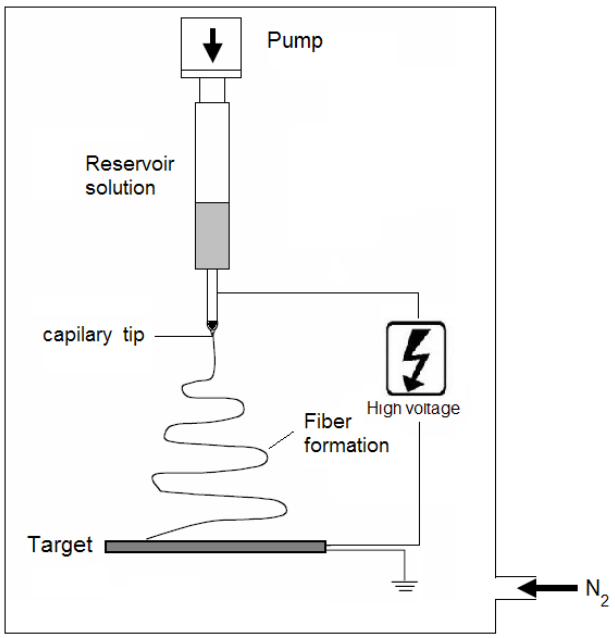

Figure 4. Experimental set-up for electrospinning, used to produce modified silk nets.

3. **Characterization of the Materials and Solutions**

3.1. *Rheological characterization*

Rheological measurements can describe the flow and deformation behaviour of materials under the effect of different parameters (shear, frequency, time, temperature, concentration)[28]. Rheological or viscoelastic evaluation is done through flow measurements and dynamical mechanical tests. The first one investigates the flow viscosity, whereas the latter evaluates small periodic deformations that determine molecular-level mobility or rearrangement of structure. For example, the time sweep test provides a means of monitoring the time-dependent behaviour of a material. It measures the storage modulus, G', which is an indicator of elastic behavior and reveals the ability of the polymer system to store elastic energy while the loss modulus, G'', is a measure of the dynamic viscous behaviour. Additionally, loss tangent (tan δ) is a parameter that represents the ratio between the viscous and elastic components of the modulus of the polymer, being a good indicator of the overall viscoelastic nature of the samples, and is dimensionless. The relationship between G´, G´´ and tan δ is calculated following the equation (2)[28].

$$\tan \delta = G''/G' \qquad \text{Equation 1}$$

In our studies, time sweep testes were performed using an Advanced Expansion System (ARES). The measurements were performed at 37°C, frequency of 5 rad/s and strain 5%. These tests served to characterize the behaviour of the CS blended solutions and to monitor the build-up of the network structure. Moreover, these tests also were used to study the behaviour of the regenerated silk fibroin solution before and after addition of genipin.

3.2. *Morphology*

The surface morphology of the materials obtained in this thesis (membranes, sponges and nanofibers) was analyzed by scanning electronic microscopy (SEM). SEM analysis was performed on samples gold-sputter coated using both Leica Cambridge S-360 and Cambridge Steroscan 100 model equipped with a with a LINK eXLII X-ray energy dispersion spectrometer for silicon microanalysis. The micrographs were taken at 10kV and different magnifications. In some cases, SEM photos were used to determine the fiber diameters of the nanofibrous membranes as described in Chapter VIII. Additionally, the CSG hydrogels prepared in Chapter VII were observed and photographed in an optical microscope with an image acquisition system (Zeiss – Axiotech; HAL 100, Germany). Besides, CSG hydrogels were freeze-dried and their morphology was studied by Environmental scanning electronic microscopy (ESEM). ESEM analysis was performed on samples without any treatment using a Philips XL 30 ESEM, Philips, Eindhoven, The Netherlands, at a vaccum pressure level of 0.8 Torr.

In the case of chitosan/silk fibroin sponges, a μCT imaging system (Skyscan 1072 X-ray microtomograph,Belgium) was used to determine the mean porosity. During the measurement, both the X-ray source and the detector are fixed while the sample rotates around a stable vertical axis. Samples were scanned at a voltage of 40kV and a current of 248μA. After reconstruction of the two-dimensional (2D) cross-sections, a Skyscan ™ CT-analyser software was used to segment of the images and determine their 3D porosity. 200 slices of a region of interest corresponding to the structure of sponges were selected from the CT data set. A customized threshold technique was used to enhance the CS contrast and remove noise.

3.3. *Surface topography*

The surface roughness of chitosan-based membranes was measured by atomic force microscopy (AFM). The analyses were performed on at least three spots per sample using TappingMode (Veeco, USA) connected to a NanoScope III (Veeco, USA) with non-contacting silicon nanoprobes (ca 300kHz, setpoint 2-3V) from Nanosensors, Switzerland. All images were fitted to a plane using the 3rd degrees flatten procedure included in the NanoScope software version 4.43r8. The surface roughness was calculated as Sq (root mean square from average flat surface) and Sa (average absolute distance from average flat surface). The values are presented as mean ± standard deviation.

3.4. *Fourier Transform Infrared with Attenuated Total Reflection (FTIR-ATR)*

The chemical structure of the surfaces and the conformational changes of the materials were assessed by FTIR-ATR and FTIR spectroscopy. FTIR-ATR spectra on chitosan-based membranes were recorded at least 32 scans with a resolution of 2 cm^{-1} in FTIR spectrophotometer (Perkin-Elmer 1600 series and Bio-Rad FTS6000). Also, FTIR spectra of KBr pellets of chitosan/siloxane hybrids were recorded (64 scans with a resolution of 4 cm^{-1}) on a Unican Mattson Mod 7000 FTIR. To examine the conformational changes on silk nanofibers a curve fitting of the bands were performed with the ORIGIN® (OriginLab Corporation, MA, USA) software and Gaussian bands shapes were employed in this procedure. Curve-fitting was limited to the 1580-1720 cm^{-1} spectrum range, since protein structure (contributions of second and third vibration) can see identified in this range [29,30] .

3.5. *Solid State Nuclear Magnetic Resonance (NMR)*

Solid state NMR is a powerful technique that has been used in analyzing miscibility, phase structure or heterogeneity in polymer mixture on a molecular scale [31]. This technique can also be used to identify the structure of materials. In the Chapter III,

both ^{13}C NMR and ^{29}Si NMR solid state spectroscopy provided the ways to evaluate the structure of chitosan/siloxane hybrid materials and to confirm the hydrolysis and condensation reactions in the sol-gel process, respectively. ^{29}Si and ^{13}C solid-state NMR spectra were recorded at 79.49 and 100.62 MHz, respectively, on a (9.4 T) Bruker Avance 400 spectrometer. ^{29}Si magic angle spinning (MAS) NMR spectra were measured with 40° rf pulses, a spinning rate of 5.0 kHz, and a recycle delay of 35 s. ^{1}H-^{29}Si cross-polarization (CP) MAS NMR spectra were recorded with 4.0 μs ^{1}H 90° pulses, a spinning rate of 5.0 KHz and 5 s recycle delays. Chemical shifts are quoted in ppm from tetramethylsilane (TMS).

On the other hand, solid state NMR is especially useful in polymer blend systems containing complex phase structures that may be beyond the resolution limits of conventional microscopic or thermal analysis. In Chapter VI, the miscibility of the components of chitosan/soy protein blended membranes was evaluated via solid-state NMR relaxation methods. In particular, the proton relaxation times in the rotating frame, $T_{1\rho}$ (^{1}H), were measured since that they are sensitive to heterogeneity in blends. The solid state NMR spectra were recorded on Bruker DRX spectrometers operating at a ^{1}H frequencies of 400 and 500 MHz. Proton spin-lattice relaxation time (T_1^H) values were determined using a ^{1}H-^{13}C cross-polarization (CP) inversion recovery sequence [32] and by fitting the ^{13}C peak intensities to a single exponential.

3.6. *X- ray photoelectron spectroscopy (XPS)*

X-ray photoelectron spectroscopy (XPS) was performed for a detailed analysis of the surface chemical composition of the chitosan membrane modified and non-modified. The XPS analysis was performed using ESCALAB 200A, VG Scientific (UK) with PISCES software for data acquisition and analysis. For analysis of the membranes, an achromatic Al (Kα) X-ray source operating at 15 kV (300 W) was used. The spectrometer was calibrated with reference to Ag 3d5/2 (368.27 eV) and

it was operated in constant analyser energy (CAE) mode with 20 eV pass energy. The measurements were carried out at a take-off angle of 90° (normal to the surface). Data acquisition was performed with a pressure lower than 10^{-6} Pa. The value of 285 eV of the hydrocarbon C1s core level was used as a calibration for the absolute energy scale. Overlapping peaks were resolved into their individual components by XPSPEAK 4.1 software.

3.7. *Powder X-ray Diffraction (XRD)*

X-ray diffraction (XRD) is a versatile, non-destructive technique that reveals detailed information about the crystallographic structure and sub-nanometric morphology of natural and manufactured materials. In our studies, the x-ray diffraction patterns of chitosan and chitosan/siloxane hybrids were analysed with a Philips X'Pert MPD diffractometer using Cu Kα radiation (λ=1.54 Å), 2θ range 1 - 80°.

3.8. *Small Angle X-Ray Scattering (SAXS)*

Small angle X-ray scattering (SAXS) is an analytical X-ray application technique for the structural characterization of solid and fluid materials in the nanometer range. When a sample is irradiated by a monochromatic X-ray beam, structural information of the scattering particles can be derived from the intensity distribution of the scattered beam at very low scattering angles. The X-ray scattering measurements on chitosan/siloxane hybrids (Chapter III) were performed in National Synchrotron Light Laboratory (LNLS), Campinas, Brazil, using its SAXS beam line which provides a monochromatic (λ=1.608 Å) and horizontally focused beam. The intensity was recorded as a function of the modulus of the scattering vector q, $q=(4\pi/\lambda)\sin(\varepsilon/2)$, ε being the scattering angle. Because of the small size of the incident beam cross section at the detection plane, no mathematical desmearing of the experimental SAXS intensity

was needed. Each spectrum corresponds to a data collection period of 300 s. The parasitic scattering intensity from air, slits and windows was subtracted from the total intensity. The scattering intensity was also normalized by taking into account the varying intensity of the direct X-ray beam, sample absorption and sample thickness.

3.9. *Contact angle measurements*

The wettability and surface energy of the chitosan-based membranes were assessed by static contact angle (θ) measurements using the sessile drop method with ultra-pure distilled water (polar) and diiodomethane (non-polar). The measurements were performed using OCA 20 equipment (DataPhysics, Germany) and SCA-20 software. The present data were averaged on six measurements. The surface energy was calculated using the Owens-Wendt equation [33].

3.10. *Photoluminescence spectroscopy*

Luminescence is the result of electron-hole recombination on delocalized states so that emission wavelength depends on excitation wavelength. Luminescence can thus be emitted in almost the entire visible spectrum and it can be tuned by choosing excitation wavelength. Amino-group-containing materials give the highest photoluminescence yield. It is, generally, expected that the presence of chemical groups with electron-donating capacity within the light-generating nanoclusters will be a favourable factor for making an efficient photoluminescent material [34]. The Emission (PL) and excitation (PLE) photoluminescence spectra and lifetime measurements of chitosan/siloxane hybrid materials were recorded between 13 and 300 K on a modular double grating excitation spectrofluorimeter with a TRIAX 320 emission monochromator (Fluorolog-3, Jobin Yvon-Spex) coupled to a R928 Hamamatsu photomultiplier, in the front-face acquisition mode.

3.11. *Dynamic mechanical analysis (DMA)*

Dynamic mechanical analysis (DMA) measures the stiffness and damping properties of materials as a function of time, temperature and frequency. When a dynamic force is applied to a polymeric material, the sample will deform as response. From this material response, an elastic modulus (E´) and a loss modulus (E´´) can be calculated. These different moduli allow better characterization of the material since they examine the ability of the material to store energy (E´), to its ability to lose energy (E´´), and the ratio between these effects (tan delta), which is related to damping [35]. In our studies, viscoelastic measurements were performed on CSG sponges using a TRITEC2000B DMA from Triton Technology (UK) equipped with a compressive mode. The samples were seccionated into rectangular cross-section geometry (5.4 x 5.7 mm). Prior the DMA experiments, the sample were equilibrated for about 50 minutes in a phosphate buffer saline (PBS) solution. All samples were analysed in wet conditions (PBS) at 37°C with heat rate at 2°C/min and frequency scans (0.1 to 100 Hz). The DMA results were presented in terms of E´ and E´´ .

3.12. *Water uptake and degradation tests*

Water uptake and weight loss are important parameters in the evaluation of biodegradable materials. They translate the degradation behaviour and the ability of the biomaterial to absorb water in their matrix (swelling), respectively. However, the rate at which a fluid penetrates into material depends, mainly on its surface area, the hydrophilic/hydrophobic character and in some cases its porosity [36].

For the determination of the degradation and water uptake profiles, non-cross-linked and cross-linked blend membranes (1 x 2 cm^2) were weighted and immersed in a phosphate buffer saline solution [37] at physiological pH (pH 7.4) and placed into a water bath at 37 °C. Sodium azide (0.02 % w/v) was added to the buffer to

prevent bacterial growth. After pre-determined time periods, the samples were removed from the vials, washed with distilled water and weighted. Water uptake was determined using equation 2:

$$\text{Water uptake (\%)} = ((W_s(t) - W_i)/W_i) \times 100 \qquad (2)$$

Where $W_s(t)$ and W_i represent the weight of the samples at time t and 0, respectively. Each experiment was repeated three times and the average value was considered as the water uptake value. After that, the samples were dried in an oven (60° C/24 h). The percentage weight loss of the soy materials was then calculated by:

$$\text{Weight loss (t)} = [(W_i - W_f(t)) / W_i] * 100 \qquad (3)$$

Where W_i is the initial dry weight of the sample. $W_f(t)$ denotes the weight loss of sample after a certain time t of immersion. Each experiment was repeated three times and the average value was taken as the weight loss.

In the case of CSG sponges, water uptake assays were performed through immersion of the materials in buffer solutions at pH 3, 7.4 and 9 instead to PBS, and incubated at 37°C under static conditions. The samples were left for 24 hours in each buffer solution prior to weight determination. The swelling ratio was determined using equation 1.

Additionally, silk mats obtained by ELE were cut into squares of 2 x 2 cm^2 and immersed in distilled water at 37°C for 8 days to test their dissolvability.

3.13. *Surface Modification and in Vitro Apatite Forming Ability*

It is known that the presence of Si-OH groups in different types of materials can induce the formation of an apatite layer. However, this ability is associated to the amount, distribution and arrangement of these groups in the material structure [38-40]. In Chapter III, chitosan/siloxane hybrids were submitted to alkaline treatments in order to obtain a structural re-arrangement of the silanol groups present in the material. *In vitro* bioactivity of a material is generally evaluated by its ability to form a calcium-phosphate (Ca-P) layer at its surface when immersed in a solution simulating the human blood plasma ionic compositions [41]. Thus, after alkaline treatment, the hybrid powders were soaked in 10 mL of the simulated body fluid (SBF) [41] prepared with ion concentrations (Na^+ 142.0, K^+ 5.0, Ca^{2+} 2.5, Mg^{2+} 1.5, Cl^- 147.8, HCO_3^- 4.2, HPO_4 2- 1.0, SO_4 2- 0.5 mM) nearly equal to those of the human blood plasma at 36.5 °C for different periods up to 21 days to evaluate the bioactivity of the samples by means of looking at the material formation of an apatite-like layer on their surface. Later on, the samples were removed from the fluid, gently rinsed with distilled water and dried at room-temperature.

3.14. *In vitro cytotoxicity and Cell Culture Studies*

- *In vitro cytotoxicity*

A material in contact with human tissues should not liberate any agent that may be toxic or have an adverse effect on the healing process. Thus, the first step in the assessment of a material biocompatibility is the screening of cellular toxicity. The cytotoxicity procedure described in this work, follows the ISO International Standards Organization (ISO/EN 10993) guidelines[42] for testing biomedical materials.

Possible toxic leachables might be released when scaffolds are incubated in a culture medium. Thus after a 24 hour incubator period at 37ºC, leachables are filtered and placed in contact to cells. This method allows to quantify the effect of a

material over the viability of a cell culture, and thus deduces about the cytotoxic behavior (or lack of) in contact to a material. In the studies, mouse fibroblast-like cells (L929) obtained from European Collection of Cell Cultures (ECACC, UK) were used to perform the cytotoxicity tests on chitosan-based membranes (Chapter IV and V) and sponges (chapter VII). L929 cells were cultured and expanded in basic medium: Dulbecco's Modified Eagle's Medium (DMEM, Sigma-Aldrich, USA) without phenol red and supplemented with 10% foetal bovine serum, (FBS, Gibco, UK) and 1% antibiotic/antimycotic (A/B, Gibco, UK) solution. L929 cells were incubated at 37 °C in an atmosphere containing 5% of CO_2 until achieving 90% of confluence. Then, L929 cells were were seeded onto adherent 96 well plates at a concentration of 8 x 10^4 cm^{-1}. After 72h leachables were placed in contact with cells and a MTS ((3-(4,5-dimethylthiazol-2-yl)-5-(3-carboxymethoxyphenyl)-2-(4-sulfophenyl)-2H-tetrazolium)) assay was performed to screen the cellular viability after 1,3,7 and 14 days.

- *Direct contact assays on the developed materials*

An evaluation of the cell supporting ability of the chitosan-based membranes and chitosan/silk (CSG) sponges was performed using L929 fibroblast-like cells and ATDC5 chondrocyte-like cells line, respectively, in direct contact tests. Chitosan-based membranes (1 cm^2 modified and non-modified) were seeded with 100 μL of a cell suspension (8 x 10^4 cells/mL) and cultured for 3, 7 and 14 days, while CSG sponges (with an approximate volume of 0.125mm^3) were seeded with a cell suspension of 2.4 x 10^5 cells per sponge. Triplicates were made for each sample formulation. The samples were incubated at 37°C in a humidified 95% air/5% CO_2 atmosphere. In the case of chitosan based membranes, L929 fibroblasts-like cells were used and maintained for 3, 7 and 14 days with culture medium containing of Dulbecco's Modified Eagle's Medium low glucose (DMEM), Sigma, USA) supplemented with 10% foetal bovine serum, FBS (Gibco, UK) and 1% antibiotic/antimycotic (A/B, Gibco, UK) solution. For CSG sponges, ATDC5 chondrocyte-like cells were seeded and cultured in DMEM-F12 (Gibco, UK)

supplemented with 10% FBS (Gibco, UK), 2mM L-Glutamine (Sigma, USA) and 1% A/B (Gibco, UK) solution for 14, 21 and 28 days. Culture medium was replaced twice a week. After each culture time, the medium was removed and the samples were washed with a PBS solution.

Characterization

- *MTS assay*

Cellular viability was quantitatively assessed by the MTS (3-(4,5-dimethylthiazol-2-yl)-5-(3-carboxymethoxyphenyl)-2-(4-sulfophenyl)-2H-tetrazolium) assay (Promega, Madison, USA) in the samples. Culture medium without FBS and without phenol red was mixed with MTS reagent at a ratio 5:1, added to the sample/cells constructs and incubated for 3 hours at 37°C. After the incubation period the optical density [5] was read in a microplate reader (Bio-Tek, USA) at 490 nm. The measurements were made in triplicate for each treatment and time point (3, 7 and 14 days).

- *Cell morphology*

The cell morphology was analysed using SEM. After each culturing period, samples were fixed with 2.5% glutaraldehyde in a PBS solution for 30 minutes in the case of cht membranes or with 4% formalin solution for 60 minutes at 4°C for sponges, respectively. After that, the samples were dehydrated using a series of ethanol solutions. The samples were dried overnight at room temperature, coated with gold by sputtering and observed by SEM.

This procedure was performed in chitosan/L929- and in sponges/ATDC5-constructs.

- *DNA (only for CSG sponges)*

DNA assay is one of the most used measurements to evaluate cell proliferation by quantifying the double strand DNA (dsDNA) content of cells cultured on the porous matrices. In order to determine ATDC5 cell proliferation onto CSG sponges a fluorimetric dsDNA quantification kit (PicoGreen, Molecular Probes, Invitrogen, UK) was used. At each time point of culture, cell-sponges constructs were transferred into 1.5 ml microtubes containing 1 ml of ultra-pure water. ATDC5 cell-sponge constructs were stored in a -80°C freezer until testing. Prior to DNA quantification, constructs were thawed and sonicated for 15 min. Samples and standards (ranging between 0 and 2 mg ml^{-1}) were prepared and mixed with a PicoGreen solution in a 200:1 ratio. Triplicates were made for each sample or standard and after 10 minute incubation in the dark, fluorescence was measured on a microplate ELISA reader (BioTek, USA) using an excitation of 485 nm and an emission wavelength of 528 nm. A standard curve was created and sample DNA values were read off from the standard graph.

- *GAGs quantification assay*

GAGs quantification assay was used to detect chondrogenic-like ECM formation after 14, 21 and 28 days of culture in ATDC5-sponge constructs. GAGs standards were obtained by preparing a chondroitin sulphate solution ranging from 0 and 30 mg ml^{-1}. In each well of a 96-well plate, samples or standards were added in triplicates and then mixed with the dimethylmethylene blue reagent (DMB, Sigma-Aldrich, USA). The optical density (OD) was measured immediately at 525 nm on a microplate ELISA reader. A standard curve was created and GAGs sample values were read off from the standard graph.

4. **References**

1. Kumar, M. N. V. R., Muzzarelli, R. A. A., Muzzarelli, C., Sashiwa, H., and Domb, A. J., Chitosan chemistry and pharmaceutical perspectives, *Chemical reviews* 104, 6017-6084, 2004.
2. Kumar, M. N. V. R., A review of chitin and chitosan applications, *Reactive & Functional Polymers* 46, 1-27, 2000.
3. Santin, M., Motta, A., Freddi, G., and Cannas, M., In vitro evaluation of the inflammatory potential of the silk fibroin, *Journal of Biomedical Materials Research* 46, 382-389, 1999.
4. Signini, R. and Filho, S. P. C., On the preparation and characterization of chitosan hydrochloride, *Polymer Bulletin* 42, 159-166, 1999.
5. Hirai, A., Odani, H., and Nakajima, A., Determination of degree of deacetylation of chitosan by 1H NMR spectroscopy, *Polymer Bulletin* 26, 87, 1991.
6. Muzzarelli, R. and Peter, M. G., *Chitin Handbook* European Chitin Society, Grottammare, 1997.
7. Illum, L., Chitosan and its use as a pharmaceutical excipient, *Pharmaceutical Research* 15, 1326-1331, 1998.
8. Swain, S. N., Biswal, S. M., Nanda, P. K., and Nayak, P. L., Biodegradable soy-based plastics: Opportunities and challenges, *Journal of Polymers and the Environment* 12, 35-42, 2004.
9. Wu, Q. and Zhang, L., Properties and structure of soy protein isolate-ethylene glycol sheets obtained by compression molding, *Industrial and Engineering Chemistry Research* 40, 1879-1883, 2001.
10. Mo, X., Sun, S., and Wang, Y., Effects of molding temperature and pressure on properties of soy protein polymers, *Journal of Applied Polymer Science* 73, 2595-2602, 1999.
11. Rangavajhyala, N., Ghorpade, V., and Hanna, M., Solubility and molecular properties of heat-cured soy protein films, *Journal of Agriculture and Food Chemistry* 45, 4204-4208, 1997.
12. Swain, S. N., Rao, K. K., and Nayak, P. L., Biodegradable Polymers. III. Spectral, Thermal,Mechanical, and Morphological Properties of Cross-linked Furfural–Soy Protein Concentrate, *Journal of Applied Polymer Science* 93, 2590-2596, 2004.
13. Vaz, C. M., Fossen, M., van Tuil, R. F., de Graaf, L. A., Reis, R. L., and Cunha, A. M., Casein and soybean protein-based thermoplastics and composites as alternative biodegradable polymers for biomedical applications, *Journal of Biomedical Materials Research Part A* 65A, 60-70, 2003.
14. Jin, H. J., Fridrikh, S. V., Rutledge, G. C., and Kaplan, D. L., Electrospinning Bombyx mori Silk with Poly(ethylene oxide), *Biomacromolecules* 3, 1233-1239, 2005.
15. Altman, G. H., Diaz, F., Jakuba, C., Calabro, T., Horan, R. L., Chen, J. S., Lu, H., Richmond, J., and Kaplan, D. L., Silk-based biomaterials, *Biomaterials* 24, 401-416, 2003.
16. Roh, D. H., Kang, S. Y., Kim, J. Y., Kwon, Y. B., Kweon, H. Y., Lee, K. G., Park, Y. H., Baek, R. M., Heo, C. Y., Choe, J., and Lee, J. H., Wound healing effect of silk fibroin/alginate-blended sponge in full thickness skin defect of rat, *Journal of Materials Science-Materials in Medicine* 17, 547-552, 2006.
17. Romero, P. G. and Sanchez, C., *Functional Hybrid Materials* Wiley-VCH, Weinheim, 2003.
18. Sanchez, C., Julian, B., Belleville, P., and Popall, M., Applications of hybrid organic–inorganic nanocomposites, *Journal of Materials Chemistry* 15, 3559-3592, 2005.
19. Chu, P. K., Chen, J. Y., Wang, L. P., and Huang, N., Plasma surface modification of biomaterials, *Materials Science and Engineering Reviews* 36, 143-206, 2002.
20. Oehr, Plasma surface modification of polymers for biomedical use, *Nuclear Instruments and Methods in Physics Research B* 208, 40-47, 2003.
21. Nadeu, O. W. and Carlson, G. M., Protein interactions captured by chemical cross-linking, in *Protein-protein interactions, a molecular cloning manual*, Golemis, E. andAdams, P. New York, 2005, pp. 105-127.

22. Monteiro, O. A. C. and Airoldi, C., Some studies of crosslinking chitosan-glutaraldehyde interaction in a homogeneous system, *International Journal of Biological Macromolecules* 26, 119-128, 1999.
23. Silva, R. M., Silva, G. A., Coutinho, O. P., Mano, J. F., and Reis, R. L., Preparation and characterization in simulated body conditions of glutaraldehyde crosslinked chitosan membranes, *Journal of Materials Science-Materials in Medicine* 15, 1105-1112, 2004.
24. Yuan, Y., Chesnut, B. M., Utturkar, G., Haggard, W. O., Yang, Y., Ong, J. L., and Bumgardner, J. D., The effect of cross-linking of chiosan microspheres with genipin on protein release, *Carbohydrate Polymers* 68, 561-567, 2007.
25. Buther, M. F., Ng, Y. F., and Pudney, P. D. A., Mechanism and kinetics of the crosslinking reaction between biopolymers containing primary amine groups and genipin, *Journal of polymer Science Part A: Polymer Chemistry* 41, 3941-3953, 2003.
26. Pham, Q. P., Sharma, U., and Mikos, A. G., Electrospinning of polymeric nanofibers for tissue engineering applications: a review, *Tissue Engineering* 12, 1197-1211, 2006.
27. Ramakrishna, S., Fujihara, K., Teo, W. E., Lim, T. C., and Ma, Z., *An introduction to electrospinning and nanofibers* World Scientific, 2005.
28. Macosko, C. W., *Rheology: Principles, measurements and applications* VCH Publishers, New York, 1994.
29. Wilson, D., Valluzi, R., and Kaplan, D., Conformational transitions in model silk peptides, *Biophysical Journal* 78, 2690-2701, 2000.
30. Chittur, K. K., FTIR/ATR for protein adsorption to biomaterial surfaces, *Biomaterials* 19, 357-369, 1998.
31. Wu, R. R., Kao, H. M., Chiang, J. C., and Woo, E. M., Solid state NMR studies on phase behaviour and motional mobility in binary blends of polystyrene and poly(cyclohexyl methacrylate), *Polymer* 43, 171-176, 2002.
32. Zhong, Z. and MI, Y., Thermal characterization and solid state 13C-NMR investigation of blends of poly(N-phenyl-2-hydroxytrimethylene amine) and poly(N-vinyl pyrrolidone), *Journal of Polymer Science Part B: Polymer Physics* 37, 237-245, 1999.
33. Owens, D. K. and Wendt, R. C., *Journal of Applied Polymer Science* 13, 1741, 1969.
34. Brankova, T., Bekiari, V., and Lianos, P., Photoluminescence from sol-gel organic/inorganic hybrid gels obtained through carboxylic acid solvolysis, *Chemistry of materials* 15, 1855-1859, 2003.
35. Menard, K. P., *Dynamic mechanical analysis - a practical introduction* CRC Press, Florida, 1999.
36. Ratner, B. D., Hoffman, A. S., Schoen, F. J., and Lemons, J. E., *Biomaterials Science- An introduction to materials in medicine*, Second edition ed. Elsevier Academic Press, 2004.
37. Silverman, R. P., Passaretti, D., Huang, W., Randolph, M. A., and Yaremchuk, M. J., Injectable tissue-engineered cartilage using a fibrin glue polymer, *Plastic Reconstruction Surgery* 103, 1809-1818, 1999.
38. Kokubo, T., Kim, H. M., and Kawashita, M., Novel bioactive materials with different mechanical properties, *Biomaterials* 24, 2161, 2003.
39. Oyane, A., Nakanishi, K., Kim, H. M., Miyaji, F., Kokubo, T., Soga, N., and Nakamura, T., Sol gel modification of silicone to induce apatite-forming ability, *Biomaterials* 20, 79-84, 1999.
40. Kokubo, T. and Takadama, H., How useful is SBF in predicting in vivo bone bioactivity? *Biomaterials* 27, 2907-2915, 2006.
41. Kokubo, T., Kushitani, H., Sakka, S., Kitsugi, T., and Yamamuro, T., Solutions able to reproduce n vivo surface-structure changes in bioactive glass-ceramic A-W, *Journal of Biomedical Materials Research* 24, 721-734, 1990.
42. ISO/ and 10993, Biological evaluation of medical devices- Part 5 test for Cytotoxicity, in vitro methods: 8.2 test on extracts, 1992.

CHAPTER III

CHAPTER III

Functional nanostructured chitosan/siloxane hybrids

Abstract

New organic-inorganic hybrids were prepared by a sol-gel method from the biopolymer chitosan and a silane coupling agent, the 3-isocyanatopropyltriethoxysilane (ICPTES), in which essentially urea bridges covalently bond the chitosan to the polysiloxane network. The structural characterization of the advanced chitosan/siloxane hybrids was performed by Fourier transform infrared spectroscopy, X-ray diffraction and ^{29}Si and ^{13}C nuclear magnetic resonance. The presence of siloxane nanodomains was detected by small angle X-ray diffraction. The chitosan/siloxane hybrids are bifunctional materials with interesting photoluminescent features and a bioactive behaviour. The photoluminescence spectra display an additional high-energy band with longer lifetime, relatively to the characteristic emission of pure chitosan. This band is associated with electron-hole recombinations arising from silicon-related defects at the surface of the siliceous nanodomains. The bioactive behaviour of these materials was also evaluated; the apatite formation was shown to depend on the amount and arrangement of silanol groups.

This chapter is based on the following publication:

S. S. Silva, R. A. S. Ferreira, L. Fu, L. D. Carlos, J. F. Mano, R. L. Reis, J. Rocha. "Functional nanostructured chitosan/siloxane hybrids", Journal of Materials Chemistry 15, 3952-3961, 2005.

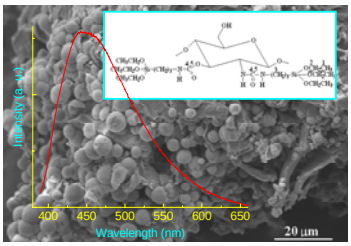

---

1. **Introduction**

The development of advanced materials from combination of macromolecules with inorganic species has become one of the most innovative research fields [1]. Following this approach the synthesised hybrid materials may allow the tailoring of properties from the atomic to the mesoscopic and the macroscopic length scales [2]. This ability to control materials properties over broad length scales suggests that research on hybrids can have a significant impact in diverse fields, such as nanoelectronics, separation techniques, catalysis, smart coatings, sensors, immobilization of enzymes, biomedical and polymer composite applications [1-6]. Currently, hybrid materials have been obtained through sol-gel chemistry, which constitutes a versatile method that allows the combination of organic and inorganic or even bioactive components in a single hybrid material [6-10]. In this method, a judicious choice of the constitutive organic and inorganic components as well as reaction parameters (pH, solvent, concentration of the reactants, catalyst, and temperature) allows to tailor the final chemical and physical properties of the materials [1,2,6]. Generally, hybrid materials are grouped in two classes based on the type of interaction or nature of chemical bonding between the organic and inorganic components [11]. In class I the organic component is bonded physically to inorganic phase, whereas in class II hybrids the organic and inorganic compounds are bonded through stronger covalent chemical bonds [11] achieved by using functionalized silanes coupling agents, such as 3-glycidyloxypropyl-trimethoxysilane (GPTMS), 3-aminopropyltriethoxysilane (APTES)[12,13], and 3-isocyanatopropyltriethoxysilane (ICPTES). The latter has been used to modify the ethylene vinyl alcohol copolymer [14] and poly (ε-caprolactone-b-perfluoropolyether-b-ε-caprolactone) [7]. Recently, the synthesis of amine-functionalized cross-linked sol-gel derived hybrids in which the siliceous backbone is covalently bonded to polyether chains by means of urea or urethane crosslinks originating from ICPTES, named as di-ureasils and di-urethanesils, respectively, have been described [6,15-21].

In particular, the preparation of efficient white-light photoluminescence (PL) siloxane-based organic-inorganic hybrids lacking metal activator ions have been reported [6,16,18-23]. The development of new full colour displays, cheaper and less aggressive to the global environment is one of the main challenging tasks for the next generation of flat-panel display systems and lighting technologies [20]. Alternatively to conventional sol-gel process (e.g. in the presence of water and ethanol and inorganic acids as the catalyst), Sailor *et al* [12], Lianos *et al* [13,17] and Carlos *et al* [15] reported that amine-functionalized sol-gel derived hybrids with attractive photoluminescence features, in particular high emission quantum yields, can also be obtained by a sol-gel derived carboxylic acid solvolysis, which occurs in the absence of water and oxygen, using APTES or ICPTES as silane coupling agents.

A different approach for the preparation of hybrid compounds based on the combination of polysaccharides and silicon-based materials was recently reported [24-27]. In this context, chitosan/siloxane hybrids have received much attention due to their potential for use in enzyme immobilization, porous materials and as electrochemical sensors [28]. Furthermore, chitosan based materials have been proposed for an all range of biomedical applications [29-31]. The methodologies reported focus on the modification of the polymer chain structure before introducing the inorganic component [32]. Alternatively, it is also possible to prepare porous silica particles by elimination of the organic phase (chitosan) [33], or by interaction of chitosan in solution with silica particles to produce aerogel composites [33,34], films and membranes [35,36]. Devoiselle *et al* [37] recently reported that porous chitosan-silica hybrid microspheres can be obtained using supercritical drying by CO_2. In these approaches [27,33-37] both organic matrix and inorganic species are physically bonded (class I). It would be interesting to move ahead with this concept by introducing chemical cross-linkages between the reactive groups of chitosan and the siliceous skeleton (class II). If so, a more effective bonding between the organic and the inorganic phases will be achieved, improving the mechanical performance, chemical stability, and controlled water absorption or hydrogel behaviour in a wide pH range. Furthermore, as the optical features of the

hybrid materials are extremely affected by the organic/inorganic interfaces, the covalently crosslinkages of these class II polysaccharides-siloxane hybrids (urea or urethane groups) may induce optical characteristics distinct from those associated with the class I polysaccharides/silicon-based materials.

The main objective of this work was therefore to develop novel functional class II polysaccharide-based hybrid materials through sol-gel derived carboxylic acid solvolysis. This paper, in fact, reports the first attempt to synthesize a polysaccharide-based hybrid material via carboxylic acid solvolysis. The photoluminescence characterization and a preliminary study of the materials eventual bioactive behaviour are also reported and discussed.

2. **Materials and Methods**

Chitosan (CHT; Sigma Aldrich medium and low molecular weight) was used as the polymeric component. Molecular viscosimetric weight (M*v* = 662 kDa) and (M*v* = 591 kDa) was determined in 0.1 M acetic acid/0.2 M sodium acetate as described previously [38]. Before the reaction the polymer was milled to obtain a fine powder. 3- isocyanatopropyltriethoxysilane (ICPTES), the inorganic constituent, was purchased from Aldrich Chemical Co and used as received. Ethanol (Et, Merck), Dimethylformamide (DMF, Merck), acetic acid (AA, Aldrich, 99.7%) were kept in contact with molecular sieves prior to be used.

2.1. **Synthesis**

The chitosan/siloxane hybrids were prepared in two steps using the sol-gel method (Figure 1). In the first stage, chitosan (fine powder) dispersed in DMF reacted with the silane coupling agent, ICPTES under a N_2 atmosphere during different times (Table 1). In a typical procedure, a sample of 1 g of chitosan (powder) was dispersed under stirring in 10 mL of DMF. Approximately 1.52 mL of ICPTES was added to this dispersion. The flask was sealed and the dispersion was stirred during

a pre-determined time (Table 1) at 105 °C under N_2 atmosphere. The reaction was monitored by IR spectroscopy until the characteristic isocyanate band at *ca.* 2274 cm^{-1} vanished. Following the solvolysis process [17,18], in the second reaction step, an acetic acid/ethanol mixture in the ratio molar ICPTES: acetic acid: ethanol of 1:3:6 and 1:6:6 was added to the dispersion prepared in step 1. The mixture was stirred in a sealed flask for 24 h at room-temperature in inert atmosphere. The materials were obtained as fine powders. Subsequently, the DMF was separated from the product by centrifugation and washed several times with methanol, after which this solvent was evaporated and the solid allowed to dry overnight in an oven at 60 °C.

Table 1. Experimental synthesis conditions of chitosan/siloxane hybrids.

Sample	Molar Ratio		Time (h)	
	NH_2/NCO	AA/Et	Step 1 (h)	Step 2 (h)
CHY1	1: 1.17	3:6	48	24
CHY2*	1: 1.17	3:6	48	24
CHY3	1: 2.34	6:6	48	24

AA – acetic acid; Et – ethanol; * hybrid sample obtained from chitosan medium molar viscosimetric weight; CHY1- chitosan hybrid 1; CHY2 – chitosan hybrid 2; CHY3 – chitosan hybrid 3.

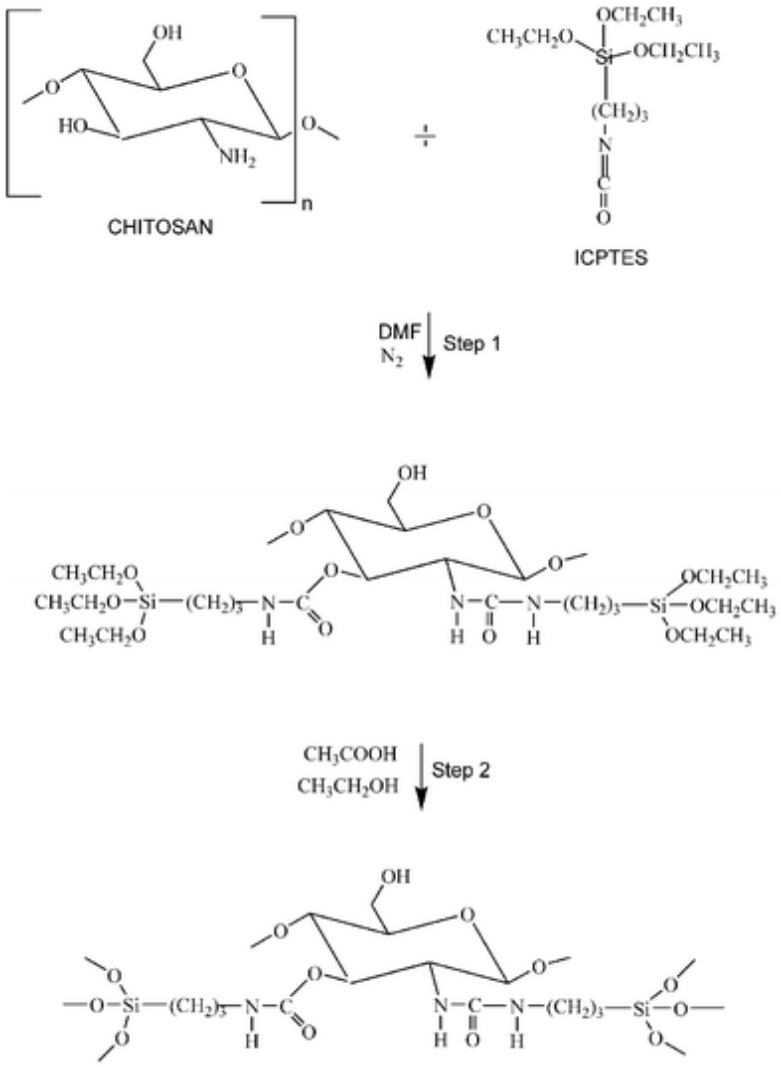

Figure 1. Scheme proposed for preparation of the chitosan–siloxane hybrids. Although urethane cross-linkages are considered in the scheme urea bridges should be preferentially formed.

2.2. **Characterization**

2.2.1. *Surface Modification and in Vitro Apatite Forming Ability*

After washing and the drying of the hybrids, they were also submitted to a surface modification using 3 M KOH for 2 h at room-temperature. In these tests the hybrid powders were soaked in 10 mL of the simulated body fluid (SBF) [39], at 36.5 °C for a period of up to 21 days to evaluate the bioactivity of the samples by means of looking at the material formation of an apatite-like layer on their surface. Later on, the samples were removed from the fluid, gently rinsed with distilled water and dried at room-temperature.

2.2.2. *Adsorption Measurements*

After outgassing the chitosan/siloxane hybrids overnight to a residual pressure of *ca.* 10^{-4} mbar, we have tried (with no success) to measure a nitrogen adsorption isotherm at 77 K. Thus, accordingly the IUPAC classification the surface area is negligible.

2.2.3. *Fourier Transform Infrared Spectroscopy (FT-IR)*

The FT-IR spectra of KBr pellets were recorded (64 scans with a resolution of 4 cm^{-1}) on a Unican Mattson Mod 7000 FTIR.

2.2.4. *Nuclear Magnetic Resonance (NMR) Spectroscopy*

^{29}Si and ^{13}C solid-state NMR spectra were recorded at 79.49 and 100.62 MHz, respectively, on a (9.4 T) Bruker Avance 400 spectrometer. ^{29}Si magic angle spinning (MAS) NMR spectra were measured with 40º rf pulses, a spinning rate of 5.0 kHz, and a recycle delay of 35 s. ^{1}H-^{29}Si cross-polarization (CP) MAS NMR spectra were recorded with 4.0 μs ^{1}H 90º pulses, a spinning rate of 5.0 KHz and 5 s recycle delays. Chemical shifts are quoted in ppm from tetramethylsilane (TMS).

2.2.5. *Powder X-ray Diffraction (XRD)*

XRD patterns were recorded on Philips X'Pert MPD diffractometer using Cu Kα radiation (λ=1.54 Å), 2θ range 1 - 80°.

2.2.6. *Photoluminescence Spectroscopy*

Emission (PL) and excitation (PLE) photoluminescence spectra and lifetime measurements were recorded between 13 and 300 K on a modular double grating excitation spectrofluorimeter with a TRIAX 320 emission monochromator (Fluorolog-3, Jobin Yvon-Spex) coupled to a R928 Hamamatsu photomultiplier, in the front-face acquisition mode.

2.2.7. *Scanning electron microscopy (SEM)*

SEM images of samples coated with gold were obtained at 10 kV on a Leica Cambridge S-360 microscope equipped with a LINK eXLII X-ray energy dispersion spectrometer for silicon microanalysis.

2.2.8. Small Angle X-Ray Scattering (SAXS)

The X-ray scattering measurements were performed in National Synchrotron Light Laboratory (LNLS), Campinas, Brazil, using its SAXS beam line which provides a monochromatic (λ=1.608 Å) and horizontally focused beam. The intensity was recorded as a function of the modulus of the scattering vector q, $q=(4\pi/\lambda)\sin(\varepsilon/2)$, ε being the scattering angle. Because of the small size of the incident beam cross section at the detection plane, no mathematical desmearing of the experimental SAXS intensity was needed. Each spectrum corresponds to a data collection period of 300 s. The parasitic scattering intensity from air, slits and windows was subtracted from the total intensity. The scattering intensity was also normalized by taking into account the varying intensity of the direct X-ray beam, sample absorption and sample thickness.

3. **Results and Discussion**

3.1. *Structural Characterization*

Chitosan/siloxane hybrids were prepared through the reaction of the reactive groups of chitosan with the isocyanate group (NCO) present in the alkoxysilane precursor, ICPTES (Figure 1) in the presence of dimethylformamide (DMF), chosen as dispersed agent. This reaction may produce either urea (–NHCONH–) or urethane (–NHCOO–) groups, which form bridges between the chitosan and the inorganic matrix. The former linkage (–NHCONH–) should be preferentially formed as NH_2 groups react faster with isocyanates than with OH moieties [40]. The formation of the chitosan hybrids is summarized in Figure 1. All reactions were performed in an inert atmosphere to ensure that the ICPTES did not react with moisture. In the second stage of Figure 1, the hydrolysis and condensation reactions of the precursor occurred with addition of acetic acid and ethanol in different molar ratios (see Experimental section - Table 1) to yield the corresponding polysiloxane Si–O–Si inorganic chain. The two-step reaction mechanism for this process, proposed by Pope and Mackenzie [41], was recently confirmed by Lianos *et al* [17] for the acetic acid solvolysis of poly(oxypropylene) 4000/siloxane hybrids in the presence of ethanol using temporal attenuated total reflection IR measurement technique [17]. In the first step, acetic acid reacts with the alkoxy groups bonded to the silicon atom (C_2H_5OSi–), forming an ester (CH_3COOSi–). During the second step, this ester reacts with ethanol, producing ethyl acetate ($CH_3COOC_2H_5$) and Si–OH groups. Then condensation of two Si–OH groups or one Si–OH group and one ethanol molecule yields the Si–O–Si network. The work of De Azevedo and Brondani focused on the development of polyaniline/silicate glass composites using formic acid as catalyst and solvent through a sol-gel process also supported this argument [42].

Hybrid materials obtained by the sol-gel method may present different forms (aerogels, films, xerogels, and powders) depending on the components and preparation conditions [6]. For the particular conditions used in this work (Table 1) it was possible to obtain powdered chitosan/siloxane hybrids. Figure 2 shows the FTIR spectra of the prepared materials. The displacement of the NH (from 1590 cm^{-1} to 1564 cm^{-1}) and CO (from 1652 cm^{-1} to 1633 cm^{-1}) deformation bands towards lower wavenumbers provides the evidence for the presence of urea and urethane groups in the hybrids. These shifts, combined with the increase of intensity of the bands, may reflect changes from primary amino groups (chitosan) to urea and urethane groups. Furthermore, the main IR bands of urea groups overlap with the characteristic absorption bands of chitosan and urethane [43], making difficult the spectral interpretation. Bermudez *et al.* [15] reported that the "amide I" and "amide II" modes are complex vibrations: amide I (1800-1600 cm^{-1}) involves the contribution of the C=O stretching, C-N stretching, and C-C-N deformation vibrations, while the amide II (1600-1500 cm^{-1}) mode has contributions from the N-H in plane bending, C-N stretching, and C-C stretching vibrations. In order to study in detail the vibrations for the urea and urethane groups spectral deconvolutions were carried out in the 1800-1500 cm^{-1} range using the ORIGIN® package and Gaussian band shapes. The results are listed in Table 2.

According to the literature, the components at *ca.* 1690 cm^{-1} and 1655 cm^{-1} are tentatively due to the vibration of urea-polyether hydrogen-bonded structures, whereas the component at about 1630 cm^{-1} results from the formation of strong self-associated hydrogen-bonded urea-urea associations [15,18]. The absence in the spectra of Fig. 2 of an individual band at *ca.*1750 cm^{-1} indicates that neither C=O nor N–H groups are left free (with no hydrogen bond interactions), in agreement with that reported before for di-ureasils with shorter polymer chains [15,18]. However, for di-urethanesil hybrids the "amide I" envelope involves essentially three bands, at *ca.* 1750 cm^{-1}, 1720 cm^{-1} and 1696 cm^{-1}, ascribed to urethane linkages in which the N-H and C=O groups are nonbonded, hydrogen-bonded C=O groups in

polyether/urethane associations, and C=O groups belonging to a considerably more ordered hydrogen-bonded urethane/urethane disordered aggregates, respectively [18,19]. Therefore, the band at *ca.* 1680-1696 cm^{-1} in Table 2 could be associated both to urea-polyether hydrogen-bonded structures and urethane/urethane hydrogen-bonded associations. However, the urea cross-linkages may exist in larger amounts in accordance with previously observations indicating that NH_2 groups react much more rapidly with isocyanates than OH moieties [40].

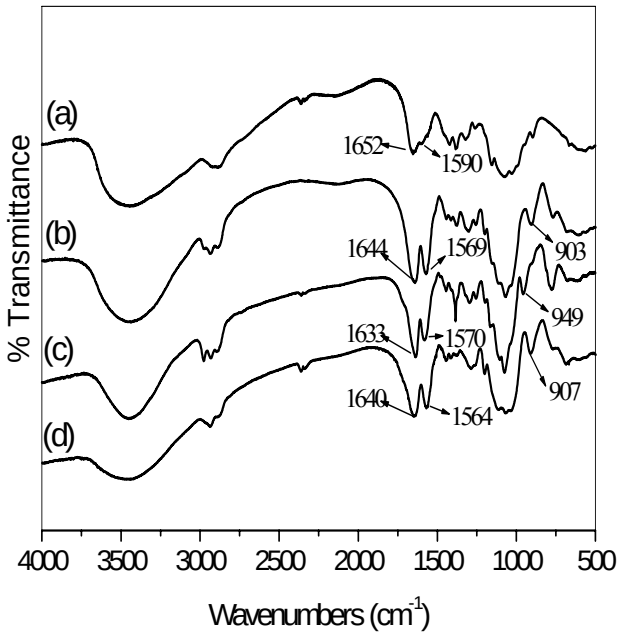

Figure 2. FTIR spectra of chitosan (a), CHY1 (b), CHY2 (c) and CHY3 (d).

Table 2. Curve-fitting results of "amide I" and "amide II" regions in the FT-IR spectra of CHY1, CHY2, and CHY3.

Sample	CHY 1	CHY2	CHY3
"Amide I"			
Wavenumber(cm^{-1})/area (%)	1689/(36)	1696/(33)	1680/(19)
	1654/(48)	1656/(39)	1651/(25)
	1629/(16)	1632/(28)	1643/(56)
Amide II			
Wavenumber (cm^{-1})	1572	1579	1568

The inorganic phase gives IR bands in the following regions: 1100-1000 cm^{-1}, 950-900 cm^{-1} and 800-700 cm^{-1} assigned, respectively, to Si–O–Si (stretch mode), Si–OH (stretch mode) and Si–O–Si [15,44]. The presence of residual silanol (Si–OH) groups is a common situation in many sol-gel derived materials, reflecting incomplete polycondensation [15]. The chitosan spectrum (Fig. 2a) displays a band at 1100-1000 cm^{-1}, attributed to –C–O–C– of glycosidic linkage [43]. In the hybrids spectra (Fig. 2b-e) this band increases intensity, possibly due to the overlapping of the Si–O band in the same frequency region.

Figure 3 shows the ^{13}C CP/MAS NMR of chitosan and derivatives. In the spectra of the hybrids (Fig. 3b-d), the bridge of the siloxane network to the polymer is confirmed by the appearance of new signals at *ca.* 23, 43 and 160-170 ppm. The peaks at *ca.* 23 and 43 ppm are given by the ester group (C_1, C_2) carbons bonded to silicon atom (–SiO$\underline{C}H_2\underline{C}H_3$) and the aliphatic $(CH_2)_3$ carbons of the silane precursor (C_3), respectively (see Figure 3). In addition, the intensity of the peak at *ca.* 18 ppm increases, as a result of the overlapping of the resonances of the methyl groups of the polymer chain [45] with the resonances of the CH_3 of ethoxy (OCH_2CH_3) groups.

Furthermore, the ^{13}C CP/MAS NMR spectra exhibit several resonances at *ca.* 160-170 ppm ($C_{4,5}$) that are associated with carbonyl groups in different environments [18,19,46]. This lends support to the suggesting that urea and urethane bridges may coexist in the hybrids. The prepared chitosan/siloxane derivatives are thus bifunctional hybrids, forming an interconnected network with the inorganic component through urea (essentially) and urethane bridges. Hence, the chitosan (amino and hydroxyl groups) functionality offers different ways of obtaining class II hybrid materials.

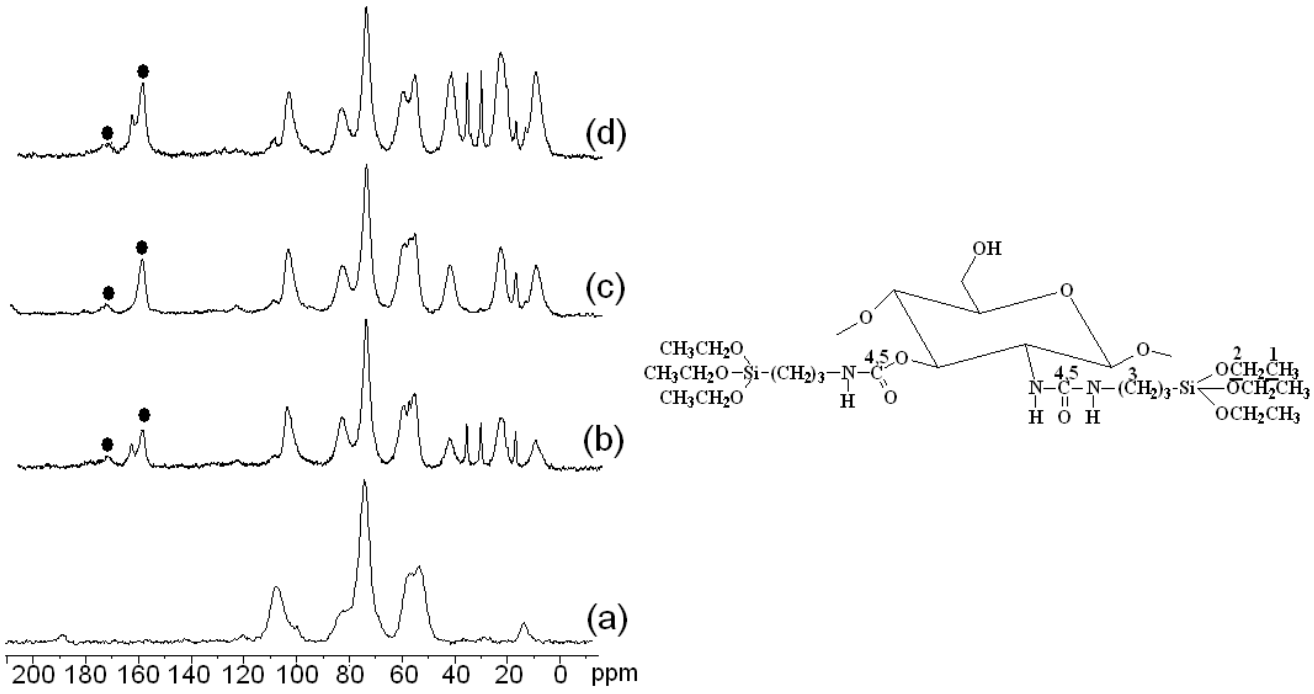

Figure 3. ^{13}C CP MAS of chitosan (a), CHY1 (b), CHY2 (c) and CHY3 (d).

Solid-state ^{29}Si MAS NMR spectroscopy is a useful technique to elucidate the structure of hybrid materials. The ^{29}Si MAS NMR spectra of the hybrids studied here (Figure 4) exhibit broad signals in three distinct regions, *ca.* -48 to -50, -58 to -59 and -66 to -68 ppm, assigned to T_1, T_2 and T_3 environments, respectively [6,18,19,21]. The silicon sites are labelled according to the conventional T_n notation, where *n* (*n*= 1, 2, 3) is the number of Si-bridging oxygen atoms. As the sol-gel process progresses, new peaks associated with the formation of the siloxane (–Si–O–Si–) and/or Si–OH groups appear. The signals from T_2 sites are stronger than the signals given by the T_3 environments for CHY1, CHY2 and CHY3 samples (Fig. 4). This suggests that partial condensation favours lightly branched structures rather than linear segments. The intensity of the CHY3 peaks at *ca.* -66.7 and *ca.* -58 ppm increases, while it decreases for the *ca.* -48.6 ppm resonance, confirming that a large population of siloxane groups is present in this hybrid. The degree of condensation *(c)* involves the population (intensity) of the distinct Si (T_1, T_2, T_3) environments and it was calculated using the equation $c = 1/3\ (\%T_1 + 2\%T_2 + 3\%T_3)$ [18,21]. The peak assignment and the relative populations of the different Si sites, estimated after deconvolution using Gaussian band shapes, are depicted in Table 3. The results show that the degree of polysiloxane formation in each hybrid is different, depending on the experimental conditions. The increase of isocyanate and acetic acid/ethanol molar ratio in CHY3 (Experimental section) increases the population of the T_2 and T_3 sites and reduces the population of the T_1 site, leading to a higher degree of condensation (71%) and, hence, a close network structure is formed. The change of the molecular weight of chitosan to prepare CHY2 did not change significantly the degree of condensation. In general, the results confirm that the siloxane network was incorporated, to different extents, into chitosan.

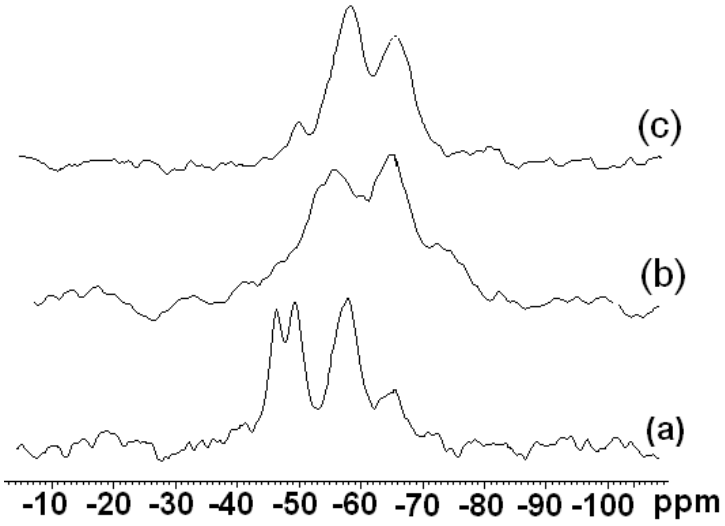

Figure 4. ^{29}Si MAS NMR spectra for CHY1 (a), CHY2 (b) and CHY3 (c).

It was worth noting that the variation of the polycondensation degree with the NCO/NH_2 ratio (Table 3) agrees well with the deconvolution of the "amide I" region (Table 2). The larger ratio of NCO/NH_2 results in more precursors formed in the first step and more complete polycondensation in the second step and consequently higher degree of condensation. This is consistent with the decrease of the amount of urea-polyether hydrogen-bonded structures and the simultaneous increase of the amount of strong self-associated hydrogen-bonded urea-urea associations as the NCO/NH_2 ratio enlarges (Table 2).

Table 3. ^{29}Si NMR chemical shifts and population of the different T_n species and degree of condensation, *c*, of the chitosan/siloxane hybrids.

Sample	**CHY 1**	**CHY2**	**CHY3**
Precursor	-45.3 (24)	-45.6 (17)	-
T1- $Si(OSi)(OR)_2$ (%)	-49.9 (27)	-49.8 (24)	-48.6 (15)
T2- $R´Si(OSi)_2(OR)$ (%)[a]	-58.2 (32)	-57.9 (42)	-58.0 (58)
T3- $R´Si(OSi)_3$ (%)	-65.7 (9)	-66.0 (10)	-66.7 (27)
c (%)[b]	39	46	71

[a] R denotes the ethoxy groups; R´denotes the polymeric chain bonded to urea groups; [b]*c* = degree of condensation; in parenthesis is the population.

The RT powder X-ray diffraction patterns of chitosan and chitosan/siloxane hybrids are shown in Figure 5A. All the patterns exhibit a main peak centred at *ca.* 20.02° associated with the chitosan crystalline structure [47]. The second-order of this peak appears as a broad hump at *ca.* 40°. Accordingly, a structural unit distance of 4.43±0.1 Å is obtained. For the chitosan/siloxane hybrids both peaks broaden due to the presence of siloxane nanodomains, whose first diffraction peak appears at *ca.* 21.0-21.7° [6,18-20]. For instance, in the pattern of the CHY1 chitosan/siloxane hybrid the full-width-at-half-maximum (fwhm) of the main peak increases *ca.* 50%, relatively to the fwhm of this peak in the chitosan matrix pattern.

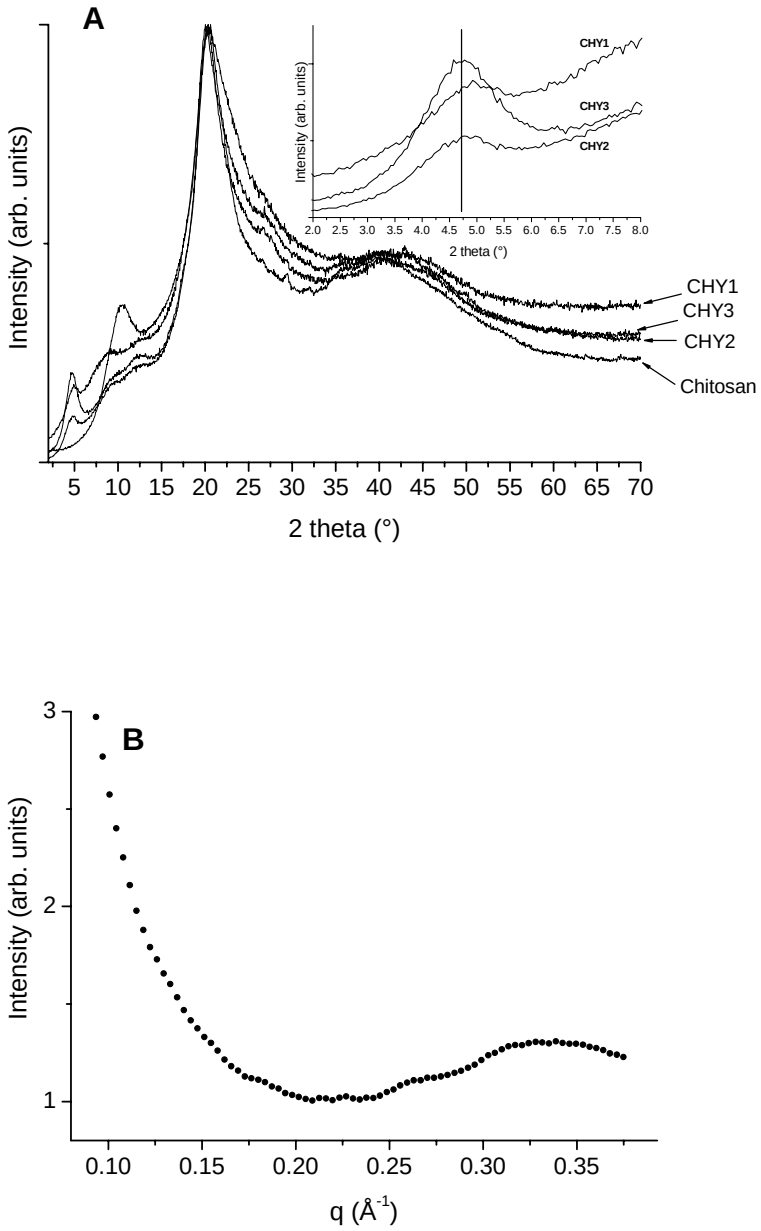

Figure 5. A: Powder X-ray diffraction patterns of chitosan/siloxane hybrids. The inset shows the XRD diffractograms in the low 2θ region. B: SAXS pattern of the CHY3 chitosan/siloxane hybrid.

In addition, a shoulder is clearly observed at *ca.* 10° in the trace of pure chitosan. This feature is ascribed to other type of ordering within the chitosan chains, with a characteristic distance of *ca.* 8.5±0.3 Å. For the chitosan/siloxane hybrids, this peak is not seen, and two broad and weak humps are present at *ca.* 8.5-9.0 and 12.0-12.5°.

The peak appearing at low angles, *ca.* 5°, in the XRD patterns of chitosan/siloxane hybrids (insert of Figure 5A) is ascribed to interparticle scattering interference and indicates a highly non-periodic fluctuation of the electronic density in these hybrid materials. This well-defined peak, which is also clearly seen in the SAXS scattering profile of the CHY3 hybrid (Figure 5B), was attributed to the liquid-like spatial correlation of siloxane-rich domains embedded in the polymer matrix and located at the ends of the organic segments [48,49]. This result suggests a diphasic structure for the morphology of the hybrids caused by local phase separation between inorganic silicon-rich domains and polymeric regions, as in the case of analogous di-ureasil and di-urethanesil hybrids [6,18-23].

From the XRD peak maximum position (Figure 5A) the average interparticle distance, *d*, is estimated to be 18-19±1 Å. From the magnitude of the SAXS scattering vector of the peak maximum, the corresponding interdomain distance is calculated as *d*=18.6±0.1 Å, matching well the value extracted from the XRD diffractogram. This distance is similar to that reported for similar organic/inorganic hybrids [6,48,49].

3.2. *In Vitro Apatite Forming Ability*

It is known that the presence of Si-OH groups in different types of materials can induce the formation of a bone-like apatite layer [50-52]. In the present work preliminary *in vitro* apatite forming ability tests in simulated body fluid (SBF) were conducted to assess the ability of the chitosan hybrids to induce the formation of an apatite layer on its surface. Pure chitosan did not show ability to induce the apatite formation (Figure 6A). For chitosan/siloxane hybrids, the formation of Ca-P

nuclei sitting on specific sites of the substrate surface was observed. It can be seen that the formation of precipitates occurs, which may be due to the apatite formation (Figure 6C) after immersion in SBF for 21 days. The EDS analysis revealed that the precipitates consisted of calcium and phosphorus elements (Figure 6D). Figure 6E shows the XRD results for chitosan/siloxane hybrids after soaking in SBF. It can be observed that apatite peaks were observed after immersion in SBF on the surface of CHY2 sample. The diffraction peaks above 30° in the XRD spectra are in agreement with the standard pattern of hydroxyapatite (JCPDS 9-432), although the partially amorphous nature of film was also evident. These results are in agreement with the ones obtained from SEM, where only apatite nuclei were observed on the surface of hybrid (seen by Fig. 6C). The results indicate that a longer soaking period (21 days) is required to form Ca-P nuclei, and this effect depends on the amount and arrangement of silanol groups in the materials structure. The results in this work suggest that such systems do in fact exhibit a bioactive behaviour. However, further improvements in the compositions, synthesis conditions and surface modification, would be necessary to minimise the time necessary to observe the apatite layer formation.

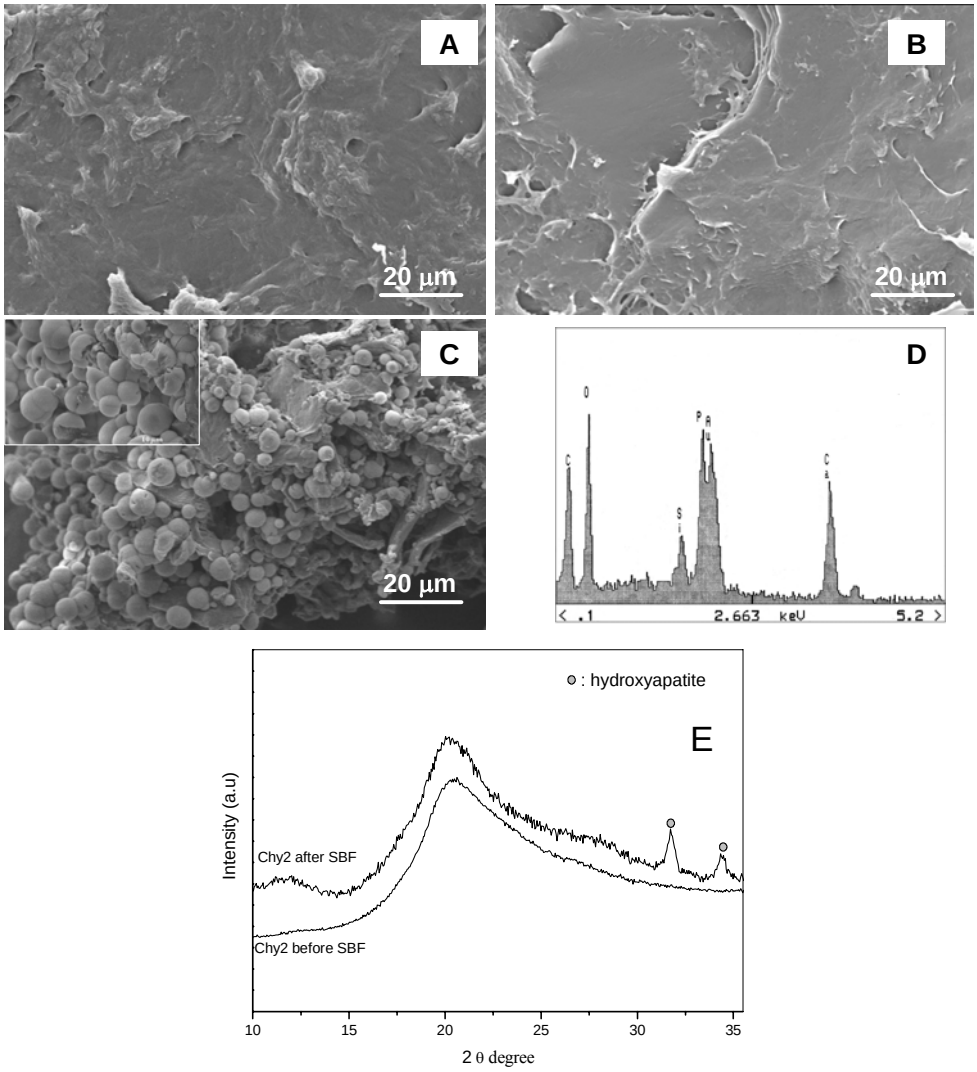

Figure 6. SEM images of the chitosan (A), CHY2 before immersion in SBF (b) after 21 days in immersion in SFF (C), EDS analysis (D) and XRD analysis.

3.3. *Photoluminescence*

Figures 7 shows the excitation (PLE) spectra of chitosan and two representative chitosan/siloxane hybrids (CHY1 and CHY3) detected between 13 and 300 K.

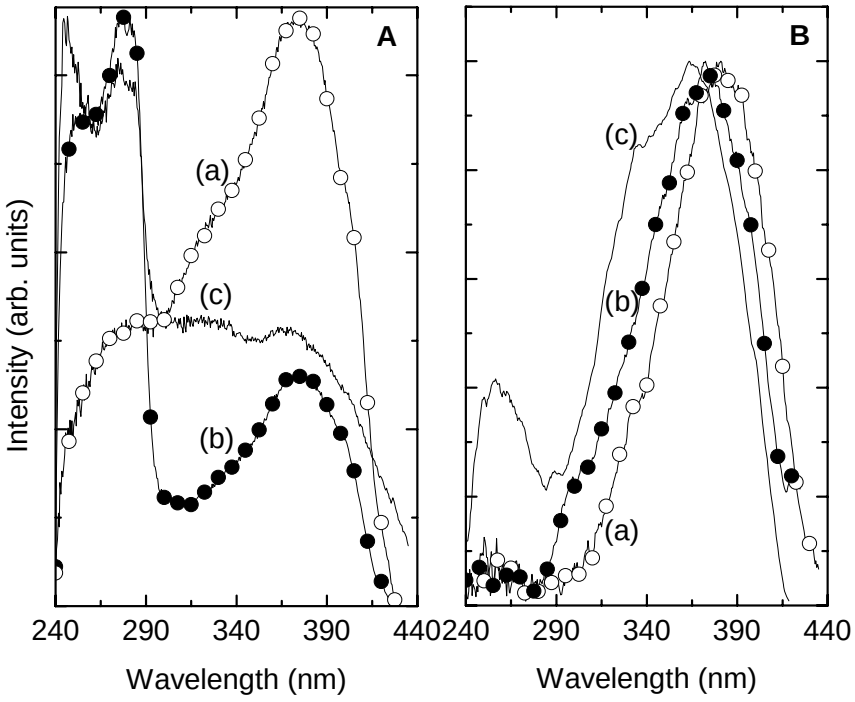

Figure 7. PLE spectra of chitosan (a), CHY1 (b), and CHY3 (c), monitored around 440-450 nm at 13 (A) and 300 K (B).

The low-temperature chitosan spectrum consists of a large broad band between 240 and 420 nm, where it is possible to discern a main component, whose peak position occurs at *ca.* 375 nm, and two lower intensity bands, located at *ca.* 290 and 335 nm. Marked changes are observed in the low-temperature PLE spectra of the chitosan/siloxane hybrids, particularly in the high-energy region. These spectra are formed by two main peaks at *ca.* 245 and 278 nm and by a lower intensity broad band region showing two main components at *ca.* 335 and 375 nm, similarly to what was observed in the chitosan spectrum. The main differences observed

between the PLE features of the two hybrids are in the relative intensity of the two peaks (245 and 278 nm) and in the higher contribution of the band centred around 335 nm for the CHY3 PLE spectrum. Raising the temperature to 300 K, all the spectra display a main band peaking around 362-378 nm, and only the spectrum of the CHY3 hybrid shows a lower intensity band at *ca.* 256 nm.

Figures 8 presents the low-temperature emission (PL) spectra of chitosan and CHY1 and CHY3 hybrids recorded at two selected excitation wavelengths (278 and 375 nm). For the lower excitation wavelength (Figure 8A), all the spectra display a large broad band peaking around 450-480 nm. For the hybrids it is also possible to clearly discern another lower-intensity component around 340 nm. For 375 nm excitation wavelength, all the spectra display a large broad band at *ca.* 450-480 nm. Comparing the PL features of CHY1 and CHY3, there is a red-shift of the more intense band of the latter hybrid, whereas the more energetic emission has a greater contribution to PL spectra of the former hybrid.

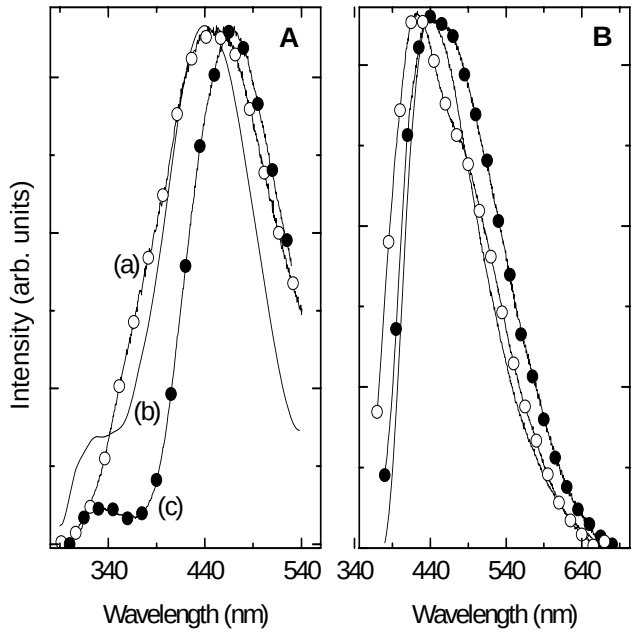

Figure 8. PL spectra measured at 13 K of chitosan (a), CHY1 (b), and CHY3 (c) excited at 278 (A) and 375 nm (B).

At room-temperature the band around 340 nm could not be detected. Apart from an intensity reduction around 30 % the spectra display only the lower energetic broad band that has been detected at 13 K (Figure 8B).

Preliminary lifetime measurements were carried out at 13 K for the chitosan and chitosan/siloxane hybrids (not shown). The lifetimes were monitored around 455-472 nm under 284-300 nm excitation wavelength with a starting delay of 0.05 ms. For such experimental conditions the data reveal a non-single exponential behaviour and therefore an effective lifetime (τ_e) for which the PL intensity is reduced to 1/e of its maximum intensity was considered. The τ_e values found for the CHY1 and CHY3 are around 350 ms and for the pure chitosan a faster $\tau_e \approx 90$ ms was estimated. At room-temperature both the hybrids' and the chitosan's emission bands have lifetimes faster than the limit detection of our experimental equipment (0.050 ms).

The hybrids' emission strongly depends on the excitation wavelength, for the whole temperature range between 13 and 300 K. Figure 9 shows the low-temperature spectra of the CHY3 hybrid for the excitation range between 350 and 420 nm. A blue-shift of the emission energy and an increase in the fwhm with the decrease of the excitation wavelength are observed. The energy dependence on the excitation wavelength has already been discussed for analogous poly(oxyethylene) (PEO)-siloxane and poly(oxypropylene) (POP)-siloxane hybrids [6,17-23], providing strong evidence of disordered-related processes, which are generally associated with transitions between localized states in amorphous structures. The origin of such behaviour is probably connected with radiative electron-hole recombinations involving localized states within the conduction and valence bands [6,20,21].

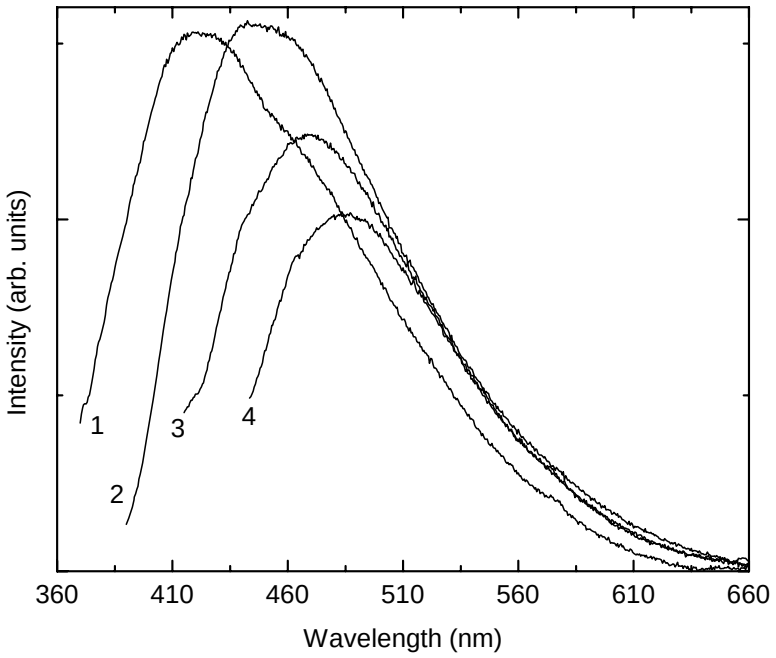

Figure 9. PL spectra measured at 13 K of CHY3 hybrid excited at 1) 350, 2) 375, 3) 400 and 4) 420nm.

The previous results for the chitosan/siloxane hybrids, namely the presence of more than one PLE component and the increase in the fwhm of the PL spectra as the excitation wavelength decreases from 420 to 350 nm strongly suggest the presence of more than one emission component. In order to further interpret the PL features a deconvoluting fitting procedure was applied to the emission spectra of the chitosan/siloxane hybrids, in the excitation wavelength range between 330 and 420 nm. The used method was similar to that reported for other classes of organic-inorganic hybrids such di-ureasils and di-urethanesils [6,18,20,21]. One Gaussian function was used to fit the emission spectrum excited within the interval 400-420 nm (2.95-3.10 eV). Since, the fwhm is determined primarily by carrier-phonon interaction, its value should not be affected by the variation of the excitation energy [6,18,20]. Therefore, for each hybrid, the fwhm-fitted values were considered to

be independent of the excitation energy. In contrast, the peak energies and their integrated intensity were, for each hybrid, free to vary for the whole excitation energy range used. For excitation wavelengths between 330 and 375 nm (3.31-4.00 eV) the fitting method revealed the presence of two Gaussian bands in the blue (≈ 2.53-2.64 eV) and in the purplish-blue (≈ 2.82-3.12 eV) spectral regions. Only the former component was observed for excitation wavelengths in the 400-420 nm (2.95-3.10 eV) interval. The fwhm reached approximately 0.50 and 0.35 eV for the blue and purplish-blue bands, respectively. It was observed that the energy of the blue band is almost independent of the excitation wavelength, whereas the energy of the purplish-blue band shifts to the red as the excitation wavelength decreases.

Comparing these fit results with those already reported for other classes of analogous organic-inorganic hybrids, such as di-ureasils and di-urethanesils, we can ascribe the origin of the blue and purplish-blue components to electron-hole recombinations that occur in the NH groups and in the siloxane nanoclusters, respectively. For the di-ureasils and di-urethanesils, it has been recently demonstrated that these two components reveal a radiative recombination mechanism typical of donor-acceptor pairs, mediated by some localized centers [21]. Photoinduced proton-transfer between defects such as NH_2^+ and N^- is proposed as the mechanism responsible for the NH-related component.

The chitosan-related emission might be originated by electron-hole recombinations that take place in the NH groups, similarly to the blue band in the chitosan/siloxane hybrids.

Returning to the fit results, the most notorious variations found in the fitting parameters are related with variations in the integrated intensity of the two PL components. The data in Figure 10 shows that the relative contribution between the integrated intensity of the NH and siliceous-related emissions strongly depends on the sample. For the CHY1 hybrid it is observed that the NH emission component dominates the overall emission independent on the selected excitation wavelength within the interval 330-400 nm. For CHY3 the previous results occur only for

excitation wavelengths higher than 350 nm, since at lower excitation wavelengths (350-330 nm) the PL associated with the siliceous domains dominates the emission features. Such range of excitation wavelengths favours the siliceous related emission, so that an increase in the emission intensity observed for the CHY3 sample with respect to the NH-related emission might be a consequence of the higher condensation degree of this hybrid (the number of defects associated with the dangling bonds, for instance, increases with the condensation degree), see Table 3.

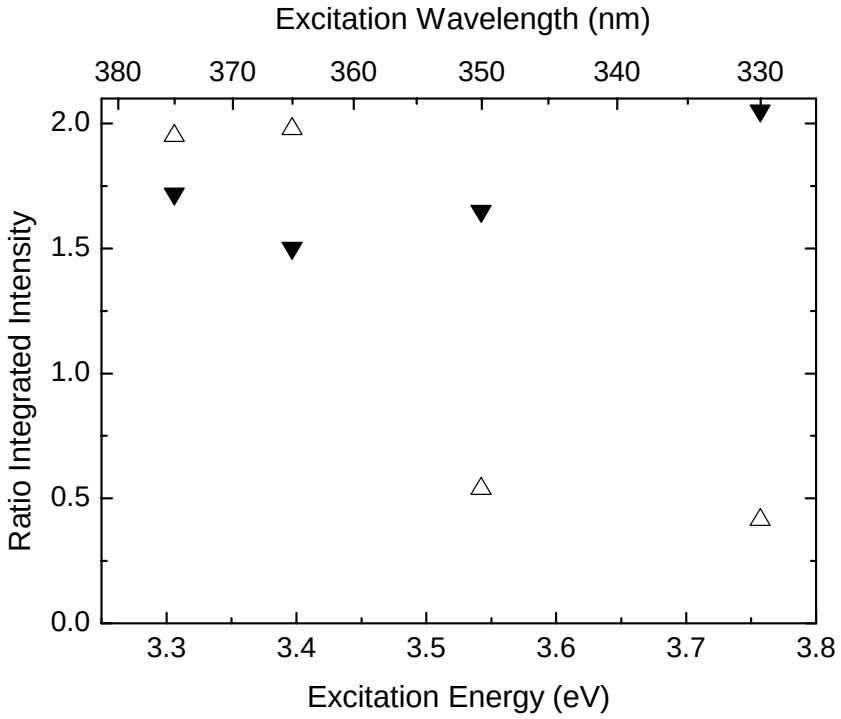

Figure 10. RT ratio of the integrated intensity of the NH (blue band) and siliceous (purplish-blue band) related emission for the CHY1 (down triangle) and CHY3 (up triangle) hybrids, obtained from the fit procedure to the PL spectra obtained at different excitation wavelengths.

The smaller contribution of the NH groups to the PL features of the CHY3 hybrid relatively to the CHY1 may be induced by the stronger hydrogen bonds established between adjacent urea groups, as pointed out by FTIR results (Table 2). The presence of stronger hydrogen bonds in CHY3 contributes to localize the proton rendering difficult its induced transfer between NH groups and, consequently, reducing the intensity of the NH-related emission.

4. **Conclusions**

Polysaccharide-inorganic hybrids based on low-molecular weight chitosan are interesting because of their chemical versatility, which allows tailoring novel functionalities accomplished by linkages between the different polymer groups and the inorganic components. Novel chitosan/siloxane hybrids were synthesized by a sol-gel derived carboxylic acid solvolysis. Structural characterization by a range of techniques (FTIR, ^{29}Si MAS NMR, ^{13}C CP/MAS NMR, powder XRD, SEM) confirmed that the derivatives are bifunctional hybrids, in which urea and urethane bridges covalently bond chitosan to the polysiloxane network. From the bioactivity tests, it can be concluded that the apatite formation mainly depends on the amount and arrangement of the silanol groups in materials structure. The PL results furnish unequivocal evidence for the presence of a new band with higher energy and long lifetime, relatively to the characteristic emission of pure low-molecular weight chitosan. Since this component is associated with electron-hole recombinations mediated by donor-acceptor pairs arising from oxygen-related defects at the surface of the siliceous nanodomains (dangling bonds, for instance), the features observed in the high-energy region of the PL spectrum of CHY3, relatively to the remaining hybrids, could be connected with the higher condensation degree of their inorganic domains (Table 3) and with the stronger hydrogen bonds established between adjacent urea groups (Table 2) . The siloxane-chitosan hybrids exhibit therefore interesting photoluminescent characteristics that may be adequate to their use as optical probes for applications *in vivo*.

5. **Acknowledgments**

The authors thank the Anabela Valente (CICECO, University of Aveiro) and Verónica de Zea Bermudez (UTAD) for their help on the adsorption measurements and synthesis process, respectively. L. D. Carlos acknowledges Karim Dahmouche (UNESP, Brazil), Nuno Silva (CICECO, University of Aveiro) and LNLS staff for their collaboration during SAXS experiments/analysis. S. S. Silva and L. Fu thank the Portuguese Foundation for Science and Technology (FCT) for providing PhD and pos-doctoral scholarships (SFRH/BD/8658/2002 and SFRH/BPD/5657/2001, respectively). This work was partially supported by FCT, through funds from the POCTI and/or FEDER programmes.

6. **References**

1. Romero, P. G. and Sanchez, c., *Functional Hybrid Materials* Wiley-VCH, 2003.
2. Sanchez, C., Soler-Illia, D. A. A., Ribot, F., and Grosso, D., Design of functional nano-structured materials through the use of controlled hybrid organic–inorganic interfaces, *Comptes Rendus Chimie* 6, 1131-1151, 2003.
3. Lebeau, B. and Clément Sanchez, C., Sol-gel derived hybrid inorganic-organic nanocomposites for optics, *Current Opinion in Solid State and Materials Science* 4, 11-23, 1999.
4. Sanchez, C. and Lebeau, B., Design and properties of hybrid organic-inorganic nanocomposites for photonics, *Materials Research Society Bulletin* 26, 377-387, 2001.
5. Messori, M., Toselli, M., Pilati, F., Mascia, L., and Tonelli, C., Synthesis and characterisation of silica hybrids based on poly(-caprolactone-b-perfluoropolyether-b-caprolactone), *European Polymer Journal* 38, 1129-1136, 2002.
6. Carlos, L. D., Ferreira, R. A. S., and Bermudez, V. Z., *Handbook of organic-inorganic hybrid materials and nanocomposites* American Scientific Publishers, California, 2003.
7. Biazzotto, J. C., Sacco, H. C., Ciuffi, K. J., Ferreira, A. G., Serra, O. A., and Iamamoto, Y., Synthesis and properties of urea porphyrinosilica, *Journal of Non-Crystalline Solids* 273, 186-192, 2000.
8. Shang, X.-Y., Zhu, Z.-K., Yin, J., and Ma, X.-D., Compatibility of soluble polyimide/silica hybrids induced by a coupling agent, *Chemistry of Materials* 14, 71-77, 2002.
9. Moreau, J. J. E., Vellutini, L., Man, M. W. C., and Catherine Bied, C., New hybrid organic-inorganic solids with helical morphology via H-bond mediated sol-gel hydrolysis of silyl derivatives of chiral (R,R)- or (S,S)-diureidocyclohexane, *Journal of the American Society* 123, 1509-1510, 2001.
10. Coradin, T., Mercey, E., Lisnard, L., and Livage, J., Design of silica-coated microcapsules for bioencapsulation, *Chemical communications* 23, 2496-2497, 2001.
11. Sanchez, C. and Ribot, F., *New Journal of Chemistry* 18, 1007, 1994.
12. Green, W. H., Le, K. P., Grey, J., Au, T. T., and Sailor, M. J., White phosphors from a silicate-carboxylate sol-gel precursor that lack metal activator ions, *Science* 276, 1826-1828, 1997.

13. Bekiari, V. and Lianos, P., Tunable photoluminescence from a material made by the interaction between (3-aminopropyl)triethoxysilane and organic acids, *Chemistry of Materials* 10, 3777-3779, 1998.
14. Ren, L., Tsuru, K., Hayakawa, S., and Osaka, A., Synthesis and characterization of gelatin-siloxane hybrids derived through sol-gel procedure, *Journal of Sol-Gel Science and Technology* 21, 115-121, 2001.
15. Bermudez, V. Z., Carlos, L. D., and Alcácer, L., Sol-gel derived urea cross-linked organically modified silicates. 1. Room Temperature Mid-Infrared Spectra, *Chemistry of Materials* 11, 569-580, 1999.
16. Stathatos, E., Lianos, P., Stangar, U. L., and Orel, B., A high-performance solid-state dye-sensitized photoelectrochemical cell employing a nanocomposite gel electrolyte made by the sol-gel route, *Advanced Materials* 14, 354-357, 2002.
17. Berkiari, V., Lianos, P., Stangar, U. L. L., Orel, B., and Judenstein, P., Optimization of the intensity of luminescence emission from silica/poy(ethylene oxide) and silica/poly(prolylene oxide) nanocomposite gels, *Chemistry of Materials* 12, 3095-3099, 2000.
18. Fu, L., Ferreira, R. A. S., Silva, M. J. O., Carlos, L. D., Bermudez, V. Z., and Rocha, J., Photoluminescence and quantum yields of urea and urethane cross-linked nanohybrids derived from carboxylic acid solvolysis, *Chemistry of Materials* 16, 1507-1516, 2004.
19. Gonçalves, M. C., Bermudez, V. Z., Ferreira, A. G., Carlos, L. D., Ostrovskii, D., and Rocha, J., Optically functional di-urethanesil nanohybrids containing Eu+ ions, *Chemistry of Materials* 16, 2530-2543, 2004.
20. Carlos, L. D., Bermudez, V. Z., Ferreira, A. G., Marques, L., and Assunção, M., Sol-gel derived urea cross-linked organically modified silicates, *Chemistry of Materials* 11, 581-588, 1999.
21. Carlos, L. D., Ferreira, A. G., Orion, I., Bermudez, V. Z., and Rocha, J., Sol–gel derived nanocomposite hybrids for full colour displays, *Journal of Luminescence* 702-705, 87, 2000.
22. Carlos, L. D., Ferreira, A. G., Bermudez, V. Z., and Ribeiro, S. J. L., Full-color phosphors from amine-functionalized crosslinked hybrids lacking metal activator ions, *Advanced Functional Materials* 2, 111-115, 2001.
23. Carlos, L. D., Ferreira, A. G., Pereira, R. N., Assunção, M., and Bermudez, V. Z., White-light emission of amine-functionalized organic/inorganic hybrids: emitting centers and recombination mechanisms, *Journal of Physical Chemistry B* 108, 14924-14932, 2004.
24. Ren, L., Tsuru, D.,Hayakawa, S. and Osaka, A. Synthesis and characterization of gelatin-siloxane hybrids derived through sol-gel procedure, Journal of Sol-Gel Science and Technology 21,115-121,2001.
25. Schipunov, Y. A., Sol–gel-derived biomaterials of silica and carrageenans, J*ournal of Colloid and Interface Science* 268, 68-76, 2003.
26. Fuentes, S., Retuert, P. J., Ubilla, A., Fernandez, J., and Gonzalez, G., Relationship between composition and structure in chitosan-based hybrid films, *Biomacromolecules* 1, 239-243, 2000.
27. Retuert, P. J., Quijada, R., Arias, V., and Pedra, M. Y., Porous silica derived from chitosan-containing hybrid composites, *Journal of Materials Research* 18, 487-494, 2003.
28. Bond, R. and McAuliffe, J. C., Silicon biotechnology: new opportunities for carbohydrate science, *Australian Journal of Chemistry* 56, 7-11, 2003.
29. Silva, S. S., Santos, M. I., Coutinho, O. P., Mano, J. F., and Reis, R. L., Physical properties and biocompatibility of chitosan/soy blended membranes, *Journal of Materials Science-Materials in Medicine* 16, 575-579, 2005.
30. Tuzlakoglu, K., Alves, C. M., Mano, J. F., and Reis, R. L., Production and characterization of chitosan fibers and 3-D fiber mesh scaffolds for tissue engineering applications, *Macromolecular Bioscience* 4, 811-819, 2004.

31. Baran, E. T., Tuzlakoglu, K., Salgado, A. J., and Reis, R. L., Multichannel mould processing of 3D structures from microporous coralline hydroxyapatite granules and chitosan support materials for guided tissue regeneration/engineering, *Journal of Materials Science-Materials in Medicine* 15, 161-165, 2004.
32. Zhu, A. P., Zhang, Z., and Shen, J., Preparation and characterization of novel silica-butyrylchitosan hybrid biomaterials, *Journal of Materials Science-Materials in Medicine* 14, 27-31, 2003.
33. Ayers, M. R. and Hunt, A. J., Synthesis and properties of chitosan-silica hybrid aerogels, *Journal of Non-Crystalline Solids* 285, 123-127, 2001.
34. Hu, X., Littrel, K., Ji, S., Pickles, D. G., and Risen, W. M., Caracterization of silica-polymer aerogel composites by small-angle neutron scattering and transmission electron microscopy, *Journal of Non-Crystalline Solids* 288, 184-190, 2001.
35. Park, S., You, J. O., Park, H. Y., Haam, S. J., and Kim, W. S., A novel pH-sensitive membrane from chitosan — TEOS IPN; preparation and its drug permeation characteristics, *Biomaterials* 22, 323-330, 2001.
36. Airoldi, C. and Monteiro, O. A. C., Chitosan-organosilane hybrids- synthesis, characterization, cooper adsorption and enzyme immobilization, *Journal of Applied Polymer Science* 77, 797-804, 2000.
37. Molvinger, K., Quignard, F., Brunel, D., Boissiere, M., and Devoisselle, J. M., Porous chitosan-silica hybrid microspheres as a potential catalyst, *Chemistry of Materials* 16, 3367-3372, 2004.
38. Muzzarelli, R. A. A. and Peter, M. G., *Chitin handbook* European chitin society, Grottammare, 1997.
39. Kokubo, T., Kushitani, H., Sakka, S., Kitusgi, T., and Yamamuro, T., Solutions able to reproduce in vivo surface-structure changes in bioactive glass-ceramic A-W3, *Journal of Biomedical Materials Research* 24, 721-734, 1990.
40. Morales, P. V., Le Nest, J.-F., and Gandini, A., Polymer electrolytes derived from chitosan/polyether networks, *Electrochimica Acta* 43, 1275-1279, 1998.
41. Pope, E. J. A. and Mackenzie, J. D., Sol-gel processing of silica: II. the role of the catalyst, *Journal of Non-Crystalline Solids* 87, 185-198, 1986.
42. Azevedo, W. M. and Brondani, D. J., Formic acid an efficient solvent to prepare polyaniline/silicate glass composite using sol-gel technique, *Journal of Non-Crystalline Solids* 296, 224-229, 2001.
43. Pawlak, A. and Mucha, M., Thermogravimetric and FTIR studies of chitosan blends, *Thermochimica Acta* 396, 153-166, 2003.
44. Bertoluzza, A., Fagnano, C., Morelli, M. A., Gottardi, V., and Gulielmi, M., Raman and infrared spectra on silica gel evolving toward glass, *Journal of Non-Crystalline Solids* 48, 117-128, 1982.
45. Monteiro, O. A. C. and Airoldi, C., Some studies of crosslinking chitosan-glutaraldehyde interaction in a homogenerous system, *International Journal of Biological Macromolecules* 26, 119-128, 1999.
46. Franville, A.-C., Mahiou, R., Zambon, D., and Cousseins, J.-C., Molecular design of luminescent organic-inorganic hybrid materials activated by europium (III) ions, *Solid State Sciences* 3, 211-222, 2001.
47. Jaworska, M., Sakurai, K., Gaudon, P., and Guibal, E., Influence of chitosan characteristics on polymer properties: I. Cystallographic properties, *Polymer International* 52, 198-205, 2003.
48. Dahmouche, K., Santilli, C. V., Pulcinelli, S. H., and Craievich, A. F., Small-angle X-ray scattering study of sol-gel-derived siloxane-PEG and siloxane-PPG hybrid materials, *Journal of Physical Chemitry B* 103, 4937-4952, 1999.

49. Dahmouche, K., Carlos, L. D., Bermudez, V. Z., Ferreira, R. A. S., Santilli, C. v., and Craievich, A. F., Structural modelling of Eu3+ based siloxane-poly(oxyethylene) nanohybrids, *Journal of Materials Chemistry* 11, 3249-3257, 2001.
50. Kokubo, T., Kim, H.-M., and Kawashita, M., Novel bioactive materials with different mechanical properties, *Biomaterials* 24, 2161-2175, 2003.
51. Rhee, S.-H., Effect of molecular weight of poly(caprolactone) on interpenetrating network structure, apatite-forming ability, and degradability of poly(caprolactone)/silica nano-hybrid materials, *Biomaterials* 24, 1721-1727, 2003.
52. Oyane, A., Nakanishi, K., Kim, H.-M., Miyaji, F., Kokubo, T., Soga, N., and Nakamura, T., Sol-gel modification of silicone to induce apatite-forming ability, *Biomaterials* 20, 79-84, 1999.

CHAPTER IV

CHAPTER IV

Plasma Surface Modification of Chitosan Membranes: Characterization and Preliminary Cell Response Studies

Abstract

Surface modification of biomaterials is a way to tailor cell responses whilst keeping the bulk properties. In this work, chitosan membranes were prepared by solvent casting and treated with nitrogen or argon plasma at 20 W for 10 – 40 minutes. Atomic force microscopy indicated an increase in the surface roughness as a result of ongoing etching process. X-ray photoelectron spectroscopy and contact angle measurements showed different surface elemental composition and higher surface free energy. MTS test and direct contact assays with L929 fibroblast cell line indicated that the plasma treatment improved the cell adhesion and proliferation. Overall, the results demonstrated that such plasma treatments could significantly improve the biocompatibility of chitosan membranes and thus improving their potential in wound dressings and tissue engineering applications.

This chapter is based on the following publication:

S. S. Silva, S. M. Luna, M. E. Gomes, J. Benesch, I. Paskuleva, J. F. Mano, R. L. Reis. "Plasma surface modification of chitosan membranes: characterization and preliminary cell response studies", Macromolecular Bioscience, 2008, 8(6):568-576.

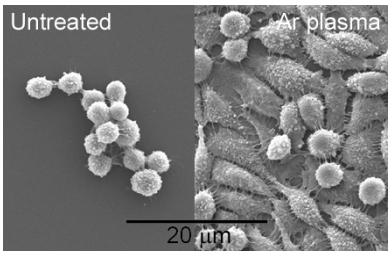

---

1. **Introduction**

Every year millions of people suffer cutaneous lesions such as burns, abrasions or wounds that need treatment. When the skin is wounded cellular damage, loss of tissue, changes in the relationship between the tissues and the surrounding environment are correlated in a complex series of cellular and chemical events[1]. It is well established that severely damaged skin requires a protective barrier for proper healing. Effective wound dressing must not only protect the wound from the surrounding environments but also to promote the healing process by providing an optimal microenvironment[2,3]. Polysaccharides have been widely used in wound management aids. Due to their relative versatility in terms of composition, structure and intrinsic properties, they can assist proper physiological reconstruction of the skin and reduce or prevent scar tissue formation[4]. Some of the thoroughly studied natural polymers for skin regeneration are alginate, chitosan, hyaluronic acid, cellulose, collagen, gelatin and their derivatives[3-10] . These polymers can be used as gelling agents, consistency excipients in creams, matrices in patches, sponge type wound dressings, hydrogels, membranes and skin adhesives in transdermal systems [3-11]. Among them, chitosan possesses several characteristics favourable for promoting dermal regeneration and accelerated wound healing [5,12]. Its biodegradability, adhesiveness, non-toxicity, bacteriostatic, fungistatic, hemostatic activities and antimicrobial effect make this polysaccharide an excellent biomaterial to treat wounds [5,12-15]. Several works [16,17] have shown that chitosan-derived membranes are not cytotoxic towards fibroblasts but tend to inhibit cell proliferation. Thus, significant research efforts have been focused on improving the host response to these materials in terms of cellular behaviour. Earlier studies have used a variety of methods such as blending[16], gamma irradiation[18], chemical reactions[19], and plasma surface modification[20-23]. The last one, plasma surface modification, is a method widely used[23-25] to tailor surface functionality by working in different atmospheres. The commonly used oxygen plasma results in the formation of different oxygen containing groups as –OH, -

C=O, -COOH. Argon and nitrogen are other examples of gases used in the plasma treatment[26-29]. As a result of the introduced changes in the surface chemistry, different cell behaviour on the modified material can be observed[26-29].

The aim of this study was to improve the biocompatibility of chitosan membranes in terms of fibroblasts responses *in vitro*. Two sets of experiments using nitrogen and argon treatments for different time were carried out. *In vitro* biological assays with L929 fibroblasts like-cells was performed to evaluate the influence of the introduced changes on cells´ behaviour on a preliminary basis. To our knowledge there is no other study that has compared the effect of these surface treatments of chitosan membranes on fibroblasts response.

2. **Materials and Methods**

2.1. *Materials and Samples preparation*

Chitosan- Cht (Sigma Aldrich, CAS 9012-76-4) with deacetylation degree of 83.8% as determined by ^{1}H NMR[30] was used. All other reagents were analytical grade and used as received. Chitosan powder was dissolved at 1wt% in 0.2M acetic acid. Chitosan membranes (average thickness of 47μm) were obtained by solvent casting technique, followed by neutralisation in a 0.1M NaOH solution for 30 min. The plasma treatment was carried out in a radio frequency plasma reactor (PlasmaPrep5, Germany). The plasma chamber was thoroughly purged with a continuous flow of the gas used during the treatment to reduce trace amounts of air and moisture. During the treatment the gas flow was adjusted in order to keep a constant pressure of 0.2 mbar insight the chamber. A power of 20W was applied. The duration of the treatment was varied from 10 min to 40 min. Two different working gases, namely nitrogen (N_2) and argon (Ar) (see Table 1 that also contains designation codes for each treatment), were used in order to evaluate the effect of the working gas on the induced changes in the surface functionalities.

Table 1. Plasma conditions used for modification of chitosan membranes

Sample	Conditions		
	Power [Watts]	**Time [min]**	**Gas**
ChtP1	20	10	N_2
ChtP2	20	20	N_2
ChtP3	20	30	N_2
ChtP4	20	40	N_2
ChtP5	20	10	Ar
ChtP6	20	20	Ar
ChtP7	20	30	Ar
ChtP8	20	40	Ar

2.2. **Characterization Methods**

2.2.1. *Scanning electron microscopy (SEM)*

The surface morphology of the samples was analyzed using a Leica Cambridge S-360 scanning electron microscope (SEM). All specimens were pre-coated with a conductive layer of sputtered gold. The micrographs were taken at 10kV at different magnifications.

2.2.2. *Atomic force microscopy (AFM)*

The roughness of the sample surface was measured by AFM. The analyses were performed on at least three spots per sample using TappingMode (Veeco, USA) connected to a NanoScope III (Veeco, USA) with non-contacting silicon nanoprobes (ca 300kHz, setpoint 2-3V) from Nanosensors, Switzerland. All images were fitted to a plane using the 3rd degrees flatten procedure included in the NanoScope

software version 4.43r8. The surface roughness was calculated as Sq (root mean square from average flat surface) and Sa (average absolute distance from average flat surface). The values are presented as mean ± standard deviation.

2.2.3. *X-ray photoelectron spectroscopy (XPS)*

The XPS analysis was performed using ESCALAB 200A, VG Scientific (UK) with PISCES software for data acquisition and analysis. For analysis an achromatic Al (Kα) X-ray source operating at 15 kV (300 W) was used. The spectrometer was calibrated with reference to Ag 3d5/2 (368.27 eV) and it was operated in constant analyser energy (CAE) mode with 20 eV pass energy. The measurements were carried out at a take-off angle of 90° (normal to the surface). Data acquisition was performed with a pressure lower than 10^{-6} Pa. The value of 285 eV of the hydrocarbon C1s core level was used as a calibration for the absolute energy scale. Overlapping peaks were resolved into their individual components by XPSPEAK 4.1 software.

2.2.4.*Contact angle measurements*

The surface wettability of the membranes was assessed by static contact angle (θ) measurements using the sessile drop method. Two different liquids were used; ultra-pure water (polar) and diiodomethane (non-polar). The measurements were performed using OCA20 equipment (DataPhysics, Germany) and SCA-20 software. The presented data were averaged on six measurements. The surface energy was calculated using the Owens, Wendt, Rabel and Kaelble (OWRK) equation[31].

2.3. ***In vitro*** **cell culture studies**

2.3.1. *Cell culture*

A mouse fibroblasts-like cell line (L929) was selected for all the biological assays in order to evaluate the effect of surface modification on cell adhesion, viability and proliferation. The L929 fibroblast cell line was obtained from European Collection of Cell Cultures (ECACC, UK). The cells were cultured in Dulbecco's Modified Eagle's Medium (DMEM; Sigma-Aldrich, USA), supplemented with 10% of heat inactivated fetal bovine serum (FBS; Biochrom AG, Germany) and 1% antibiotic/antimycotic solution (Invitrogen, Portugal) incubated at 37°C in a humidified atmosphere with 5% of CO_2. The culture medium was changed every 2 days.

2.3.2. *Direct Contact assay – cell adhesion and proliferation on chitosan membranes*

Chitosan membranes (1 cm^2 modified and non-modified) were seeded with 100μL of a cell suspension (8 x 10^4 cells/mL) and cultured for 3, 7 and 14 days at 37ºC. Tissue culture polystyrene coverslips (TCPS, Sarstedt, USA), were used as controls. After each incubation period the samples were rinsed with a phosphate buffer saline (PBS; Sigma-Aldrich, USA) and prepared for further analysis (MTS assay and SEM observations).

Prior to culturing, all the membranes were sterilized with ethylene oxide at previously described conditions[32].

2.3.3. *MTS assay*

Cellular viability was quantitatively assessed by the MTS (3-(4,5-dimethylthiazol-2-yl)-5-(3-carboxymethoxyphenyl)-2-(4-sulfophenyl)-2H-tetrazolium) assay (Promega, Madison, USA) [33]. Culture medium without FBS and without phenol red was mixed with MTS at a ratio 5:1, added to the membrane/cells constructs until totally cover them and incubated for 3 hours at 37°C in 5% CO_2 atmosphere. After the incubation period the optical density (OD) was read in a microplate reader (Bio-Tek,

USA) at 490 nm. The measurements were made in triplicate for each treatment and time point (3, 7 and 14 days).

2.3.4. *SEM analysis of the membranes*

Prior to SEM measurements the seeded membranes were fixed with 2.5% glutaraldehyde (Sigma-Aldrich, Germany) in a PBS solution and then dehydrated using a series of ethanol solutions (25, 30, 50, 70, 80, 90, 100%, v/v). The samples were dried overnight at room temperature, coated with gold by sputtering and observed by SEM.

3. **Results and Discussion**

When a polymer is exposed to plasma, two competitive processes, namely functionalization and etching, take place. In a typical plasma process the radicals created on the polymer surface by hydrogen removal combine with the radicals from the working gas to modify the surface. Alternatively, cross-linking could occur when the created radicals on the surface recombine with themselves. On the other hand, etching will also take place. The working conditions determine which processes will be dominant [24,25]. SEM images of the modified membranes did not show any significant changes of the surface morphology induced by the treatments (data not shown). Nevertheless, ongoing etching processes were confirmed by AFM. Changes of the surface topography after the performed modification were observed at the nanoscale (Figure 1). This effect was more significant after longer exposure time (30 and 40 minutes) when nitrogen was used as a working gas. Contrary, shorter exposure time (10 and 20 minutes) was more effective when the modification was performed in an argon plasma atmosphere. The roughness of the argon plasma treated membranes (Fig. 2B) decreases with longer exposure time (40 minutes) but the modified membranes were thinner compared to the untreated. Additionally, the treated membranes were more brittle which indicates cross-linking processes.

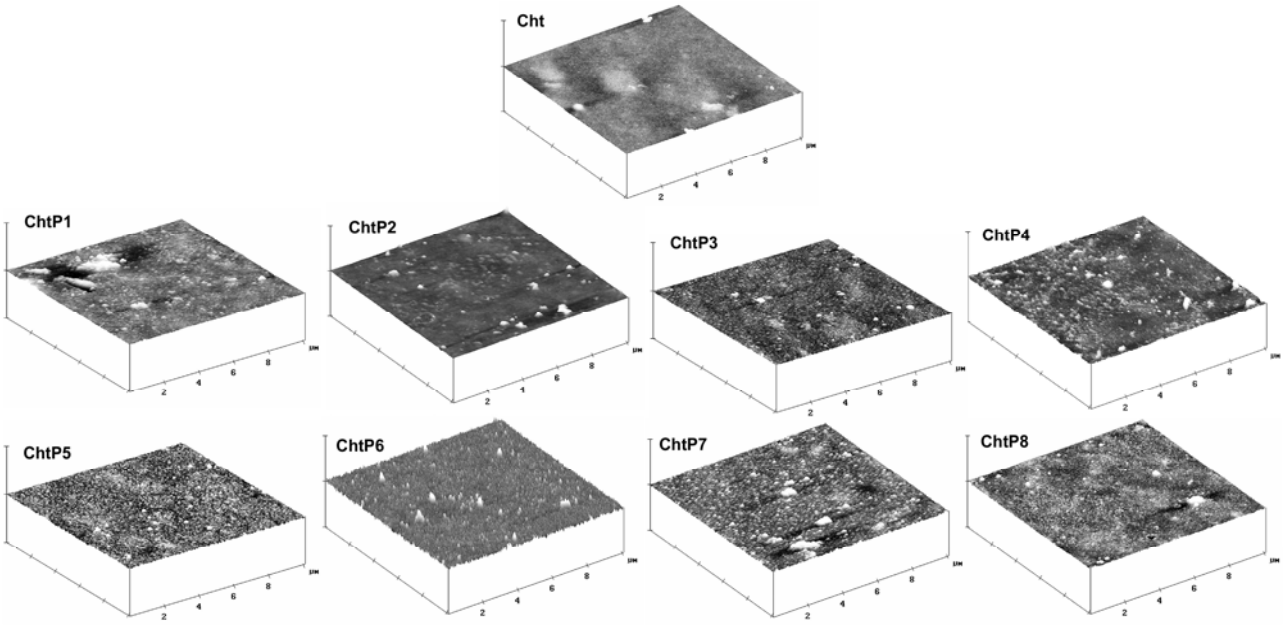

Figure 1. AFM images of chitosan membranes before (Cht) and after plasma treatment; ChtP1, ChtP2, ChtP3, ChtP4 - nitrogen plasma, and ChtP5, ChtP6, ChtP7, ChtP8 - argon plasma.

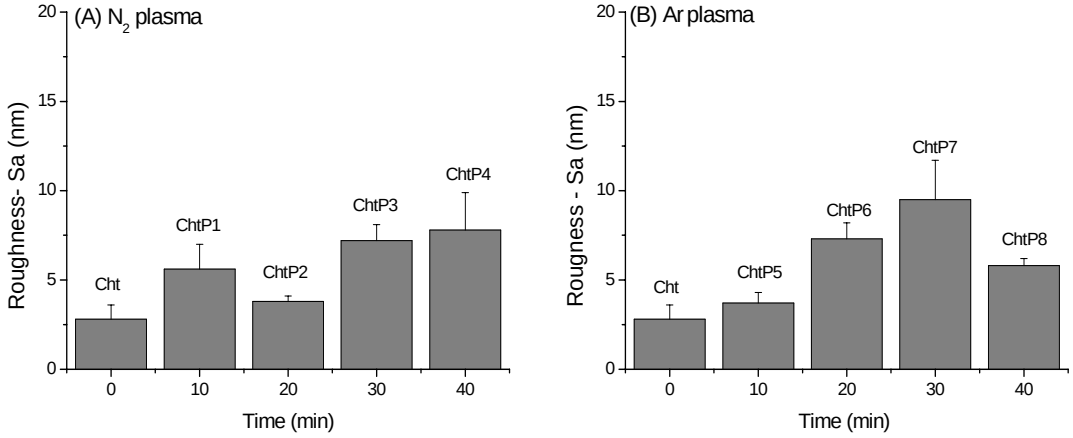

Figure 2. Mean roughness of chitosan membranes before and after nitrogen (A) and argon (B) plasma treatment.

The surface chemistry of modified and non-modified samples was investigated by XPS. Since the argon atmosphere is a non-reactive gas, mainly etching was expected to be observed after this treatment. As can be seen from Table 2 a significant increase in the nitrogen content was observed for shorter treatment times (10 and 20 minutes). Cleavage of the remaining -$COCH_3$ groups of chitosan is most probably the reason for the obtained results. This hypothesis was confirmed by the observed decrease of the intensity of the carbon peak in the ChtP5 spectrum. However, when the treatment was extended this relation was not that straightforward. For longer treatment time the reactive species created by plasma etch the already modified surface and therefore reveal non-modified surface. Hence, the values for C and N content obtained from the XPS spectra of the samples treated for 40 minutes (the longest time) are very similar to the initial ones for untreated chitosan (Table 2). When nitrogen is used as a working gas, not only etching but also functionalization with N-containing groups (-NH_2, -NH, =NH, $CONH_2$ or C≡N) must be observed [28]. Longer exposure times (30 and 40 minutes) resulted in higher nitrogen content (Table 2) that confirms the incorporation of those groups on the material surface.

Table 2. Surface composition and atomic ratios determined by XPS for original and modified membranes

Treatment	Sample	Surface composition			Atomic ratio %	
		%C	% O	% N	C/O ratio	C/N ratio
	Chitosan	66.41	27.97	5.62	2.37	11.82
N_2 plasma	ChtP1	64.06	30.24	5.70	2.12	11.24
	ChtP2	70.33	24.24	5.33	2.90	13.20
	ChtP3	70.04	21.43	8.53	3.27	8.21
	ChtP4	67.88	24.61	7.50	2.76	9.05
Ar plasma	ChtP5	63.31	28.61	8.08	2.21	7.84
	ChtP6	66.80	24.43	8.78	2.73	7.61
	ChtP7	69.15	24.31	6.54	2.84	10.57
	ChtP8	65.61	28.61	5.79	2.29	11.33

Changes in the high-resolution C_{1s} core level spectra before and after nitrogen and argon-plasma treatment are shown in Figure 3. The C_{1s} core level spectrum of chitosan membranes revealed three peaks. The C_{1s} peak at 285.0 eV was assigned for the main backbone carbon peak, which also overlaps C-NH_2 chemical bindings. The peak at 286.6 eV was assigned to C–O/ C–OH and the peak at 288.3 eV to O-C-O and N–C=O chemical bindings [34,35]. The same components were present in the C_{1s} core level spectra of the treated membranes but changes in the relative intensities of all peaks were observed (Figure 3, Table 3). Generally an increase of the relative intensity of C-H component was observed after treatment. This change was accompanied by a decrease in C-O intensity in almost all the treated membranes compared to untreated one. These results confirm the acetate cleavage and the ongoing etching processes. Significant quantities of oxygen moieties (mainly C=O) were introduced on the surface for ChtP5 and ChtP8 (Table 2).

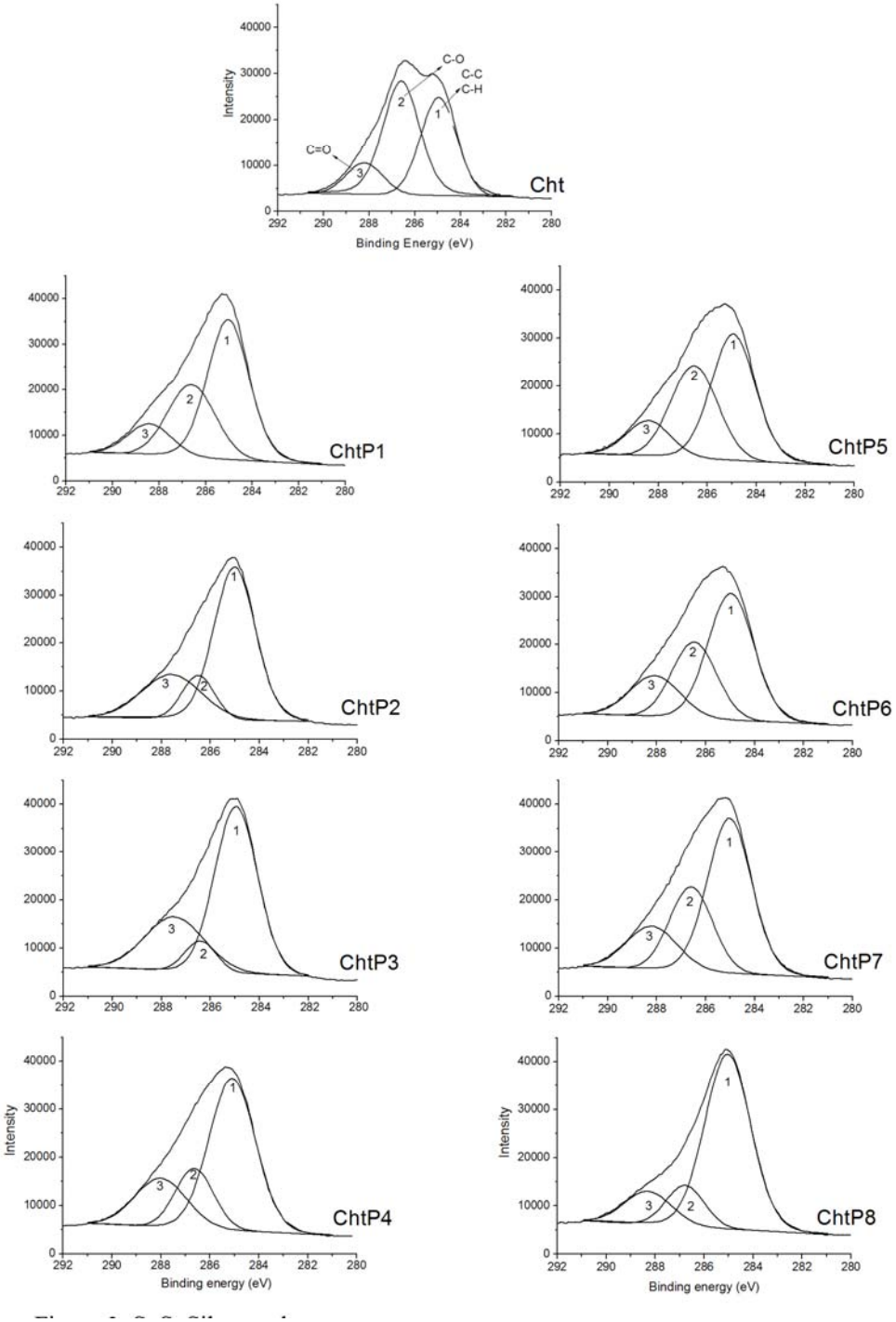

Figure 3. C_{1s} core level spectra of untreated chitosan (Cht) and modified samples; ChtP1, ChtP2, ChtP3, ChtP4 – samples after nitrogen plasma; ChtP5, ChtP6, ChtP7 and ChtP8 – samples after argon plasma.

Table 3. Relative intensities of the fitted C1s peak of untreated and modified plasma membranes.

Treatment	Sample	Binding energy/ev (relative intensity %)	Assignments
	Cht	285.0 (39)	C-C, C-H
		286.6 (44)	C-O
		288.2 (16)	C-O-C, N-C=O
N_2 plasma	ChtP1	285.0 (56)	C-C, C-H
		286.6 (31)	C-O
		288.4 (12)	C-O-C, N-C=O
	ChtP2	285.0 (63)	C-C, C-H
		286.5 (13)	C-O
		287.6 (25)	C-O-C, N-C=O
	ChtP3	284.9 (64)	C-C, C-H
		286.4 (8)	C-O
		287.5 (28)	C-O-C, N-C=O
	ChtP4	285.1 (60)	C-C, C-H
		286.6 (19)	C-O
		288.0 (21)	C-O-C, N-C=O
Ar plasma	ChtP5	284.9 (49)	C-C, C-H
		286.5 (37)	C-O
		288.4 (14)	C-O-C, N-C=O
	ChtP6	284.9 (52)	C-C, C-H
		286.5 (30)	C-O
		288.1 (18)	C-O-C, N-C=O
	ChtP7	285.0 (55)	C-C, C-H
		286.6 (28)	C-O
		288.2 (17)	C-O-C, N-C=O
	ChtP8	285.0 (73)	C-C, C-H
		286.8 (14)	C-O
		288.3 (14)	C-O-C, N-C=O

Modifications in the surface chemistry and morphology can change the surface hydrophilicity[24] which is one of key surface parameters determining the material/bioenvironment interactions. The measured contact angles and calculated surface energies of the prepared membranes are summarized in Table 4. Generally all the treatments resulted in more hydrophilic surfaces. Previous works [29,36] have demonstrated that short time (1-3 min) treatments in nitrogen atmosphere results in more hydrophilic surfaces. In contrast longer treatments (i.e. » 3 min) decrease the surface hydrophilicity. The obtained results for the surface energy are in agreement with the ones from XPS analysis. Different trends were observed for the used working atmospheres. A slight increase of the surface energy with the treatment time was observed for the samples treated by nitrogen plasma. Intermediate exposure time was found to result in highest surface energy, when argon was used as a working gas. Earlier studies [37,38] reported that materials with high surface energy promote rapid cellular adhesion and spreading, whereas low surface energy does not favour such behaviour. It has been also shown by different studies [24,39] that changes in the surface charge, chemical surface composition and roughness can affect the biocompatibility of a polymer.

Table 4. Water contact angles (θ) and surface energy (γ) of untreated and plasma-treated chitosan membranes.

Treatment	Sample	θ_{Water} (º)	γ (mN.m^{-1})
	CHT	88.5 ± 1.6	30.8 ± 0.1
N_2 plasma	ChtP1	87.7 ± 1.7	20.7 ± 0.1
	ChtP2	85.1 ± 9.4	21.6± 0.1
	ChtP3	83.5 ± 5.6	28.8 ± 0.2
	ChtP4	84.7 ± 7.1	38.6 ± 0.1
Ar plasma	ChtP5	78.3 ± 9.4	21.9 ± 0.1
	ChtP6	88.1 ± 3.3	31.8 ± 0.1
	ChtP7	84.9 ± 4.4	32.4 ± 0.3
	ChtP8	93.7 ± 2.6	18.0 ± 0.2

The results obtained from the MTS assay (Figure 4) showed that both nitrogen and argon plasma treated-membranes promoted a higher cell viability than untreated chitosan membranes. This effect was observed for all studied time periods. After 14 days of culture, the ChtP2 sample presented the highest cell viability among the nitrogen-plasma treated membranes. The values obtained for the membranes treated with argon plasma were more consistent regardless the culture time.

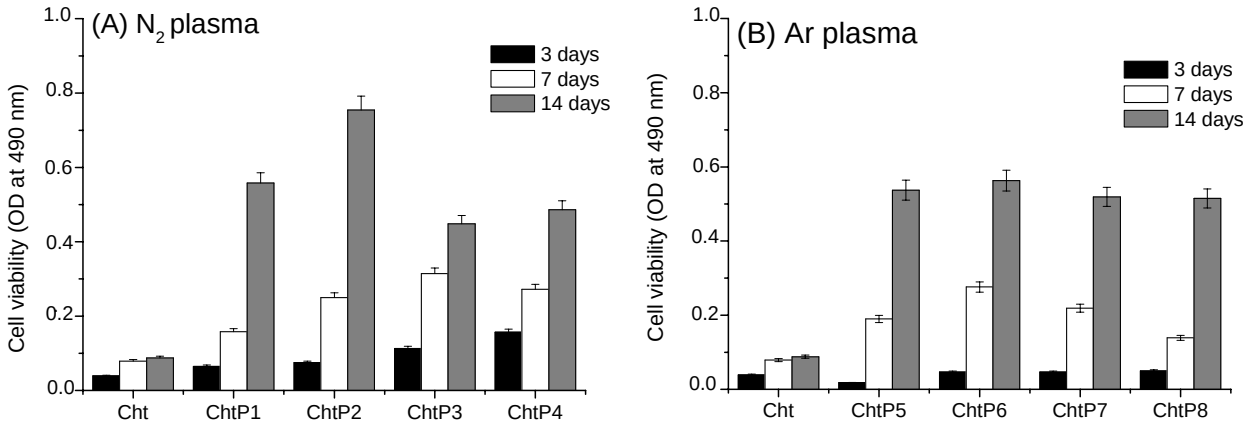

Figure 4. Viability levels of L929 fibroblasts-like cells on the untreated and treated plasma membranes assessed by MTS assay. (A) ChtP1, ChtP2, ChtP3, ChtP4 – samples after nitrogen plasma, and (B) ChtP5, ChtP6, ChtP7 and ChtP8 – samples after argon plasma.

Cell morphology on both untreated and modified membranes was observed by SEM. Fibroblasts like-cells were able to attach and stretch on all the types of modified membranes after different culture time. ChtP2 sample, which presented the best results among nitrogen-treated membranes, was selected to be studied for different culture periods. The ChtP6 from the argon modified membranes was also chosen in order to evaluate the effect of the working gas on cell morphology. After 3 days of culture, there is significant number of L929 cells on the surface of both nitrogen and argon-treated plasma membranes (Figure 5).

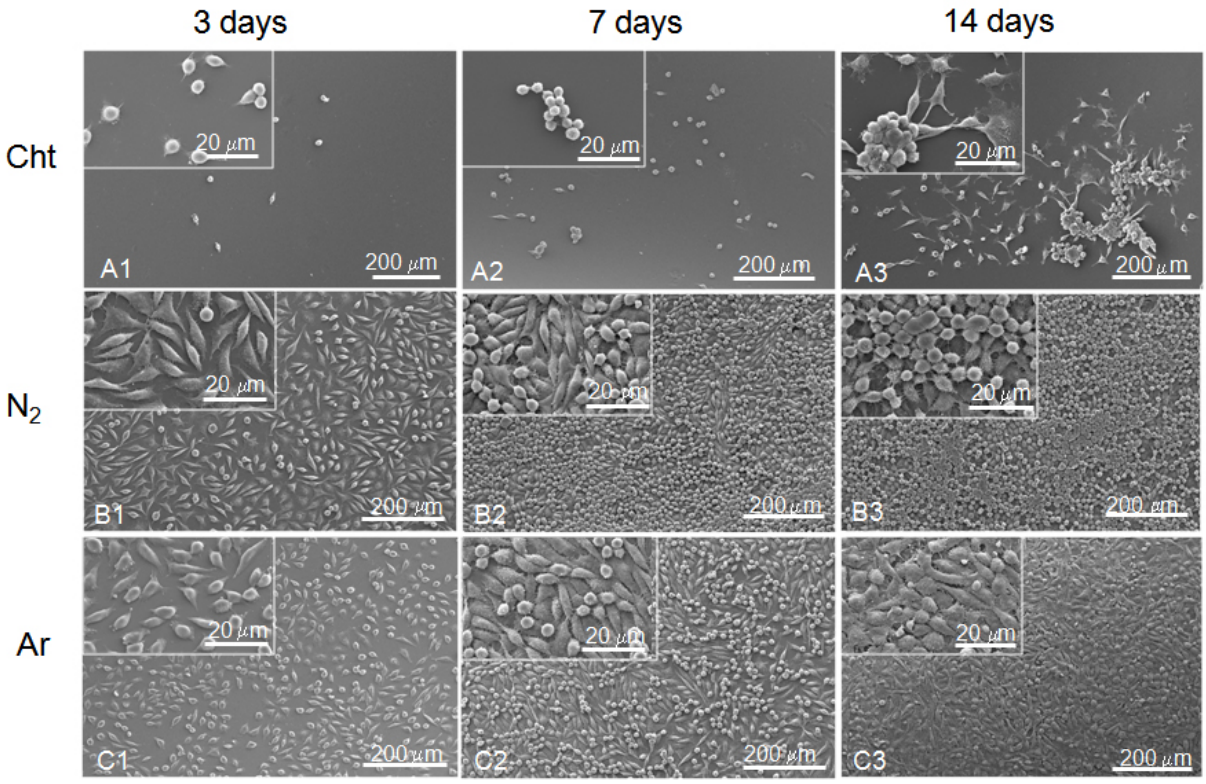

Figure 5. SEM micrographs of L929 fibroblasts-like cells cultured on: A) Cht (untreated membranes-control); B) ChtP2 (chitosan membranes modified by nitrogen plasma); C) ChtP6 (chitosan membranes modified by argon plasma), after 3, 7 and 14 days of culture.

The attached cells presented typical morphology for fibroblast with elongate shape. The number of the attached cells increases with the culture time and after 14 days a dense cellular monolayer was covering both modified membranes. On the contrary and as previously described [16, 17], poor cell attachment was observed for the untreated membranes. After 3 days of culture only a few rounded cells can be seen on their surface. This number increases with the time of culture but at the end of the studied period it was still insignificant compared to the number of cells, adhered to the modified membranes.

4. **Conclusions**

Surface modification of chitosan membranes was performed by nitrogen and argon plasma. Higher surface roughness (nanoscale) measured for the modified materials indicate etching processes. This effect increases with the exposure time and does not depend on the used working atmosphere. The surface energy increased for the treated membranes compared to untreated. The XPS measurements confirmed the incorporation of oxygen- and nitrogen- containing groups on the surface after treatments. *In vitro* preliminary biological studies showed that modified chitosan membranes displayed higher cell viability on the surface when compared to untreated chitosan membranes. The results demonstrated that either nitrogen or argon plasma treatments can be a way to improve the fibroblast adhesion and proliferation of chitosan membranes. The proposed modifications would facilitate the use of chitosan and chitosan based materials as wound dressing and tissue engineering applications.

5. **Acknowledgements**

The authors acknowledge funding from Portuguese Foundation for Science and Technology (FCT), Portugal for providing the grants SFRH/BD/8658/2002, SFRH/BPD/17584/2004 and SFRH/BPD/8191/2002. Programme Alβan, the European Union Programme of High Level Scholarships for Latin America (E04M041362CO), and the EU funded Project HIPPOCRATES (NMP3-CT-2003-505758). This work was carried out under the scope of the European NoE EXPERTISSUES (NMP3-CT-2004-500283).

6. **References**

1. Lanza, R. and Langer, R., *Principles of Tissue Engineering* Academic press, 2000.
2. Bradley, M., Cullum, N., Nelson, E. A., Petticrew, M., Sheldon, T., and Torgerson, D., Systematic reviews of wound care management: (2) Dressings and topical agents used in the healing of chronic wounds, *Health Technology Assessment* 3, 1-47, 1999.
3. Qin, Y., Absorption characteristics of alginate wound dressings, *Journal of Applied Polymer Science* 91, 953-957, 2004.
4. Lloyd, L. L., Kennedy, J. F., Methacanon, P., Paterson, M., and Knill, J., Carbohydrate polymers as wound management aids, *Carbohydrate Polymers* 37, 315-322, 1998.
5. Paul, W. and Sharma, C. P., Chitosan and alginate wound dressings: a short review, *Trends Biomaterials Artificial Organs* 18, 18-23, 2004.
6. Silva, R. M., Mano, J. F., and Reis, R. L., Preparation and characterization in simulated body conditions of glutaraldehyde crosslinked chitosan membranes, *Journal of Materials Science-Materials in Medicine* 15, 1105-112, 2004.
7. Kirker, K. R., Luo, Y., Nielson, J. H., Shelby, J., and Prestwich, G. D., Glycosaminoglycan hydrogel films as bio-interactive dressings for wound healing, *Biomaterials* 23, 3661-3671, 2002.
8. Azad, A. K., Sermsintham, N., Chandrkrachang, S., and Stevens, W. F., Chitosan membrane as a wound-healing dressing: Characterization and clinical application, *Journal of Biomedical Materials Research Part B-Applied Biomaterials* 69B, 216-222, 2004.
9. Jeschke, M. G., Sandmann, G., Schubert, T., and Klein, D., Effect of oxidized regenerated cellulose/collagen matrix on dermal and epidermal healing and growth factors in an acute wound, *Wound Repair and Regulation* 13, 324-331, 2005.
10. Chang, W. H., Chang, Y., Lai, P. H., and Sung, H. W., A genipin-crosslinked gelatin membrane as wound-dressing material: in vitro and in vivo studies, *Journal of Biomaterials Science-Polymer Edition* 14, 481-495, 2003.
11. Valenta, C. and Auner, B. G., The use of polymers for dermal and transdermal delivery, *European Journal of Pharmaceutics and Biopharmaceutics* 58, 279-289, 2004.
12. Kumar, M. N. V. R., Chitosan chemistry and pharmaceutical perspectives, *Chemistry Reviews* 104, 6017-6084, 2004.
13. Campos, M. G. N., Grosso, C. R. F., Cardenas, G., and Mei, L. H. I., Effects of neutralization process on preparation and characterization of chitosan membranes for wound dressing, *Macromolecular Symposia* 229, 253-257, 2005.
14. Zheng, H., Du, Y., Yu, K., Huang, R., and Zhang, L., Preparation and characterization of chitosan/poly(vinyl alcohol) blend fibers, *Journal of Applied Polymer Science* 80, 2558-2565, 2001.
15. Peniche, C., Monal, W. a., Peniche, H., and Acosta, N., Chitosan: an attractive biocompatible polymer for microencapsulation, *Macromolecular Bioscience* 3, 512-520, 2003.
16. Silva, S. S., Santos, M. I., Coutinho, O. P., Mano, J. F., and Reis, R. L., Physical properties and biocompatibility of chitosan/soy blended membranes, *Journal of Materials Science-Materials in Medicine* 16, 575-579, 2005.
17. Chatelet, C., Damour, O., and Domard, A., Influence of the degree of acetylation on some biological properties of chitosan films, *Biomaterials* 22, 261-268, 2001.
18. Yang, F., Li, X., Cheng, M., Gong, Y., Zhao, N., and Zhang, X., Performance modification of chitosan membranes induced by gamma irradiation, *Journal of Biomaterials Applications* 16, 215-226, 2002.
19. Tangpasuthadol, V., Pongchaisirikul, N., and Hoven, V. P., Surface modification of chitosan films. Effects of hydrophobicity on protein adsorption, *Carbohydrate Research* 338, 937-942, 2003.

20. Wang, H. T., Fang, Y. E., and Yan, Y. S., Surface modification of chitosan membranes by alkane vapor plasma, *Journal of Materials Chemistry* 11, 1374-1377, 2001.
21. Li, Y. P., Liu, L., and Fang, Y. E., Plasma-induced grafting of hydroxyethyl methacrylate (HEMA) onto chitosan membranes by a swelling method, *Polymer International* 52, 285-290, 2003.
22. Zhu, X., Chian, K. S., Chan-Park, M. B. E., and Lee, S. T., Effect of argon-plasma treatment on proliferation of human-skin-derived fibroblast on chitosan membrane in vitro, *Journal of Biomedical Materials Research Part A* 73A, 264-274, 2005.
23. Pérez, P. M. L., Marques, A. P., Silva, R. M. P., Pashkuleva, I., and Reis, R. L., Effect of chitosan´surface modification via plasma induced polymerization on the adhesion of Osteoblast-like cells, *Journal of Materials Chemistry* 17, 4064-4071, 2007.
24. Chu, P. K., Chen, J. Y., Wang, L. P., and Huang, N., Plasma-surface modification of biomaterials, *Materials Science & Engineering R-Reports* 36, 143-206, 2002.
25. Khonsari, F. A., Tatoulian, M., Shahidzadeh, N., and Amouroux, J., Study of the plasma treated polymers and the stability of the surface properties, in *Plasma processing of polymers*, Agostino, R., Favia, P., and Fracassi, F. 2003, pp. 165-193.
26. Alves, C. M., Yang, Y., Carnes, D. L., Ong, J. L., Sylvia, V. L., Dean, D. D., Agrawal, C. M., and Reis, R. L., Modulating bone cells response onto starch-based biomaterials by surface plasma treatment and protein adsorption, *Biomaterials* 28, 307-315, 2007.
27. Plath, A. A. M., Schroder, K., Finke, B., and Ohl, A., Current trends in biomaterial surface functionalization— nitrogen-containing plasma assisted processes with enhanced selectivity, *Vacuum* 71, 391-406, 2003.
28. Gerenser, L. J., Grace, J. M., Apai, G., and Thompson, P. M., Surface chemistry of nitrogen plasma-treated poly(ethylene-2,6-naphthalate): XPS, HREELS and static SIMS analysis, *Surface and Interface Analysis* 29, 12-22, 2000.
29. Bhat, N. V. and Upadhyay, D. J., Plasma-induced surface modification and adhesion enhancement of polypropylene surface, *Journal of Applied Polymer Science 86*, 925-936, 2002.
30. Hirai, A., Odani, H., and Nakajima, A., Determination of degree of deacetylation of chitosan by 1H NMR spectroscopy, *Polymer Bulletin* 26, 87-94, 1991.
31. Owens, D. K. and Wendt, R. C., Estimation of the surface free energy of polymers, *Journal of Applied Polymer Science* 13, 1741-1747, 1969.
32. Reis, R. L., Mendes, S. C., Cunha, a. M., and Bevis, M. J., Processing and in vitro degradation of starch/EVOH thermoplastic blends, *Polymer International* 43, 347-352, 1997.
33. Salgado, A. J., Gomes, M. E., Chou, A., Coutinho, O. P., Reis, R. L., and Hutmacher, D. W., Preliminary study on the adhesion and proliferation of human osteoblasts on starch-based scaffolds, *Materials Science and Engineering C* 20, 27-33, 2002.
34. Beamson, G. and Briggs, D., *High Resolution XPS of Organic Polymers*, Chichester, UK, 1992.
35. Matienzo, L. J. and Winnacker, S. K., Dry processes for surface modification of a biopolymer: chitosan, *Macromolecular Materials and Engineering* 287, 871-880, 2002.
36. Chan, C. M., Ko, T. M., and Hiraoka, H., Polymer surface modification by plasmas and photons, *Surface Science and Reports* 24, 1-54, 1996.
37. Mitchell, S. A., Davidson, M. R., and Bradley, R. H., Improved cellular adhesion to acetone plasma modified polystyrene surfaces, *Journal of Colloid and Interface Science* 281, 122-129, 2005.
38. Anselme, K., Osteoblast adhesion on biomaterials, *Biomaterials* 21, 667-681, 2001.
39. Ratner, B. D., Hoffman, A. S., Schoen, F. J., and Lemos, J. E., *Biomaterials Science: An Introduction to Materials in Medicine* Academic Press, New York, 1996.

CHAPTER V

CHAPTER V

Physical Properties and Biocompatibility of Chitosan/Soy Blended Membranes

Abstract

Blends of polysaccharides and proteins are a source for the development of novel materials with interesting and tailorable properties, with potential to be used in a range of biomedical applications. In this work a series of blended membranes composed by chitosan and soy protein isolate was prepared by solvent casting methodology. In addition, cross-linking was performed *in situ* with glutaraldehyde solutions in the range 5.10^{-3}M- 0.1M. Furthermore, the influence of the composition and cross-linking on the degradation behaviour, water uptake and cell adhesion was investigated. The obtained results showed that the incorporation of chitosan, associated to network formation by cross linking, promoted a slight decrease of water absorption and a slower degradability of the membranes. Moreover, direct contact biocompatibility studies, with L929 cells, indicate that the cross-linking enhances the capability of the material to support cell growth.

This chapter is based on the following publication:

S. S. Silva, M. I. Santos, O. P. Coutinho, J. F. Mano, R. L. Reis. "Physical properties and biocompatibility of chitosan/soy blended membranes", Journal of Materials Science: Materials Science 16,575-579, 2005

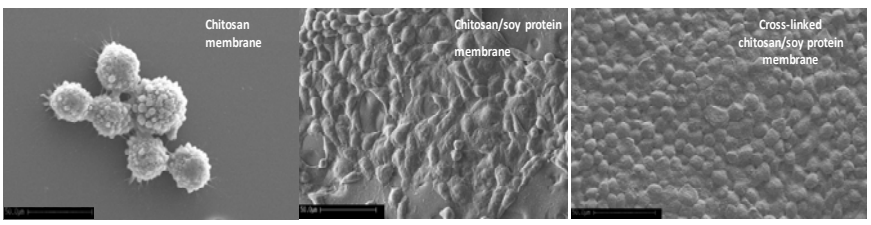

---

1. **Introduction**

There is an increasing need to develop new biodegradable materials to be used in skin tissue engineering, wound cover or as dressings and barrier-membranes, since there is a high demand for skin replacements and skin repair treatments. For instance, an ideal material to be use as a wound dressing should associate availability with minimal storage requirements, long shelf-life, versatility and, biocompatible behaviour [1]. Many polymeric membranes have been investigated for the purpose of wound covering on account its importance in the treatment of burns, prevention of post surgical adhesions and cosmetic surgery. These materials include synthetic polymers like polyurethane, polyethylene and polylactides, polyglycolides, polyacrylonitrile. However some of these polymers have disadvantages in such applications, i.e. poor biocompatibility and release of acidic degradation products [2,3]. One alternative approach involves the use of biodegradable polymers from renewable resources, it including starch, collagen, gelatin, chitosan and proteins (soy protein, casein, silk fibroin and wheat), since these polymers are widely available in nature, and are biodegradable and non-toxic [1, 4-8]. Among these renewable polymers, soy protein, the major component of the soybean, has the advantages of being economically competitive and present good water resistance as well as storage stability. The combination of these properties with a similarity to tissue constituents and a reduced susceptibility to thermal degradation makes soy an ideal template to be used as a biomaterial for skin tissue engineering. Soy proteins are rich in polar groups, such as hydroxyl, amide and carboxyl groups among others, which enable soy protein to associate with many different types of compounds [9]. Some studies reported that the combination of soy protein with other proteins such as wheat gluten [10] or, casein [7], may promote physical and chemical interactions which improve some properties. Combination of polysaccharides such as carrageenan, xanthan [11,] dialdehyde starch [12] with soy protein has also been investigated.

This work explored the combination of chitosan with a colloidal suspension formed from the soy protein, in the form of membranes, through chemical and/or physical means, which can allow to control the degradation rate, or the hydrolytic resistance, and to induce antibacterial properties in soy protein membranes. It is expected that the characteristics of a blend membrane system formed by these components can be tailored by controlling the particle charge of protein, which can be dependent, among other factors, on the pH medium and the composition of the blend. In addition, the blend membrane system can potentially be used for the delivery of water-soluble compounds that aid wound healing, such as antibiotics or anti-inflammatory agents. In a previous study, which also involved the combination of chitosan with soy protein[13], β-radiation was shown to be as a suitable sterilisation methodology to be used on chitosan/soy protein membranes aiming to be used in guide bone regeneration. The results showed that no substantial changes were detected in the studied properties, with the exception of the surface energy that was found to be slightly increased for higher applied doses.

The aim of this work was to evaluate the influence of chemical cross-linking in the water uptake, degradation rate and biocompatibility of the blend system composed by chitosan and soy protein. Cytotoxicity tests, both extract and direct contact tests were performed on these materials in order to evaluate the potential toxicity of the degradation products, and the ability of the membranes to promote cell attachment and growth.

2. **Materials and methods**

Chitosan- CHT (Sigma) with deacetylation degree about 85% was used. Soy protein isolate (SI) was provided by Loders Crocklaan (The Netherlands). All other reagents were analytical grade and used as received.

Chitosan/soy protein blended membranes (CS) (average thickness from 40 to 84μm) were prepared by solvent casting. Chitosan flakes were dissolved in aqueous

acetic acid 2% (v/v) solution at a concentration of 1%wt. A soy suspension (1% wt.) was prepared by slowly suspending the soy protein powders, under constant stirring, in distilled water with glycerol. After adjusting the pH to 8.0± 0.3 with 1M sodium hydroxide, the dispersion was heated in a water bath at 50 ºC for 30 min. Studies reported that the alkaline conditions favour soy film formation by aiding protein dispersion in film-forming solutions [14]. Then, the two solutions were mixed in different ratios, namely CS75, CS50 and CS25 corresponding to 75/25, 50/50, 25/75 wt% chitosan/soy. Glutaraldehyde (Ga) solutions in the range 5.10^{-3}M- 0.1M were prepared diluting 50 wt% Ga solution as it was provided by the manufacturer. After that, glutaraldehyde solutions were added to the mixture, to study the effect of crosslinking on the blend properties. After the chitosan/soy solutions had been homogenized, they were casted into Petri dishes and dried at room temperature for about 6 days. In order to neutralize acetic acid, the dried membranes were immersed in 0.1M sodium hydroxide for about 10 minutes, and then washed with distilled water to remove all traces of alkali, followed by drying at room temperature. After that, the structural changes were assessed by FTIR-ATR spectroscopy (Perkin-Elmer 1600 Series).

Non-cross-linked and cross-linked blend membranes (1x 2 cm) were submitted to swelling and *in vitro* degradation tests. Pre-weighed dried membranes were immersed for 0, 2, 7, 14, 30 and 60 days, at 37ºC, in a phosphate buffer saline solution, pH 7.4 (PBS). Sodium azide (0.02% w/v) was added to the buffer to prevent bacterial growth. After each ageing period, the samples were removed from the degradation solution, washed with distilled water and weighed. The water uptake was obtained by weighing the initial and swollen samples in various time intervals:

$$\text{Water uptake (\%)} = ((W_s(t) - W_i)/W_i) \times 100 \qquad (1)$$

Where $W_s(t)$ and W_i represent the weight of the samples at time t and 0, respectively.

After that, the samples were dried in an oven (60º C/24 h). The percentage weight loss of the soy materials was then calculated by:

$$\text{Weight loss (t)} = [(W_i - W_f(t)) / Wi\ ]*100 \qquad (2)$$

Where W_i is the initial dry weight of the sample. $W_f(t)$ denotes the weight loss of sample after a certain time t of immersion. Each experiment was repeated three times and the average value was taken as the weight loss.

In according to ISO standards [15] two categories of *in vitro* cytotoxicity evaluation were made: extract tests and direct contact tests. In extract tests the samples were extracted in culture medium for 24 h at 37ºC, 60 rpm. The filtered extracts were placed in contact with a monolayer of L929 cells (mouse fibroblasts) for 72 hrs. A control with cells grown in the presence of complete culture medium was included. Then, cell viability was evaluated by MTT assay and the results were expressed as percentage of cell viability. In direct contact test, L929 cells ($8x10^4$ cells/cm^2) were seeded on the biomaterials and incubated under standard culture conditions for 3 days.

3. **Results and Discussion**

The FTIR-ATR spectra of chitosan and soy protein films were analysed (Figure 1a) and compared with the spectra of the blended membranes (Figure 1b). The ATR analysis of membranes was based on the identification of bands related to the functional groups present in chitosan and soybean, among others [16,17].

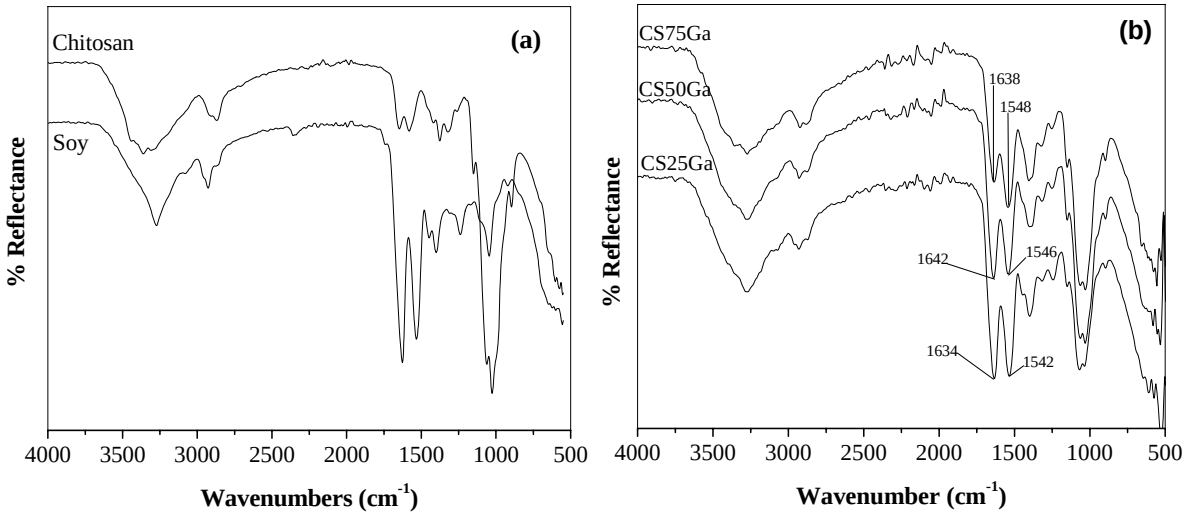

Figure 1. (a) FTIR-ATR spectra of chitosan and soy pure membranes; (b) CS75Ga, CS50Ga and CS25Ga blended membranes cross-linked with 5.10^{-2}M glutaraldehyde, after neutralization. (CS75, CS50 and CS25 corresponding to 75/25, 50/50, 25/75 wt% chitosan/soy).

As can be seen in Figure 1a, the main characteristic absorption bands of chitosan appear at 1650 cm^{-1} (C=O stretching), 1560 cm^{-1} (-NH angular deformation), 3450 cm^{-1} (OH hydroxyl group) and 1150-1040 cm^{-1} (-C-O-C- in glycosidic linkage) [16]. The soy protein spectrum (Figure 1a) showed an amide I band at 1632 cm^{-1} and a amide II band at 1536 cm^{-1} [17]. The amide I can be composed of several overlapping components due to various protein segments with different secondary structures [17]. Figure 1b is one spectra representative of the cross-linked blended membranes, which showed the characteristic absorptions bands of both chitosan and soy being its proportional to ratio between the components of the blend. As a result, the absorbance of NH and CO deformation bands in the range 1580-1490 cm^{-1} and 1700-1630 cm^{-1} respectively, became gradually higher with the increase of soy content in the blend. Similar results were found for non-cross-linked membranes. Even though new peaks did not appear before and after the crosslinking reaction, we noted a displacement of these bands for lower wave-numbers (NH from 1584 to 1542 cm^{-1} and CO - from 1650 to 1634 cm^{-1}) with respect to pure chitosan. The above findings suggest that the chitosan and soy may

have participated in a specific intermolecular interaction. In this case, more details about the protein-polysaccharide interactions and miscibility of this blend system, using measurements of proton spin-lattice relaxation times by solid state ^{13}C nuclear magnetic resonance (^{13}C NMR,) spectroscopy, are in progress.

On the other hand, water absorption ability of the blended membranes was evaluated through the monitoring of the water absorption ratio determined in phosphate buffer solution- PBS (pH 7.4). As expected, the samples showed high water uptake (ca.160-200%), as result of the hydrophilic character predominant of blend components but, after cross-linking the samples presents a decreasing trend. Some results can be associated to a preferential cross linking of chitosan instead of soy or vice-versa as well as the occurrence of a partial cross linking. In a previous work, Silva *et al* [8] observed that for pure chitosan, slightly cross-linked films did not exhibit such decrease, mainly due to the stronger effect of crystallisation suppression during crosslinking. Also it was observed that both water sorption and degradation behaviour results obtained for CS50 blend composition presented an irregular behaviour (data not shown) compared to other blend compositions. This may be attributed to an irregularity found in the miscibility between soy protein and chitosan at this composition.

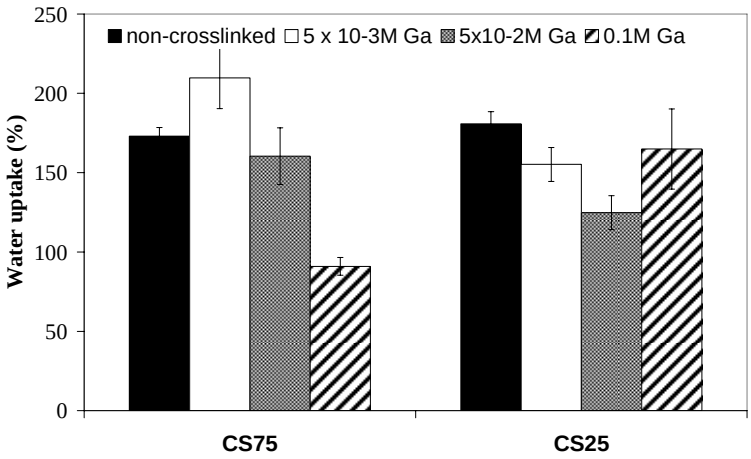

Figure 2. Water uptake of chitosan/soy blended membranes after 2 hours in PBS: (■) CS75 and CS25 membranes non-cross-linked ; (□) CS75 and CS25 membranes cross-linked with 5.10^{-3}M Ga ; (■) CS75 and CS25 membranes cross-linked with 5.10^{-2}M Ga; (▨) CS75 and CS25 membranes cross-linked with 0.1M Ga. (CS75 and CS25 corresponding to 75/25, 25/75 wt% chitosan/soy).

All the samples revealed to be stable in the phosphate buffer solution (PBS), but with different degradation pattern in function of immersion time. In fact, it was observed that the degradation pattern of blended membranes occurs in three stages (Figure 3a). The first one, between 0 and 14 days, can be related with the leaching of plasticizers (glycerol) and low molecular weight polymeric chains, as observed in composites based on casein and soy protein [7]. The second degradation stage, between 15 and 30 days, probably involves the degradation of a protein fraction, followed by third stage of degradation, correspondent to the final weight loss of the blend. Figures 3a, shows that the weight loss in the blended membranes increased with the percentage of soy in the blend. In the cross-linked samples (Figure 3b-c), the weight loss tends to stabilize, mainly after 30 days in immersion. In particular, a positive influence of crosslinking on the degradation behaviour was more evident in the CS25 composition, since its weight loss along the time was reduced (Figure 3b-c). On contrary, in the presence of the 0.1M Ga, the weight loss of CS25 blend reached the highest value of 59% after 30 days of immersion (data

not shown), probably due the brittleness of the samples. Furthermore, it is observed that the blend cross-linked membranes also present a degradation profile similar to the non-cross-linked membranes. In this case, the second stage degradation pattern can be related to degradation of the non-cross-linked protein fraction. The third stage can be associated to final weight loss (%) or stabilization due the presence of the chitosan/soy network, respectively. It is worth mentioning that the cross-linked membranes with higher chitosan content (CS75) maintained its physical integrity even after long immersion time (60days).

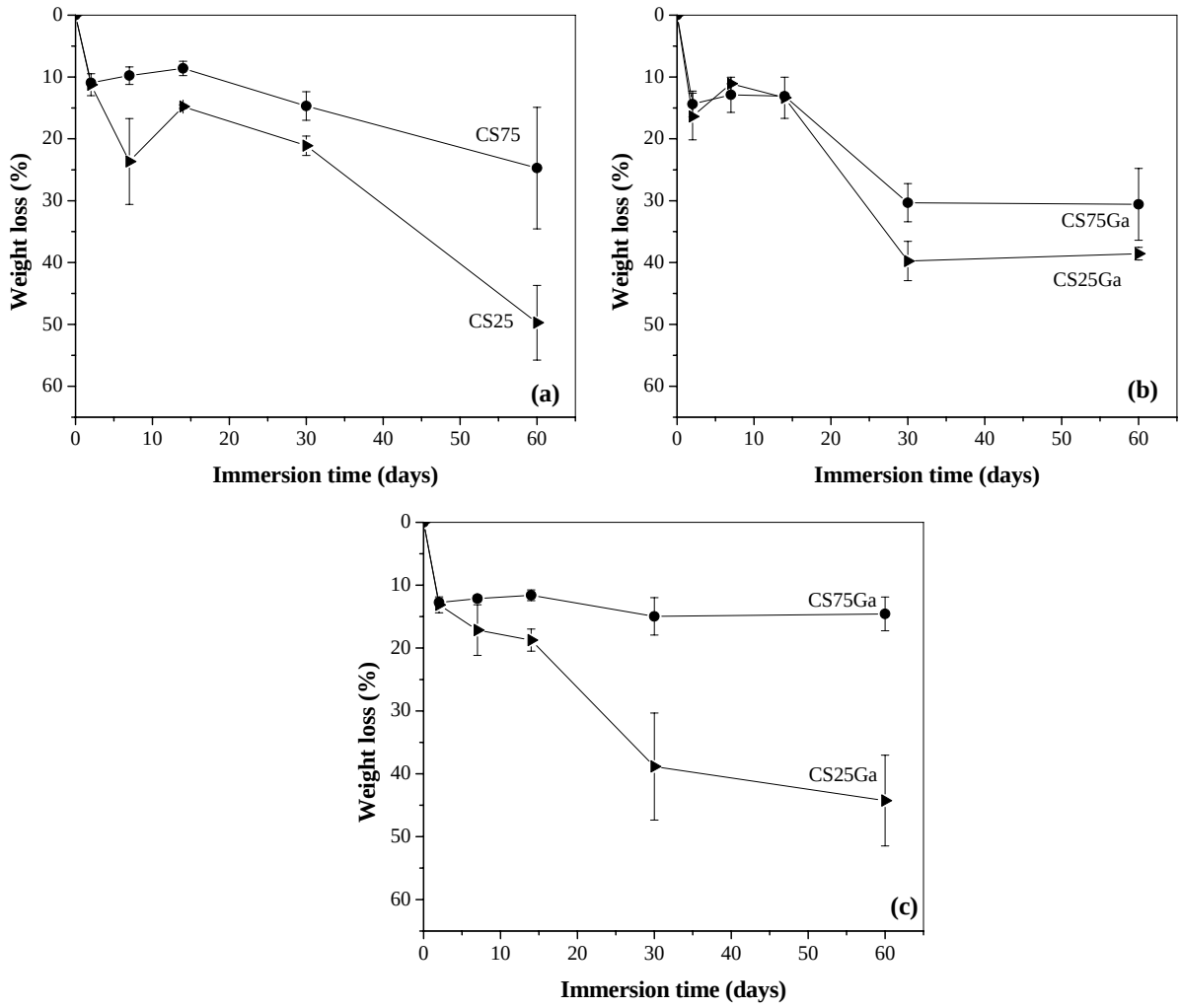

Figure 3. Weight loss of blended membranes as function of immersion time on a phosphate buffer solution at 37ºC: (a) CS75 and CS25 membranes non-cross-linked; (b) CS75 and CS25 membranes cross-linked with 5.10^{-3}M Ga; (c) CS75 and CS25 membranes cross-linked with 5.10^{-2}M Ga. (CS75 and CS25 corresponding to 75/25, 25/75 wt% chitosan/soy).

The MTT studies with extracts demonstrated that for chitosan, CS75 and CS50 membranes cross-linked with $5x10^{-2}$ M Ga, the percentage of viable L929 cells was around 90%, thus comparable to the control. However, the viability of L929 cells slightly decreased in contact with the extracts of CS75 and CS50 blended cross-linked membranes prepared with higher Ga concentration (0.1 M) and CS75 (data not shown) but even in these cases the values were acceptable. On the other hand, cell adhesion studies, after 3 days of culture, show that L929 cells on the surface of chitosan membrane (CHT) were still spherical and with microvilli-like projections in appearance (Fig. 4a). It appears that cells on CHT were able to attach but unable to follow this attachment with spreading. Domard *et al* [18] observed similar results in which chitosan is not cytotoxic towards fibroblasts but inhibits cell proliferation. In contrast, as can be observed (Fig. 4b-d) the C75 membranes show elongated and flattened cells, suggesting a tight cell adhesion to the membranes. This noteworthy improvement in cellular adhesion in comparison with chitosan membrane can be due the incorporation of the soy protein, which can provide more protein-binding sites on the membranes. In addition, the increased cellular adhesion in the cross-linked membranes CS75 (Fig. 4c-d) relative to the non-cross-linked membrane CS75 (Fig. 4b) suggests that the cross-linking with Ga has changed the surface membrane. Probably this is due to a better interaction between the blend components and, then improves the cellular adhesion of the blended membranes. The collective results from these experiments assure that chitosan/soy protein blended membranes and their extracts were noncytotoxic and were able to support cell growth and proliferation.

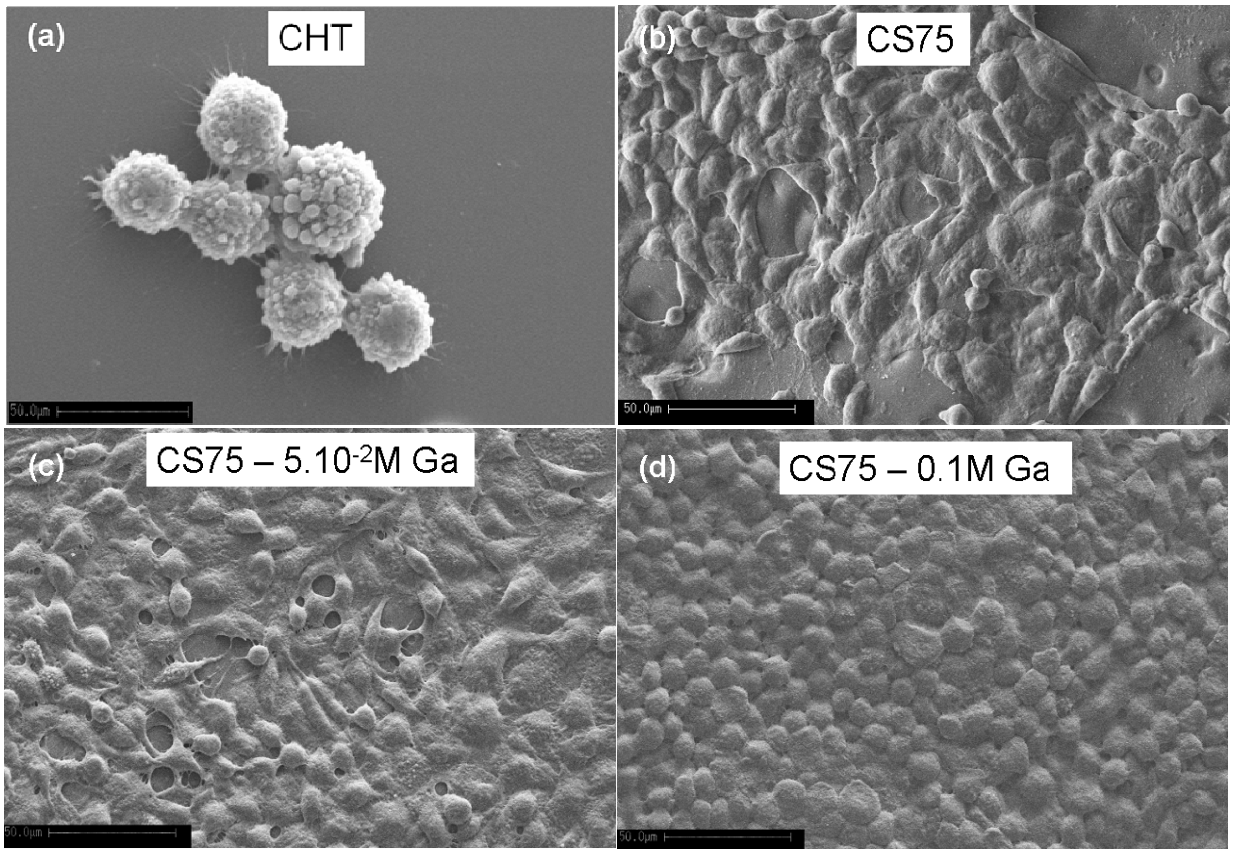

Figure 4. SEM micrographs of L929 cells cultured on chitosan/soy protein blended membranes after 3 days of culture: (a) chitosan membrane (CHT); (b) CS75 membrane non-cross-linked; (c) CS75 membrane cross-linked with 5.10^{-2}M Ga; (d) CS75 membrane cross-linked with 0.1M Ga. (CS75 corresponding to 75/25 wt% chitosan/soy).

4. **Conclusions**

Chitosan/soy protein isolate blended membranes were successfully prepared by means of a solvent casting methodology. The membranes exhibited different degradation pattern and, improved cell spreading with respect to pure chitosan. By the results, the incorporation of chitosan associated to network formation by cross linking promoted a slight decrease of water absorption and a slower degradability of the membranes. The biological studies performed suggest that the cross-linking with low glutaraldehyde concentration changed the membrane surfaces, promoting a better cell adhesion of the membranes.

5. **Acknowledgements**

S. S. Silva and M. I. Santos, thank the Portuguese Foundation for Science and Technology (FCT) for providing PhD scholarships (SFRH/BD/8658/2002 and, SFRH/BD/13428/2003, respectively). This work was partially supported by FCT, through funds from the POCTI and/or FEDER programmes.

6. **References**

1. Khan, T. A. and Peh, K. K., A preliminary investigation of chitosan film as dressing for punch biopsy wounds in rats, *Journal of Pharmacy and Pharmaceutical Sciences* 6, 20-26, 2003.
2. Mi, F. L., Wu, Y. B., Shyu, S. S., Chao, A. C., Lai, J. Y., and Su, C. C., Assymetric chitosan membranes prepared by dry/wet phase separation: a new type of wound dressing for controlled antibacterial release, *Journal of Membrane Science* 212, 237-254, 2003.
3. Gunatilake, P. A. and Adhikari, R., Biodegradable synthetic polymers for tissue engineering, *European Cells & Materials Journal* 5, 1-16, 2003.
4. Bakos, D. and Koller, J., Membranes and Hydrogels in Reconstructive Surgery, in *Polymer Based Systems on Tissue Engineering, Replacement and Regeneration*, Reis, R. L. and Cohn, D. Kluwer Academic Publishers, 2002.
5. Dermirgoz, D., Elvira, C., Mano, J. F., Cunha, A. M., Piskin, E., and Reis, R. L., Chemical modification of starch based biodegradable polymeric blends: effects on water uptake, degradation behaviour and mechanical properties, *Polymer Degradation and Stability* 70, 161-170, 2000.
6. Mi, F. L., Shyu, S. S., Wu, Y. B., Lee, S. T., Shyong, J. Y., and Huang, R. N., Fabrication and characterization of a sponge-like asymetric chitosan membrane as a wound dressing, *Biomaterials* 22, 165-173, 2001.

7. Vaz, C. M., Fossen, M., van Tuil, R. F., de Graaf, L. A., Reis, R. L., and Cunha, A. M., Casein and soybean protein-based thermoplastics and composites as alternative biodegradable polymers for biomedical applications, *Journal of Biomedical Materials Research Part A* 65, 60-70, 2003.
8. Silva, R. M., Silva, G. A., Coutinho, O. P., Mano, J. F., and Reis, R. L., Preparation and characterisation in simulated body conditions of glutaraldehyde cross-linked chitosan membranes, *Journal of Materials Science: Materials in Medicine* 15 , 1105-1112, 2003.
9. Mo, X., Hu, J., Sun, S., and Ratto, J. A., Compression and tensile strength of low-density straw-protein particle board, *Industrial Crops and Products* 14, 1-9, 2001.
10. Were, L., Hettiarachchy, N. S., and Coleman, M., Properties of cysteine-added soy protein-wheat gluten films, *Journal of Food Science* 64, 514-518, 1999.
11. Hua, Y., Cui, S. W., and Wang, Q., Gelling property of soy protein-gum mixtures, *Food Hydrocolloids* 17, 889-894, 2003.
12. Rhim, J. W., Gennadios, A., Weller, C. L., Cezeirat, C., and Hanna, M. A., Soy protein isolate-dialdehyde starch films, *Industrial Crops and Products* 8, 195-203, 1998.
13. Silva, R. M., Elvira, C., Mano, J. F., San Roman, J., and Reis, R. L., Influence of β-radiation sterilisation in properties of new chitosan/soybean protein isolate membranes for guided bone regeneration, *Journal of Materials Science: Materials in Medicine* 15, 523-528, 2004.
14. Rhim, J. W., Gennadios, A., Handa, A., Weller, C. L., and Hanna, M. A., Solubility, tensile and color properties of modified soy protein isolate films, *Jornal of Agriculture and Food Chemistry* 48, 4937-4941, 2000.
15. ISO/ and 10993, Biological evaluation of medical devices- Part 5 test for Cytotoxicity, in vitro methods: 8.2 test on extracts, 1992.
16. Pawlak, A. and Mucha, M., Thermogravimetric and FTIR studies of chitosan blends, *Thermochimica Acta* 396, 153-166, 2003.
17. Subirade, M., Kelly, I., Guéguen, J., and Pézolet, M., Molecular basis of film formation from a soybean protein: comparison between the conformation of glycinin in aqueous solution and in films, *International Journal of Biological Macromolecules* 23, 241-249, 1998.
18. Chatelet, C., Damour, O., and Domard, A., Influence of the degree of acetylation on some biological properties of chitosan films, *Bioamaterials* 22, 261-268, 2001.

CHAPTER VI

CHAPTER VI

Morphology and Miscibility of Chitosan/Soy Protein Blended Membranes

Abstract

A physico-chemical characterization of blended membranes composed by chitosan and soy protein has been carried out in order to probe the interactions that allow membranes to be formed from these biopolymer mixtures. These membranes are developed aiming at applications in wound healing and skin tissue engineering scaffolding. The structural features of chitosan/soy blended membranes were investigated by means of solid state carbon nuclear magnetic resonance (NMR), infrared spectroscopy (FTIR), contact angle, and atomic force microscopy. FTIR investigations suggested that chitosan and soy may have participated in a specific intermolecular interaction. The proton spin-lattice relaxation experiments in the rotating frame on blended membranes indicated that independently of the preparation conditions, the blend components are not completely miscible possibly due to a weak polymer-protein interaction. It was also shown that the blended systems showed a rougher surface morphology which was dependent of soy content in the blend system.

This chapter is based on the following publication:

S. S. Silva, B. J. Goodfellow, J. Benesch, J. Rocha, J. F. Mano, R. L. Reis. "Morphology and miscibility of chitosan/soy protein blended membranes", Carbohydrate Polymers, 70, 2007, 25-31.

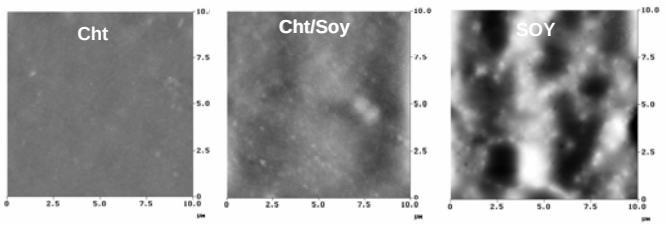

1. **Introduction**

Over the last decade, membranes obtained by combining proteins (e.g. soy protein, collagen, gelatin) with a natural polymer (e. cellulose, chitosan) have been developed in an attempt to supply the high demand for new materials for skin repair as wound dressings in the treatment of wounds caused by burns [1-3]. The presence of a protein in a polysaccharide-protein blend may improve the cell adhesion response of the resultant material due the presence of more protein-binding sites[3]. However, mixtures of protein and polysaccharide are often unstable, which leads to separation into two phases [4,5]. If the biopolymers are incompatible, i.e. they repel each other, thermodynamic phase separation occurs, also called segregation or depletion interaction. After phase separation, the mixture exhibits two phases: one rich in protein and the other rich in polysaccharide [4,6]. Bourriot [5] observed that the phase separation occurred in different casein-carrageenan systems at 50°C. The phase separation leads to the formation of a casein-rich phase and a k-carrageenan-rich phase. Some researchers support the evidence of interactions between protein and polysaccharides at fluid interfaces in conditions of limited thermodynamic compatibility between the protein and polysaccharide, *i.e.* above the protein isoelectric point in the diluted concentration region [7].

The production and successful use of materials obtained from mixtures of protein-polysaccharide require that their properties, including intermolecular interactions, miscibility, morphology, and compatibility are known.

Soy protein, the major component of the soybean, is biodegradable, environmentally friendly, and readily available from an abundant renewable resource. It had been considered an interesting starting material for the development of new materials ad devices for biotechnological and biomedical utilization [3,8,9]. However, soy protein films are very brittle and hydroscopic [10]. To overcome this limitation, soy protein has been blended with other proteins [11] or polysaccharides [3,12,13] and this has been shown to improve some of the resultant properties, such as mechanical and water vapour barrier of protein films.

Chitosan-based materials have been used for a wide range of biomedical applications [3,13-16]. Chemically, chitosan is a natural polymer, which contains β-1-4 linked 2-amino-2-deoxy-D-glucopyranose repeat units and is readily obtained by the N-deacetylation of chitin, a naturally abundant polysaccharide [1,14]. This polymer is soluble in low pH (pH $<$ 6.5), and insoluble in a neutral and alkaline medium. In an aqueous acid medium, the amine group of chitosan is protonated, the polymer behaves like cationic polyelectrolyte [14]. Previous studies [3,13,17,18] have shown that chitosan can interact with proteins to form insoluble complexes and biofilms. For example, the presence of chitosan has been shown to increase the thermal stability of collagen films, probably due to an increase in the denaturation temperature of collagen-chitosan films over that of collagen alone [17]. It has also been shown that chitosan will form covalent complexes with β-lactoglobulin [18] through a Maillard type reaction. The results of a previous study [3] demonstrate that the combination of chitosan with a colloidal suspension formed from soy protein, in a form of blended membranes exhibit different degradation patterns and improved cellular adhesion with respect to pure chitosan. The results indicate that the characteristics of this blend system are dependent on the composition of the blend, as well as the interaction between chitosan and the soy protein. However, the way in which chitosan and soy interact has not been fully studied. Therefore the aim of this work is to analyze the miscibility and the morphological aspects of chitosan/soy blended membranes, using measurements of proton spin-lattice relaxation times by solid state carbon nuclear magnetic resonance (^{13}C CP/MAS NMR), Fourier transform infrared spectroscopy (FTIR), contact angle measurements, atomic force microscopy (AFM), and scanning electron microscopy (SEM).

2. **Materials and Methods**

2.1. *Materials and Samples preparation*

Chitosan (CHT, Sigma) with ca. 85% deacetylation was used. Soy protein isolate was provided by Loders Crocklaan (The Netherlands). All other reagents were analytical grade and used as received.

Chitosan/soy protein blended membranes (CS) (average thickness from 40 to 84μm) were prepared by solvent casting, as described previously (Silva et al, 2005). Briefly, chitosan flakes were dissolved in an aqueous acetic acid 2% (v/v) solution at a concentration of 1% (w/v). A soy suspension, 1% (w/v), was prepared by slowly suspending the soy protein powder, under constant stirring, in distilled water with glycerol (water/glycerol (10 % w/v)). After adjusting the pH to 8.0± 0.3 with 1M sodium hydroxide, the dispersion was heated in a water bath at 50 ºC for 30 min. The two solutions were then mixed at different ratios, namely CS75, CS50 and CS25 corresponding to 75/25, 50/50, 25/75 w/w (chitosan/soy). After homogenization, the solutions were cast into Petri dishes and dried at room temperature.

2.2*. Fourier Transform Infrared with Attenuated Total Reflection (FTIR-ATR)*

Surface changes on membranes were assessed by FTIR-ATR spectroscopy (Unican Mattson 7000 FTIR spectrometer). All spectra were an average of 64 scans at a resolution of 4 cm^{-1}.

2.3. *Solid State Nuclear Magnetic Resonance (NMR)*

The solid state NMR spectra were recorded on Bruker DRX spectrometers operating at a ^{1}H frequencies of 400 and 500MHz. Proton spin-lattice relaxation time (T_1^H) values were determined using a ^{1}H-^{13}C cross-polarization (CP) inversion recovery sequence [19] and by fitting the ^{13}C peak intensities to a single exponential.

2.4. *Contact angle measurements*

The surface properties of the membranes were assessed by means of static contact angle (θ) measurements using the sessile drop method with ultra-pure distilled water (polar) and diiodomethane (non-polar) (OCA equipment, Germany and SCA-20 software). Six measurements were carried out for each sample. The presented data was calculated using the final averaged values. The polarity of the surface as well as the surface tension was calculated using the Owens-Wendt equation.

2.5. *Scanning electron microscopy (SEM)*

SEM images of samples coated with gold were obtained at 10kV on a Leica Cambridge S-360 microscope equipped with a LINK eXLII X-ray energy dispersion spectrometer for silicon microanalysis.

2.6. *Atomic force microscopy (AFM)*

The samples were measured on at least three spots using TappingMode™ with a MultiMode connected to a NanoScope, both supplied from Veeco, USA, with non-contacting silicon nanoprobes (ca 300kHz, setpoint 2-3V) from Nanosensors, Switzerland. All images (10 μm wide) were fitted to a plane using the 3rd degree flatten procedure included in the NanoScope software version 4.43r8. The surface roughness was calculated as Sq (root mean square from average flat surface) and Sa (average absolute distance from average flat surface). The values are presented as mean (standard deviation).

3. **Results and discussion**

Blend solutions of chitosan and soy protein prepared at different ratios appeared to be homogeneous at a macroscopic level. A mixed biopolymer system is thermodynamically unstable, and a phase separation may not be observed on the experimental time scale because of kinetic energy barriers associated with the restricted movement of molecules through biopolymer networks [20]. After casting, the as-prepared membranes presented a yellowish color. In addition, it was found that the blended membranes became brittle with increasing soy protein content. Cho *et al* [21] reported that films formed from purely protein tend to be brittle, and plasticizers should be added to overcome the brittleness of films.

As expected, the SEM images of the CS blended membranes showed a rougher surface morphology than the pure chitosan membrane (Figure 1). Additionally, the AFM images (Figure 2) show that the morphology of the blended membranes appear as a dispersion of one polymer in the matrix of the other, as it is commonly found in heterogeneous blends [22]. From AFM measurements it was noted that the surface roughness increased with increasing soy protein content from 11.8 $\pm$ 2.8 nm (CS75) to 18.8 $\pm$ 6.4 nm (CS25), in comparison to the roughness of soy protein (35.5 $\pm$ 4.5 nm) and chitosan (1.8 $\pm$ 0.9 nm) membrane alone, in accordance with the SEM results. Soy (**) and chitosan (*) alone were significantly different from all other samples. In contrast, considering experimental error, only the CS25-CS75 pair shows a significant difference.

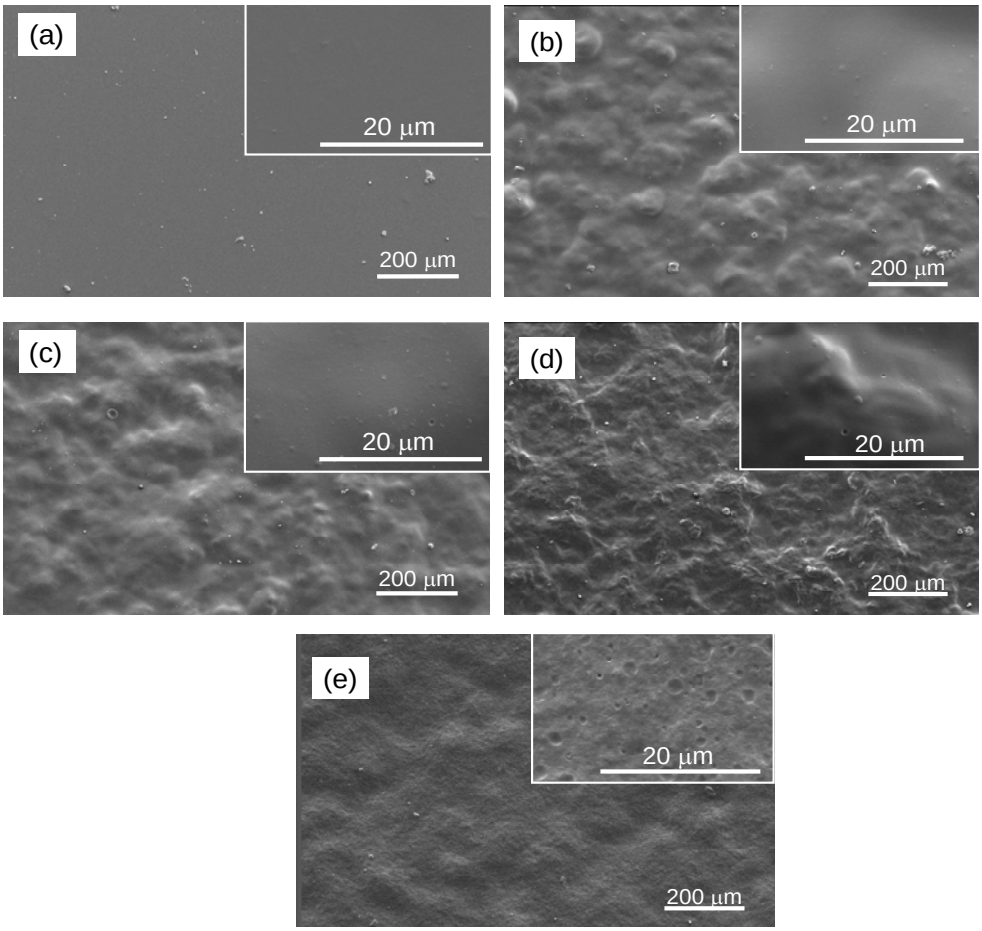

Figure 1. SEM micrographs of chitosan membrane (a), soy protein membrane (b), CS75 (c), CS50 (d) and, CS25 (e). The inset pictures present a higher magnification of the membranes surfaces. (CS75, CS50 and CS25 corresponding to 75/25, 50/50, 25/75 wt% chitosan/soy)

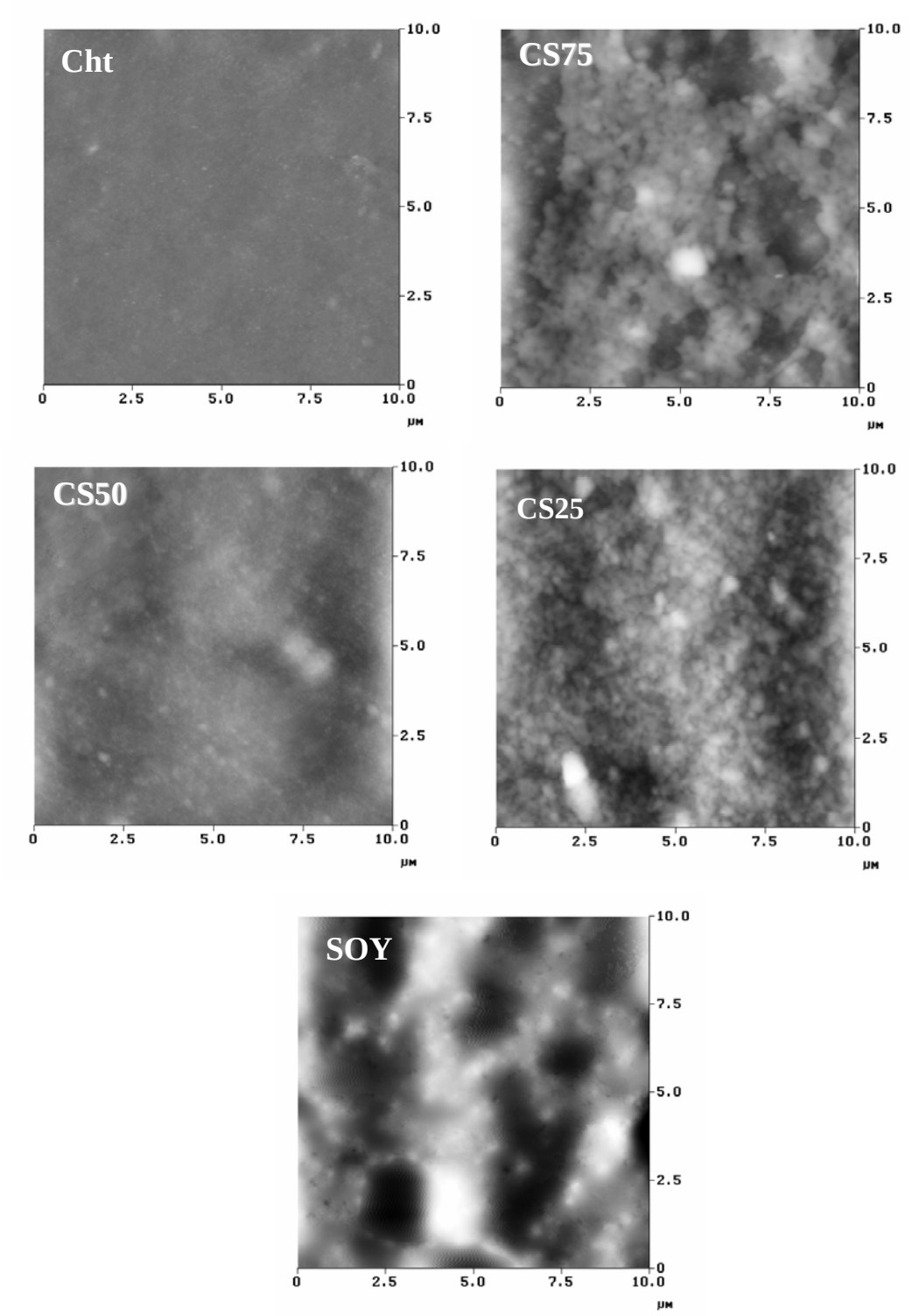

Figure 2. AFM images of membranes: chitosan membranes (CHT), CS75, CS50, CS25 and soy protein membrane. (CS75, CS50 and CS25 corresponding to 75/25, 50/50, 25/75 wt% chitosan/soy)

The measured contact angles and the calculated surface energy of the prepared membranes are summarized in Table 1. It can be seen from this data that the soy protein films are more hydrophilic than the chitosan membranes. As expected, the blending of chitosan with the soy protein resulted in a decrease in the values of the water contact angles of the blended membranes with an increase in the soy protein ratio. The surface energy (γ) of CS blended membranes increases in comparison to pure chitosan, as a result of the mixing of chitosan and soy protein in these blended system. However, no significant changes were seen for the non-polar and polar components of the surface energy.

Table 1. Contact angles (θ) and surface energy (γ) of chitosan, soy protein and their blended membranes.

Membrane	θ_{Water} **(º)**	$\theta_{Diiodomethane}$ **(º)**	γ_d **(mN.m^{-1})**	γ_p**(mN.m^{-1})**	γ **(mN.m^{-1})**
CHT	103.1± 3.2	61.3 ± 0.5	27.4 ± 0.1	0.4 ± 0.1	27.8 ± 0.2
CS75	92.4 ± 2.8	61.7 ± 2.4	24.7 ± 0.1	2.1 ± 0.0	26.8 ± 0.1
CS50	88.2 ± 2.0	55.3 ± 2.4	29.2 ± 0.1	2.0 ± 0.0	31.2 ± 0.1
CS25	75.2 ± 3.8	53.1 ± 1.8	26.1 ± 0.1	8.7 ± 0.06	34.8 ± 0.1
SOY	67.6 ± 4.2	63.5 ± 1.9	19.4 ± 0.1	14.5 ± 0.2	33.9 ± 0.3

The FTIR-ATR spectra of chitosan, soy protein and blended membranes are shown in Figure 3. The ATR analysis of membranes was based on the identification of bands related to the functional groups present in chitosan and soybean, among others [23,24]. The main characteristics absorption bands of chitosan appear at 1650 cm^{-1} (C=O stretching), 1584 cm^{-1} (-NH angular deformation) and 1150-1040 cm^{-1} (-C-O-C- in glycosidic linkage) [23]. The soy protein spectrum showed an amide I band at 1632 cm^{-1} and a amide II band at 1536 cm^{-1} [24]. The amide I can be composed of several overlapping components due to various protein segments with different secondary structures [24]. As can be seen in spectra of the blended membranes, the characteristic absorptions bands of both chitosan and soy protein

appears in proportion to the ratio between the components of the blend. As a result, the absorbance of NH and CO deformation bands in the range 1580-1490 cm^{-1} and 1700-1630 cm^{-1} respectively, increase with the increase in soy content of the blend. A small displacement of these bands to lower wave-numbers (NH from 1584 to 1536 cm^{-1} and CO - from 1650 to 1630 cm^{-1}) with respect to pure chitosan was also noted. These shifts suggest that there may be a specific chemical interaction occurring between chitosan and soy.

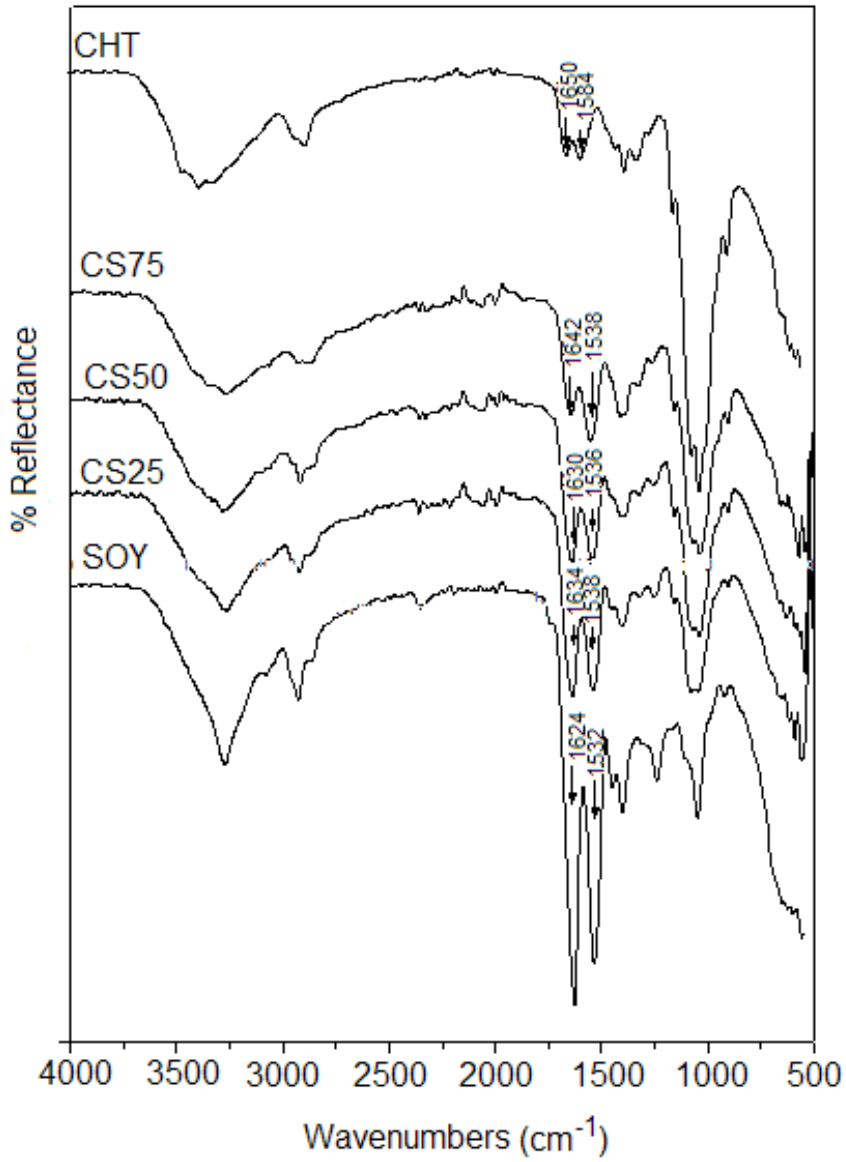

Figure 3. FTIR-ATR of the CS blended membranes. (CS75, CS50 and CS25 corresponding to 75/25, 50/50, 25/75 wt% chitosan/soy).

Figure 4 shows the ^{13}C CP/MAS NMR spectra of chitosan, soy protein and their blends. Comparing the ^{13}C CP/MAS NMR spectra of chitosan and soy protein it was possible to identify a characteristic ^{13}C peak for the polysaccharide at 104 ppm (C1 ring carbon) and for the protein at 172 ppm (backbone carbonyl group) [25,26]. These resonances are distinct from one another and can be used to probe the components of the membrane. Chitosan has a very weak peak at around 175 ppm from the acetyl group carbonyl carbon which does not interfere with the soy carbonyl resonance (Fig. 4C). The ^{13}C peak at 104 ppm in the soy spectra (Fig. 4B) is a spinning side band. To examine the miscibility of the components of chitosan/soy protein blended membranes at length scales of the order of nm, the proton spin-lattice relaxation times in the rotating frame, $T_{1\rho}$ (^1H), were measured. The results are summarized in Table 2. If there is intimate mixing of the polysaccharide and protein molecules the $T_{1\rho}$ (^1H) values will be equal. If, however, the polysaccharide/protein zones are larger than approximately 20nm (i.e. physically separated) then their relaxation times will differ. It is clear that the CS50 $T_{1\rho}$ (^1H) values for the protein and polysaccharide that are clearly different. Therefore it appears that the blend components (at a CS50 ratio), independent of the preparation conditions, are not miscible, possibly as a result of a weak chitosan-protein interaction. However, anomalous behavior has been seen before for water absorption and degradation in CS50 blends (Silva *et al*, 2005) and these results may be further indication of this phenomenon. Even so, the $T_{1\rho}$ (^1H) value for the chitosan component is quite different from pure chitosan therefore the dynamic characteristics of chitosan in the CS50 blend must be significantly different.

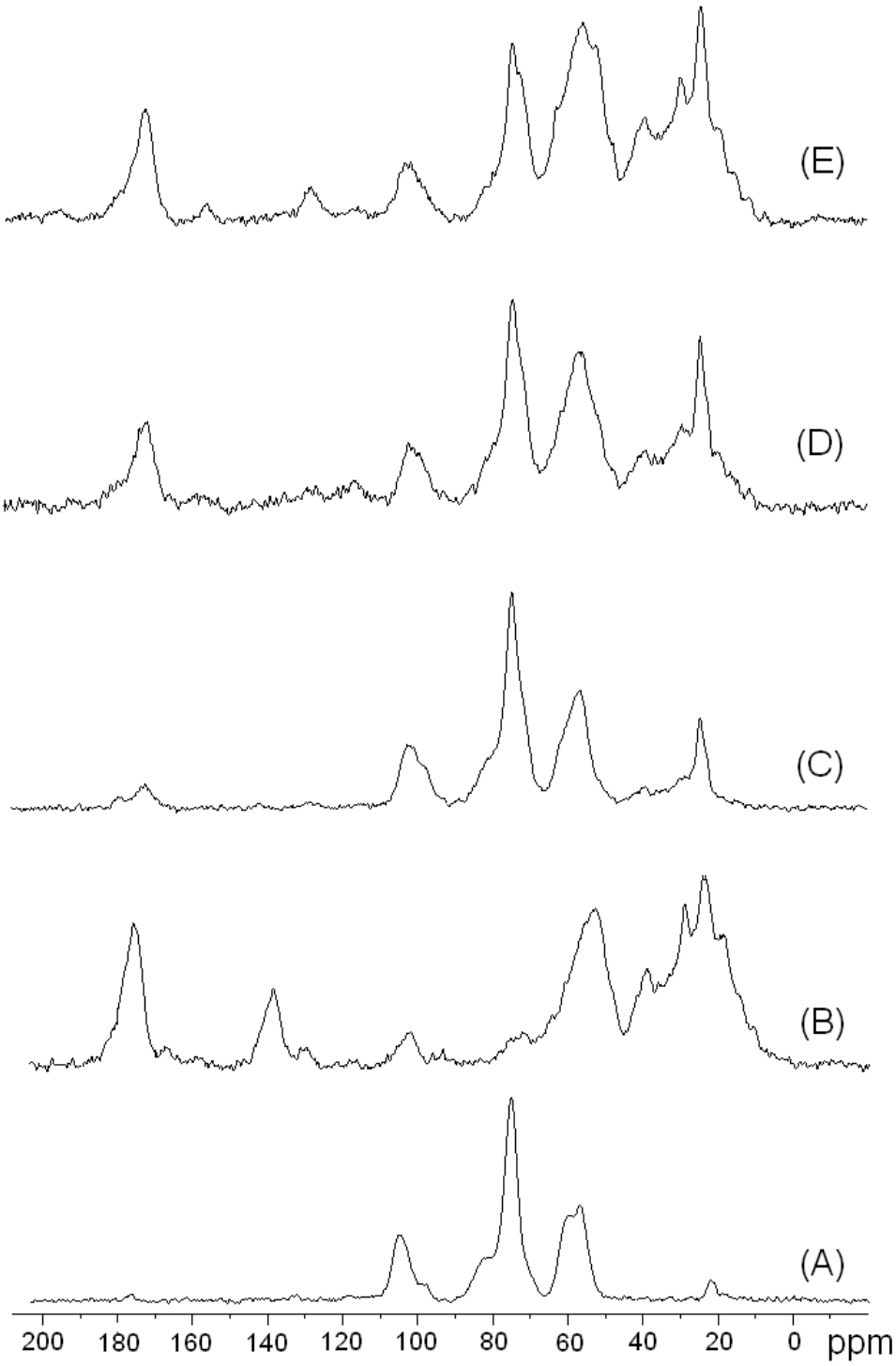

Figure 4. ^{13}C NMR spectra of the chitosan (A), soy protein (B), CS75 (C), CS50 (D), and CS25 (E). The labeled peaks correspond to overlapping of resonance signals of the carbons related to chitosan and soy protein. (CS75, CS50 and CS25 corresponding to 75/25, 50/50, 25/75 wt% chitosan/soy).

Table 2. $T_{1\rho}$ (^{1}H)[ms] values measured for selected resonances to chitosan, soy protein and their blend membranes

Sample	Peak 172-180 [ms]	Peak 104 [ms]
Chitosan	-	697.6 ± 2.7
Soy protein	602.2 ± 14.7	-
CS75	639.8 ± 4.2	619.4 ± 8.0
CS50	627.6 ± 12.0	392.9 ± 11.3
CS25	480.0 ± 12.7	459.6 ± 15.4

Increasing chitosan amount ↑

On the other hand, the CS75 and CS25 samples have $T_{1\rho}$ (^{1}H) values for each component that are that same (within experimental error, Table 2). Therefore, it appears that these samples (CS75 and CS25) may have protein and polysaccharide regions that are miscible. However, it is possible that as the percentage of one of the components is low the blends may be immiscible but due to the small physical size of one of the component pools spin diffusion is occurring. The lower $T_{1\rho}$ (^{1}H)values of the CS25 blend compared to the CS75 blend, however, imply that the dynamic characteristics for both biopolymers are different in the two blends and that the degree of homogeneity of the CS25 blend is higher than of the CS75. This is most probably due to better interaction of the soy protein-rich phase with the chitosan phase in the CS25 blend.

4. **Conclusions**

A physico-chemical characterization of chitosan/soy protein blends has been carried out in order to probe existing interactions, and the ultra-structure of membranes containing different amounts of the two biopolymers. The use of SEM and AFM indicated that the surface morphology of the membrane blends increased in roughness as the amount of soy protein increased, suggesting increasing heterogeneity. The surface energy of the blended membranes was found to increase when compared to the separate constituents and was highest for the CS25 blend. The source and extent of the interaction between the polysaccharide and protein constituents of the blends was probed using FTIR and NMR. The shift in the NH and C=O bands in the FTIR spectra of the blends compared to pure chitosan suggests a weak interaction is occurring between the two phases. The results from the NMR relaxation studies suggest that there is probably no intimate mixing for CS75 and CS50 although the lower $T_{1\rho}$ (^{1}H) values for the CS25 blend suggests that this blend may be the most homogeneous and that the biopolymers have dynamic characteristics different from the isolated components.

5. **Acknowledgements**

S. S. Silva and J. Benesch, thank the Portuguese Foundation for Science and Technology (FCT) for providing PhD and postdoctoral scholarships (SFRH/BD/8658/2002 and SFRH/BPD/20412/2004/0670, respectively) under POCTI program. This work was also partially supported by the European Union funded STREP Project HIPPOCRATES (NMP3-CT-2003-505758).

6. **References**

1. Azad, A. K., Sermsintham, N., Chandrkrachang, S., and Stevens, W. F., Chitosan membrane as a wound-healing dressing: characterization and clinical application, *Journal of Biomedical Materials Research Part B-Applied Biomaterials* 69B, 216-222, 2004.
2. Jeschke, M. G., Sandmann, G., Schubert, T., and Klein, D., Effect of oxidized regenerated cellulose/collagen matrix on dermal and epidermal healing and growth factors in an acute wound, *Wound Repair Rregulation* 13, 324-331, 2005.
3. Silva, S. S., Santos, M. I., Coutinho, O. P., Mano, J. F., and Reis, R. L., Physical properties and biocompatibility of chitosan/soy blended membranes, *Journal of Materials Science-Materials in Medicine* 16, 575-579, 2005.
4. Tolstoguzov, V., Phase behaviour of macromolecular components in biological and food systems, *Nahrung-Food* 44, 299-308, 2000.
5. Bourriot, S., Garnier, C., and Doublier, J. L., Micellar-casein-kcarrageenan mixtures. I. Phase separation and ultrastructure, *Carbohydrate Polymers* 40, 145-157, 1999.
6. de Kruif, C. G. and Tuinier, R., Polysaccharide protein interactions, *Food Hydrocolloids* 15, 555-563, 2001.
7. Baeza, R., Carrera, S. C., Pilosof, A. M. R., and Rodriguez, P. J. M., Interactions of polysaccharides with b-lactoglobulin spread monolayers at the air-water interface, *Food Hydrocolloids* 18, 959-966, 2004.
8. Vaz, C. M., Doeveren, P. F. N. M., Yilmaz, G., Graaf, L. A., Reis, R. L., and Cunha, A. M., Processing and characterization of biodegradable soy plastics: effects of crosslinking with glyoxal and thermal treatment, *Journal of Applied Polymer Science* 97, 604-610, 2005.
9. Vaz, C. M., Graaf, L. A., Reis, R. L., and Cunha, A. M., Soy protein based systems for different tissue regeneration applications, in *NATO/ASI Series Polymer Based Systems on Tissue Engineering, Replacement and Regeneration*, Reis, R. L. andCohn, D. Kluwer Academic Publishers, Dordrecht, 2002.
10. Rhim, J. W., Gennadios, A., Handa, A., Weller, C. L., and Hanna, M. A., Solubility, tensile, and color properties of modified soy protein isolate films, *Journal of Agricultural and Food Chemistry* 48, 4937-4941, 2000.
11. Silva, G. A., Vaz, C. M., Coutinho, O. P., Cunha, A. M., and Reis, R. L., In vitro degradation and cytocompatibility evaluation of novel soy and sodium caseinate-based membrane biomaterials, *Journal of Materials Science-Materials in Medicine* 14, 1055-1066, 2003.
12. Tang, R. P., Du, Y. M., Zheng, H., and Fan, L. H., Preparation and characterization of soy protein isolate-carboxymethylated konjac glucomannan blend films, *Journal of Applied Polymer Science* 88, 1095-1099, 2003.
13. Silva, R. M., Elvira, C., Mano, J. F., San Roman, J., and Reis, R. L., Influence of beta-radiation sterilisation in properties of new chitosan/soybean protein isolate membranes for guided bone regeneration, *Journal of Materials Science-Materials in Medicine* 15, 523-528, 2004.
14. Mi, F. L., Shyu, S. S., Wu, Y. B., Lee, S. T., Shyong, J. Y., and Huang, R. N., Fabrication and characterization of a sponge-like asymmetric chitosan membrane as a wound dressing, *Biomaterials* 22, 165-173, 2001.
15. Tuzlakoglu, K., Alves, C. M., Mano, J. F., and Reis, R. L., Production and characterization of chitosan fibers and 3-D fiber mesh scaffolds for tissue enginering applications, *Macromolecular Bioscience* 4, 811-819, 2004.
16. Suh, J. K. F. and Matthew, H. W. T., Application of chitosan-based polysaccharide biomaterials in cartilage tissue engineering: a review, *Biomaterials* 21, 2589-2598, 2000.
17. Silva, C. C., Lima, C. G. A., Pinheiro, A. G., Goe´s, J. C., and Figueiro, A. S. B., On the piezoelectricity of collagen-chitosan films, *Physical chemistry physics* 3, 4154-4157, 2001.

18. Hattori, M., Numamoto, K., Kobayashi, K., and Takahashi, K., Functional changes in beta-lactoglobulin by conjugation with cationic saccharides, *Journal of Agricultural and Food Chemistry* 48, 2050-2056, 2000.
19. Zhong, Z. and MI, Y., Thermal characterization and solid-state 13C-NMR investigation of blends of poly(N-phenyl-2-hydroxytrimethylene amine) and poly(N-vinyl pyrrolidone), *Journal of Polymer Science Part B: Polymer Physics* 37, 237-245, 1999.
20. Bryant, C. M. and McClements, D. J., Influence of xanthan gum on physical characteristics of heat-denatured whey protein solutions and gels, *Food Hydrocolloids* 14, 383-390, 2000.
21. Cho, S. Y. and Rhee, C., Sorption characteristics of soy protein films and their relation to mechanical properties, *Lebensmittel-Wissenschaft und-Technologie* 35, 151-157, 2002.
22. Koning, C., van Duin, M., Pagnoulle, C., and Jerome, R., Strategies for compatibilization of polymer blends, *Progress in Polymer Science* 23, 707-757, 1998.
23. Pawlak, A. and Mucha, M., Thermogravimetric and FTIR studies of chitosan blends, *Thermochimica Acta* 396, 153-166, 2003.
24. Subirade, M., Kelly, I., Gueguen, J., and Pezolet, M., Molecular basis of film formation from a soybean protein: comparison between the conformation of glycinin in aqueous solution and in films, *International Journal of Biological Macromolecules* 23, 241-249, 1998.
25. Mizuno, A., Mitsuiki, M., Motoki, M., Ebisawa, K., and Suzuki, E., Relationship between the glass transition of soy protein and molecular structure, *Journal of Agricultural and Food Chemistry* 48, 3292-3297, 2000.
26. Cervera, M. F., Heinamaki, J., Rasanen, M., Maunu, S. L., Karjalainen, M., Acosta, O. M. N., I.Colarte, A., and Yliruusi, J., Solid-state characterization of chitosans derived from lobster chitin, *Carbohydrate Polymers* 58, 401-408, 2004.

CHAPTER VII

CHAPTER VII

Novel Genipin Cross-linked Chitosan/Silk Fibroin Sponges for Cartilage Engineering Strategies

ABSTRACT

The positively interaction of materials with tissues is an important step in regenerative medicine strategies. Hydrogels obtained from polysaccharides and proteins are expected to mimic the natural cartilage environment thus providing an optimum milleu for tissue growth and regeneration. In this work, novel hydrogels composed of blends of chitosan and *Bombyx mori* silk fibroin were cross-linked with genipin (G) and freeze-dried to obtain chitosan/silk (CSG) sponges. CSG sponges possess stable and ordered structures due to protein conformation changes from α helix/random coil to β-sheet structure, distinct surface morphologies, and pH/swelling dependence at pH 3, 7.4 and 9. The cytotoxicity of CSG sponge extracts was investigated using L929 fibroblast-like cells. Furthermore, ATDC5 cells were cultured onto the sponges to evaluate the CSG sponges' potential in cartilage repair strategies. These novel sponges promoted adhesion, proliferation and matrix production of chondrocyte-like cells. Sponges' intrinsic properties and biological results suggest that CSG sponges may be potential candidates for cartilage TE strategies.

This chapter is based on the following publication:

S. S. Silva, A. Motta, M. T. Rodrigues, A. F. M. Pinheiro, M. E. Gomes, J. F. Mano, R. L. Reis, C. Migliaresi. "Novel genipin cross-linked chitosan-silk sponges for cartilage tissue engineering strategies". Biomacromolecules 2008, Submitted.

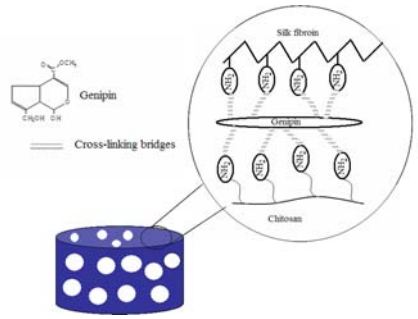

---

1. **Introduction**

The development of materials that positively interact with tissues is an important step for the success of regenerative medicine strategies. Articular cartilage presents a specialized architecture, comprising of chondrocytes embedded within an extracellular matrix (ECM) of collagen and proteoglycans [1,2], and a limited repair capacity which, together with a high physical loading demand over this tissue, make damaged cartilage exceedingly difficult to treat and heal. Different strategies have been developed to promote the repair or regeneration of cartilage tissue or osteochondral defects[1,3,4]. Several *in vivo* studies stated the importance of cell seeded biomaterials to treat cartilage lesions[5-7]. The cell-carrier material should mimic the naturally occurring ECM, as matrix components play a critical role in both *in vitro* and *in vivo* chondrogenesis[8]. Porous matrices with adequate structural and mechanical properties such as hydrogels, sponges and fibrous meshes have been widely used as three dimensional (3D) supports for cell adhesion, proliferation and ECM formation[4,9]. Natural-based porous matrices synthesized from biopolymers, namely hyaluronic acid [10], collagen [11], chitosan [8,12], starch [13] and silk fibroin [14] have been proposed for cartilage tissue engineering (TE) since they represent a suitable and structural cellular environment. Chitosan (cht) and *Bombyx mori* silk fibroin (SF) are excellent natural raw materials for porous matrices designing with potential advantages in terms of biocompatibility, chemistry versatility and controlled degradability due to their intrinsic characteristics[8,14]. Chitosan, a copolymer of D-glucosamine and N-acetylglucosamine groups derived from N-deacetylation of chitin in arthropod exoskeletons[8], is well known for its susceptibility to chemical modification, non-toxicity and enzymatic degradability[8,12]. Chitosan is also structurally similar to various glycosaminoglycans present in articular cartilage, which makes chitosan a promising candidate for cartilage TE applications[8]. Conversely, silk fibroin (SF), a fibrous protein derived from silk *Bombyx* cocoon, is composed by 18 short side chain amino acid that form antiparallel β-sheets in the spun fibers [14,15]. SF has been considered a suitable material for skeletal TE due to

an excellent biocompatibility, good oxygen and water-vapour permeabilities, and to an *in vivo* minimal inflammatory reaction [15-17].

Cell-biopolymer interactions can be improved by the conjugation of different biopolymers and/or with bioactive agents (*e.g.* growth factors or RGD)[18,19]. Additionally, the possibility of conjugating the peculiar biocompatibility of SF with mechanical and biodegradation/biostability properties, typical of polymeric materials such as chitosan, is particularly attractive for designing a tissue engineered 3D scaffold. Thus, we hypothesized the cross-linking of chitosan/silk fibroin blended systems will favor the formation of stable matrices as 3D supports for chondrocyte proliferation and matrix production towards cartilage regeneration. The present work reports the first attempt to develop cross-linked hydrogels from chitosan/silk fibroin (CS) blended systems with different CS ratios and using genipin (G). Genipin, a natural cross-linking agent with lower cytotoxicity [20], is isolated from the fruits of the plant, *Gardenial jasminoides* Ellis[20] and obtained from geniposide, a component of traditional chinese medicine [20]. Genipin has been used to fix biological tissues[8] and to cross-link amino group-containing biomaterials such as chitosan [21-23] and gelatin [22,24] in different forms as *e.g.* microspheres, membranes, and nanofibers. However, to our knowledge, only few approaches have involved genipin reactions with silk fibroin [25,26]. In our work, hydrogels produced by the cross-linking of chitosan/silk fibroin systems were freeze-dried to obtain the cross-linked chitosan/silk (CSG) sponges. The cross-linking degree of the CSG sponges was determined using ninhydrin assay. The viscoelastic properties of the CS and CSG solutions, structural changes, morphological aspects and mechanical properties of the CSG sponges were studied using different techniques namely, Rheological measurements, Fourier Transform Infrared (FTIR) Spectroscopy, Environmental Scanning Electron Microscopy (ESEM), Micro-Computed Tomography (μ-CT) and Dynamical Mechanical Analysis (DMA). To investigate a possible cytotoxicity effect of the developed materials, CSG sponges extracts were placed in contact to fibroblast-like cells (L929 cell line) and a cellular viability assay (MTS) was performed for different culture time points. Furthermore,

the potential use of the developed materials in cartilage repair strategies was also assessed by seeding and culturing ATDC5 chondrocyte-like cells onto the developed CSG sponges. ATDC5 cells, previously described to follow the chondrogenic differentiation pathway [27], constitute an interesting and functional model system for primary chondrocytes in cell culturing methodologies. ATDC5 proliferation and morphology were assessed by the DNA quantification assay and SEM, respectively. To detect the formation of a cartilage-like ECM, glycosaminoglycans (GAGs) were quantified in ATDC5-CSG sponge constructs.

2. **Materials and Methods**

2.1. *Materials*

Reagent grade medium molecular weight chitosan- cht (Sigma Aldrich, CAS 9012-76-4) with a deacetylation degree of 84%, determined by ^{1}H NMR [28] was used. Silk from cocoons of *Bombyx mori* was kindly provided from Cooperativa Socio lario, Como, Italy. Genipin was a product of Wako Chemicals, USA. All other chemicals were reagent grade and used as received.

2.1.1. *Preparation of chitosan*

Chitosan was purified by a re-precipitation method [29]. Briefly, cht powder was dissolved at a concentration of 1% (w/v) in 2% (v/v) aqueous acetic acid. The system was maintained under stirring overnight at room temperature (RT). After that, the solution was filtered twice to remove impurities. Chitosan was then precipitated using 1M aqueous sodium hydroxide (NaOH), while stirring. Finally, the cht was washed with distilled water until neutrality. White flakes of cht purified were obtained after lyophilization for 4 days.

2.1.2. *Preparation of silk fibroin*

Silk from cocoons of *Bombyx mori* was first degummed in order to remove sericins. The degumming process was achieved by boiling the silk filaments for 1 h in water containing 1.1 g/L of Na_2CO_3 (anhydrous) followed by 30 min in water with 0.4 g/L of Na_2CO_3. Finally the resulting fibroin filaments were extensively rinsed in boiling distilled water and air-dried at RT. To prepare solutions to be used in the preparation of the materials, fibroin was dissolved in 9.3M LiBr overnight at 65°C. Then, the silk fibroin (SF) was dialysed in a Slide-A-Lyzer Cassette (Pierce, USA), MWCO 3500 Da against distilled water for 3 days at RT. The water was changed every 2h. After that, the cassettes were transferred to a new dialysis process where the silk fibroin water solution was concentrated by dialysis against polyethylene glycol (PEG) aqueous solution at concentration of 25% (w/v) for 2 hours. After dialysis, the final concentration of silk fibroin aqueous solution was determined using a NanoDrop® ND-1000 Spectrophotometer **(**Delaware, USA). The amino acid composition of silk fibroin was obtained by HPLC analysis.

2.1.3. *Preparation of the CS blended solutions, cross-linking reactions and formation of sponges*

Cht powder was dissolved at a concentration of 5 % (w/v) in an aqueous acetic acid (3%, v/v) overnight at RT. Silk fibroin was dissolved in water at a concentration of 7 wt%. The two solutions were mixed in different ratios, namely CS80, CS50 and CS20 corresponding to 80/20, 50/50 and 20/80 wt% chitosan/silk fibroin (CS), and homogenized, under constant agitation during 30 min at RT. Subsequently, genipin powder (12% related to total weight of solute in solution) was added to the CS blended solutions under constant stirring for 5 min at RT. Then, the CS blended system was maintained under stirring for 5 and 24 hours at 37°C. The resulting hydrogels were washed with distilled water. By this turn, sponges were obtained by hydrogels into a mould, freezing at -80°C overnight, followed by freeze-drying for the period of 2 days to completely remove the solvent. CS sponges without genipin

were used as control materials prepared according to the process described above. The identification of the cross-linked chitosan/silk fibroin sponges was CSXGY, where X, G and Y indicate chitosan content in the blend, genipin and reaction time, respectively.

2.2. **Characterization**

2.2.1. *Rheological studies*

Rheological measurements were carried out in an Advanced Rheometric Expansion System (ARES, Shear Strain Controlled). The geometry was a stainless steal plate/plate (diameter 2 mm and gap 0.4 mm). The plate was equipped with a solvent trap to reduce evaporation during measurement. The measuring device is equipped with a temperature unit (Peltier plate) that provides a rapid change of the temperature and gives a very good temperature control over an extended time. Dynamic rheological tests (time sweep) were used to characterize the behavior of the CS blended solutions and the build-up of the network structure (hydrogel). Measurements were performed at 37°C using a frequency of 5 rad/s and strain 5%. The gelling process was monitored up to 3 hours. The measurements were used to determine the following parameters: elastic modulus, G´, viscous modulus, G´´, dynamic viscosity, η', and phase angle δ in function of time. The elastic modulus is a measure of the solid-like response of the material, whereas the viscous modulus is a measure of the liquid-like response of the material. Loss tangent (tan δ), a parameter that represents the ratio between the viscous and elastic components of the modulus of the polymer, was also calculated (tan $\delta = G''/G'$) [30].

2.2.2. *Optical microscopy*

The optical micrographs were recorded at room temperature in an optical microscope Zeiss – Axiotech (HAL 100, Germany).

2.2.3. *Environmental Scanning Electron Microscopy (ESEM) and micro-computed tomography (μ-CT)*

The morphology of the samples was observed using an environmental scanning electron microscope (E-SEM, Philips XL 30 ESEM, Philips, Eindhoven, The Netherlands) in low vacuum mode. Samples were observed without any treatment at a vacuum pressure level of 0.8 Torr. The qualitative information of the porosity of the CSG sponge architectures was obtained by microtomography imaging using a Skyscan 1072 X-ray microtomograph (Belgium). During the, both the X-ray source and the detector are fixed while the sample rotates around a stable vertical axis. Samples were scanned at a voltage of 40kV and a current of 248μA. After reconstruction of the two-dimensional (2D) cross-sections, a Skyscan ^{TM} CT-analyser software was used to segment of the images and determine their 3D porosity. 200 slices of a region of interest corresponding to the structure of sponges were selected from the CT data set.

2.2.4. *Fourier Transform Infrared (FTIR) Spectroscopy*

The infrared spectra of CS and CSG sponges were obtained with a Perkin Elmer (SPECTRUM ONE FTIR, USA) spectrometer in the spectral region of 4000-650 cm^{-1} with resolution of 2cm^{-1}.

2.2.5. *Cross-linking degree determination (Ninhydrin assay)*

The cross-linking degree for each test group of samples was determined using the ninhydrin assay [23,31]. In a ninhydrin assay [23], the sample was firstly lyophilized for 24 hours, and then was weighed (3 mg). Subsequently, the lyophilized sample was heated with a ninhydrin solution (2 wt %, v/v) at 100°C for 20 min. After the heating with ninhydrin, the optical absorbance of the solution was recorded with a spectrophotometer (Bio-Rad SmartSpec^{TM} 3000, CA, USA) at a wavelength of 570

nm. Glycine solutions at various known concentrations were used as standard. After heating with ninhydrin, the number of free amino groups in the test sample was proportional to the optical absorbance of the solution. Triplicates were made for each sample. The degree of cross-linking of sample was then calculated following the equation 1 [23]:

$$\text{Eq. 1: Degree of cross-linking} = \frac{[(\text{NH reactive amine})_{\text{fresh}} - (\text{NH reactive amine})_{\text{fixed}}]}{(\text{NH reactive amine})_{\text{fresh}}} \times 100$$

Where "fresh" is the mole fraction of free NH_2 in non cross-linked samples and "fixed" is mole fraction of free NH_2 remaining in cross-linked samples.

2.2.6. *Swelling tests*

A weighed amount of CSG sponge of each formulation was immersed in buffer solutions (pH 3, 7.4 and 9) incubated at 37°C under static conditions. The samples were left for 24h in each buffer solution prior to weight determination. The swelling ratio was calculated from the Equation 2, where W_s is the swollen sample weight at specified environmental conditions and W_d is the dry sample weight:

$$\text{Eq.2} \qquad Q = [(W_s - W_d)/W_d] * 100$$

To measure W_s, swollen samples were weighed after removal of excessive surface water with filter paper. Dry samples were obtained by placing swollen hydrogels into a vacuum oven at 65°C for 2 days and then weighed. Each experiment was repeated three times and the average value was considered as the water uptake value.

2.2.7. *Dynamic mechanical analysis (DMA) measurements*

All of the viscoelastic measurements were performed with a TRITEC2000B DMA from Triton Technology (UK) equipped with a compressive mode. The samples were sectioned into rectangular geometry (5.4 x 5.7 mm). Prior the DMA experiments, the sample were equilibrated for about 50 minutes in a phosphate buffer saline (PBS) solution. All samples were analysed in wet conditions, using PBS, placed in a Teflon reservoir. The temperature was controlled by a sensor located in the bath. The frequency scans (0.1 to 100 Hz) with acquisitions of 15 points per decade were performed at 37°C with heat rate at 2°C/min. The DMA results were presented in terms of two main parameters: storage modulus (E´) and loss modulus (E´´).

3. *In vitro cell culture studies*

Prior to cell culture studies, CS80G, CS50G and CS20G sponges were sterilized by immersion in a 70% ethanol solution overnight, washed twice in sterile ultra-pure water and air dried in a sterile environment.

3.1. *Cytotoxicity screening*

In order to assess the eventual cytotoxicity of the developed CSG sponges, extracts of all sponges were prepared and placed in contact with a mouse fibroblast-like cell line, L929, (L929 cells; ECACC, UK) and tested using a MTS assay in accordance to protocols described in ISO/EN 10993[32]. Cells were cultured in basic medium: Dulbecco's Modified Eagle's Medium (DMEM, Sigma-Aldrich, USA) without phenol red and supplemented with 10% foetal bovine serum, (FBS, Gibco, UK) and 1% antibiotic/antimycotic (A/B, Gibco, UK) solution. L929 cells were incubated at 37 °C in an atmosphere containing 5% of CO_2 until achieving 90% of confluence. Then, a cell suspension was prepared with a concentration of 8 x 10^4 cells ml^{-1} and seeded onto 96-well plates. L929 cells were incubated for 3, 7 and 14 days. Sponge extracts from CS80G, CS50G and CS20G were prepared as described in previous works[33].

L929 cells relative viability (%) was determined for each CSG sponges extracts and compared to tissue culture polystyrene (TCPS), used as a negative control of cell death. Latex extracts were considered as a positive control of cellular death. After each time point, extract solutions were removed and cells washed in a phosphate buffer saline (PBS; Sigma-Aldrich, USA) solution. Then, MTS (3-(4,5-dimethylthiazol-2-yl)-5-(3-carboxymethoxyphenyl)-2-(4-sulfophenyl)-2H-tetrazolium) test was performed to assess cellular viability of L929 cells in contact with CSG sponge extracts. For this assay, an MTS solution was prepared using a 1:5 ratio of MTS reagent and culture medium containing DMEM without phenol red, 10% FBS and 1% A/B solution, followed by a 3 hours incubation period at 37ºC. Finally, the optical density (OD) was read at 490 nm, on a multiwell microplate reader (Synergy HT, Bio-Tek Instruments). All cytotoxicity screening tests were performed using 6 replicates.

3.2. *Direct contact assay – cell adhesion and proliferation on sponges*

In vitro cell tests were performed using a cell suspension of ATDC5 chondrocytes like-cells (mouse 129 teratocarcinoma AT805 derived, ECACC, UK) at a concentration of 2.4 x 10^5 cells per sponge (with an approximate volume of 0.125mm^3). Triplicates were made for each sample. Cell-sponges constructs were incubated at 37°C in a humidified 95% air/5% CO_2 atmosphere and maintained for 14, 21 and 28 days using a culture medium consisting of Dulbecco's Modified Eagle's Medium-F12 Ham (DMEM-F12), Gibco, UK) supplemented with 10% foetal bovine serum, FBS (Gibco, UK), 2 mM L-Glutamine (Sigma, USA) and antibiotic/antimycotic (1% A/B, Gibco, UK) solution. Culture medium was replaced twice a week. After 14, 21 and 28 days of culture, the medium was removed, samples were washed with a PBS solution and assessed for SEM analysis, DNA quantification and GAGs detection.

3.3. *Scanning electron microscopy (SEM) analysis of the cell seeded sponges*

Cell morphology and proliferation of ATDC5 seeded CSG sponges were observed by SEM (Leica Cambridge S-360, UK). For this purpose, after each culturing period, ATDC5 cells-sponge constructs were fixed in a 4% formalin solution (Sigma, USA) for 60 minutes at +4°C, and dehydrated using a series of ethanol solutions (25, 50, 70, 100%, v/v). Afterwards, constructs were air-dried overnight at RT, and sputter coated with gold using a Fisons Instruments Coater (Polaron SC 502, UK) with a current set at 18 mA, for a coating time of 120 s, before observation in the SEM.

3.4. *Assessment of cellular behaviour: proliferation and matrix production of ATDC5 cells onto CSG sponges*

ATDC5 cell proliferation onto CSG sponges was determined using a fluorimetric double strand DNA quantification kit (PicoGreen, Molecular Probes, Invitrogen, UK). For this purpose, samples collected at 14, 21 and 28 days were transferred into 1.5 ml microtubes containing 1 ml of ultra-pure water. ATDC5 cells-sponge constructs were incubated for 1 h at 37°C in a water-bath and then stored in a -80°C freezer until testing. Prior to dsDNA quantification, constructs were thawed and sonicated for 15 min. Samples and standards (ranging between 0 and 2 mg ml^{-1}) were prepared and mixed with a PicoGreen solution in a 200:1 ratio, and placed on an opaque 96 well plate. Triplicates were made for each sample or standard. The plate was incubated for 10 min in the dark and fluorescence was measured on a microplate ELISA reader (BioTek, USA) using an excitation of 485/20 nm and an emission of 528/20 nm. A standard curve was created and sample DNA values were read off from the standard graph.

GAGs quantification assay[34] was used to detect chondrogenic ECM formation after 14, 21 and 28 days of culture. GAGs standards were obtained by preparing a chondroitin sulphate solution ranging from 0 and 30 mg ml^{-1}. In each well of a 96-

well plate, samples or standards were added in triplicates and then the dimethylmethylene blue reagent (DMB, Sigma-Aldrich, USA) was added and mixed. The optical density (OD) was measured immediately at 525 nm on a microplate ELISA reader. A standard curve was created and GAGs sample values were read off from the standard graph.

3.5. *Statistical analysis*

All quantitative data are presented as mean $\pm$ standard deviation. Statistic analysis was performed by Student's *t*-test (independent-difference). Results were considered significant at $p < 0.05$.

4. **Results and Discussion**

4.1. *Chitosan- silk fibroin (CS) blended solution characterization*

Prior to the preparation of CSG hydrogel network, the CS blended solution behaviors were examined by means of rheological measurements. Figure 1a-1c shows that both moduli of all CS blended solutions increases with time, demonstrating the gel-like properties of the CS blended solutions. Some rheological studies[34] reported that the gel-like properties of chitosan solutions may be associated to the worm-like character of chitosan chain solution, which may favor the macromolecular ordering and self-association through hydrophobic interactions, rendering a weak network. Also, the acid medium induces the formation of a gel from native *Bombyx mori* silk, detected by a rise in storage modulus [35]. During genipin cross-linking, the physical chain entanglements within the CS blended system are replaced by chemical cross-linkages, which would be able to form CSG hydrogels. The build-up hydrogel network formation was also monitored by the behavior of the curves G´(t), G´´(t), η´(t) and tan δ up to 3 hours. Prior to gelation, loss modulus, G´´(t) was greater than elastic modulus, G´(t)

indicating a liquid-like behavior in the beginning of the reaction. When chemical cross-linkages are introduced, the physical chain entanglements of the polymeric chains is gradually replaced by a permanent covalent network, favoring the increase of G´(t) observed in Figure 1d-1f. With the progress of reaction, the increasing rate of G´ (t) was higher than the G´´ (t), leading to a G´/G´´ crossover described as gelation time or gel point [36], where the transition from the liquid-like to the solid-like behavior takes place. From time sweep results (Figure 1d-1f) the measured values of the gelation time were 12 min, 39 min and 20 min for CS80G, CS50G and CS20G, respectively. The speed of the reactions may be associated to different interactions of genipin with the blend components. Previous studies [22] involving gelatin and chitosan indicated that genipin could efficiently cross-link chitosan much faster than with gelatin. As expected, the viscosity and both moduli increase for all CSG solutions (Figure 1d-1f) when compared to CS blended solutions (Figure 1a-1c). Additionally, the tan δ values of CSG solutions tended to decrease to less than 0.3 upon gelation (Figure 1d-1f). It is worth mentioning that the inflection of the rheological curves of CS50G (Fig. 1e) and CS20G (Fig. 1f) in both moduli at 80 min (CS20G) and 108 min (CS50G), suggest that the SF fraction reacts slower with genipin.

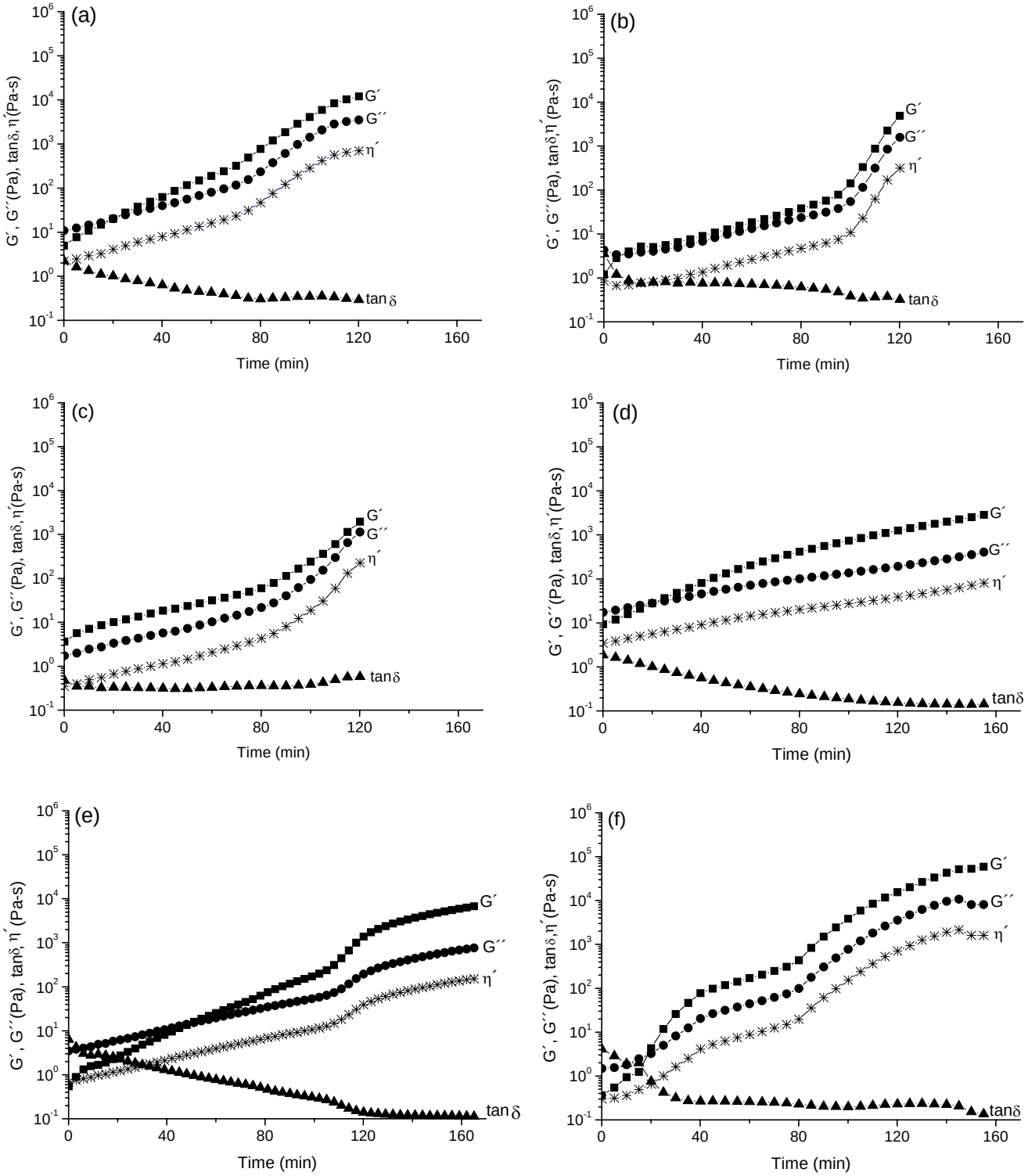

Figure 1. Time sweep profiles for non- and cross-linked CS blended solutions: (a) CS80, (b) CS50, (c) CS20, (d) CS80G, (e) CS50G and (f) CS20G. Measurements were made at ω = 5 rad/s at 37°C. Symbols correspond to storage modulus, G´ (■), loss modulus, G´´ (●) , dynamic viscosity, η´ (∗) and tanδ (▲).

4.2. *Cross-linking reactions and formation of CSG hydrogels*

Considering that the cross-linking of compounds containing amino groups with genipin is a moderate reaction [37], all reactions were conducted for 24 hours at 37°C. Table 1 summarizes the details of the cross-linking reactions in function of time. It was observed that the lightly yellow color of the solutions turned gradually into a dark blue gel. In all hydrogels, the blue coloration was deepest near the surface exposed to air, and gradually moved further into the sample with the increase of cross-linking reaction time. The dark blue color that appeared in the hydrogels is associated to oxygen radical-induced polymerization of genipin as well as its reaction with amino groups/amino acids [21,38]. The speed of the reactions was found to be dependent on the CS ratio, as evidenced by the rheological data. For example, the CS80G formulation has the highest chitosan content, and formed a dark blue gel within 3 hours (Table 1), while the others reactions take longer times up to the formation of a consistent dark blue gel. Fully gelled dark blue hydrogels with a symmetric structure were formed after 24 hours at 37°C (Fig.2a, Table 1). Previous studies [39] demonstrated that an increase of efficacy of genipin reaction can be reached with the increasing of temperature and a decreasing of pH. Chen *et al* [21] reported that the speed of the reaction of chitosan with genipin at 37°C was faster than at lower temperatures due to the higher level of molecular mobility at this temperature. Motta *et al* [25] observed that genipin cross-linked silk fibroin films were formed after 5 hours of reaction at 65°C, followed by casting of the solutions at room temperature.

Table 1. Effect of reaction time on the physical appearance of the cross-linked CS based sponges during reaction genipin at 37°C.

Blended System *	Reaction time (h)				
	0	**1**	**3**	**5**	**24**
CS80G	Lightly yellow	Gelled green blue	Gelled, dark blue gel	Fully gelled dark blue gel	Fully gelled dark blue
CS50G	Lightly yellow	Viscous green- blue	Blue gel (top)/ blue -green (bottom)	Dark blue gel (top)/ green blue (bottom)	Fully gelled dark blue
CS20G	Lightly yellow	Viscous green blue	Blue gel (top)/ blue- green (bottom)	Dark blue gel (top)/ green blue (bottom)	Fully gelled dark blue

CS80G, CS50G and CS20G corresponding to 80/20, 50/50 and 20/80 wt% chitosan/silk fibroin (CS) cross-linked with genipin.

Representative optical micrographs of hydrogels are presented in Fig.2b, suggesting that their surface were dark blue, homogeneous and globular. Though the mechanism of interaction of genipin with silk fibroin is currently unknown, the reaction mechanism can be similar to the observed for amino-group-containing compounds [21,40]. In the reaction mechanism described in these studies, the ester groups of genipin interact with the amino groups in chitosan and/or proteins leading to the formation of secondary amide linkages. Additionally, the amino groups initiate nucleophilic attacks at genipin, resulting in the opening of the dihydropyran ring followed by a number of reaction steps. Besides, some authors [38] reported that genipin reacts preferentially with the aminoacids lysine and arginine of certain proteins. In our studies, the fibroin chain contains these aminoacids in a very low percentage (lysine 0.6% and arginine 0.6%), mainly in the hydrophilic blocks. For this reason, the cross-linking sites are low in number and the kinetic should be reasonably slow on silk fibroin fraction. However, chitosan has a high

percentage of amine groups, which can be directly cross-linked with genipin[41]. Hence, the association of silk fibroin with chitosan favoured the genipin cross-linking and, as result the formation of stable and ordered hydrogels was obtained. Moreover, as the cross-linking reactions on CSG solutions took place in acidic conditions (≈ pH 4.4), the intermediate compounds could further associate to form cross-linked polymeric networks with short chains of cross-linking bridges, as reported in others studies [37]. After production, the CSG hydrogels were freeze-dried and, a schematic representation of the resulting CSG sponges was showed in Figure 2c. The cross-linking degree values of CSG sponges were determined using ninhydrin assay[31]. The values obtained were respectively: 45.2 ± 0.1%, 29.3 ± 1.7, and 23.9 ± 3.1 for CS80G, CS50G and CS20G.

(a)

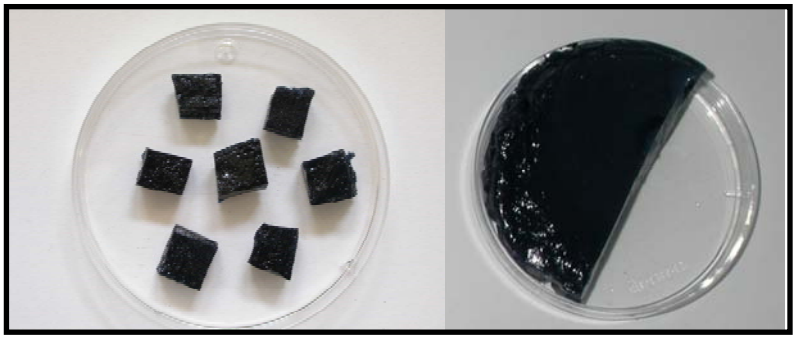

(b)

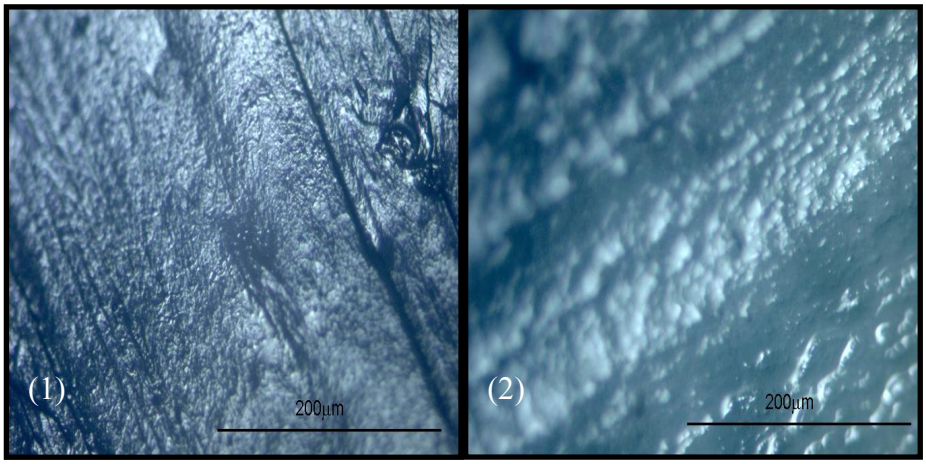

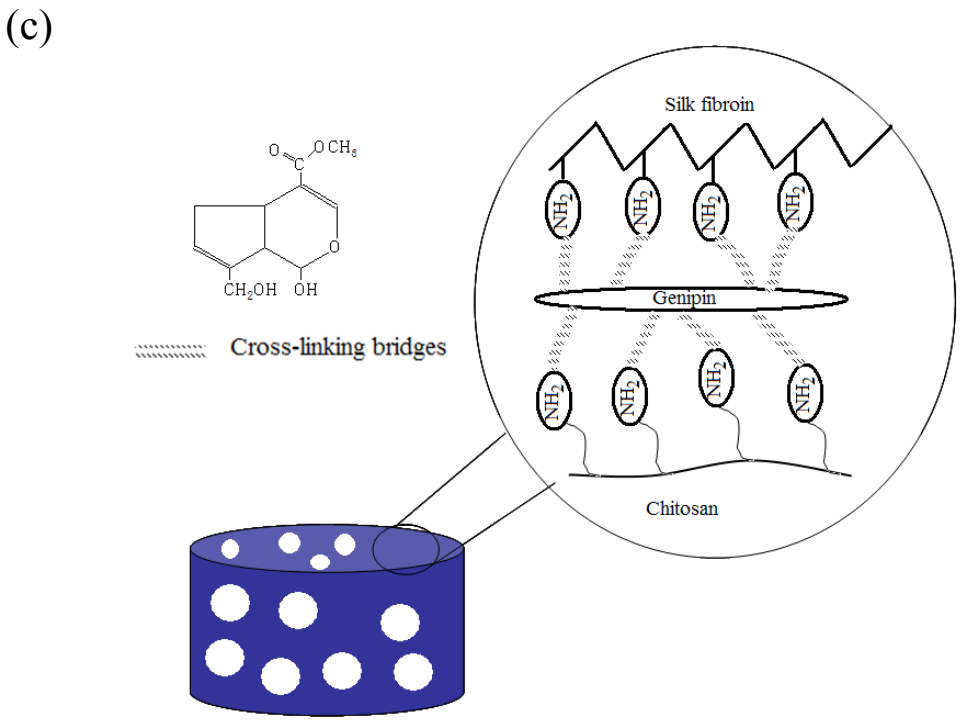

Figure 2. CSG hydrogels as obtained (a), (b) Optical micrographs of CSG hydrogels in wet state: (1) CSG20G and (2) CSG80G and, (c) Schematic representation of the CSG hydrogels.

4.3. *FTIR results*

When CS blended systems were submitted to cross-linking with genipin, conformational changes may occur as a result of structural rearrangement chains to form covalent bonds. In order to evaluate the effect of genipin on the conformation of the materials developed, FTIR spectra of non- cross-linked CS samples were acquired (see Figure 3). The main characteristics absorption bands of chitosan appear at 1637 cm^{-1} , 1541 cm^{-1} and 1150-1040 cm^{-1}, which corresponded to amide I (C=O) and amide II (NH_2) and glycosidic linkage, respectively [43]. Silk protein exists in three conformations, namely random coil, silk I (α-form), and silk II (β-sheet conformation) [44]. The silk fibroin spectrum shows bands at 1644 cm^{-1},1531 cm^{-1} assigned, respectively, to amide I and amide II bands of a random coil or silk I conformation[44]. As expected, the characteristic absorptions bands of both silk fibroin and chitosan appear in proportion to the CS ratio. The CS spectra (Fig. 3a) showed absorption bands in the range of 1654-1644 cm^{-1} (amide I), 1543-1518 cm^{-1} (amide II) and 1249-1235 cm^{-1} (amide III), in which the bands at 1653-1647 cm^{-1}

and 1250-1240 cm^{-1} were assigned to the random α helix/random coil conformation[45], while the 1532-1514 cm^{-1} belonged to beta-sheet conformation[45]. Even though new peaks did not appear after the reaction, the structural changes, caused by the genipin cross-linking can be revealed by analysing the amide I (C=O, stretching), II (N-H deformation) and III (C-N stretching and N-H deformation) in the spectra (Fig. 3b and 3c). Comparing the both spectra (Fig. 3a and 3b), the amide I (1644-1620 cm^{-1}) and amide II (1529-1517 cm^{-1}) bands shifts to lower wavenumbers in the samples obtained with different reaction time. The results suggested that CSG hydrogels produced after 5 hours of reaction had a heterogeneous structure, consisting mainly of a β-sheet structure with small contributions of α helix/random coil conformation [45]. A more prolonged reaction time (24h) seems to lead to the formation of a stable β-sheet structure (silk II structure) on all CSG matrices, which was associated to the characteristics absorption bands at 1621 (amide I), 1517 (amide II) and 1254 cm^{-1} [44,45] (Fig. 3c). Collectively, these structural aspects evidenced that the genipin cross-linking into CS blended systems was followed by protein conformational changes, promoting the formation of CSG matrices with stable and ordered structures.

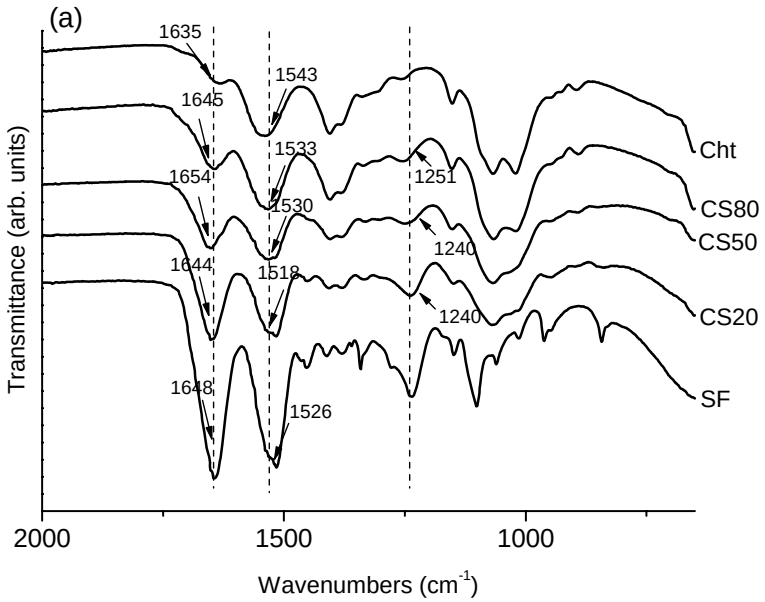

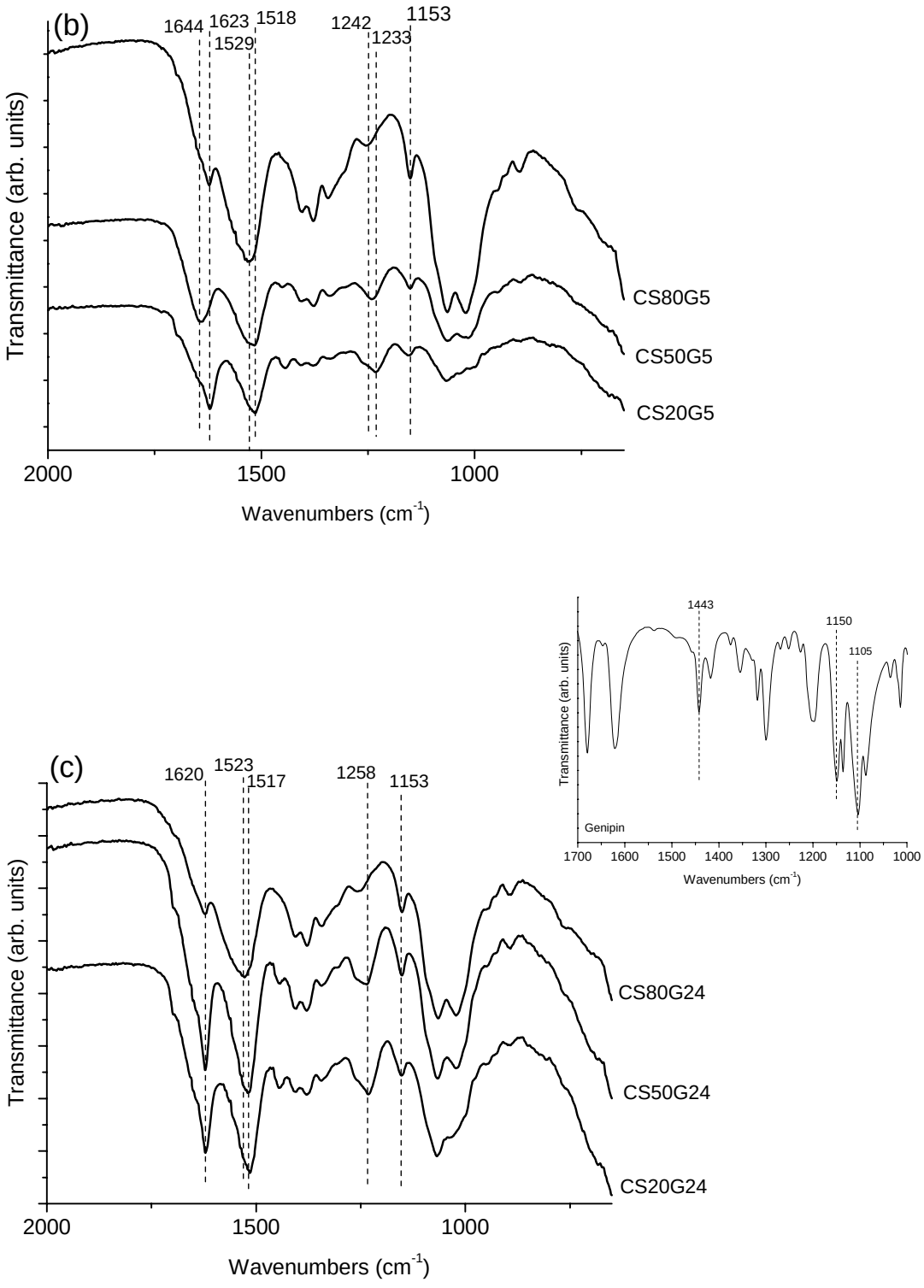

Figure 3. FTIR spectra of CS blended solutions (a), and the CSG sponges obtained after 5 (b) and 24 (c) hours of reaction time.

4.4. **Morphological characterization**

In tissue engineering applications it is important that the scaffolds maintains its porous structure under physiological immersion conditions, similar to those found *in vitro* and *in vivo*. Therefore, especially for systems that have the ability to uptake water such the ones studied in this work (see next sections), the observation of the porous architecture should be preferably performed in wet conditions. In this work, the morphology of the developed sponges was investigated by environmental microscopy (ESEM). ESEM micrographs of the surface of CSG sponges showed well distinct surface morphologies (Fig. 4) with pore sizes ranging from 29 to 167 μm, depending on the composition, where a decreasing tendency was found for the pore size of sponges with an increasing in the SF content. These different morphological features may influence the biological behaviour of the sponges, since that the hydrophilic nature of the sponges (as it will discussed in the next section) enable the complete and rapid wetting of the entire matrix by the culture medium, allowing that the cells be entrapped by the pore structure. Additionally, the μ-CT analysis enabled to estimate the mean porosity of the CSG sponges. The obtained values were 81.2 ± 1.5 %, 83.3 ± 2.4% and 80.3 ± 0.21 for CS80G, CS50G and CS20G, respectively. Even though the mean porosity of the sponges was not significantly different regardless of composition of the sponges, the hydrophilicity of the sponges combined with its 80% mean porosity can promote uniform cell distribution in the entire sponge volume.

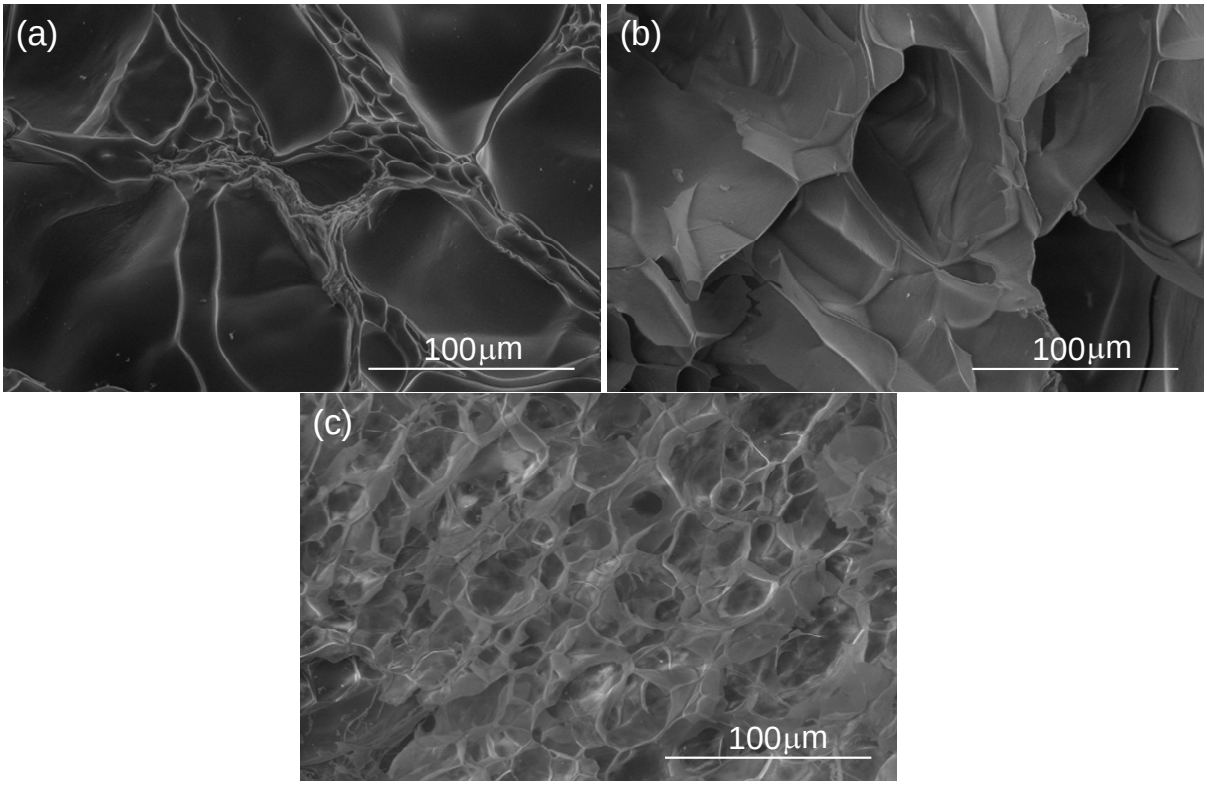

Figure 4. ESEM images of the CSG sponges: CS80G (a), CS50G (b) and CS20G (c).

4.5. *Swelling behaviour*

An important aspect of the extracellular matrix (ECM) is its ability to store water, which supports various cellular activities and functions [46]. In order to study the water uptake ability of the materials, and its response to the external pH conditions, the sponges were immersed in buffer solutions at pH 3, 7.4 and 9 at 37°C for pre-determined time. The swelling degree of CSG sponges were higher in acidic solution (pH 3) and became lower in neutral (pH 7.4) and alkaline (pH 9) medium (Fig. 5a-5d). At low pH, CSG sponges presented higher swelling degrees due essentially to the protonation of the free amino groups of chitosan. The protonation promote the solubility of the polymeric segments and leads to polymer chain repulsion, and the interaction with water molecules allowing the uptake of more water into the gel network. However, with an increasing pH, the CSG sponges exhibit a lower swelling degree after 24 hours (Figure 5d), probably due to the

influence of unprotonated amine groups, and to cross links that restrict the swelling of the sponges. Generally, the swelling degree of sponges, often with a pH stimuli-responsive character, can be controlled adjusting its composition as well as the cross-linking extent of the material. Besides, in CSG sponges, the introduced cross-links created stable structures avoiding the dissolution of the hydrophilic polymer chains/segments into the aqueous phase. Collectively, the swelling results demonstrated that the developed CSG sponges exhibited a pH-dependent pattern in the range of pH studied.

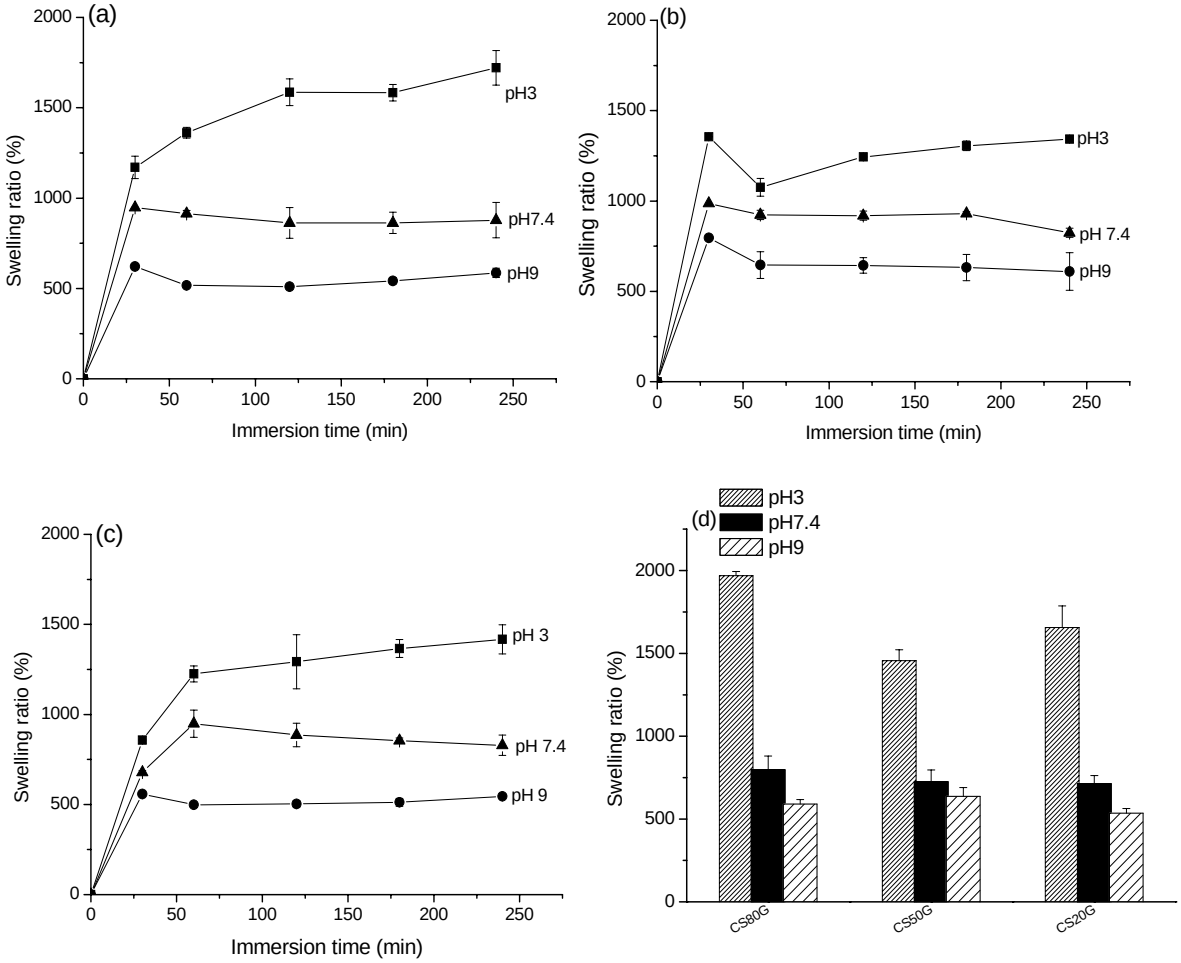

Figure 5. The pH-dependent swelling behaviour of CSG sponges after 4 hours of immersion time at 37 °C in PBS: (a) CS80G, (b) CS50G, (c) CS20G and (d) Comparative swelling ratio of the cross-linked samples after 24 hours of immersion time in PBS. Data represent the mean ± standard deviation, *n*=3.

4.6. *Mechanical properties*

To examine the mechanical properties of the CSG sponges, compression tests were conducted, in wet conditions. Dynamic mechanical analysis (DMA) is a suitable technique that enables to investigate the solid-state rheological properties of materials and biomaterials as function of temperature and frequency [47,48]. In this work the samples were kept in solution up to equilibrium and tested in that state. The results are summarized in Figure 6, where both moduli components are represented within a frequency range that could be relevant in a practical point of view. In all materials E´ was higher than E´´ indicating a solid-like behaviour consistent with the previous rheological tests. Although a small increase in both variables could be observed with increasing frequency, it may be conclude that the viscoelastic properties are kept stable within the frequency range investigated. The DMA results indicate that the incorporation of silk fibroin to chitosan associated to genipin cross-linking allows producing stiffer hydrogels. From FTIR results, it was suggested that the genipin cross-linking promoted the formation of beta-sheets into CSG sponges. The increased regions of beta-sheets imply an increase of amount of crystalline organized domains, increase stiffness, and consequently increase of the moduli of the material.

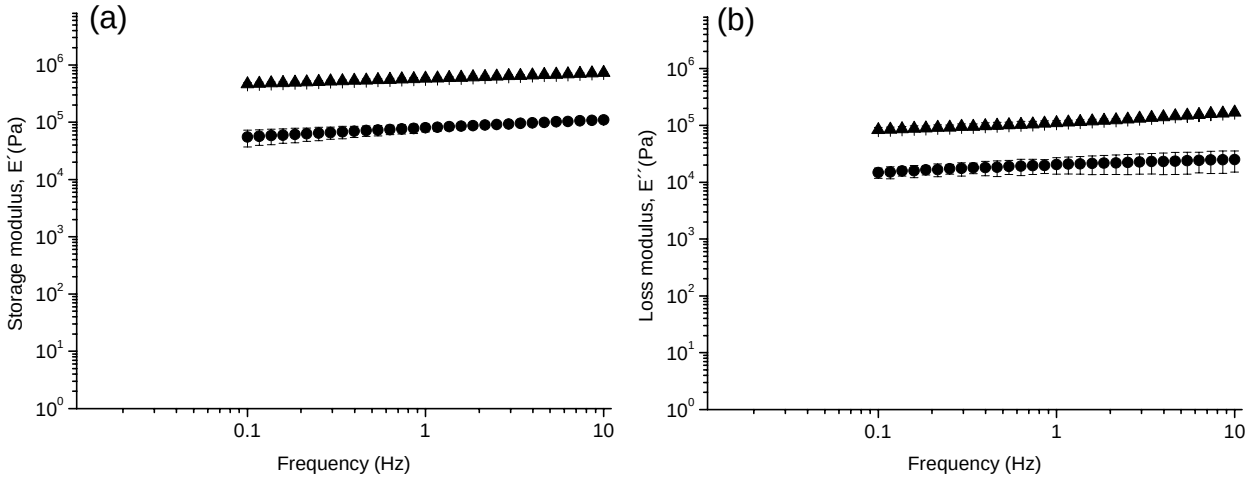

Figure 6. Storage (E´), and loss (E´´) modulus curves of the CSG sponges measured as a function of frequency. (a) E´ and (b) E´´, measured as a function of frequency. Symbols correspond to CS80G (●) and CS20G (▲).

4.7. *Biological studies*

4.7.1. *Cytotoxicity assays*

The cytotoxicity assessment of sponge extracts was carried out as a preliminary approach to assess the biocompatibility of CSG sponges. Table 2 shows the cell viability results obtained from the MTS test performed using extracts of the materials under study. Results indicate that L929 cells are viable in the presence cross-linked CS sponges' extracts. In fact, the cell viability was about 100% in all sponges when compared to tissue culture polystyrene (TCPs). This demonstrates the extremely low cytotoxicity levels of the CSG sponges.

Table 2. Results obtained from cytotoxicity tests performed using extracts of cross-linked CS based sponges.

Sample	Cell viability (%)*			
	1 day	**3 days**	**7 days**	**14 days**
CS80G	79.1 ± 13.3	95.4 ± 23.2	110.8 ± 5.5	125.1 ± 12.4
CS50G	53.5 ± 21.1	101.1 ± 16.9	96.3 ± 6.9	122.0 ± 3.4
CS20G	69.5 ± 29.7	132.9 ± 53.2	101.8± 9.5	122.2 ± 7.6

* The values were determined taking into account the TCPs (negative control) corresponded to 100%. Latex was used as a positive control of cell death, producing cell viability values which were considered negligible (less than 0.5%).

4.7.2. *Direct Contact assay – cell adhesion and proliferation on sponges*

SEM micrographs obtained from samples resulting from culturing ATDC5-chondrocytes like cells on CSG sponges for 14, 21 and 28 days are described in Figure 7, where a high cellular density on the surface of the CSG sponges was

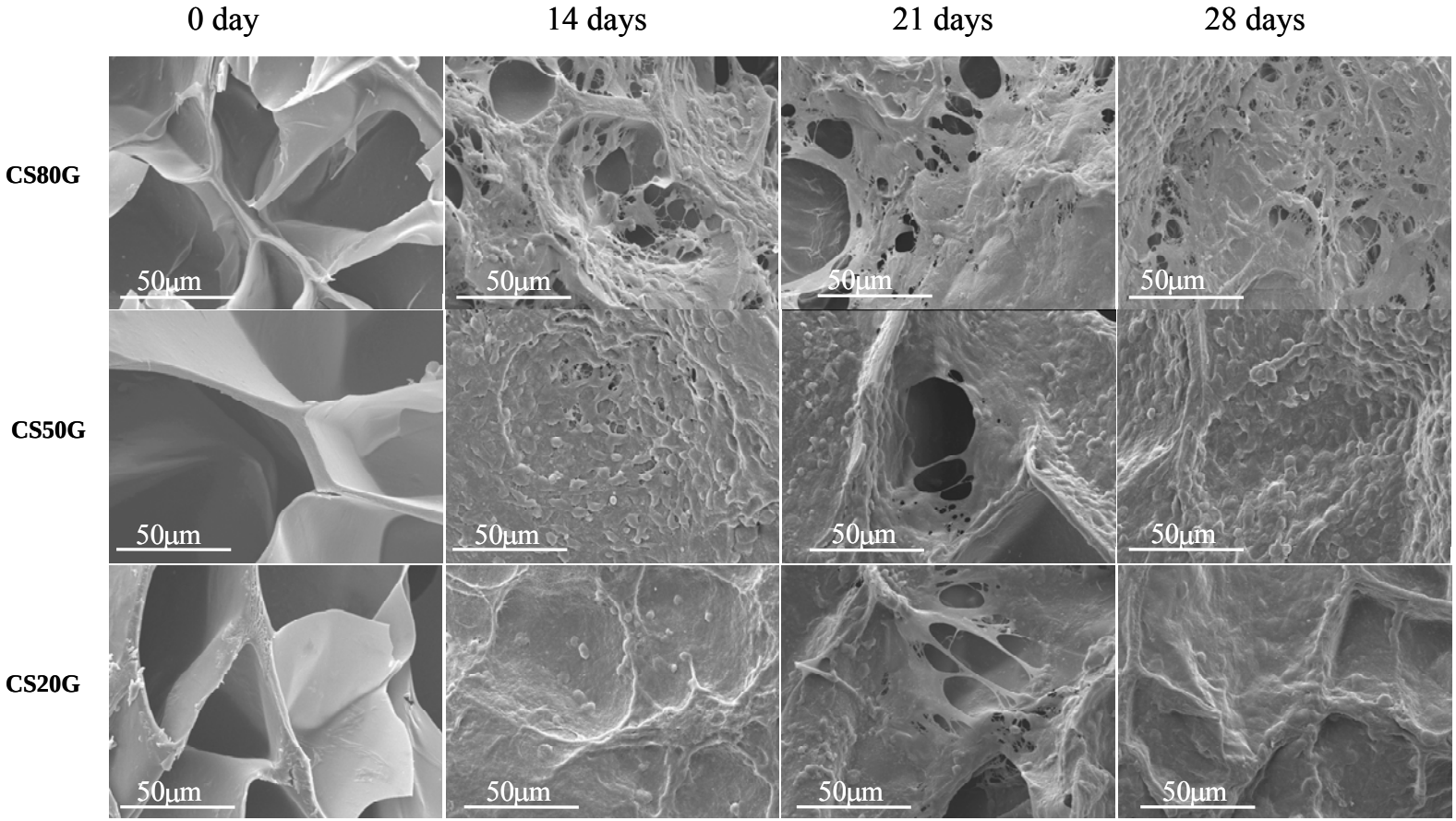

Figure 7. SEM micrographs of ATDC5 cells cultured on CS80G, CS50G and CS20G after 0, 14, 21 and 28 days.

observed. Additionally, cells were able to proliferate and maintain their chondrocyte morphology in all CSG sponges.

The results obtained from the DNA biochemical analysis showed that the proliferation of ATDC5-chondrocytes like cells seeded onto CSG sponges tend to increase with the culturing time (Figure 8). In SEM micrographs (Fig. 7) a great number of cells was observed throughout the sponges and thus supporting these findings. The synthesis of GAGs in ECM is an important function of chondrocytes and plays a significant role in regulating the chondrocyte phenotype [49] and determining the cartilage natural structure. Figure 9 shows that the GAGs content increased, especially after 28 days in culture for the different sponge compositions. These findings indicated that the incorporation of SF component to Cht as well as genipin cross-linking promoted an improvement of the properties of the resulting CSG sponges in terms of ATDC5 chondrocytes-like cells adhesion and proliferation. Although an increase in the amount of silk was expected to enhance the cell studied parameters due to its excellent biocompatibility[14,15], these results might be related to structural differences promoted by genipin cross-linking reaction.

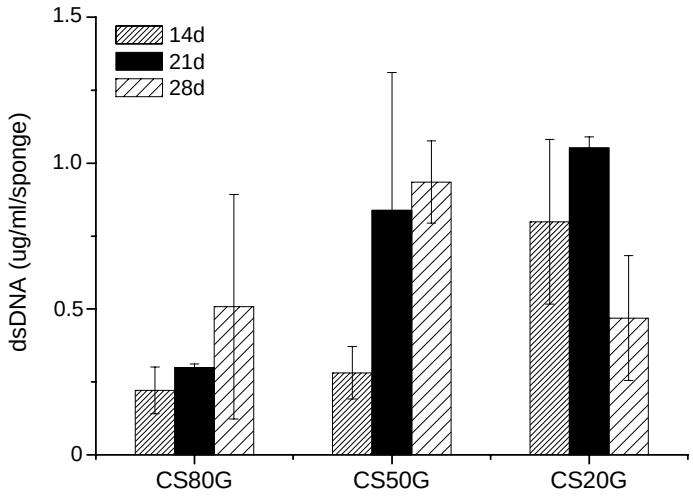

Figure 8. DNA content of ATDC5 cells on cross-linked CS sponges in function of time.

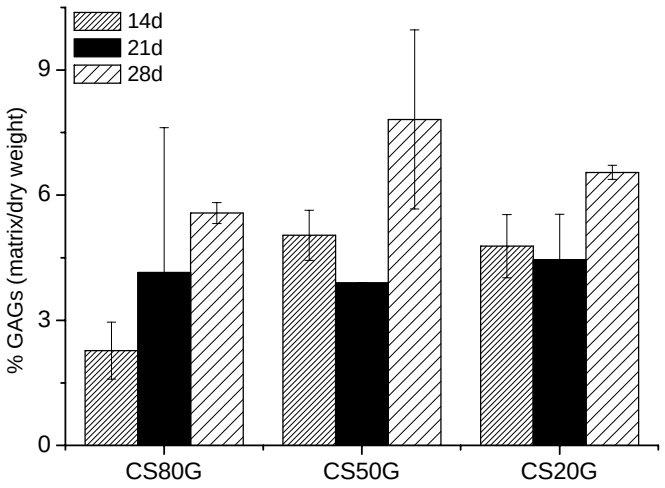

Figure 9. GAGs quantification assay of ATDC5 cells cultured on cross-linked CS sponges.

5. **Conclusions**

Novel biodegradable cross-linked chitosan/silk fibroin (CSG) blended-based hydrogels were successfully prepared. The resultant CSG sponges were fully gelled dark blue with a symmetric structure showing interesting characteristics such as (*i)* stable and ordered structures presumably due to protein conformation changes from α helix/random coil to β-sheet structure, *(ii)* different pore size and distinct morphologies, which are related to CS ratio, *(iii)* pH/swelling dependence at pH 3, 7.4 and 9, and *(iv)* stiffer sponges. In accordance to the tests performed in this work, the blending of silk fibroin to chitosan and, subsequently, genipin cross-linking promoted the formation of stable structures which favoured adhesion, proliferation and matrix production of chondrocyte-like cells. The variation of pore size of the CSG sponges did not appear to affect the cellular adhesion. Seeded cells showed a high adhesion and proliferation as well as matrix production. The positive cellular response together with the sponges' intrinsic properties suggested that cross-linked chitosan/silk fibroin based sponges may be good candidates for cartilage TE scaffolding.

6. **Acknowledgements**

S. S. Silva and M. T. Rodrigues thank the Portuguese Foundation for Science and Technology (FCT) for a PhD scholarship (SFRH/BD/8658/2002 and SFRH/BD/30745/2006, respectively). Ana F. M. Pinheiro thank the FCT and FEDER for a grant (POCI/FIS/61621/2004). This work was partially supported by the European Union funded STREP Project HIPPOCRATES (NMP3-CT-2003-505758) and was carried out under the scope of the European NoE EXPERTISSUES (NMP3-CT-2004-500283). The authors would also like to acknowledge Adriano Pedro for his contribution in the μ-CT analysis.

7. **References**

1. Vinatier C., Guicheux J., Daculsi, G., Layrolle, P., Weiss, P. Cartilage and bone tissue engineering using hydrogels. *Bio-Medical Materials and Engineering* 2006; 16: S107-S113.
2. Cartilage, in *Basic Histology*, Junqueira L. C. and Carneiro J. McGrawHill, USA, 2005; p. 128.
3. Mano, J.F., Reis, R.L. Osteochondral defects: present situation and tissue engineering approaches. *Journal of Tissue Engineering and Regenerative Medicine* 2007; 1: 261-273.
4. Chung, C., Burdick, J.A. Engineering cartilage tissue. *Advanced Drug Delivery Reviews* 2008; 60: 243-262.
5. Yan, J.H., Qi, N.M., Zhang, Q.Q. Rabbit articular chondrocytes seeded on collagen-chitosan-GAG scaffold for cartilage tissue engineering in vivo. *Artificial Cells Blood Substitutes and Biotechnology* 2007; 35: 333-344.
6. Stoltz, J.F., Bensoussan, D., Decot, V., Netter, P., Ciree, A., Gillet, P. Cell and tissue engineering and clinical applications: An overview. *Bio-Medical Materials and Engineering 2006*; 16: S3-S18.
7. De Franceschi, L., Grigolo, B., Roseti, L., Facchini, A., Fini, M., Giavaresi, G., Tschon, M., Giardino, R. Transplantation of chondrocytes seeded on collagen-based scaffold in cartilage defects in rabbits. *Journal of Biomedical Materials Research Part A* 2005; 74: 612-622.
8. Suh, J.K.F., Matthew, H.W.T. Application of chitosan-based polysaccharide biomaterials in cartilage tissue engineering: a review. *Biomaterials* 2000; 21: 2589-2598.
9. Chen, G., Ushida, T., Tateishi, T. Development of biodegradable porous scaffolds for tissue engineering. *Materials Science and Engineering C* 2001; 17: 63-69.
10. Liao, E., Yaszemski, M., Krebsbach, P., Hollister, S. Tissue-engineered cartilage constructs using composite hyaluronic acid/collagen I hydrogels and designed poly(propylene fumarate) scaffolds. *Tissue Engineering* 2007; 13: 537-550.
11. Aigner, T., Stove, J. Collagens- major component of the physiological cartilage matrix, major target of cartilage degeneration, major tool in cartilage repair. *Advanced Drug Delivery Reviews* 2003; 55: 1569-1593.
12. Kumar, M.N.V.R., Muzzarelli, R.A.A., Muzzarelli, C., Sashiwa, H., Domb, A.J. Chitosan chemistry and pharmaceutical perspectives. *Chemical Reviews* 2004; 104: 6017-6084.

13. Oliveira, J.T., Crawford, A., Mundy, J.M., Moreira, A.R., Gomes, M.E., Hatton, P.V., Reis, R.L. A cartilage tissue engineering approach combining starch-polycaprolactone fibre mesh scaffolds with bovine articular chondrocytes. *Journal of Materials Science- Materials in Medicine* 2007; 18: 295-302.
14. Vepari, C., Kaplan, D.L. Silk as a biomaterial. *Progress in Polymer Science* 2007; 32: 991-1007.
15. Altman, G.H., Diaz, F., Jakuba, C., Calabro, T., Horan, R.L., Chen, J., Lu, H., Richmond, J., Kaplan, D.L. Silk-based biomaterials. *Biomaterials* 2003; 24: 401-416.
16. Santin, M., Motta, A., Freddi, G., Cannas, M. In vitro evaluation of the inflammatory potential of the silk fibroin. *Journal of Biomedical Materials Research* 1999;46: 382-389.
17. Unger, R.E., Sartoris, A., Peters, K., Motta, A., Migliaresi, C., Kunkel, M., Bulnheim, U., Rychly, J., Kirkpatrick, C.J. Tissue-like self-assembly in cocultures of endotheilial cells and osteoblasts and the formation of microcapillary-like structures on three-dimensional porous biomaterials. *Biomaterials* 2007; 28: 3895-3976.
18. Li, Z., Zhang, M. Chitosan-alginate as scaffolding material for cartilage tissue engineering. *Journal of Biomedical Materials Research Part A* 2005; 75: 485-493.
19. Hsu, S.H., Whu, S.W., Hsieh, S.C., Tsai, C.L., Chen, D.C., Tan, H.S. Evaluation of chitosan-alginate-hyaluronate complexes modified by an RGD-containing protein as tissue-engineering scaffolds for cartilage regeneration. *Artificial Organs* 2004; 28: 693-703.
20. Koo, H.J., Song, Y.S., Kim, H.J., Lee, Y.H., Hong, S.M., Kim, S.J., Kim, B.C., Jin, C., Lim, C.J., Park, E.H. Antiinflammatory effects of genipin, an active principle of gardenia. *European Journal of Pharmacology* 2004; 495: 201-208.
21. Chen, H.M., Wei, O.Y., Bisi, L.Y., Martoni, C., Prakash, S. Reaction of chitosan with genipin and its fluorogenic attributes for potential microcapsule membrane characterization. *Journal of Biomedical Materials Research Part A* 2005; 75A: 917-927.
22. Mi, F.L. Synthesis and characterization of a novel chitosan-gelatin bioconjugate with fluorescence emission. *Biomacromolecules* 2005; 6: 975-987.
23. Yuan, Y., Chesnut, B.M., Utturkar, G., Haggard, W.O., Yang, Y., Ong, J.L., Bumgardner, J.D. The effect of cross-linking of chitosan microspheres with genipin on protein release. *Carbohydrate Polymers* 2007; 68: 561-567.
24. Chang, W.H., Chang, Y., Lai, P.H., Sung, H.W. A genipin-crosslinked gelatin membrane as wound dressing material: in vitro and in vivo studies. *Journal of Biomaterials Science- Polymer Edition* 2003; 14: 481-495.
25. Motta, A., Barbato, B., Torricelli, P., Migliaresi, C. Physical and preliminary biological properties of cross-linked fibroin-sericin films. *Bioactive and Compatible Polymers* 2007, Submitted.
26. Silva, S.S., Maniglio, D., Motta, A., Mano, J.F., Reis, R.L., Migliaresi, C. Genipin modified silk fibroin nanometric nets. *Macromolecular Bioscience* 2008*;* DOI: 10.1002/mabi.200700300.
27. Atsumi, T., Miwa, Y., Kimata, K., Ikawa, Y. A chondrogenic cell line derived from a differentiating culture of ATDC5 teratocarcinoma cells. *Cell Differentiation and Developm*ent 1990; 30: 109-116.
28. Hirai, A., Odani, H., Nakajima, A. Determination of degree of acetylation of chitosan by 1H NMR spectroscopy. *Polymer Bulletin* 1991; 26: 87-94.
29. Signini, R., Filho, S.P.C. On the preparation and characterization. *Polymer Bulletin* 1999; 42: 159-166.
30. Macosko, C.W. *Rheology: Principles, Measurements and Applications* VCH Publishers, Inc., New York, 1994.
31. Friedman, M. Applications of the ninhydrin reaction for analysis of amino acids, peptides, and proteins to agricultural and biomedical sciences. *Journal of Agriculture and Food Chemistry* 2004; 52: 385-406.

32. ISO/10993, Biological evaluation of medical devices- Part 5 test for Cytotoxicity, in vitro methods: 8.2 test on extracts 1992.
33. Gomes, M.E., Reis, R.L., Cunha, A.M., Blitterswijk, C.A., Bruijn, J.D. Cytocompatibility and response of osteoblastic-like cells to starch-based polymers: effect of several additives and processing conditions. *Biomaterials* 2001;22: 1911-1917.
34. Hollander, A.P., Hatton, P.V. *Biopolymer methods in tissue engineering* Human Press Incorporation, New York, 2004.
35. Monal, W.A., Goycoolea, F.M., Peniche, C., Ciapara, H. Rheological study of the chitosan/glutaraldehyde chemical gel system. *Polymer Gels and Networks* 1998; 6: 429-440.
36. Terry, A.E., Knight, D.P., Porter, D., Vollrath, F. pH induced changes in the rheology of silk fibroin solution from the middle division of Bombyx mori silkworn. *Biomacromolecules,* 2004; 5: 768-772.
37. Tang, Y.F., Du, Y.M., Hu, X.W., Shi, X.W., Kennedy, J.F. Rheological characterisation of a novel thermosensitive chitosan/poly(vinyl alcohol) blend hydrogel. *Carbohydrate Polymers* 2007; 67: 491-499.
38. Mi, F.L., Sung, H.W., Shyu, S.S. Synthesis and characterization of a novel chitosan-based network prepared using naturally occurring crosslinker. *Journal of Polymer Science- Part A-Polymer Chemistry* 2000; 38: 2804-2814.
39. Sung, H.W., Huang, R.N., Huang, L.L.H., Tsai, C.C., Chiu, C.T. Feasibility study of a natural crosslinking reagent for biological tissue fixation. *Journal of Biomedical Materials Research* 1998; 42: 560-567.
40. Sung, H.W., Chang, Y., Liang, I.L., Chang, W.H., Chen, Y.C. Fixation of biological tissues with a naturally occurring crosslinking agent: Fixation rate and effects of pH, temperature, and initial fixative concentration. *Journal of Biomedical Materials Research* 2000*; 52*: 77-87.
41. Butler, M.F., Ng, Y.F., Pudney, P.D.A. Mechanism and kinetics of the crosslinking reaction between biopolymers containing primary amine groups and genipin. *Journal of Polymer Science Part A- Polymer Chemistry* 2003;41: 3941-3953.
42. Mi, F.L., Sung, H.W., Shyu, S.S. Release of indomethacin from a novel chitosan microsphere prepared by a naturally occurring crosslinker: examination of crosslinking and polycation-anionic drug interaction. *Journal of Applied Polymer Science* 2001; 81: 1700-1711.
43. Pawlak, A., Mucha, A. Thermogravimetric and FTIR studies of chitosan blends. *Thermochimic Acta* 2003; 396: 153-166.
44. Um, I.C., Kweon, H.Y., Park, Y.H., Hudson, S. Structural characteristics and properties of the regenerated silk fibroin prepared from formic acid. *International Journal of Biological Macromolecules* 2001; 29: 91-97.
45. Wilson, D., Valluzi, R., Kaplan, D. Conformational transitions in model silk peptides. *Biophysical Journal* 2000; 78: 2690-2701.
46. Cooper, G.M. *The Cell - The Molecular Approach,* Sinauer Associates, Sunderland, MA, 2000.
47. Menard, K.P. *Dynamic mechanical analysis - a practical introduction* CRC Press, Florida, 1999.
48. Mano, J.F., Reis, R.L., Cunha, A.M. In *Polymer based systems on tissue engineering, replacement and regeneration*, Reis, R.L. and Cohn, D. Kluwer Academic Publishers, Netherlands, 2002; p. 139.
49. Lee, C.-T., Huang, C.P., Lee, Y.-D. Biomimetic porous scaffolds made from poly(L-lactide)-g-chondroitin sulfate blend with poly(L-lactide) for cartilage tissue engineering. *Biomacromolecules* 2006; 7: 2200-2209.

CHAPTER VIII

CHAPTER VIII

Genipin Modified Silk Fibroin Nanometric-Nets

Abstract

Nanometric silk fibroin nets were fabricated by electrospinning from regenerated *Bombyx mori* silk fibroin (SF)/formic acid solutions with the addition of genipin (GE), 2, 15 and 24 hours after the solution preparation. After spinning pure fibroin nanofibers were water soluble and needed a further stabilization process, whereas the reaction of fibroin with genipin resulted in water insoluble fibroin nets due to conformational changes induced in fibroin by genipin. SFGE nanofibers presented diameters ranging from 140 nm to 590 nm and were generally thinner than pure SF nanofibers. The secondary structure of SF into SFGE nanofibers showed the presence of β-sheet conformation together with β-turns intermediate (turns and bends). The approach described in this paper provided an alternative to design SF nanofibers already water insoluble without any stability post-treatment need.

This chapter is based on the following publication:

S. S. Silva, D. Maniglio, A. Motta, J. F. Mano, R. L. Reis, C. Migliaresi. "Genipin Modified silk fibroin-nanometric nets", Macromolecular Bioscience, 2008, DOI:mabi.200700300.

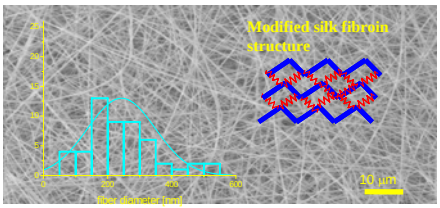

1. **Introduction**

Nature hierarchical organization at nano-level scale has been inspiring materials scientists in the design of novel nanofibers biomaterials for improving functionality and mechanical performance. The production of nanofibers from biopolymers solutions has gained a great deal of attention for biomedical uses, since the high porosity electrospun mats, that are formed by ultra-fine fibers with high specific surface, could mimic the structure of native extracellular matrix (ECM). Furthermore, interactions between cells and ECM are crucial to cellular differentiation and in modulation cell function [1,2]. The electrospinning technique has been recognized as an efficient, rapid and inexpensive method to manufacture nanoscale fibrous structures for a number of biomedical applications [3,4]. In the electrospinning process, a high voltage is applied to create electrically charged jets of a polymer solution. As the conical jet of polymer fluid propagates through the air, the solvent evaporates and nanofibers are collected on the target as a nonwoven matrice [2,3]. This technique has been utilized to generate non-woven mats of nanometer-sized fibers from biopolymers [5-11]. Among them, silk fibroin (SF), the natural biomacromolecule spun by *Bombyx mori* silkworm has been used in the preparation of matrices (*e.g.* tissue-engineered scaffolds, films, nanofibers) for a range of biomedical applications due to its unique properties such as good biocompatibility, good oxygen and water vapour permeability and minimal inflammatory reaction [9,10,12-15]. Non-woven matrices of electrospun nanofibers have been obtained from a regenerated SF solution using different spinning solvents [9-11,16]. However, electrospun SF nanofibers as well as others types of SF matrices such as films are water soluble and should be treated with an aqueous alcohol solution [13,15,17] or with water vapour [11] to enhance their crystallinity and stability in the presence of water. The main objective of this work was to obtain modified SF nanofibers stable in aqueous environment in a single processing step. This paper reports the first attempt to use genipin (GE) to modify regenerated SF solutions for electrospinning process. Actually, genipin is considered a natural

cross-linking agent with lower cytotoxicity as compared with alternative cross-linkers such as glutaraldehyde [18]. It has been reported that genipin binds with biological tissues [19,20] and biopolymers [18,21], leading to matrices with good mechanical properties, reduced swelling extent and good biocompatibility. Our aim was to investigate the effect of the addition of genipin to SF solution on the processability, morphology and stability of electrospun fibroin nets. In fact, an increase of both water-resistant ability and mechanical performance of the resulting silk nanofibrous membranes could facilitate their practical applications. Properties of GE added fibroin solutions, structural changes and morphological features of electrospun SFGE nanofibers were examined using Rheological measurements, Attenuated Total Reflection Fourier Transform Infrared (ATR-FTIR) Spectroscopy and Scanning Electronic Microscopy (SEM).

2. **Materials and Methods**

2.1. *Materials*

Silk from cocoons of *Bombyx mori* was kindly provided from Cooperativa Socio Lario, Como, Italy. Genipin was a product of Wako Chemicals, USA. All other chemicals were reagent grade and used as received.

2.2. *Preparation of silk fibroin*

Silk from cocoons of *Bombyx mori* was first degummed in order to remove sericins. Degumming was achieved by boiling the silk filaments for 1 h in water containing 1.1 g/L of Na_2CO_3 (anhydrous) and, then for 30 min in water with 0.4 g/L of Na_2CO_3. Finally the resulting fibroin filaments were extensively rinsed in hot distilled water and dried in the air at room temperature. To prepare solutions to be used in the preparation of the materials, fibroin was dissolved in 9.3M LiBr overnight at 65°C. Then, the solution was dialysed in a Slide-A-Lyzer Cassette (Pierce), MWCO 3500 Da against distilled water for 3 days at room temperature. The water was changed

every 2h. After that, the silk fibroin water solution was frozen in liquid nitrogen and lyophilized to obtain pure fibroin powder. The amino acid composition of silk fibroin was obtained by HPLC analysis.

2.3. *Spinning silk fibroin solution preparation*

Regenerated silk fibroin (SF) dissolved in neat formic acid at concentration 12 wt% was used. Genipin powder (12% related to total weight of fibroin in solution, *i.e.* 6.29 x 10^{-3}M) was added to the silk fibroin solution under stirring conditions for 5 min at room temperature until complete dissolution. The system was maintained under stirring for pre-determined time (2, 15 and 24 hours) at 37°C and then the conductivities of the solutions were measured using a conductimeter instrument 525 CRISON. Subsequently, the SF solutions were submitted to electrospinning process. The identification of the modified SF solutions was SFGEX, where GE and X indicate genipin and reaction time, respectively. As control materials, SF and SFGE films were also prepared by casting the solutions on Petri dishes. After casting, the films were dried at room temperature for at least two days before any further use.

2.4. *Production of nanonetworks by electrospinning process*

In the experimental electrospinning the SF solution was loaded into a 20 ml syringe and a needle was attached. The positive electrode of a high-voltage power supply (Gamma High Voltage Research Inc.) was directly connected to the needle to charge the spinning drop of protein solution, and the negative electrode was clipped in the down part of the system. The syringe was placed on an automatic syringe pump to maintain a constant volume flow rate. The electric potential, solution flow rate, and the distance between the needle tip and the aluminium foil were adjusted till a stable jet was obtained. The operating parameters selected to produce the nanofibers were the following: voltage 21kV, flow rate 0.005 ml/min, distance between the needle tip and the target (aluminium foil set at ground

voltage) 10 cm and room temperature. All the apparatus was mounted under a hood and nitrogen gas was insufflated continuously around the system during the electrospinning process to control the humidity, which was regulated to a range of 20-30%. After preparation, all samples were dried in vacuum for 1 week prior the analysis.

2.5. *Characterization*

Rheological measurements were carried out on Advanced Rheometric Expansion System (ARES, Shear Strain Controlled). The geometry was a stainless steal plate/plate (diameter 2 mm and gap 0.4 mm). The plate was equipped with a solvent trap to reduce evaporation during measurement Dynamic rheological tests (time sweep) at frequency of 5 rad/sec and strain 5% were used to characterize the behaviour of the solution before and after addition of genipin at 37°C.

The electropun nanofiber morphology was observed under a scanning electron microscope (SEM) (Cambridge Stereoscan 100) operated at an acceleration voltage of 10kV. SEM photos, fiber diameters of the nanofibrous membranes were analysed using image visualization software ImageJ developed by National Institute of Health (http://rsb.info.nih.gov/).

The mats obtained by electrospinning were cut into squares of 2 x 2 cm^2 and immersed in distilled water at 37°C for 8 days to test their dissolution/stability.

The infrared spectra of SF and SFGE nanofibers and films were obtained using a Perkin Elmer and a Bio-rad FTS6000 spectrometer, respectively in the spectral region of 4000-650 cm^{-1}. Curve fitting of the bands were performed with the ORIGIN® (OriginLab Corporation, MA, USA) software Gaussian bands shapes were employed in this procedure. Curve-fitting was limited to the 1580-1720 cm^{-1}

spectrum range, since protein structure (contributions of second and third vibration) can see identified in this range [22,23].

3. **Results and Discussion**

3.1. *Silk fibroin solution characterization*

Amino acid composition of the fibroin used in this work was assessed by HPLC analysis. Silk fibroin molecule was formed mainly of Glycine (46.7%), Alanine (31.4%), and Serine (8.5%). Prior to the preparation of non-woven silk fibroin mats by electrospinning, silk fibroin solutions behaviors after addition of genipin were examined by rheology measurements (Figure 1A). Both storage shear modulus G´(t) and loss shear modulus G´´(t) were found increase with the time, until G´ became over G´´ due to formation of a protein network structure. The gel point defined when G´=G´´, was observed after 3.5 min. However, the stiffness of the gel keeps increasing for longer times. Based on such results, SF solutions were electrospun 2, 15 and 24 hours after preparation. Furthermore, dynamic time sweep studies were performed on these SF and SFGE solutions. The rheological data of all SF solutions showed that G´(t), G´´(t) and $\eta'(t)$ values increase with the time (Figure 1B-D). This effect could be due to a slight gelation of the fibroin solution induced by the applied shear stress, a phenomenon well known for fibroin solutions. Moreover, values of G´(t), G´´(t) and $\eta'(t)$ were higher for the SFGE15 solution as compared with SFGE24, so indicating the occurrence of some degradation at higher times.

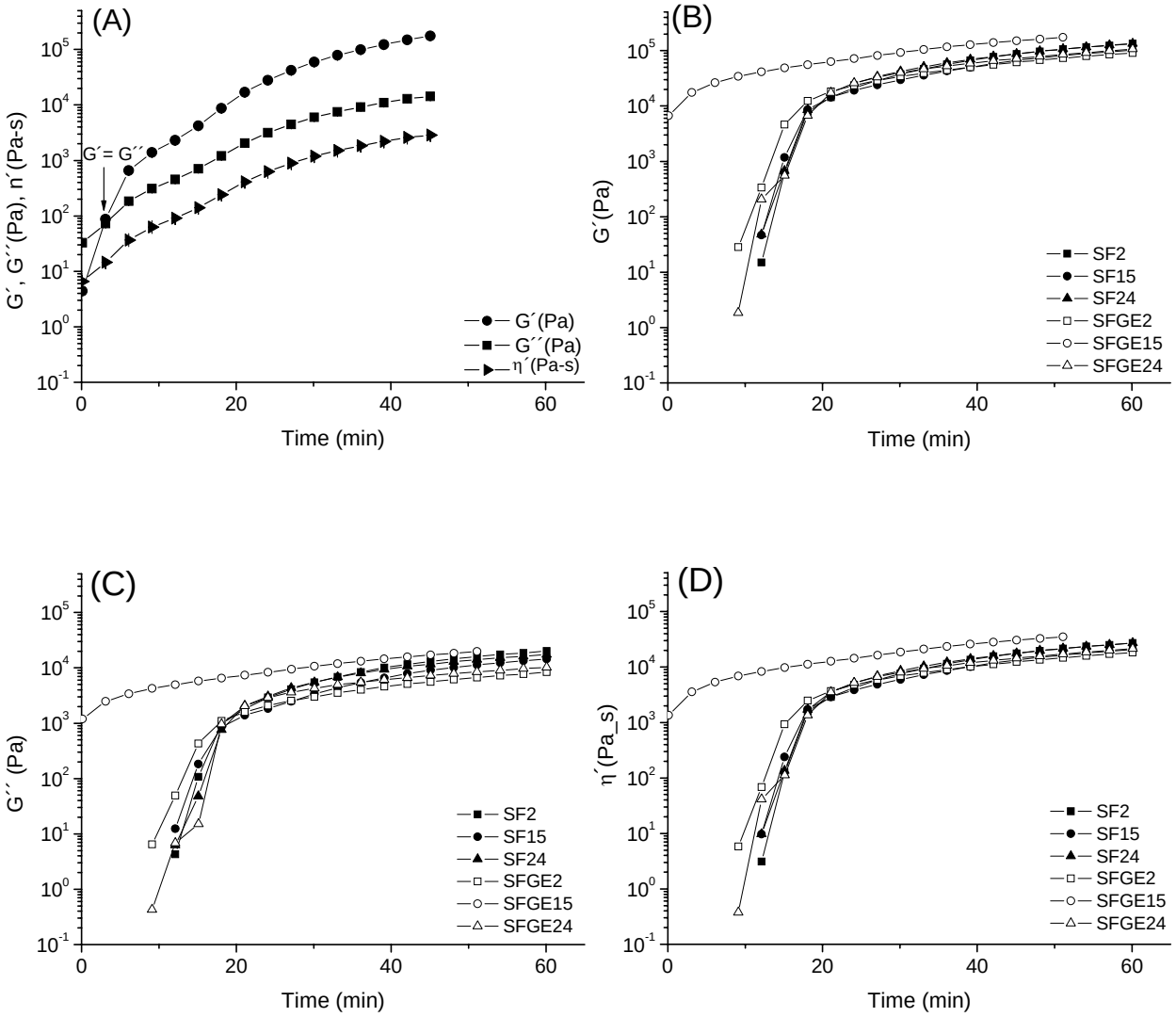

Figure 1. (A) Storage shear modulus G´ (t), loss shear modulus G´´ (t) and viscosity of SFGE solutions; (B) Time dependence of storage shear modulus, G´(t), (C) loss shear modulus, G´´ (t), and (D) Viscosity ,η´(t), of SF and SFGE solutions after different reaction time. Measurements were made at ω = 5 rad/s at 37°C. The close (■, ●,▲) and open (□, ○, △) symbols correspond to SF and SFGE solutions, respectively.

Electrical conductivities of SFGE solutions were higher than regenerated SF solutions (Table 1). The higher conductivity, resulting in more charges accumulated in the electrospinning jet, associated to viscoelastic behavior of the modified SF solutions promoted the formation of a more stable jet and the production of nanofibers with average smaller diameters (Figure 2). Nevertheless, SF nanofibers were obtained only when the humidity of the system was controlled in the range of 20-30%, using nitrogen gas. Higher humidity, in fact, could slow down solvent evaporation so hindering the formation of nanofibers [3].

Table 1. Characteristics of the SF and SFGE solutions and average fiber diameter of the SF nanofibers obtained before and after water- stability tests.

System	Colour of the solution	Conductivity (μS/cm)*	Fiber diameter (μm)	
			Before water-stability tests	After water-stability tests
SF	Pale rose	874	480 ± 140	900 ± 280
SFGE2	Pink	892	590 ± 170	1020 ± 370
SFGE15	Dark pink	925	240 ± 110	380 ± 120
SFGE24	Dark red	1160	140 ± 70	-

*Formic acid conductivity = 396 μS/cm

3.2. *Morphological characterization*

SEM micrographs (Fig. 2) showed that as-spun SF and SFGE nanofibers were randomly distributed in the mats with an average fiber diameter that varied from 140 nm to 590 nm (Table 1). Also, the morphology of the SF nanofibers changed from a uniform fiber structure (Fig. 2A-2C1) to fibers linked together with beads (Fig. 2D1). The high conductivity of SFGE solutions (Table 1) might increase the stretching of the polymer solution in electrospinning, so resulting in small diameter fibers [3]. It is evident that the properties of SFGE solutions (viscosity, conductivity) had a clear influence on both morphology and average diameter of the resulting fibers. Additionally, it is known that genipin reacts with amino acids or proteins to form dark blue pigments [19] . After mixing, the colour of SF-GE solutions changed gradually from pale rose transparent to dark red (Table 1), so indicating the progress of a reaction between SF and GE. This fact also suggests that the reaction mechanism involving genipin and silk fibroin with formic acid as solvent may be different those reported in literature [18,24].

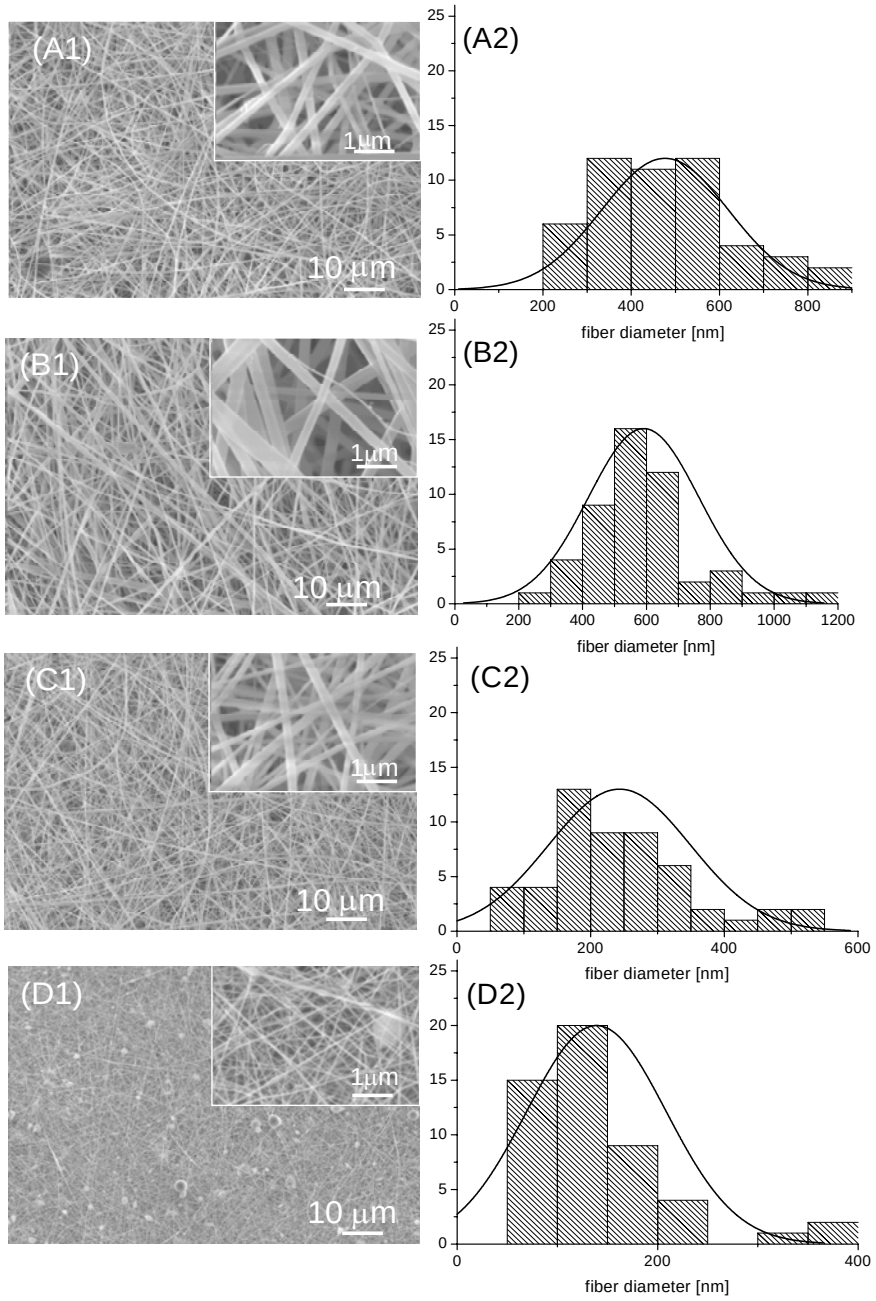

Figure 2. SEM micrographs of as-prepared SF and SFGE nanofibers: A1) SF nanofibers, and A2) the corresponding histogram of the fiber diameter distribution; B1) nanofiber SFGE2, and B2) the corresponding histogram of the fiber diameter distribution; C1) nanofiber SFGE15 and, C2) the corresponding histogram of the fiber diameter distribution; D1) nanofiber SFGE24 and, D2) the corresponding histogram of the fiber diameter distribution. The insets are the high magnification SEM micrographs.

Water-stability of the SF nanofibers prepared from different reaction time (2, 15 and 24 hours) was evaluated through immersion of the nonwoven net in distilled water at 37°C for 8 days. As expected, the SF nanofibres without any stabilization post-treatment (Fig. 3A1), lost their integrity as reported in others studies [11]. Fibers at junctions were fused together forming agglomerates on the surface (Figure 3A1), probably due the gradual dissolution of the material. Compared with the SF nanofibers, SFGE2 preserved their original fibrous form (Figure 3B1). Among all fibres, SFGE15 showed the highest stability in water with a small increase of the fiber diameter (Figure 3C1, Table 1). The interaction mechanism of genipin with silk fibroin is currently unknown, some authors [20] reported that genipin reacts preferentially with the aminoacids lysine and arginine of proteins. In our studies, the fibroin chain contains those aminoacids in a very low percentage (lysine 0.6% and arginine 0.6%), mainly in the hydrophilic blocks. For this reason, the reaction kinetic should be reasonably slow, but efficient enough to render the system stable in water.

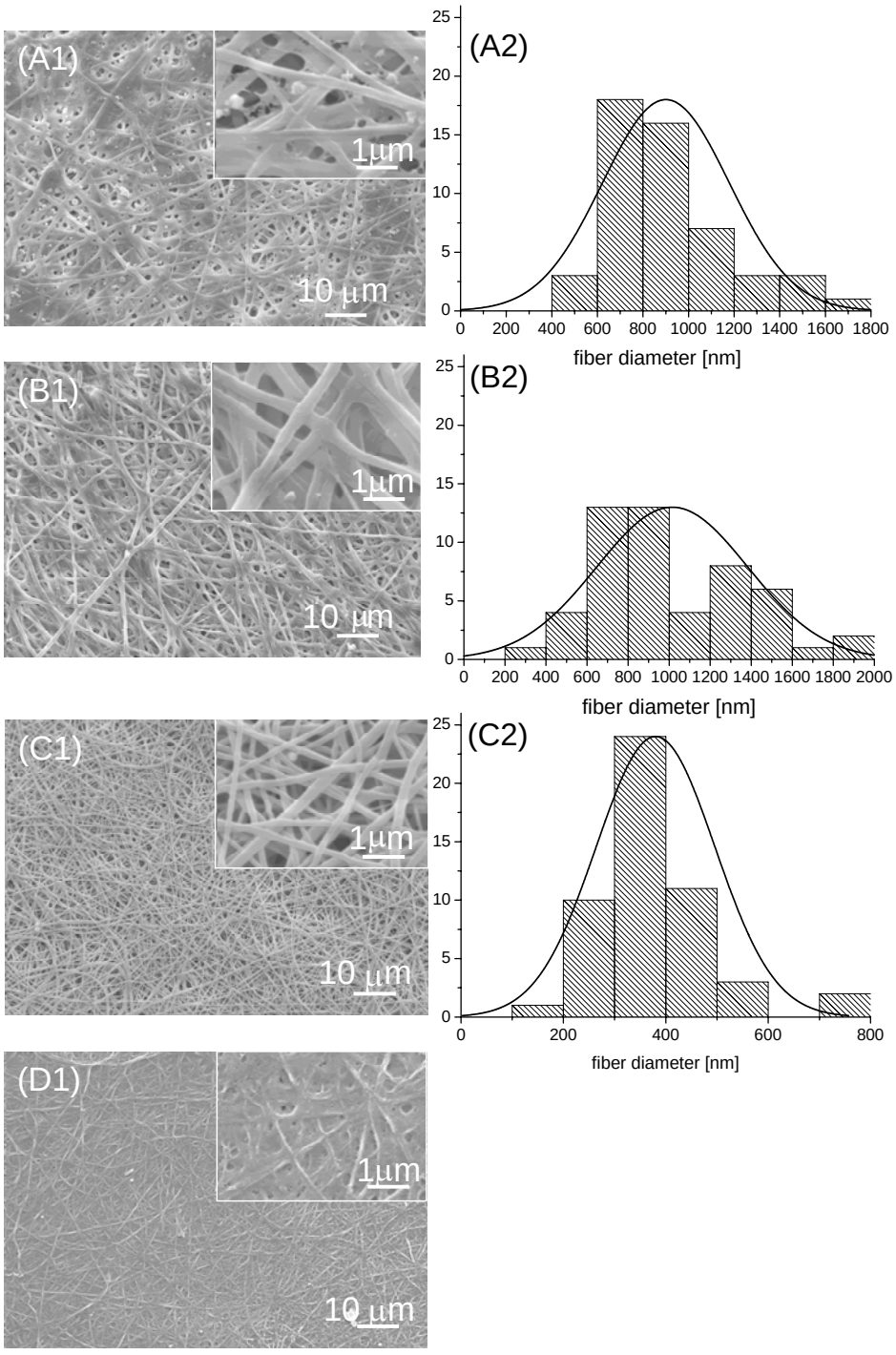

Figure 3. SEM micrographs of SF and SFGE nanofibers after 8 days immersed in distilled water at 37°C: A1) SF nanofibers and A2) the corresponding histogram of the fiber diameter distribution; B1) nanofiber SFGE2, and B2) the corresponding histogram of the fiber diameter distribution; C1) nanofiber SFGE15 and, C2) the corresponding histogram of the fiber diameter distribution; D1) nanofiber SFGE24. The insets are the high magnification SEM micrographs. All samples were dried in vaccum for 1 week prior the SEM observations.

3.3. *FTIR results*

Fibroin protein exists in three conformations, namely random coil, silk I (α-form), and silk II (β-sheet conformation). SF in formic acid exhibits random coil conformation similar to the aqueous SF solution [25]. It is hypothesized that the SF molecules could structurally rearrange due to the changes in the hydrogen bonding caused by presence of the genipin as well as by the processing effect. In order to evaluate the effect of genipin on the final conformation of fibroin, FTIR spectra of SF and SFGE nanofibers and films were acquired (see Figure 4). Even though new peaks did not appear after the reaction, structural changes can be revealed by analysing the amide I (C=O) stretching and II (N-H deformation) in the spectra (Fig. 4a and 4b). Comparing spectra acquired on both samples, the amide I (1640-1620 cm^{-1}) and amide II (1529-1517 cm^{-1}) bands, which are associated to the antiparallel β-structural conformation[11,22,23], shifted to lower wavenumbers (1620 cm^{-1} , amide I and at 1514 cm^{-1} , amide II), mainly in the films spectra (Fig. 4a). These peaks in the SFGE samples suggest the presence of β-sheet structure (silk II structure). Furthermore, some characteristic bands of genipin at 1443 ($-CH_3$, CH_2), 1150 (-COH) and 1105 (-COH) cm^{-1} (Figure 4, insert spectrum) [26] appeared displaced in the spectra (Figure 4). These displacements could be attributed to modifications on SF molecules due to the reaction with genipin. When modified SF solutions undergo electrospinning, further conformational changes may occur, with a further transition of random coils to a more stable antiparallel β-sheet conformation throughout intermediate forms such as β-turns and β-bends.

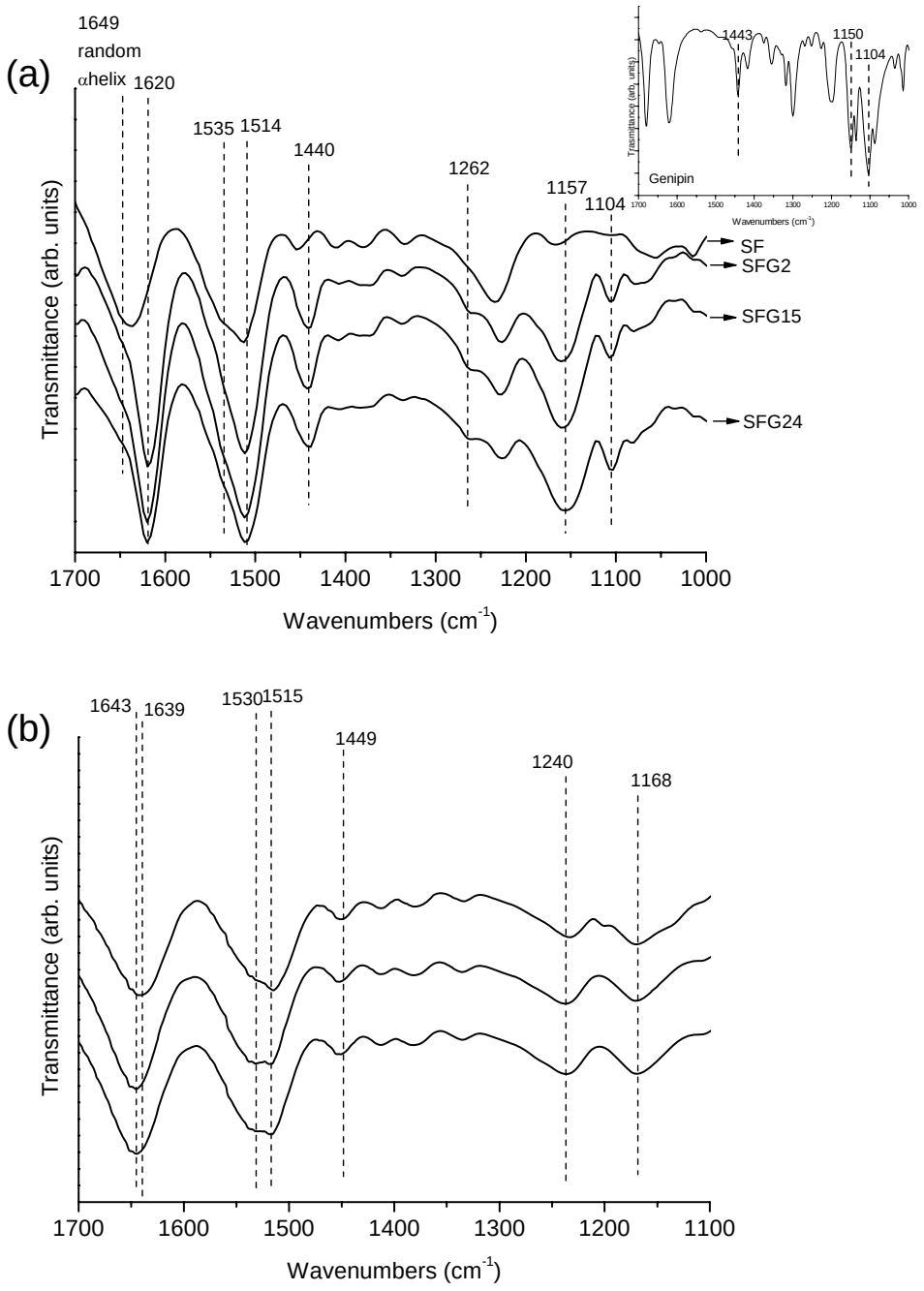

Figure 4. FTIR spectra of the samples: (a) SF and SFGE films, and (b) SFGE nanofibers. Insert in the (a) shows the genipin spectrum.

To confirm this change, ATR-FTIR spectra of SF nanofibers were examined more carefully in the amide I region (1700-1650 cm^{-1}) – see Figure 5. The amide I spectral region was resolved into three or four main components for each sample, assuming a Gaussian behaviour for each individual process. The curve-fitting results (Figure 5 and Table 2) showed that SFGE nanofibers have contributions of different conformations such as random coil (1640-1648 cm^{-1}), α-helix (1651-1657 cm^{-1}), β-sheet (1625-1640 cm^{-1}), and some intermediate forms such as turn and bends (1658-1666 cm^{-1}) [22,23]. The addition of genipin and/or electrospinning process promoted particular conformational changes in the silk fibroin secondary structure of each sample. Particularly, in the SFGE15 sample, the frequency of the peaks (92.4%) ascribed to β-sheet structure as well as turns and bends structures (7.6%) revealed a more stable structure compared to others samples (Table 2). Additionally, the presence of a small percentage of random coil was observed, mainly in SFGE2 (23.3%) and SFGE24 (17.3%) samples. The higher percentage of beta sheet found in the modified SF nanofibers, supports the hypothesis that SF molecules were structurally rearranged by addition of genipin as well as by the processing effect. The findings suggested also that SFGE15 system represents the optimal condition to formation of SFGE nanofibers in terms of structure and water stability.

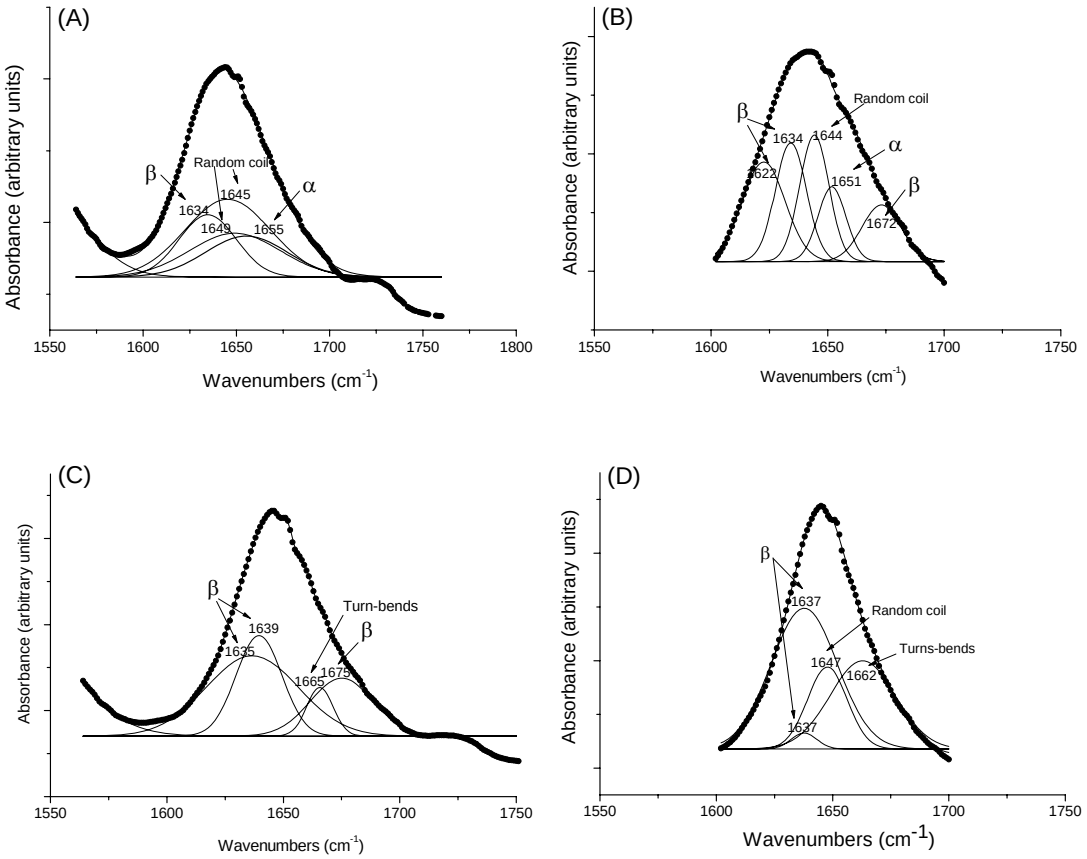

Figure 5. Curve-fitting results of the ATR-FTIR data of amide II region of the silk fibroin nanofibers: (A) SF, (B) SFGE2, (C) SFGE15 and (D) SFGE24.

Table 2. Curve-fitting results of "amide I" regions in the ATR-FTIR spectra of SF nanofibers.

Samples	Wavenumber/cm^{-1} (area)*	Secondary structure**
SF	1634 (19.7%)	β-structure
	1645 (38.5%)	Random coil
	1649 (23.1%)	
	1655 (18.7%)	α-helix
SFGE2	1622 (26.7%)	β-structure
	1634 (23.3%)	
	1672 (13.9%)	
	1644 (23.3%)	Random coil
	1651 (12.8%)	α-helix
SFGE15	1635 (44.3%)	β-structure
	1639 (26.6%)	
	1675 (21.5%)	
	1665 (7.6%)	Turns and bends
SFGE24	1637 (51.9%)	β-structure
	1647 (17.3%)	Random coil
	1662 (30.8%)	Turns and bends

* Percentage total pick area / ** Secondary structure attributed to amide I band frequencies [22].

4. **Conclusions**

Nanometric-nets were successfully obtained by electrospinning from regenerated silk fibroin-genipin (SFGE) solutions. The resulting SFGE nanofibers had a fiber diameter from 140 to 590 nm and were generally thinner than non-modified SF nanofibers. SFGE15 nanofibers maintained their integrity in water even after 8 days of aging. The evaluation of the secondary structure of SFGE nanofibers revealed the presence of both β-turn intermediates and β-sheet conformation, induced by the reaction of silk fibroin with genipin. This result was more evident in the fibres produced from SFGE15 and SFGE24 solutions. Water stability and structure of the investigated SFGE nanofibres makes the process suitable for the fabrication of fibroin nets that do not need any stabilization treatment after spinning and that could be used in a variety of biomedical applications, *e.g.* wound dressings or, with appropriate modifications for tissue engineering.

5. **Acknowledgments**

We gratefully acknowledge Prof. Rolando Barbucci (Department of Chemical and Biosystem Sciences and Technologies, University of Siena, Italy) for assistance with FTIR studies. The authors acknowledge funding from Portuguese Foundation for Science and Technology (FCT), Portugal for SFRH/BD/8658/2002 and the EU funded Project HIPPOCRATES (NMP3-CT-2003-505758). This work was carried out under the scope of the European NoE EXPERTISSUES (NMP3-CT-2004-500283).

6. **References**

1. Li, M. Y., Mondrinos, M. J., Gandhi, M. R., Ko, F. K., Weiss, A. S., and Lelkes, P. I., Electrospun protein fibers as matrices for tissue engineering, *Biomaterials* 26, 5999-6008, 2005.
2. Pham, Q. P., Sharma, U., and Mikos, A. G., Electrospinning of polymeric nanofibers for tissue engineering applications: a review, *Tissue Engineering* 12, 1197-1211, 2006.
3. Ramakrishna, S., Fujihara, K., Teo, W. E., Lim, T. C., and Ma, Z., *An introduction to electrospinning and nanofibers* World Scientific, 2005.
4. Murugan, R. and Ramakrishna, S., Nano-featured scaffolds for tissue enginnering: a review of spinning methodologies, *Tissue Engineering* 12, 435-447, 2006.
5. Bhattarai, N., Edmondson, D., Veiseh, O., Matsen, F. A., and Zhang, M., Electrospun chitosan-based nanofibers and their cellular compatibility, *Biomaterials* 26, 6176-6184, 2005.
6. Lu, J. W., Zhu, Y. L., Guo, Z. X., Hu, P., and Yu, J., Electrospinning of sodium alginate with poly(ethylene oxide), *Polymer* 47, 8026-8031, 2006.
7. Huang, Z. M., Zhang, Y. Z., Ramakrishna, S., and Lim, C. T., Electrospinning and mechanical characterization of gelatin nanofibers, *Polymer* 45, 5361-5368, 2004.
8. Buttafoco, L., Kolkman, N. G., Engbers-Buijtenhuijs, P., Poot, A. A., Dijkstra, P. J., Vermes, I., and Feijen, J., Electrospinning of collagen and elastin for tissue engineering applications, *Biomaterials* 27, 724-734, 2006.
9. Jin, H. J., Fridrikh, S. V., Rutledge, G. C., and Kaplan, D. L., Electrospinning Bombyx mori silk with poly(ethylene oxide), *Biomacromolecules* 3, 1233-1239, 2002.
10. Ayutsede, J., Gandhi, M., Sukigara, S., Micklus, M., Chen, H. E., and Ko, F., Regeneration of Bombyx mori silk by electrospinning. Part 3: characterization of electrospun nonwoven mat, *Polymer* 46, 1625-1634, 2005.
11. Min, B. M., Jeong, L., Lee, K. Y., and Park, W. H., Regenerated silk fibroin nanofibers: Water vapor-induced structural changes and their effects on the behavior of normal human cells, *Macromolecular Bioscience* 6, 285-292, 2006.
12. Vepari, C. and Kaplan, D. L., Silk as a biomaterial, *Progress in Polymer Science* 32, 991-1007, 2007.
13. Servoli, E., Maniglio, D., Motta, A., Predazzer, R., and Migliaresi, C., Surface properties of silk fibroin films and their interaction with fibroblasts, *Macromolecular Bioscience* 5, 1175-1183, 2005.
14. Unger, R. E., Peters, K.,Wolf, M., Motta, A., Migliaresib, C., Kirkpatrick,J., Endothelialization of a non-woven silk fibroin net for use in tissue engineering: growth and gene regulation of human endothelial cells, *Biomaterials* 25, 5137-5146, 2004.
15. Santin, M., Motta, A., Freddi, G., and Cannas, M., In vitro evaluation of the inflammatory potential of the silk fibroin, *Journal of Biomedical Materials Research* 46, 382-389, 1999.
16. Ohgo, K., Zhao, C. H., Kobayashi, M., and Asakura, T., Preparation of non-woven nanofibers of Bombyx mori silk, Samia cynthia ricini silk and recombinant hybrid silk with electrospinning method, *Polymer* 44, 841-846, 2003.
17. Chen, C., Chuanbao, C., Xilan, M., Yin, T., and Hesun, Z., Preparation of non-woven mats from all-aqueous silk fibroin solutions with electrospinning method, *Polymer* 47, 6322-6327, 2006.
18. Butler, M. F., Ng, Y. F., and Pudney, P. D. A., Mechanism and kinetics of the crosslinking reaction between biopolymers containing primary amine groups and genipin, *Journal of Polymer Science Part a-Polymer Chemistry* 41, 3941-3953, 2003.
19. Sung, H. W., Liang, I. L., Chen, C. N., Huang, R. N., and Liang, H. F., Stability of a biological tissue fixed with a naturally occurring crosslinking agent (genipin), *Journal of Biomedical Materials Research* 55, 538-546, 2001.

20. Sung, H. W., Huang, R. N., Huang, L. L. H., Tsai, C. C., and Chiu, C. T., Feasibility study of a natural crosslinking reagent for biological tissue fixation, *Journal of Biomedical Materials Research* 42, 560-567, 1998.
21. Chen, H. M., Wei, O. Y., Bisi, L. Y., Martoni, C., and Prakash, S., Reaction of chitosan with genipin and its fluorogenic attributes for potential microcapsule membrane characterization, *Journal of Biomedical Materials Research Part A* 75A, 917-927, 2005.
22. Wilson, D., Valluzi, R., and Kaplan, D., Conformational transitions in model silk peptides, *Biophysical Journal* 78, 2690-2701, 2000.
23. Chittur, K. K., FTIR/ATR for protein adsorption to biomaterial surfaces, *Biomaterials* 19, 357-369, 1998.
24. Mi, F. L., Shyu, S. S., and Peng, C. K., Characterization of ring-opening polymerization of genipin and pH-dependent cross-linking reactions between chitosan and genipin, *Journal of Applied Polymer Science Part A: Polymer Chemistry* 43, 1985-2000, 2005.
25. Um, I. C., Kweon, H. Y., Lee, K. G., and Park, Y. H., The role of formic acid in solution stability and crystallization of silk protein polymer, *International Journal of Biological Macromolecules* 33, 203-213, 2003.
26. Mi, F. L., Sung, H. W., and SHYU, S. S., Release of indomethacin from a novel chitosan microsphere prepared by a naturally occuring crosslinker: examination of crosslinking and polycation-anionic drug interaction, *Journal of Applied Polymer Science* 81, 1700-1711, 2001.

CHAPTER IX

CHAPTER IX

General Conclusions

Nature-inspired routes involving the development of natural origin polymer-based systems constitute an alternative to produce useful novel materials. Chemical and surface modification can additionally be performed on these systems to further tailor their properties according the requirements for tissue engineering applications. The main goal of the present thesis was to develop and modify natural origin polymer-based systems using simple methodologies such as a sol-gel method, plasma surface modification and blending of chitosan with proteins like soy protein isolate and silk fibroin.

Chitosan has been considered in a wide range of biomaterials and tissue engineering works due to its intrinsic characteristics. However, when chitosan is used without further modification the findings showed different degree of success, which justified the interest in studies of chemical and surface modification of this natural polymer.

Sol-gel method is a versatile wet-chemical technique for the preparation of materials involving the transition of a system from a liquid “sol” (mostly colloidal) into a solid “gel” phase (formation of an inorganic network). This method is an important tool to create ceramics, glass materials, microspheres, biosensors, and also acts in the immobilization of biomolecules. Different hybrid materials can be used and/or adapted to tissue engineering. Alternatively to conventional sol-gel process (*e.g.* in the presence of water and ethanol and inorganic acids as the catalyst), a sol-gel derived carboxylic acid solvolysis was used for the first time to synthesize chitosan-based hybrid material (class II) via carboxylic acid solvolysis. This method occurred in the absence of water and oxygen using isocyanatopropyltriethyoxysilane (ICPTES) as silane coupling agent. The developed bifunctional hybrid materials were formed by covalent cross linking (urea or

urethane groups) bridges that bonded chitosan to the inorganic matrix, whereas the siloxane network was incorporated, in different extents, into polysaccharide. These structural features may provide to photoluminescence characteristics and a bioactive behaviour of these hybrids, which can be advantageous to create new advanced materials. The photoluminescence nature of the hybrids was correlated with the condensation degree of the inorganic domains and with the stronger hydrogen bonds established between adjacent urea groups. Besides, the amount, distribution and structural re-arrangement of residual silanol groups could be associated to the formation of Ca-P layer at the surface of the hybrids. In spite of the success achieved in inorganic incorporation in chitosan, it was not possible to obtain a mouldable structure to be used as three dimensional material due to the difficulties associated with the insolubility of this polysaccharide in usual organic solvents (*e.g.* tetrahydrofuran) used for this particular sol-gel process. In respect to potential of sol-gel process, it is important to use new solvents that make possible to obtain stable structures like gels, which make easy the moulding of the structure for a determined biomedical applications.

Together with the so-called good bulk properties of a biomaterial, their surface characteristics also play a fundamental role on how the living host tissue interacts with the implant. Plasma surface treatment is a widely used method to tailor surface functionality, which might for instances determine the cell attachment and proliferation on the materials, its interactions with bioactive agents, namely drugs, growth factors, as well as the possibility of use on the regeneration of hard/soft tissues. In our work, surface properties of chitosan membranes were modified through nitrogen and argon plasma treatment. In preliminary studies, oxygen was also tested. However, the treated membranes were fragile and highly hydrophilic while membranes treated with argon and nitrogen showed good handling with a good hydrophilic/hydrophobic balance. Based on these results, argon and nitrogen were chosen. Both plasma treatments resulted in membranes with higher surface roughness (nanoscale), indicating the occurrence of an etching process. When

argon plasma was used there was a trend to enhance the roughness with the increase of the exposure time. Moreover, the incorporation of oxygen and nitrogen- containing groups on the surface and an increase in the surface energy contributed to the modification of the surface chemistry and wettability of the chitosan surface, respectively. After plasma treatment, the treated membranes were stored in a desiccator overnight to allow the recombination of the radicals. Post-reactions of radicals with the environment can have influenced some of these obtained results. In addition, the cell studies showed that the changes on surface properties of chitosan membranes were sufficient to influence effectively and positively on fibroblast adhesion and proliferation. These modifications on chitosan membranes confirmed their potential as wound dressing materials, and also open opportunities to create patterns on the polymeric surface controlled by exposure time, which might reflect in the cell adhesion.

The combination of polysaccharides and proteins in a unique material offers a useful route to obtain new biomaterials with superior properties when compared to individual components towards specific biomedical purposes, as revised in the introduction section of this thesis. The presence of proteins into matrix materials may improve its cell behaviour because they are able to interact favourably with cells through specific recognition domains present in their structure. A severe inflammatory tissue reaction was obtained when soy protein (powders) were injected into the intraperitoneal cavity of rats. With the purpose to study the influence of blending of soy protein with chitosan solution, a series of blended membranes were prepared using three different compositions and *in situ* cross-linking with glutaraldehyde solutions. The features used in this methodology were dependent on the amount of soy protein used and demonstrated to be adequate to produce rough membranes with high surface energy. Membranes obtained with higher soy protein content were fragile and presented high weight loss, whereas the reduction of soy protein content overcomes these effects. The solid state carbon nuclear magnetic resonance (^{13}C NMR) suggested that a weak interaction

occurred between chitosan and soy protein phases. The proton spin-lattice relaxation times in the rotating frame, $T_{1\rho}$ (1H) were measured, and indicated that the formulations with lower and higher soy content may have protein and polysaccharide regions that are miscible. *In situ* chemical cross-linking with glutaraldehyde on chitosan/soy protein blended systems was chosen as an alternative approach to enhance the interaction between chitosan and soy protein thus overcoming the immiscibility drawback. The cross-linking step resulted in blended membranes with decreased water absorption and different degradation profiles. The findings from cell culture studies demonstrated that the addition of soy protein associated with the cross-linking with low glutaraldehyde concentration have a positive effect on enhancing cell attachment of the chitosan/soy protein blended membranes in comparison to chitosan membranes. Recent *in vivo* studies demonstrated that chitosan/soy protein blended membranes accelerated skin wound healing in rats after two weeks of dressings compared to the positive control (Eppigard). All these findings support the suitability of the chitosan/soy protein to be used as wound dressing materials.

Based on our previous studies, the association of proteins and chitosan produces chitosan-based materials with improved physical and mechanical properties, and cell adhesion. New hydrogels were produced in this thesis combining *Bombyx mori* silk fibroin and chitosan. In this case, the systems were cross-linked with genipin. These hydrogels were freeze-dried to obtain cross-linked chitosan/silk sponges. These sponges were stable and quite ordered due to the protein conformation changes from α helix/random coil to β sheet structure promoted by genipin cross-linking. The mechanism of interaction of genipin with silk fibroin is currently unknown, but most probably it is similar to one the observed for amino-group-containing compound like chitosan. In addition, genipin reacts preferentially with the aminoacids lysine and arginine of certain proteins, where the used fibroin chain contains these aminoacids in a very low percentage (lysine 0.6% and arginine 0.6%), mainly in the hydrophilic blocks. For this reason, the number of cross-linking

sites is low and the kinetics is reasonably slow on the silk fibroin fraction. The cross-linking degree values obtained for the sponges were 45.2 ± 0.1%, 29.3 ± 1.7, and 23.9 ± 3.1 for CS80G, CS50G and CS20G, respectively. The formulation with higher silk fibroin content (CS20G) resulted in the lower cross-linking degree while the sample with higher chitosan (higher percentage of available amine groups) (CS80G) presented higher cross-linking degree. These results are in agreement with the hypothesis that the association of chitosan with fibroin favoured the genipin cross-linking and, the formation of stable and ordered hydrogels. In addition, the sponges showed swelling capability that depended on the pH, and good mechanical properties.

The cell studies using chondrocyte-like cells seeded onto sponges indicated that the introduction of silk component to chitosan, as well as genipin cross-linking, promoted favourable adhesion, proliferation and matrix production of chondrocytes-like cells. This positive cellular response together with the sponges' intrinsic properties suggested that cross-linked chitosan/silk fibroin based sponges may be a potential candidate for cartilage tissue engineering scaffolding.

In parallel to this study of blending of silk fibroin and chitosan, the possibility of obtaining modified silk nanometric nets using an electrospinning process was explored. Electrospinning has emerged as a very widespread technology to produce nanofibrous structures. These structures have morphology and fiber diameters in a range comparable with those found in the extracellular matrix of human tissues. The construction of nanofibrous scaffolds is intended to provide improved environments for cell attachment as well as may facilitate their use as local drug-release systems and wound dressings. Normally, electrospun silk fibroin nanofibers as well as other types of silk fibroin matrices should be treated with an aqueous alcohol solution to enhance their crystallinity and stability in the presence of water. In our strategy, nanometric silk fibroin nets were fabricated by electrospinning from regenerated *Bombyx mori* silk fibroin (SF)/formic acid solutions with the addition of genipin, 2, 15 and 24 hours after the solution preparation. The effect of

the addition of genipin to SF solution on the processability, morphology and stability of electrospun fibroin nets was studied. It was possible to obtain modified silk fibroin nanometric nets with fiber diameter ranging from 140 nm to 590 nm, which were generally thinner than pure silk fibroin nanofibers. In addition, the reaction was efficient enough to render modified silk nanometric nets more stable in water, mainly those obtained with 15 hours of time reaction. Structural characterization showed that the higher percentage of β- sheet found in the modified SF nanofibers, supported the hypothesis that SF molecules were structurally rearranged by addition of genipin as well as by the processing effect. The main advantage of this approach consisted on the fabrication of fibroin nets that do not require any stabilization treatment after the spinning process. This approach with appropriate modifications can be helpful in the construction of different three dimensional architectures with nano and microfibers for tissue engineering applications.